THE UNIVERSITY
of EDINBURGH

The functional and diagnostic role of microRNAs in *Schistosoma mansoni* infection

Anna Maria Hoy

Doctor of Philosophy The University of Edinburgh 2014

DECLARATION

I, the undersigned, hereby declare that the content of this thesis has been composed by myself, that the work described herein is my own unless acknowledged otherwise, and that the work has not been submitted for any other degree or professional qualification

I, the undersigned, confirm that the work submitted is my own, except where work which has formed part of jointly-authored publications has been included. The contribution of the other authors to this work has been explicitly indicated below. I confirm that appropriate credit has been given within the thesis where reference has been made to the work of others.

Anna Maria Hoy Date:

PUBLICATIONS & CONTRIBUTIONS

Publication 1	**Hoy A.M.**, Lundie JR, Ivens A, Quintana JF, Nausch N, Forster T, Jones F, Kabatereine NB, Dunne DW, Mutapi F, MacDonald AS, Buck AH (2014). Parasite-derived microRNAs in host serum as novel biomarkers of helminth infection. PLOS Neglected Tropical Diseases. 8(8(2): e2701
Authors Contributions-General	Conceived and designed the experiments: **AMH** RJL ASM AHB. Performed the experiments: **AMH** RJL JFQ AHB. Analyzed the data: **AMH** TF AI AHB. Contributed reagents/materials/analysis tools: NN FM NBK FJ DWD. Wrote the paper: **AMH** AHB.
Candidate's Contributions-Specific	*1) S. mansoni c.180 infection, liver tissue harvest, RNA extraction - RJL, miRNA array & analysis- AHB, TF, miRNA array validation- **AMH**. 2) S.mansoni time course experiments: S.mansoni infection- RJL & **AMH**, Tissue harvest, Blood collection, Liver RNA extraction **-AMH**, RJL, Serum and RNA extraction- **AMH**. Reverse transcription, PCR & data analysis - **AMH*** 3) Illumina sequencing: Small RNA library preparation- **AMH**, JFQ. Illumina sequencing analysis- AHB, AI. 4) Human serum samples: Sample collection & parasitology- FJ, NN, FN, DDW. RNA extraction- **AMH**, *Reverse transcription, PCR and data analysis - **AMH**, ROC curve analysis- **AMH***
Confirmation:	*Date: Signature:* *Print Full Name: Amy Buck*
Publication 2	**Hoy, A.M.** & Buck, A.H. (2012). Extracellular small RNAs: what, where, why? *Biochem Soc Trans. 40(4); 886-90*
Authors Contributions-General	Literature review: **AMH**, AHB, Wrote the paper: **AMH**, AHB, Figure construction: **AMH**
Confirmation:	*Date: Signature:* *Print Full Name: Amy Buck*

The microarray experiment data detailed in Chapter 3 of this thesis is a result of work of Dr Rachel J. Lundie (*S.mansoni* infection and liver RNA extraction), Dr Amy Buck (microarray experiment) and Thorsten Forster (microarray analysis).

I would like to thank Dr Rachel J. Lundie and Ms Rinku Rajan for their contribution in planning and setting up the *S.mansoni* infections, help with organ harvest and RNA extraction.

Dr Jess G. Borger carried out the miRNA in-situ hybridization experiment for which data is presented in Appendix 5 and provided *S.mansoni* time course histology pictures Fig 3.4 A.

The experimental data detailed in Chapter 4 is a result of collaborative work. The Small RNA library preparation for deep - sequencing (experiment 2) was carried out by Juan F. Quintana. The analysis of the sequencing data was carried out by Dr Alasdair Ivens and Dr Amy H. Buck. I would also like to thank Dr Fabio Simbari, Dr Nouf Laqtom, Gillian Coakley, Marissa Lear for their assistance with organ harvests, Sujai Kumar for processing initial sequencing data and Dr Dan Frank and Margo Chase-Topping for helpful discussions on analysis. The human serum samples collection and human parasitology was carried out by Dr Norman Nausch and Frances Jones.

I would like to thank Dr James Hewitson for his help with size exclusion chromatography experiment (Chapter 5).

Dr Andrew S. MacDonald was involved in the planning and comprehension of Chapters 3 and 4

Dr Amy H. Buck was involved in the planning and comprehension of all chapters.

NERC funded this PhD.

The Wellcome Trust UK funded the laboratory of Dr Amy H. Buck.

ACKNOWLEDGEMENTS

Amy, thank you for teaching, guiding and supporting me during my PhD. Thank you for always “having a minute” to discuss exciting data, horrible data and no data. I loved working in the Buck lab and will miss it a lot. Thank you for pushing me to do better and be better. It was a pleasure to be your student.

Andrew, thank you for your supervision and support during my PhD. Thank you for all the encouragement and advice. I have been lucky to have you as my second supervisor.

Many thanks to the wonderful past and present members of the Buck Lab: Nouf, Diwa, Hannah, Valentina, Alessandro, Marissa, Fabio, Divya, Lek, Gillian, Juan, Kat, Kashyap, Jana and Zamoyska lab members, especially: Kaija, Shini, Jess, Stefano and Celine. Thank you for your advice, help and your support. Thank you for coffee breaks, lunch breaks, journeys on the bus, dinning out, conferencing, and all the fun we had together. You are truly amazing! Big thank you to MacDonald lab members for their *S.mansoni* expertise. Rachel, thank you for being the most patient teacher ever. Rinku, thank you so much for helping me with animal work. Many thanks to Martin for help with blood-related matters, to Al for bioinformatics, and Betty for smiles, good words and cheerfulness. To everyone in the IIIR, thank you for your advice, help and suggestions whenever I needed them.

Mamo, Tato, Mlody, tralalalala wreszcie koniec studiów! Dziekuję za Wasze wsparcie. Kocham Was.

Chris, thank you for your support and love, for driving me to and from the lab, feeding me, reminding me to drink and telling me ‘ you can do it!’. I would not have done it without you. I love you.

Zosiu, my precious little kluseczko, thank you for being so wonderful. Thank you for making me the happiest person na świecie. Kocham Cię so very much.

ABSTRACT

Schistosomiasis caused by the parasitic helminth *Schistosoma mansoni* is a major health problem in tropical and subtropical regions. Its detection is crucial for patient management, evaluation of treatment, and monitoring of disease transmission, thus the development of novel diagnostic assays is of immense importance. The pathology of *S.mansoni* infection is characterised by formation of granulomatous lesions, hepatic fibrosis and portal hypertension. Liver fibrosis itself, regardless of the causative agent is an important health problem. The fact that there is no treatment for hepatic fibrosis other than transplantation in end stage liver failure emphasizes the importance of investigating the molecular basis of fibrogenesis and development of better therapeutic tools.

MicroRNAs (miRNAs) are a class of short non-coding RNA that play important roles in disease processes in animals. Several miRNAs have been implicated in hepatic fibrogenesis; however, the expression profile and the role of miRNAs in *S. mansoni* infection are yet to be determined.

This thesis focuses on the characterization of miRNAs in the liver and serum of mice during *S.mansoni* infection in order to determine their therapeutic and diagnostic potential in this disease.

Profiling of miRNA expression in the liver of mice infected with *S.mansoni* revealed a set of mouse miRNAs that were differentially expressed in infected compared to naïve mice including miR-199a-3p, miR-199a-5p, miR-214 and miR-21, which have previously been associated with liver fibrosis in other settings. Further, inhibition of one of the up-regulated miRNAs, miR-199a-3p, in the liver upon *S.mansoni* infection resulted in reduced levels of collagen and other fibrosis related genes. Our results are consistent with a model where miRNA inhibition influences the clearance or reversion of hepatic stellate cells (HSCs) from a “myofibroblast-like” to an inactivated state. Thus, these results suggest miR-199a-3p inhibitor as potential therapeutic in treatment of liver fibrosis.

miRNAs have been shown to be altered in disease process and are present in body fluids in a stable form, indicating that they can be used as novel diagnostic

biomarkers. Studies of miRNAs in the circulation revealed that 5 of the mouse miRNAs altered in the liver were also significantly elevated in serum by 12 weeks post-infection. Sequencing of small RNAs from serum confirmed the presence of these miRNAs and further revealed 11 parasite-derived miRNAs that were detectable by 8 weeks post infection. Analysis of host and parasite miRNA abundance by qRT-PCR was extended to the serum of patients from low- and high-infection sites in Zimbabwe and Uganda. The host-derived miRNAs failed to distinguish uninfected from infected individuals. However, analysis of three of the parasite-derived miRNAs (miR-277, miR-3479-3p and bantam) could detect infected individuals from low- and high-infection intensity sites with specificity/sensitivity values of 89%/80% and 80%/90%, respectively.

Moreover, sequencing of small RNAs from serum revealed that specific tRNA fragments of 29-33 nt exist in mouse serum and occur at a >10 fold higher copy number than known microRNAs. The tRNA fragments appear to be the product of a specific cleavage event near the anti-codon loop, which has previously been associated with oxidative stress inside cells. We detected a clear bias in the abundance of 5' versus 3' products of $tRNA^{Gly}$(GCC), indicating specificity in the mechanism of stabilization of these products following cleavage. Our findings suggest that these specific tRNA cleavage products are either generated in, or exported to, serum and are protected against serum RNase activity by protein rather than encapsulation within vesicles. Further work is necessary to investigate the role and potential involvement of tRNA halves in cell-to-cell communication in oxidative stress induced by *S.mansoni* infection.

In summary, this thesis reveals three major findings, which provide an important base for further studies of the role of miRNAs in *S.mansoni* infection and liver fibrosis. Firstly, it characterises host miRNAs dysregulated during *S.mansoni* infection in the liver and identifies a miR-199a-3p inhibitor as a potential anti-fibrotic agent. Secondly, it identifies parasite-derived miRNAs as novel markers of *S. mansoni* infection in the serum of both mice and humans, with the potential to be used with existing techniques to improve *S.mansoni* diagnosis. Lastly, it identifies

and characterises novel tRNA-derived fragments in the serum, whose properties as biomarkers awaits further characterisation.

LAY ABSTRACT

Schistosomiasis is a chronic disease caused by blood flukes that affect over 200 million people worldwide, of which 90% live in Africa. Infection with one of the *Schistosoma* flukes, called *Schistosoma mansoni (S.mansoni)* leads to scaring (fibrosis) of the liver.

In this thesis we studied the role of a class of small RNAs, microRNAs (miRNAs) in *S. mansoni* infection and investigated their potential in diagnosis of the infection and treatment of liver fibrosis.

By measuring the levels of miRNAs in the liver of mice infected with *S.mansoni* we identified a subset of mouse miRNAs that are either expressed at higher or lower levels in infected compared to uninfected mice. Some of these miRNAs have previously been linked with liver fibrosis caused by other insults. Further, we showed that blocking one of the miRNAs in the liver during *S.mansoni* infection lowered the levels of genes that are normally elevated during liver fibrosis, suggesting that this miRNA inhibitor could be used as a new medicine of liver fibrosis. Studies of miRNAs in serum of mouse and human infected with *S.mansoni* showed the presence of miRNAs derived from *S.mansoni*. Further analysis of these miRNAs revealed that they can be used to detect infected individuals with good specificity and sensitivity. This thesis provides an important base for further studies of the role of miRNAs in *S.mansoni* infection and liver fibrosis and identifies a set of miRNAs that can be used to diagnose this infection.

ABBREVIATION

µl	Microliter
µ	Micro
µg	Microgram
µM	Micromolar
~	Approximately
°C	Degrees Celsius
aaRSs	Aminoacyl-tRNA synthetases
ACTA2	Smooth Muscle α Actin
AGO	Argonaute
aHSCs	Activated hepatic stellate cells
AMI	Acute myocardial infarction
ANG	Angiogenin
ASH	Alcohol steatohepatits
BCL-2	B-cell lymphoma-2
bp	Base pairs
CAA	Circulating anodic antigens
CAF1	Chromatin assembly factor-1
CB1	Cannabinoid receptor 1
CCA	Circulating cathodic antigens
CCL4	Carbon tetrachloride
CCND1	Cyclin D 1
CCR	C-C chemokine receptor
CDS	Coding sequence
CNE1	Cyclin E1
COL1A1	Collagen, type I, alpha 1
COL3A1	Collagen, type III, alpha 1
CTGF	Connective tissue growth factor
DCP2	Decapping MRNA 2
ddH20	Double-distilled water
DDR2	Discoidin domain receptor tyrosine kinase 2
DDX6	DEAD-box protein
DGCR8	DiGeorge Syndrome Critical Region 8 Protein
DMN	Dimethylnitrosamine
DNA	Deoxyribonucleic acid
DNMT2	DNA (cytosine-5-)-methyltransferase 2
ECM	Extracellular matrix

EDC4	Enhancer of mRNA decapping 4
EDTA	Ethylenediaminetetraacetic acid
eIF4G	Eukaryotic translation initiation factor 4G
epg	Eggs per gram
FBN1	Fibrilin 1
FN1	Fibronectin 1
FXR1	Fragile X mental retardation, autosomal homolog 1
g	Gravitational force or grams
GAPDH	Glyceraldehyde-3-phosphate dehydrogenase
GW182	Glycine-tryptophan protein of 182 kDa
HBV	Hepatitis B virus
HCC	Hepatocellular carcinoma
HCV	Hepatitis C virus
HDL	High-density lipoprotein
HIF1a	Hypoxia inducible factor 1, alpha subunit
HNF	Hepatocyte nuclear factor
HSCs	Hepatic stellate cells
HSP-90	Heat Shock Protein 90
IFN	Interferon
IL	Interleukin
Inh.	Inhibitor
ITGB1	Integrin beta-1
kb	Kilobase
kDa	Kilodalton
KLF6	Kruppel-like factor 6
LNA	Lock nucleic acid
lncRNAs	Long non-coding RNAs
LX2	Human hepatic stellate cell line
M	Molar
m^7G	7-methylguanosine (m^7G) cap
MEF-2	Myocyte enhancer factor-2
min	Minute
miRNA	MicroRNA
ml	Millilitre
mM	Millimolar
MMP	Matrix metalloproteinase
mRNA	Messenger RNA
MVB	Multivesicular bodies

Mw	Molecular weight
NAFLD	Non-alcoholic fatty liver disease
NASH	Non-alcoholic steatohepatitis
ncRNA	Non-coding RNAs
nM	Nanomolar
CNOT4	CCR4-NOT transcription complex, subunit 1
NPM1	Nucleophosmin
NSCLC	Non-small cell lung cancer
nt	Nucleotides
ORF	Open reading frame
P	Probability value
p.i	Post infection
P4HA1	Prolyl 4-hydroxylase subunit alpha-1
PABP1	Poly(A)-binding protein 1
PACT	Protein kinase R-activating protein
PAN2	poly(A) specific ribonuclease subunit homolog
PBMC	Peripheral-blood mononuclear cells
PBS	Phosphate buffered saline
PDGF	Platelet-derived growth factor
pH	Measure for the hydrogen ion concentration
piRNA	Piwi-interacting RNAs
PMN	Polymorphonuclear cells
Pol	Polymerase
PPAR-α	Peroxisome proliferator activated receptor-alpha
pre-	Precursor microRNA
pri-	Primary microRNA
PZQ	Praziquantel
qRT-PCR	Quantitative reverse transcription polymerase chain reaction
RBC	Red blood cells
RGS16	Regulator of G protein signaling 16
RISC	RNA-induced silencing complex
RLC	RISC loading complex
RNA	Ribonucleic acid
RNase P	Endoribonuclease P
RNase Z	Endoribonuclease Z
RNases	Ribonucleases
RNH1	Ribonuclease/angiogenin inhibitor 1
Rny1	Ro-associated Y1

ROCK1	Rho-associated, coiled-coil containing protein kinase 1
rRNA	Ribosomal RNA
SDS	Sodium dodecyl sulfate
SEA	Soluble egg antigens
SEC	Size exclusion chromatography
siRNA	Small interfering ribonucleic acid
snoRNA	Small nucleolar RNAs
snRNA	Small nuclear RNAs
SSC	Sodium chloride-sodium citrate buffer
TDP-43	TAR DNA binding protein 43
TGF-β	Transforming growth factor-beta
TIMP	Tissue inhibitor of matrix metalloproteinases
TNC	Tenascin-C
TNF-α	Tumour necrosis factor alpha
TRBP	Transactivation-response RNA-binding protein
tRNA	Transfer RNA
U6 snRNA	Small nuclear RNA U6
UTR	Untranslated region of mRNA
VEDF	Vascular endothelial growth factor
WHO	World Health Organization
XPO5	Exportin 5
XRN1	5'-3' exoribonuclease 1
YB-1	Y box binding protein 1
α-SMA	α smooth muscle actin

Table of Contents

List of Figures

List of Tables

List of Appendices

Chapter 1: **Introduction**

1.1 Schistosomiasis

Schistosomiasis, also known as bilharzia, is a chronic disease caused by parasitic helminths of the genus *Schistosoma* and is second to malaria as the most important parasitic infection in the world in terms of economic and public health impact (Gray et al., 2011; Gryseels et al., 2006; Ross et al., 2002). It has been estimated that 200 million people are infected across Africa, Asia & South America with an estimated 800 million people at risk (Steinmann et al., 2006; WHO, 2013a). However, new research suggests that the true number of infections is considerably higher (Schur et al., 2011a; Schur et al., 2011b). The annual mortality rate due to schistosomiasis is approximately 280,000 per year (WHO, 2013a). Five species of *Schistosoma* infect humans: *Schistosoma haematobium, S.mansoni, S.japonicum, S.mekongi* and *S.intercalatum*. These same parasites can also infect a range of animals including non-human primates and rodents (Rollinson et al., 2013). Depending on the *Schistosoma* species, the immunopathological reaction against the parasite eggs trapped in the tissue lead to inflammation and urinary disease (*S. haematobium*) or intestinal disease, hepatosplenic inflammation and hepatic fibrosis (*S.mansoni, S.japonicum, S.mekongi*) (Gryseels et al., 2006). The distribution of schistosomiasis is shown in Fig 1.1.

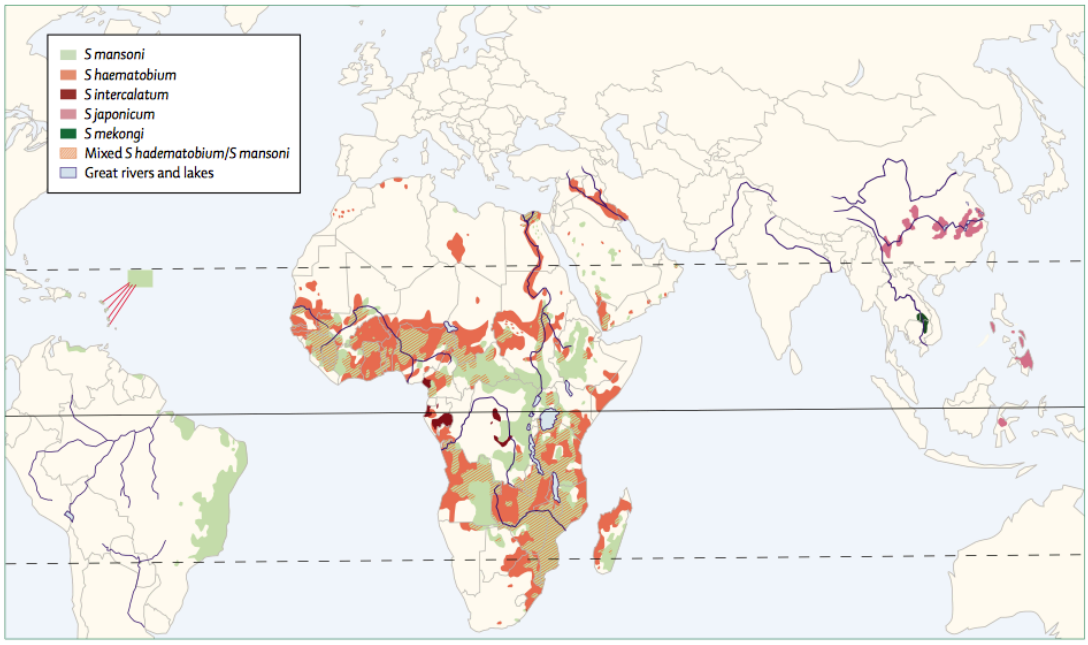

Figure 1.1 The distribution of schistosomiasis
S.haematobium infections occur across Africa and in the Middle East. *S.mansoni* occurs mainly in Sub-Saharan Africa, South America (parts of Venezuela, Brazil and the Caribbean), and the Arabian Peninsula. *S.japonicum* infections occur in Southeast Asia (People's Republic of China, Philippines) and small parts of Indonesia. *S. intercalatum* is endemic in Central and West Africa and *S.mekongi* is found only in Cambodia and Lao People's Democratic. The figure is from (Gryseels et al., 2006).

1.1.1 Biology and life cycle of Schistosoma mansoni

The complex life cycle of *S. mansoni* involves the sexual reproduction phase in the human definitive host and the asexual reproduction phase in the intermediate host (Fig.1.2). The *S.mansoni* eggs released from the infected individuals hatch upon contact with fresh water and release the miracidia (Pearce and MacDonald, 2002). The ciliated miracidia infect the intermediate host, which is a snail of the genus *Biomphalaria,* and undergoes a series of transformations including generation of sporocysts and the production of cercariae (free-swimming larval stage) (Rollinson, 1987). The cercariae present in the infected water initiates infection of the definitive host by penetrating the skin. They then loose their tails and becoming schistosomulae, which migrate through the blood system via the lung to the mesenteric veins where they can live 5-10 years (Pearce and MacDonald, 2002). Mature worms are elongated, have cylindrical bodies of 7-20 mm long, two terminal suckers (oral and ventral), a complex tegument, blind digestive tract and reproductive organs. The mature male worm pairs with the immature female in the portal vein. The presence of the male worm is necessary for maturation and the development of reproductive function of the female (Popiel et al., 1984). The male worm has a gynecophoral canal where the thinner female worm resides (Skelly, 2008). After approximately 4-6 weeks post infection the mature female starts producing up to 300 eggs per day (Wynn et al., 2004). Some of the eggs successfully traverse from the vasculature to the intestinal tracts and are released to the gut lumen to be excreted in faeces. The contact of mature *S.mansoni* eggs with water closes the life cycle. However, more than 50% of the eggs are carried by the blood-flow to the liver where they become trapped (Wynn et al., 2004) thus, the liver is the key organ of *S.mansoni* pathology (Pearce and MacDonald, 2002). The host immune response induced by the presence of the egg antigens in the liver leads to the formation of granulomatous lesions, fibrosis and portal hypertension (Booth et al., 2004; de Jesus et al., 2004; Wynn et al., 2004).

.

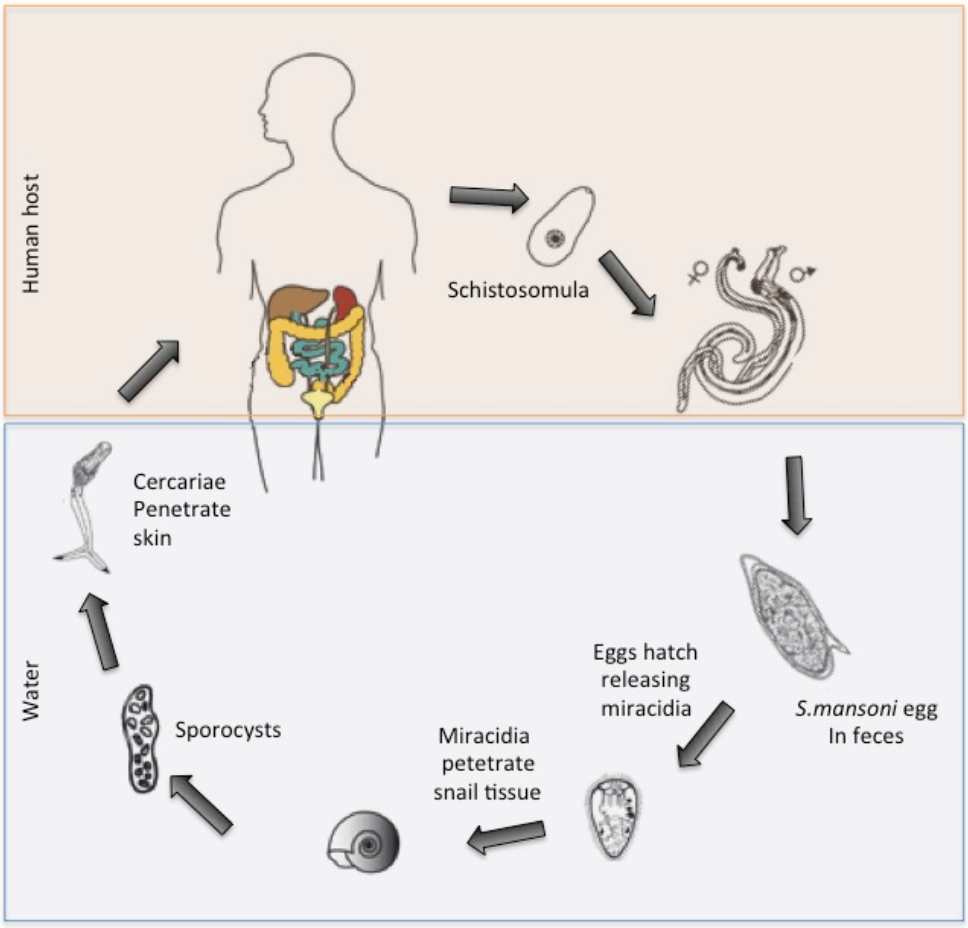

Figure 1.2 Life cycle of *S.mansoni*.
The *S.mansoni* eggs released in feces from the infected individuals, hatch upon contact with fresh water and release the miracidia. The miracidia infect snails of the genus *Biomphalaria* and undergo a series of transformations including generation of sporocysts and the production of cercariae (free-swimming larval stage). *S.mansoni* infection in the definitive host (human) is initiated by *S.mansoni* cercariae present in the infested water. The cercariae penetrate the skin, loose their tail and become schistosomulae, which migrate through the blood system via lung to the mesenteric veins. The mature male worm pairs with the immature female in the portal vein and after approximately 4-6 weeks the mature female start producing up to 300 eggs per day. Some of the eggs successfully traverse from the vasculature to the intestinal tracts and are released to the gut lumen to be excreted in feces. This figure is adapted from a figure by the Centers for Disease Control & Prevention: Division of Parasitic Diseases, USA. (http://www.cdc.gov/parasites/schistosomiasis)

1.1.2 Symptoms and immunopathology

The clinical symptoms associated with *S.mansoni* infection can be divided into three phases: cercarial dermatitis, acute and chronic infection.

The percutaneous penetration of the cercariae can result in a temporary rash with maculopapular eruptions and erythematous lesions and occurs mainly in tourists or migrants that are infected for the first time (Bottieau et al., 2006). A similar rash called "swimmer's itch" is an effect of the immune reaction to cercariae of non-human *Schistosoma* species (Horak and Kolarova, 2005).

Acute schistosomiasis is rarely seen in areas of chronic exposure, but it is common in tourists. This hypersensitive reaction to the migration and maturation of schistosomulae occurs several weeks post infection. Symptoms observed in the acute schistosomiasis may include fever, abdominal pain, fatigue, headache, malaise, myalgia, dry cough, neck pain and diarrhoea. Neurological, pulmonary and cardiac complications have also been reported (Gray et al., 2011; Gryseels et al., 2006). It has been shown that during the acute phase the levels of pro-inflammatory cytokines tumour necrosis factor alpha (TNF-α), interleukin (IL) - 1 and IL- 6 are raised in peripheral-blood mononuclear cells (PBMCs), and the levels of TNF-α are also increased in serum (de Jesus et al., 2004).

The chronic pathology of *S.mansoni* infection is due to the host immune response to the egg trapped in the liver and gut and is characterized by granulomatous inflammation around the parasite egg, portal hypertension, splenomegaly, gastrointestinal varices and peri-portal (Symmers') fibrosis (Gray et al., 2011; Gryseels et al., 2006). The studies in animal models of *S.mansoni* infection have made substantial contribution to understanding the immunopathology of this infection. It is important to note that *S.mansoni* infection in mice differs compared to the infection in humans. Specifically, the pathology of infection in mice is associated primarily with the granulomatous response in the liver and intestines and does not cause Symmers' fibrosis which is known to be associated with morbidity in humans (Hams et al., 2013).

In the first 3-5 weeks post infection, the initial host immune response, targeted against the migrating immature parasites antigens, is strongly Th1-like, characterized by increased production of interferon-γ (IFN- γ) and IL-12. However, the type-2 responses are also primed during the first weeks of infection (Pearce and MacDonald, 2002). After 5-6 weeks, the mature parasites mate and female worms start laying eggs. Some eggs are carried via sinusoids to the liver where they become trapped (Wynn, 2004). The presence of the egg antigen leads to the modulation of the host immune response from the Th1 to a strong Th2 response. The Th2 response leads to up-regulation of IL-4, IL-5, IL-13 as well as immunoglobulin (Ig) E levels and an increase in circulating eosinophils. It has been demonstrated that the eggs produce IL-4 inducing factor (IPSE/alpha-1), which stimulates the expression of IL-4 and IL-13, which are considered to be important for induction of the Th2 response (Dunne et al., 1981; Schramm et al., 2006). Further, a major component of the soluble egg antigen (SEA), Omega-1, has been shown to be involved in Th2 polarisation of dendritic cells (Dunne et al., 1991; Dunne et al., 1981; Everts et al., 2009). The Th2 cytokine response peaks at week 8 post infection, correlating with the peak of granulomatous inflammation around the parasite egg, and decreases significantly after approximately 3 months post infection (Pearce and MacDonald, 2002).

The characteristic feature of *S.mansoni* infection is the development of granulomas around the trapped *S.mansoni* eggs which is orchestrated primarily by $CD4^+$ T cells, although $CD8^+$ T cells, B cells and M2 macrophages are also involved. The granulomas are composed of collagen fibres and cells including eosinophils, macrophages and $CD4^+$ T cells (Hams et al., 2013; Pearce and MacDonald, 2002). Although granulomas are pathogenic and contribute to the development of fibrosis they also serve a host-protective role (Pearce and MacDonald, 2002). In mice with depleted $CD4^+$ T cells an acute disease with striking mortality occurs, with the granuloma formation around the *S.mansoni* eggs being distorted (Fallon et al., 1998). As opposed to immunologically intact mice where eosinophil-rich granulomas are observed, the granulomas of $CD4^+$ T cell deficient mice are neutrophil-dominated. Further, the absence of the functional granuloma leads to hepatocyte damage (Dunne

et al., 1991; Hams et al., 2013). The role of Th2 cytokines on granuloma formation and *S.mansoni* pathology has been reported. It has been demonstrated that *S.mansoni* infection in IL-4 deficient mice causes pathology similar to acute schistosomiasis with significant hepatotoxicity and death (Brunet et al., 1997; Fallon et al., 2000). This is further exaggerated in the IL-10 and IL-4 double-deficient mice, demonstrating the importance of IL-10 in preventing the development of excessive Th1- and Th2-mediated pathologies (Hoffmann et al., 2000).

Fibrosis of the liver is the main pathology associated with *S.mansoni* infection and depends on the interaction of many factors. IL-13 is thought to be the dominant Th2 cytokine responsible for development of liver fibrosis (Pearce and MacDonald, 2002). The *S.mansoni* infection in IL-13 deficient mice or in mice where IL-13 is ineffective (IL-4 receptor α-chain – knockouts IL4Rα-/-) or neutralised by the treatment with the soluble IL-13Rα2-Fc, leads to down-modulation of granulomatous inflammation and prolonged survival (Chiaramonte et al., 1999; Fallon et al., 2000; Jankovic et al., 1999). In addition, it has been shown that IL-13 directly induces the synthesis of collagen type I, III and V in fibroblasts and stimulates collagen synthesis in hepatic stellate cells (HSCs), which are recognised as the main producer of extracellular matrix (ECM) components (Wynn et al., 2004). In HSCs, IL-13 which binds to IL-13Rα1 activates JAK/STAT6 signalling pathway leading to liver fibrosis (de Jesus et al., 2004). IL-13Rα2 is a negative regulator of IL-13 and was shown to reduce the volume of granulomas in the liver and reduction of liver fibrosis (Mentink-Kane et al., 2004). Importantly, Kavirante et al., showed that fibrosis related genes such as collagens, MMPs (MMP-2, MMP-9, MMP-13 and TIMP-1 were upregulated in TGF-β1 -/- mice in response to IL-13 treatment providing evidence that fibrosis induced by *S.mansoni* infection is IL-13 dependent but TGF-β1 independent (Kaviratne et al., 2004).

1.1.3 Diagnosis of schistosomiasis

Early diagnosis of schistosomiasis is important to prevent associated pathology. Schistosomiasis can be diagnosed using parasitological (qualitative sedimentation method, Kato-Katz method), histopathological (rectum biopsy), serological (antigen

and antibody detection) and molecular (PCR) methods reviewed in (Gomes et al., 2014). Microscopic examination of stool or urine (e.g. Kato-Katz or ether-concentration techniques used for diagnosis of *S.mansoni*) are gold standard tests for diagnosis of schistosomiasis (Glinz et al., 2010). These techniques are simple, inexpensive and 100% specific, however they have poor sensitivity in detecting low-intensity infections, are unable to detect pre-patent or single sex infection and fail to detect infection in individuals where eggs are trapped in tissues and are not excreted (Stothard et al., 2011). Antibody-based assays are useful for diagnosis in specific circumstances such as in individuals who excrete eggs less efficiently (e.g. individuals with HIV-1 (Karanja et al., 1998)) or have low egg burden, but they cannot differentiate past and active infection and can also cross-react with antigens from other helminths (Doenhoff et al., 2004). Recent studies have shown success with point-of-care tests for *Schistosoma* circulating cathodic and anodic antigens (CCA and CAA, respectively) in serum and urine, which decrease rapidly after chemotherapy (Coulibaly et al., 2013; Shane et al., 2011; Sousa-Figueiredo et al., 2013; Stothard et al., 2011; van Dam et al., 1996; van Lieshout et al., 1993) and these are now being further developed for use in the field (van Dam et al., 2013). Specific and highly sensitive PCR based assays for the detection of schistosome DNA in urine and stool samples or plasma have been recently developed and offer yet another strategy for diagnosis of infection (Enk et al., 2012; Ibironke et al., 2011; Lodh et al., 2013; Pontes et al., 2003a; Wichmann et al., 2009).

Better methods for diagnosing schistosomiasis are important for patient management, evaluation of treatment efficiency, monitoring of disease transmission and success of control strategies as emphasized recently by the World Health Organization (WHO) (WHO, 2008, 2013b).

1.2 miRNAs- Background

With the completion of the Human Genome Project it has been discovered that protein-coding sequences account for only ~1.1% of the entire genome (Venter et al., 2001). The advancement in microarray and next generation sequencing technologies revealed that the ‘dark matter” of the human genome encodes multiple classes of

non-coding RNAs (ncRNAs) including: ribosomal RNAs (rRNAs), transfer RNAs (tRNAs), small nucleolar RNAs (snoRNAs), small nuclear RNAs (snRNAs), small interfering RNAs (siRNAs), piwi-interacting RNAs (piRNAs), microRNAs (miRNAs), long non-coding RNAs (lncRNAs), unusually small RNAs (usRNA) or enhancer transcribed RNAs (eRNAs). This thesis focuses primarily on miRNAs but also touches on small RNAs derived from tRNAs.

MicroRNAs (miRNAs) are short (19-24 nt), single-stranded RNAs that are known to negatively regulate gene expression at the post-transcriptional level. The very first miRNA, lin-4, was discovered in the nematode *Caenorhabditis elegans* in the labs of Victor Ambros and Gary Ruvkun in 1993 who studied the timing of larval development in *C.elegans* (Lee et al., 1993; Wightman et al., 1993). They showed that the *lin-4* gene did not encode a protein but gave rise to two small RNA transcripts of 22 and 61 nt. They further showed that lin-4 acts by negatively regulating the level of lin-14 mRNA via an antisense interaction with the 3' untranslated region (UTR) of lin-14 mRNA (Lee et al., 1993; Wightman et al., 1993). Seven years later, a second miRNA, let-7, was identified in *C.elegans*. Reinhart and colleagues showed that this 21nt long RNA is required for transition of the larval stage to an adult (Reinhart et al., 2000). Soon after this, let-7 was found to be conserved in other animals, including mammals (Pasquinelli et al., 2000). Subsequently, hundreds of miRNA were identified and an online miRNA database - miRBase was established to facilitate classification of miRNAs (available at: http://www.mirbase.org). To date (June 2014), 30,424 mature miRNAs in 206 species have been registered in the miRBase version 20 including 2578 in *Homo sapiens*. Each of these is predicted to target hundreds of mRNAs (Bartel, 2009). Given the vast scope for combinatorial regulation of targets, it is difficult to find a cellular pathway that is not regulated at some level by a miRNA. Indeed, the majority of protein-coding genes contain miRNA binding sites under selective pressure (Friedman et al., 2009) and mis-expression of miRNAs is associated with many disease processes, encompassing all cancers, as well as metabolic, cardiovascular, neuronal and immune-related diseases (Chang and Mendell, 2007).

1.2.1 Biogenesis

The biogenesis of miRNAs involves two consecutive steps: processing of the pri-miRNA in the nucleus followed by pre-miRNA maturation in the cytoplasm (Fig 1.3).

miRNA Transcription

miRNAs are transcribed in the nucleus from the exons and introns of protein-coding genes or transcribed from "intergenic" regions of the genome by RNA polymerase II (RNA Pol II), although some miRNAs are transcribed by RNA polymerase III. Generated primary miRNA (pri-miRNA) is of 1000-3000 bases long (Borchert et al., 2006; Cai et al., 2004; Han et al., 2006; Lee et al., 2004). The pri-miRNAs generated by RNA Pol II have a 7-methylguanosine cap (m^7Gppp) on the 5' end and poly(A) tail on the 3' end (Cai et al., 2004). The pri-miRNA is cleaved to form 60-70 nt long pre-miRNAs. The cleavage is executed in the nucleus by RNase III enzyme Drosha which interacts with the dsRNA-binding protein, DiGeorge Syndrome Critical Region 8 Protein (named DGCR8 in mammals and Pasha in *D. melanogaster* and *C. elegans*) to form a microprocessor complex (Denli et al., 2004; Gregory et al., 2004; Han et al., 2004; Landthaler et al., 2004; Lee et al., 2003; Lee et al., 2002). Independent transcription units within exons, introns and intergenic regions can carry monocystronic miRNAs, dicistronic miRNAs or polycistronic miRNA clusters that are transcribed from the same promoter (Lee et al., 2004) or can be transcribed independently of each other by using overlapping genomic regions (Song and Wang, 2008). miRNAs that are processed in a Drosha-DGCR8 independent manner have also been described in mammals, *D.melanogaster* and *C.elegans*, and named mitrons (Berezikov et al., 2007; Okamura et al., 2007; Ruby et al., 2007). The nuclear transport receptor Exportin 5 (XPO5) in complex with Ran-GTP recognises the 3' overhang of the pre-miRNA and exports it from the nucleus to the cytoplasm (Bohnsack et al., 2004; Lund et al., 2004; Yi et al., 2003).

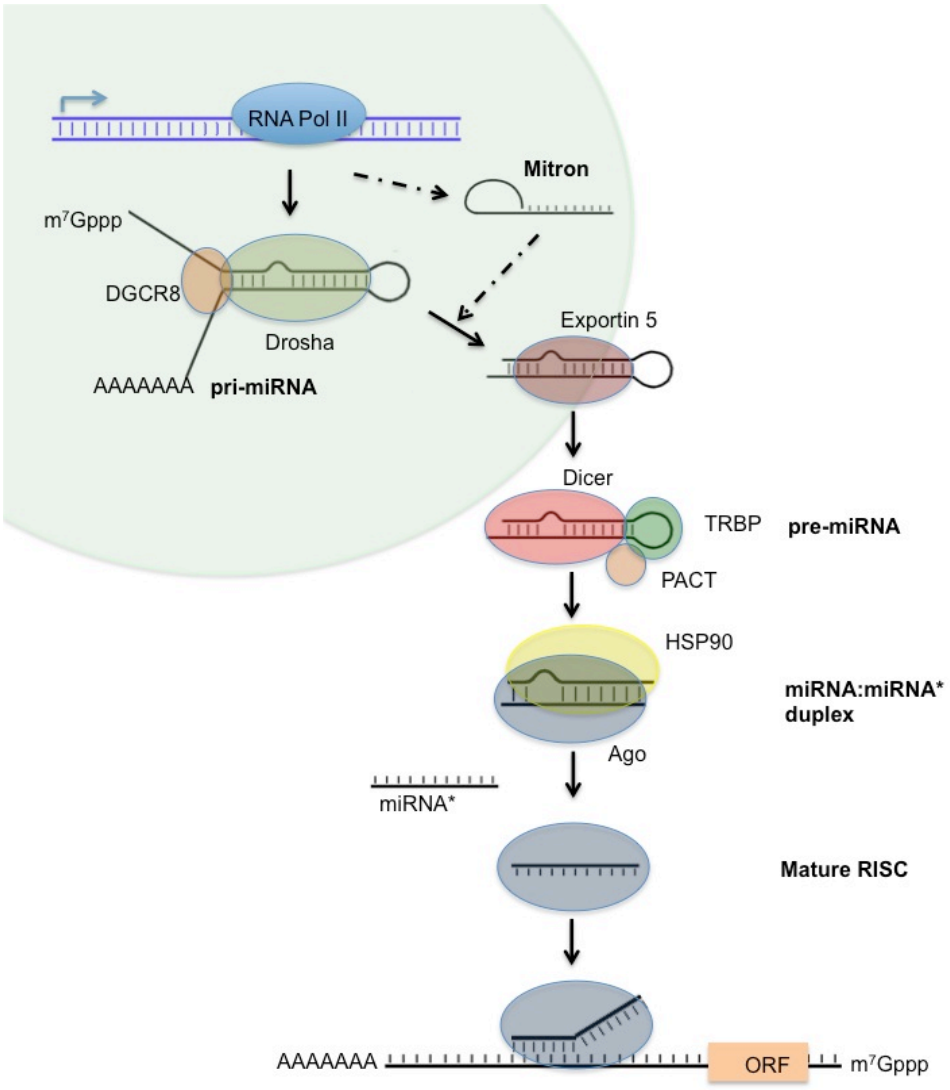

Figure 1.3 miRNA biogenesis.
The pri-miRNA is generated by RNA Pol II. Drosha interacts with DGCR8 to form a microprocessor complex and cleaves pri-miRNA to form the 60-70nt pre-miRNAs. miRNAs that are processed in Drosha-DGCR8 independent manner have been described in mammals, *D. melanogaster* and *C. elegans*, and named mitrons. The nuclear transport receptor Exportin 5 exports pre-miRNA from the nucleus to the cytoplasm. Dicer interacts with TRBP and PACT, cleaves off the loop of the pre-miRNA and generates a ~22 nt long miRNA:miRNA* duplex. The double-stranded miRNA:miRNA* duplex is separated into the functional 'guide' strand that is preferentially loaded into Ago protein and becomes the mature miRNA, and the 'passenger' miRNA* strand. The guide strand is incorporated into the RISC complex and binds to mRNAs at specific sites with base-pair complementarity to the miRNA. This figure is adapted from a figure available at http://commons.wikimedia.org/wiki/File:MiRNA-biogenesis.jpg

miRNA Maturation and RISC assembly

In the cytoplasm RNase III enzyme Dicer cleaves off the loop of the pre-miRNA and generates a ~22 nt long miRNA:miRNA* duplex with a 2nt overhang at the 3' end (Grishok et al., 2001; Hutvagner et al., 2001; Ketting et al., 2001; Zhang et al., 2004). Although most miRNAs are processed by Dicer, Dicer-independent processing has also been described. For example, in zebrafish a 39 nt long pre-miR-451 is too short to be recognised by Dicer and it is loaded directly into RNA-induced silencing complex (RISC) and processed by the Argonaute 2 (Ago2) protein (Cheloufi et al., 2010; Cifuentes et al., 2010; Yang et al., 2010). Similarly to Drosha, Dicer acts as part of a larger complex. In mammals Dicer interacts with transactivation-response RNA-binding protein (TRBP, also known as TRBP2) and protein kinase R-activating protein (PACT, also known as PRKRA) (Chendrimada et al., 2005; Haase et al., 2005; Lee et al., 2006; Perron and Provost, 2008). It has been shown that TRBP and PACT are not essential for Dicer-mediated cleavage but TRBP facilitates Dicers' stability and acts as a sensor for the thermodynamic asymmetry within an miRNA duplex and together with PACT participates in the recruitment of Argonaute 2 (Ago 2) protein to the RISC loading complex (RLC) (Chendrimada et al., 2005; Diederichs and Haber, 2007; Lee et al., 2006).

After the Dicer cleavage, the double-stranded miRNA:miRNA* duplex is separated into the functional 'guide' strand (with the less stable base pair at its 5' end) that is preferentially loaded into Ago protein and becomes the mature miRNA, and the 'passenger' strand (Khvorova et al., 2003; Schwarz et al., 2003). The transfer of the miRNA duplex to Ago is facilitated by Heat Shock Protein 90 (HSP-90). Four Ago (Ago1-4) proteins are found in humans (Burroughs et al., 2011). Structural studies revealed that Ago proteins are characterized by amino-terminal (N), PAZ (PIWI-ARGONAUTE-ZWILLE), MID (middle) and PIWI domains (Elkayam et al., 2012; Schirle and MacRae, 2012; Song et al., 2004). The PAZ domain anchors the 3' end, and the MID domain anchors the 5' end of the miRNA, whereas the N domain mediates miRNA loading and unwinding of the miRNA:miRNA* duplex (Jinek and Doudna, 2009; Lingel et al., 2004). All four Agos can bind miRNA but Ago2 is the

only catalytic Ago protein in mammals and is capable of cleaving target mRNA strands that are perfectly complementary to the mature miRNA (Liu et al., 2004; Meister et al., 2004).

The guide strand incorporated into the RISC complex binds to messenger RNAs (mRNAs) at specific sites with base-pair complementarity to the miRNA (Lee et al., 1993). Most miRNAs bind to 3' UTR of mRNA via the 'seed' region, which is located at position 2-7 nt or 2-8 nt of the 5' end of the miRNA (canonical seed match) (Brennecke et al., 2005; Doench and Sharp, 2004; Krek et al., 2005; Lewis et al., 2003). The interaction between a miRNA and the 5'UTR or coding sequences (CDS) of mRNAs have also been show (Zhou et al., 2009). Pairing between the 3' UTR and miRNA at position 13 to 16 of the miRNA ('supplementary' base pairing) can reduce the off rate of RISC from the target RNA and improve target inhibition. It has also been shown that pairing at the 3' end of miRNA and 3'UTR can compensate for mismatch in the seed and is called compensatory pairing (Grimson et al., 2007; Wee et al., 2012). Furthermore, other features such as: i) presence of adenosine across from the first base of a miRNA, ii) the position of the target site within 3' UTR or iii) sequence motifs within miRNA, can affect miRNA binding to its target mRNA (Grimson et al., 2007; Lewis et al., 2005; Obernosterer et al., 2008; Tafer et al., 2008). The interactions of the miRNA and mRNA within RISC leads to destabilization of the mRNA and/or inhibition of translation, resulting in decreased levels of the protein (Bartel, 2009). The passenger strand is often degraded although recent reports show that it can play a role in miRNA homeostasis and gene regulation (Mah et al., 2010).

1.2.2 Mechanism of action

Studies have shown that miRNAs regulate gene expression post-transcriptionally; however, the mechanism of miRNA- mediated repression or activation of gene expression remains controversial. There are two main mechanisms of miRNA-mediate regulation of target mRNAs: translation repression and mRNA degradation (Ameres and Zamore, 2013; Gu and Kay, 2010; Huntzinger and Izaurralde, 2011).

miRNA-mediated direct endonucleolytic cleavage of fully complementary mRNA by Ago occurs between nucleotide 10 and 11, opposite the miRNA strand. This mode of target regulation is common in plants but rarely occurs in animals (Llave et al., 2002; Yekta et al., 2004). Rather, in animals targets are not perfectly complementary and mRNA degradation occurs through the 5'-to-3' decay pathway (Fig 1.4). In this pathway the mRNA poly (A) tail is removed by deadenylases which is followed by decapping and degradation by exonuclease XRN1 in the 5'-to-3' direction (Carthew and Sontheimer, 2009; Eulalio et al., 2008; Filipowicz et al., 2008).

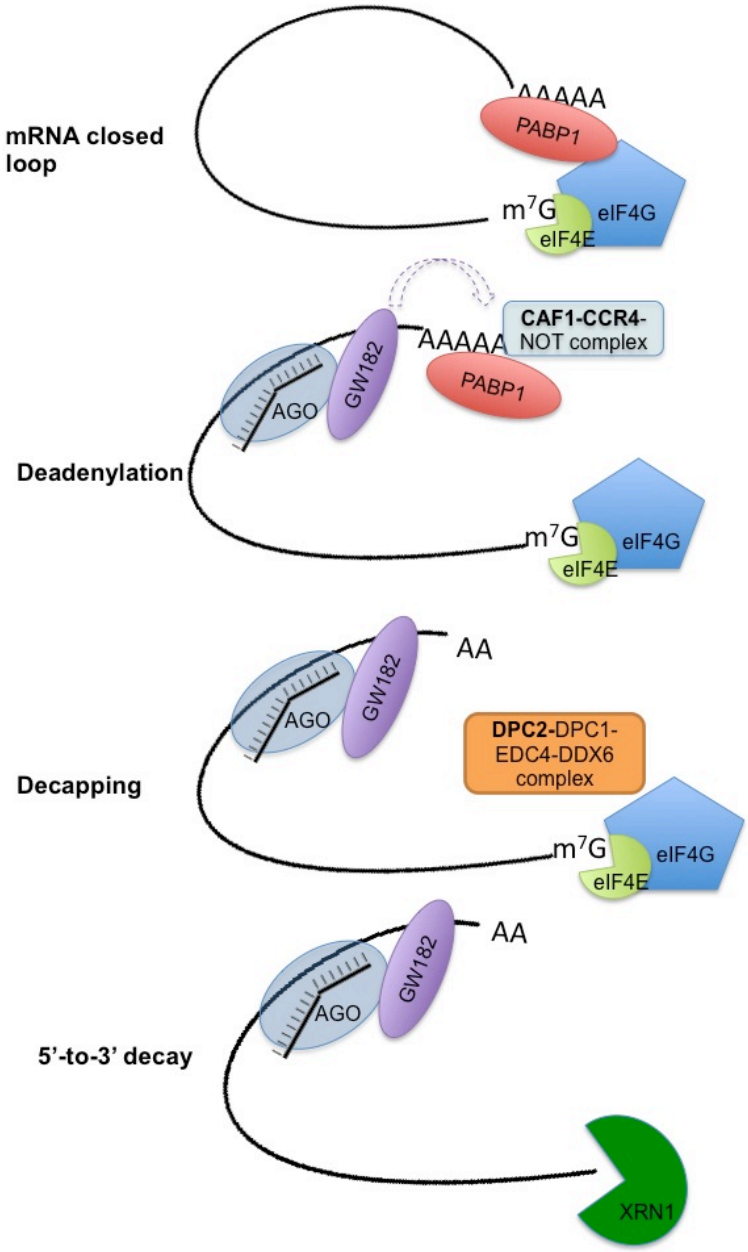

Figure 1.4 Mechanism of miRNA-mediated gene silencing
A closed loop confirmation of a target mRNA is a result of interaction between PABP1 which binds to 3' poly (A) tail and eIF4G, which is bound to the cap binding protein- eIF4E. miRNA- Ago complex recognizes the partially complementary site of the target mRNA by base-pairing. Ago interacts with GW182, which interacts with PABPC and recruits CAF1-CCR4-NOT; mRNA poly (A) tail is removed by deadenylases. The removal of the mRNA 5' cap is catalysed by a decapping enzyme DCP2, which requires association with DCP1, DDX6 and EDC4 for its full activity and stability. This is followed by mRNA degradation by exonuclease XRN1 in the 5'-to-3' manner.

mRNA deadenylation requires CAF1-CCR4-NOT1 and, to a lesser extent, PAN2-PAN3 deadenylase complexes which are recruited through interaction with GW182 protein (Bagga et al., 2005; Behm-Ansmant et al., 2006; Braun et al., 2011; Fabian et al., 2011; Kuzuoglu-Ozturk et al., 2012; Rehwinkel et al., 2005; Wu et al., 2006). The removal of the mRNA 5' cap is catalysed by a decapping enzyme DCP2 which requires association with decapping activators for its full activity and stability (Eulalio et al., 2007; Haas et al., 2010; Nishihara et al., 2013; Rehwinkel et al., 2005). Recent studies have shown that miRNA-RISC complex recruit the decapping activators onto mRNA which is independent of deadenylation (Fabian and Sonenberg, 2012)

Next-generation sequencing and ribosome profiling data have revealed that the decrease in protein level observed in miRNA-mediated regulation of mRNA is primarily due to mRNA decay and only in 11-16% of cases derives from translational inhibition (Guo et al., 2010). Recent studies investigated whether the initiation and post-initiation mechanism of mRNA regulation are mutually exclusive and whether target deadenylation and degradation occurs as a consequence of the translation inhibition. Djuranovic et al., have shown that in Drosophila S2 cells mRNAs are first subject to translational inhibition, followed by deadenylation and decay (Djuranovic et al., 2012). Moreover, it has been shown that in mammalian cell lines translation repression is the dominant effect of miRNA on its target and precedes deadenylation and decay (Bethune et al., 2012). mRNA translation consists of three steps: initiation, elongation and termination. The initiation of translation begins with the recognition and binding of the 5'-terminal 7-methylguanosine (m^7G) cap by eukaryotic translation initiation factor complex eIF4F which is composed of eIF4E (binds mRNA cap), eIF4G (a scaffold for the assembly of translation initiation factor complex) and eIF4A (an RNA helicase). eIF4G together with eIF3 facilitate the recruitment of ribosomal subunit 40S (Kapp and Lorsch, 2004; Merrick, 2004). eIF4G also interacts with the poly(A)-binding protein 1 (PABP1) which leads to circularisation of mRNA (Derry et al., 2006; Wells et al., 1998). With 60S ribosomal subunit joining at the AUG codon the elongation phase begins. Studies demonstrated that miRNA-RISC inhibit translation initiation via interaction with eIF4F and

PABP1 (Fabian et al., 2009; Mathonnet et al., 2007; Zekri et al., 2009). Further, miRNA-RISC complex can repress elongation via promoting dissociation of ribosome from mRNA or prevent association between small and large ribosomal subunit (Fabian et al., 2009; Petersen et al., 2006; Zekri et al., 2009).

Some miRNAs have also been linked to translational activation. Liver specific miR-122 has been shown to bind to complementary sites within the 5' UTR of the hepatitis C virus RNA and stimulate HCV RNA accumulation and translation (Henke et al., 2008; Jopling et al., 2005). Another example of direct activation of gene expression has been shown following G1/G0 cell-cycle arrest. In serum starved cells, but not in the proliferating cells, miR-369-3p binds to 3' UTR of tumour necrosis factor α (TNFα) mRNA and promotes translation (Vasudevan et al., 2007). Translation activation has also been observed in response to stress or amino acid starvation. In these specific conditions, miR-10a binds to 5' UTR of ribosomal protein mRNAs and promotes their translation (Orom et al., 2008).

Although the mechanism of miRNA-mediated gene expression is still a matter of debate, it is generally accepted that the majority of miRNAs act as 'fine tuners' of the expression of most targets. However, recent works propose that mRNA targets can act as competitive inhibitors 'sponges' of miRNA and therefore affect the concentration of miRNAs (Ebert et al., 2007; Ebert and Sharp, 2010; Hansen et al., 2013). This adds another layer of complexity to the miRNA-mediated post-transcriptional regulation of targets.

1.3 miRNAs in human disease

It has been shown that miRNAs play important roles in development, apoptosis, proliferation, differentiation, organ development, host-pathogen interactions and that altered miRNA expression is related with the development of multiple diseases including liver disease.

1.3.1 Liver fibrosis

The liver is the largest organ in the human body receiving 25% of the total blood supply. It performs the essential functions of carbohydrate metabolism, lipid metabolism, protein metabolism, bile acid synthesis, vitamin D activation, drug and hormone inactivation as well as immunological surveillance. Fulminant hepatic failure (i.e. abrupt cessation of liver function) without transplantation leads to death, demonstrating the essential role of this organ in the maintenance of life (Kumar, 2000).

Hepatic fibrosis is one of the most serious problems of human health. The main causes of liver fibrosis are: alcohol and drug abuse, chronic viral hepatitis, non-alcoholic fatty liver disease, schistosomiasis, autoimmune and congenital metabolic diseases. The ongoing inflammatory stimulus associated with these aetiologies results in fibrotic changes in which normal parenchymal tissue is replaced with connective tissue in order to slow or remove the occurring tissue damage. This wound-healing process of tissue remodelling, when uncontrolled, causes significant scarring and dysfunction of the liver and it is known as cirrhosis (Bataller and Brenner, 2005; Hernandez-Gea and Friedman, 2011; Pellicoro et al., 2014).

Hepatic fibrosis is associated with significant changes in the extracellular matrix (ECM) composition which is a result of increased synthesis of collagens, fibronectin, elastin, laminin, hyaluronan, proteoglycans and undulin, and simultaneous decreased activity of ECM-degrading matrix metalloproteinases (MMPs) and overexpression of their inhibitors, tissue inhibitors of matrix metalloproteinases (TIMPs) (Arthur, 2000; Friedman, 2008; Sato et al., 2003). Various cell types, growth factors, cytokines and enzymes are involved in the process of fibrogenesis, but hepatic stellate cells (HSCs) (Ito cells, fat-storing cells) are the main producer of ECM components and are thought to be the key cell type responsible for fibrogenesis (Friedman, 2008). In a normal liver these vitamin A storing cells reside in a subendothelial space, between the anti-luminal site of sinusoidal endothelial cells and the basolateral surface of hepatocytes and account for ~15% of all resident cells (Friedman, 2008). Upon liver injury, HSCs undergo activation or transdifferentiation from quiescent to a

"myofibroblast-like" phenotype (aHSCs) and migrate to the site of tissue repair where they secrete excessive ECM components, which have been shown to play a role in development of liver fibrosis (Bartley et al., 2006; Chang et al., 2006; Kresina et al., 1994). Activated HSCs express myogenic markers (α smooth muscle actin (α-SMA), c-myb, myocyte enhancer factor-2 (MEF-2)) of which α-SMA is the most reliable marker of HSCs activation as it is not expressed by any other liver cell type in either normal or injured liver (Friedman, 2008). The balance between MMPs and their inhibitors, TIMPs, play a significant role in the ECM remodelling, and therefore, fibrosis progression and resolution. MMPs are calcium-dependent enzymes that degrade collagens and noncollagenous substrates including: collagenases (MMP-1,-8,-13, -18), gelatinases (MMP-2, -9), stromelysins (MMP-3,-10,-11), matrylisins (MMP-7,-26) metalloelastase (MMP-12) and membrane type-MMPs (MMP-14, -15, -16, -17, -24, -25) and others. The inactivation of MMPs activity occurs by binding to their inhibitors TIMPs (Nagase et al., 2006). Interestingly, Madala et al., demonstrated a regulatory role between MMP-12 and EMC-degrading MMPs upon *S.mansoni* infection. Specifically, they showed that upon *S.mansoni* infection, mice-deficient in MMP-12 display higher level of MMP-2 and MMP-13 expression and significant reduction in liver fibrosis, suggesting that MMP-12 acts as an inducer of fibrosis by limiting the expression of MMP-2 and MMP-13 Further, the absence of MMP-12 leads to reduction of IL-13 decoy receptor, IL-13Rα2, providing explanation for the increase in IL-13- driven MMP-13 levels and reduction in fibrosis (Madala et al., 2010).

Despite the rapid progress in understanding the pathology of liver fibrosis and attempts to develop serum-based biomarkers, biopsy of the liver is still regarded as a 'gold standard' for accurate confirmation of the severity and type of liver disease. More importantly, there is no treatment for liver cirrhosis other than transplantation which is effective but very expensive and limited by donation from matched living donors or cadavers (Bal *et al*., 2009; Rockey, 2008), emphasizing the importance of investigating the molecular basis of fibrogenesis and development of better diagnostic and therapeutic tools.

1.3.2 miRNA in liver fibrosis

Dysregulation of miRNA in liver fibrosis

Studies have shown that miRNAs are implicated in the progression and resolution of liver fibrosis and regulation of the activation, proliferation and apoptosis of HSCs. The miRNA profile has been shown to be altered upon liver fibrosis caused by different etiologies. miR-122, a liver specific miRNA that accounts for more than 70% of all miRNA in hepatocytes (Jopling, 2012; Jopling et al., 2005), has been reported to be down regulated in liver injury and fibrosis induced by chronic hepatitis C (HCV) infection or non-alcoholic fatty liver disease (NAFLD) (Cheung et al., 2008; Marquez et al., 2010; Trebicka et al., 2013). This is thought to be due to the down-regulation of transcription factors: hepatocyte nuclear factor (HNF) 1 and HNF4, which control miR-122 gene expression (Coulouarn et al., 2009). miR-125b and miR-22 which are also expressed in the liver at a high level have been shown to be reduced in liver biopsies of patients with chronic HCV. Other miRNAs, such as the members of the miR-29 family, miR-150, miR-194, miR-19b are also down-regulated during fibrogenesis (Kwiecinski et al., 2012; Lakner et al., 2012; Roderburg et al., 2011). miR-29 family members, specifically miR-29a and miR-29b, were found to be down-regulated in experimental models of liver fibrosis as a result of intoxication or cholestasis and the levels of miR-29c has been show to be increased in the mouse model of the dietary non-alcoholic steatohepatitis (NASH) (Bandyopadhyay et al., 2011; Pogribny et al., 2010; Roderburg et al., 2011). A few miRNAs such as the members of the miR-199/200 family, miR-221/222 family and miR-34 family and miR-21 are up-regulated during liver fibrosis induced by different etiologies including HCV infection, NASH and alcoholic steatohepatits (ASH) as well as in animal models of liver fibrosis such as carbon tetrachloride (CCL4) intoxication, and a fat diet mouse model (Meng et al., 2012; Murakami et al., 2011; Ogawa et al., 2012; Pogribny et al., 2010; Ramachandran et al., 2013). In mice treated with dimethylnitrosamine (DMN), the levels of miR-34, miR-199/200, miR-221/222 family members, miR-146b, miR-214, miR-199-5p, miR-199-3p, miR-223 and miR-324-5p are increased and correlate with progression of liver fibrosis in rats (Li et al., 2011a).

HSCs regulation by miRNAs

Recent reports have shown that miRNAs are implicated in the activation, migration, proliferation and apoptosis of HSCs (Table 1.1) based on the finding that miRNAs are dysregulated during these processes.

Among the pro-fibrotic miRNAs identified are miR-15/16, miR-21, miR-33a and miR-181b. miR-15/16 has been shown to be down-regulated in the HSCs and regulates proliferation and apoptosis by targeting mitochondrial associated anti-apoptotic protein B-cell lymphoma-2 (BCL-2) and cyclin D 1 (CCND1) (Guo et al., 2009a; Guo et al., 2009b). miR-181b is elevated in HSCs activated by TGF- β1 and promotes HSC proliferation *in vitro* by targeting the cell cycle regulator p27 and cell cycle progression by increasing the number of S phase cells.

In addition, miR-181 is also elevated in serum of patients with liver cirrhosis (Wang et al., 2012a). miR-221/222 expression is increased in the HSCs activated by nuclear factor kappa B (NF-kB) and correlates with the expression of COL1A1 and αSMA mRNA expression (Ogawa et al., 2012). Wei et al., demonstrated that upon stimulation of the human HSC cell line LX2 with platelet-derived growth factor (PDGF)-BB, the levels of miR-21 increase. Further analysis revealed that miR-21 regulates the activation of HSCs via the PTEN/Act pathway. Recent work has shown that miR-21 is up-regulated in the human cirrhotic livers and in mouse liver fibrosis induced by CCL4 and thioacetamide intoxication and maintains its high levels by using a miRNA-21/programmed cell death protein 4/activation protein-1 (miR-21/PDCD4/AP-1) autoregulatory feedback loop and promotes TGF-β signalling pathway thus influencing activation of HSCs and driving fibrosis progression (Wei et al., 2013; Zhang et al., 2013). miR-33a has been shown to be up-regulated in TGF-β1 induced HSCs. The inhibition of this miRNA *in vitro* leads to decrease in activation of HSCs and ECM production at least in part via activation of the PI3K/AKT pathway and targeting peroxisome proliferator activated receptor-alpha (PPAR-α)(Li et al., 2014b).

Table 1.1 miRNAs involved in HSCs regulation.

Up	Down	Effect	Target	Putative Role in HSC/ Fibrosis	Reference
	miR-15b	-	Reporter assay (BCL-2)	Apoptosis	Guo et al., 2009
	miR-16	-	Reporter assay (BCL-2)	Apoptosis	Guo et al., 2009
	miR-29	+	Reporter gene assays (COL1a1, COL4, PDGF-C, IGF-I)	Cell activation, ECM synthesis	Ogawa et al., 2010, Roderburg et al., 2011, Sekiya et al., 2011, Kwiecinski et al., 2011, Kwiecinski et al., 2012
	miR-150	+	Target protein change (c-MYB, SP1, COL4A4)	Cell activation, Cell proliferation	Venugopal et al.2010, Zheng et al., 2013
	miR-146a	+	Reporter gene assays (SMAD4)	TGF-β signaling	He et al., 2012
	miR-194	+	Target protein change (RAC-1)	Cell activation, Cell proliferation	Venugopal et al.2010
	miR-126	+	Reporter gene assay (VEGFA)	Cell proliferation	Guo et al., 2013
	miR-122	+	Target mRNA changes (P4HA1)	Collagen production, Cell proliferation	Li et al., 2013
	miR-19b	+	Reporter gene assays (TGF-βRII)	TGF-β signaling	Lankner et al., 2012
	miR-195	+	Reporter gene assays (CCNE1)	Cell proliferation	Sekiya et al., 2011
	miR-335	+	Target mRNA changes (TNC)	Cell activation and migration	Chen et al., 2011
	miR-34a		Reporter gene assay (ACSL1)	Lipids biosynthesis	Li et al., 2011a
	miR-483-5p/3p	+	Reporter gene assay (PDGFβ, TIMP2)	Cell activation	Li et al., 2014a
	miR-101a	+	Reporter gene assay (TβRI, KLF6)	Cell activation, migration, proliferation	Tu et al., 2014
miR-21		+	Target protein changes (PTEN)	PTEN/Akt pathway	Wei et al., 2013
miR-221/222		+	Reporter gene assay (CDKN1B)	Cell activation	Ogawa et al., 2012
miR-181b		+	Reporter gene assay (CDNK1B)	Cell proliferation	Wang et al., 2012
miR-27a/b		-	Reporter assay (RXR-α)	Fat metabolism, proliferation	Ji et al., 2009
miR-33a		-	Target protein change (PPAR-α)	Cell activation, EMC synthesis	Li et al.,2014b

+ indicates pro-fibrotic and – anti-fibrotic effect of miRNA

Several miRNA such as: miR-27a/b, miR-29, miR-150, mir-146, miR-126, miR-122, miR-19b, miR-195, miR-335, miR-34, miR-483 and miR-101a have been demonstrated to have anti-fibrotic properties. Transforming growth factor-beta1 (TGF-β1) is thought to be the main stimulating factor in the HCS activation and plays an important role in liver fibrosis. Tu et al., (2014) showed that miR-101 is significantly down-regulated in liver fibrosis induced by CCL4 intoxication and that it acts as a suppressor of TGFβ signaling by targeting TGFβ receptor I (TβRI) and its transcriptional activator Kruppel-like factor 6 (KLF6) during liver fibrogenesis (Tu et al., 2014). They demonstrated that in HSCs, overexpression of miR-101 led to reduction of COL1A1, aSMA and TIMP-1, affecting activation, proliferation and migration of HSCs. Moreover, miR-101 could efficiently inhibit the TGF-β-induced TGF-β1, PDGF, CTGF, TIMP-1 and collagen I productions in hepatocytes (Tu et al., 2014). In addition to miR-101's effect on TGF-β, miR-19b was shown to inhibit TGF-β signalling through targeting TGF-β receptor II (TGF-βRII) which resulted in decrease in collagen type I mRNA level and inhibition of HSCs activation (Lakner et al., 2012).

Several miRNAs have been shown to play a role in activation, proliferation and migration of HSCs. miR-146a expression is down-regulated in HSCs in response to TGF-β1 stimulation and in liver fibrosis induced by CCL4 intoxication. The overexpression of miR-146a in HSCs leads to inhibition of cell activation and proliferation and induced apoptosis (He et al., 2012a). miR-483-5p/3p, which is also down-regulated in the CCL4-induced liver fibrosis in mice, has been reported to supress the TGF-β1 induced activation of human HSCs cell line LX2 via targeting platelet-derived growth factor-β (PDGF-β) and TIMP-2 and inhibit liver fibrosis in mice (Li et al., 2014a). miR-335 has been reported to influence the activity and migration of HSCs, at least in part, via targeting extracellular matrix glycoprotein tenascin-C (TNC) (Chen et al., 2011a).

MiRNAs altered in HSCs have been shown to influence accumulation of ECM components. miR-29 family members (miR-29a/b/c) have been demonstrated to be down-regulated in activated HSCs during liver fibrosis due to profibrotic stimulation

by TGF-β and PDGF-BB (Kwiecinski et al., 2011; Ogawa et al., 2010). It was reported that miR-29 is an effective inhibitor of collagen I via targeting COL1A1 (Ogawa et al., 2010; Roderburg et al., 2011). Further, Sekiya et al., demonstrated that overexpression of miR-29b led to inhibition of COL1A1 and COL1A2 mRNAs and reduced expression of α-SMA, DDR2, FN1, ITGB1, and PDGFR-β, which are key genes involved in the activation of HSCs (Sekiya et al., 2011b). Kwiecinski et al., reported recently that apart form regulating ECM accumulation, miR-29a and miR-29b target insulin-like growth factor (IGF)-I and platelet-derived growth factor (PDGF)-C and thus interfere with the profibrotic cell communication (Kwiecinski et al., 2012). miR-126* is significantly down-regulated during activation of HSCs. The *in vivo* and *in vitro* studies have shown that overexpression of miR-126* lead to induction of G0/G1 phase arrest in aHSCs, partially by regulating the VEDF-A/PI3K/AKT/CCND1 pathway and interplays with VEGF-A/Ca2+ pathway which leads to inhibition of ECM accumulation and contraction of HSCs, respectively (Guo et al., 2013). miR-150 and miR-194 are down-regulated in HSCs isolated from fibrotic rats. Overexpression of these miRNAs in the HSC cell line LX2 lead to inhibition of cell proliferation and activation and inhibition of ECM production which, at least in part, occurs via targeting c-MYB (miR-150) and RAC1 (miR-194) (Venugopal et al., 2010). Further, Zheng et al., revealed that miR-150 affects collagen type I and IV synthesis via targeting Sp1, a mediator of α-1 (I) collagen (Col1A1) expression, and Col4A4 (Zheng et al., 2013). Liver specific miR-122 has been shown to influence collagen maturation and ECM production in HSCs *in vitro* by targeting prolyl 4-hydroxylase subunit alpha-1 (P4HA1) (Li et al., 2013).

Sekiya et al., showed that miR-195 is significantly down-regulated in mouse primary HSCs. The treatment of HSCs with IFN-β, which is know to have an antifibrotic effect in the liver independent of its antiviral effect, induced miR-195 expression and inhibited HSCs (LX2) proliferation by delaying G1 to S phase of the cell cycle, partially by inhibition of miR-195 target cyclin E1 (CNE1). These results revealed a new mechanistic aspect of the antifibrotic effect of INFs in the liver fibrosis (Sekiya et al., 2011a).

The importance of miRNAs in activation and proliferation of HSCs has been underscored by studies showing the inhibition of Dicer, a key enzyme in miRNA biogenesis pathway. Inhibition of Dicer *in vitro* in HSCs resulted in decreased levels of miR-138, miR-143, miR-140 and miR-122, of which miR-138 showed the biggest reduction. Further, it reduced expression of fibrosis-related genes such as COL1A1 and TIMPs on mRNA and protein level and reduced the proliferation rate of HSCs (Yu et al., 2014).

1.3.3 miRNA therapeutics

The fact that miRNAs have the ability to function as gene regulators potentially makes them good therapeutic candidates. Studies of miRNA profile and role in fibrogenesis allow translating this knowledge into clinical applications including development of novel diagnostics and anti-fibrotic therapeutics. In recent years, extensive work has been carried out to develop miRNA-based therapies (Bennett and Swayze, 2010; Bumcrot et al., 2006; Wahid et al., 2010).

Depending on the function of miRNA candidate and its expression level in the abnormal tissue, two strategies have been used: miRNA antagonists and miRNA mimics (Pottier et al., 2014). In cases where the miRNAs are up-regulated in the diseased tissue (e.g. pro-fibrotic miRNAs), miRNA antagonists can be used to inhibit their expression. These chemically modified anti-sense miRNA oligonucleotides (e.g. anti-miRs, antagomirs or lock nucleic acid (LNA), tiny LNA) bind irreversibly to the miRNA of interest and block interaction with its targets. The main drawback of this strategy is that miRNA antagonist can bind to other complementary RNAs and thereby lead to side effects. In cases where the miRNA is down-regulated (e.g. anti-fibrotic miRNAs) miRNA mimics are used to restore the miRNA levels (Pottier et al., 2014).

The activity of the first miRNA antagonist was examined *in vivo* in 2004. Hutvagner et al., have shown that in *C.elegans* injection of the 2'-*O*-methyl oligonucleotide complementary to the miRNA *let-7* can induce a *let-7* loss-of-function phenocopy (Hutvagner et al., 2004). A year later, Krutzfield et al., demonstrated that intravenous

administration of miR-16, miR-122, miR-192 and miR-94 antagomirs led to the inhibition of corresponding miRNAs in various tissues including liver, lung, kidney, heart, intestine, fat, skin, bone marrow, muscle, ovaries and adrenals (Krutzfeldt et al., 2005). The therapeutic potential of miR-122 in treatment of HCV infection has been initially addressed by Lanford and colleagues. They found that treatment of HCV infected chimpanzees with an LNA-modified oligonucleotide complementary to miR-122 has a long-lasting anti-viral effect without induction of side effects. The inhibition of miR-122 resulted in the de-repression of miR-122 mRNA targets, down-regulation of IFN genes and improvement in liver pathology (Lanford et al., 2010). The recent results of a phase 2a clinical trial show that subcutaneous administration of miR-122 antagonist (miravirsen) to patient with HCV genotype 1 resulted in the dose-dependant reduction in HCV RNA levels without evidence for viral resistance (Santaris Pharma; ClinicalTrials.gov number, NCT01200420) (Janssen et al., 2013). The therapeutic effects of miRNA mimics have also been examined *in vivo*. The intravenous administration of miR-34a mimic to mice with non-small cell lung cancer (NSCLC) showed a significant reduction in tumour growth without induction of an immune response (Wiggins et al., 2010). Further works on the applicability of miR-34a mimic as therapeutic agents are now taking place. A clinical phase 1 trial examining the effect of MRX34 (mimic of miR-34) in treatment of primary liver cancer, advanced or metastatic cancer were initiated in May 2013 (ClinicalTrials.gov Identifier: NCT01829971).

Many miRNAs have been identified as potential targets for development of treatment for liver fibrosis (He et al., 2012b; Szabo and Bala, 2013; Vettori et al., 2012). Several pre-clinical studies were conducted to develop miRNA-based therapeutics and test their efficacy in various animal models of disease. Importantly, recent successes of phase 1 and 2 clinical trials suggest that miRNA-based therapeutics will become important medical tools in the near future. However, before they can be brought to the clinic, several challenges need to be overcome including specific delivery to the diseased tissue or organ and targeting the exact pathway responsible for the disease. Additional questions also need to be answered, including whether the

inhibition of miRNAs in chronic disease will have a clinical effect (Pottier et al., 2014).

1.4 Small RNAs in extracellular environment

In 1948 Mandel and Métais described extracellular nucleic acids in human blood for the first time (Mandel and Metais, 1948); however it was not until 1970s that the attention was put back on the significance of cell-free RNA. In 1972, Kolodny et al., showed that RNA can be secreted by normal and transformed fibroblasts to their culture media (Kolodny, 1971, 1972) and a few years later Stroun et al., further demonstrated the presence of highly methylated, small in size (sedimenting between 2.5 to 4S) RNA, released by two different cell types, normal human lymphocytes and frog auricles, into the cell culture media through a process not associated with cell death (Stroun et al., 1978). A range of reports in the 1960s also suggested that RNA from one tissue (e.g. liver) could induce tissue-specific expression in another cell type (Niu et al., 1962), although the mechanisms of such import were never described. The recent discovery of RNA encapsulation within extracellular vesicles (Valadi et al., 2007) is consistent with some of these earlier studies and provides a base for conceptualizing RNA transport in mammals.

In 2007 Valadi et al., reported the first evidence of miRNAs outside the cell. They showed that exosomes secreted by mast cell lines contain both mRNA and miRNA (Valadi et al., 2007). Moreover, several reports in 2008 demonstrated that miRNAs are present in a cell-free form in human and mouse serum based on small RNA sequencing and/or RT-PCR analysis (Chen et al., 2008b; Lawrie et al., 2008; Mitchell et al., 2008). Since then, miRNA have been shown to be present in various body fluids including serum, plasma, saliva, tears, urine, amniotic fluid, colostrum, breast milk, bronchial lavage, cerebrospinal fluid, peritoneal fluid, pleural fluid, and seminal fluid (Weber et al., 2010).

Analyses of small RNA content in bodily fluids has been largely focused on miRNAs, given their tissue-specific expression, the precedence for their differential expression in disease, and their diagnostic potential (Calin and Croce, 2006).

However, an increasing number of reports suggest that other classes of small RNAs can also play a variety of roles in gene regulation. For example, tRNAs can be processed into small RNA fragments that associate with Argonaute (Ago) proteins and can silence genes, reviewed in (Tuck and Tollervey, 2011). Semenov et al., showed that 3' end fragments of rRNAs and tRNAs are detectable in human milk (Semenov et al., 2004). Appaiah et al., also reported up regulation of U6 RNA in the sera of cancer patients (this study was originally focused on miRNA content and analysis of U6 expression was included for purposes of normalization) (Appaiah et al., 2011). It is possible, therefore, that various small RNAs exist in an extracellular form that may be of diagnostic or biological interest.

1.4.1 Stability of extracellular RNA

miRNAs have been shown in various body fluids including serum and plasma, yet, the blood of a healthy human contains high levels of stable ribonucleases: the concentrations of RNases in human serum or plasma are estimated at several hundred ng/mL, and can be elevated in cancer patients, which could degrade exogenous RNA within seconds (Blank and Dekker, 1981; Kamm and Smith, 1972). The surprising fact that cell-free RNA can be therefore detected in RNase rich environment has been examined in various studies. Tsui et al., showed that synthetic RNA is degraded in less than 5 sec when incubated with human plasma, but they found that RNAs present in serum and plasma are stable at 4°C for at least 24 h and the concentration of endogenous RNA in serum is not affected by freezing-thawing (Tsui et al., 2002). Further studies (prior to analysis of miRNAs) have confirmed this apparent stability of RNA: El-Hefnawy et al., showed that plasma RNA is stable for at least 3 h at room temperature and that neither RNase H, RNase A/T or DNase affect RNA concentration in plasma. They have also reported that the addition of detergents (Triton-X or SDS) to the sample significantly reduced 18S rRNA levels quantified by qRT-PCR suggesting that extracellular RNAs are protected by proteins (El-Hefnawy et al., 2004), arguing against the possibility that mRNA is stabilized by association with DNA as suggested previously by (Stroun et al., 1978). A range of reports have shown similar results with miRNAs, and have gone on to test the stability of miRNA in serum and plasma under extreme conditions including

incubation for long periods at room temperature, multiple cycles of freeze-thawing, exposure to boiling and different pH solution treatments (Chen et al., 2008b; Li et al., 2011b; Mitchell et al., 2008). These and other investigations suggest that a large component of the RNA found in fluids is extremely stable. The observation that pre-treatment of serum or plasma with detergents (e.g. Triton-X or SDS) makes mRNAs susceptible to degradation by RNases (El-Hefnawy et al., 2004; Tsui et al., 2002), and miRNAs secreted from human monocyte cell line derived from an acute monocytic leukemia patients (THP-1) similarly lose protection following treatment with detergents (Zhang et al., 2010b) led to suggestion that stability of miRNAs is related to their natural encapsulation in vesicles or proteins (Ng et al., 2002).

miRNA encapsulated within vesicles

Cell-derived membrane vesicles are secreted by many, if not all, cell types and have been detected in body fluids through density sedimentation, electron microscopy and analysis of specific markers on their surfaces. Due to a lack of precise nomenclature, many terms are used in literature to describe extracellular vesicles, including microparticles, microvesicles, exosomes, and membrane particles; here we refer to exosomes, apoptotic bodies and shedding microvesicles as defined in a recent review (Gyorgy et al., 2011). The term exosome is used to describe vesicles ~ 40-100 nm in diameter, of endocytic origin, derived from multivesicular bodies (MVB) that fuse with the plasma membrane (Stoorvogel et al., 2002). Shedding microvesicles are ~ 100-1000 nm in diameter and derive directly from cell membranes by budding. Apoptotic bodies are ~ 50-5000 nm in diameter and are membranous vesicles shed from the plasma membranes of dying/apoptotic cells via blebbing. A description of the biogenesis and distinguishing features of these vesicles is summarized in (Gyorgy et al., 2011). Of interest is the fact that RNA has been shown to be associated with vesicles (Fig 1.5). In 2007, Valadi et al., showed for the first time that exosomes derived from mouse and human mast cell lines (MC/p and HMC-1 respectively) contain, apart from mRNA, small RNA including miRNA. They have shown that RNA is encapsulated in vesicles and is resistant to RNase treatment (Valadi et al., 2007). Interestingly Valadi et al., and others, observed that levels of

specific miRNAs are enriched in vesicles in relation to the pool of intracellular small RNA (Pigati et al., 2010; Valadi et al., 2007). This specificity implies function, and secreted small RNAs provide one media for cell-to-cell communication.

Cell-to-cell communication

It is know that cell-to-cell communication occurs through secreted growth factors, cytokines, hormones and chemokines, direct cell contact or cell synapses. Given the findings of miRNAs in exosomes, miRNAs are also considered as a mediator of cell-to-cell communication.

For example, Zhang et al., showed that miR-150 is selectively packaged into exosomes secreted by THP-1 cells, which can be taken up by human microvascular endothelial HMEC-1 cells. Increased concentrations of miR-150 in HMEC-1 cells leads to down-regulation of miR-150 targets, including the transcription factor c-MYB, resulting in enhanced cell migration (Zhang et al., 2010b). In a study carried out by Kosaka et al., it has been shown that tumour suppressive miR-146a can be transferred from COS-7 or HEK293 cells to recipient COS-7 cells. The analysis also showed that an addition of media from cells transfected with pri-miR-146a can suppress miR-146a target, ROCK1, in recipient tumour cells and result in tumour cell growth inhibition (Kosaka et al., 2010c). Functional RNA transfer also occurs via apoptotic bodies. miR-126 is the most abundant miRNA in endothelial-derived apoptotic bodies generated during atherosclerosis and can be transferred and taken up by recipient vascular cells. Using a variety of controls, including apoptotic bodies from cells derived from miR-126-/- mice, Zernecke et al., demonstrated that the uptake of miR-126 is responsible for the down regulation of its target, RGS16, an inhibitor of a G-protein-coupled receptor. Regulation of RGS16 by miR-126 leads to an increase in CXCL12, which causes mobilization of progenitor cells and incorporation into plaques, conferring protective effects in diet-induced atherosclerosis (Aad et al., 2014; Zernecke et al., 2009). A range of cell-to-cell communication associated with immune and neuronal signalling as well as tissue repair was reviewed in (Thery, 2011). Although it seems that the RNA within vesicles could play a wide range of functional roles within recipient cells, the actual

mechanisms by which RNAs are selectively packaged into different vesicles remain unknown. Gibbings et al., demonstrated that exosomes secreted from monocytes contain components of the RISC machinery, including Argonaute 2 (Ago2) and GW182, which co-migrate with endosomal-MVB fractions in density gradients (Gibbings et al., 2009). Lee et al., found that silencing miRNA-RISC activity is enhanced when MVB turnover is impaired and MVBs positively regulate RISC loading (Lee et al., 2009a). However, there is no experimental support for a mechanism whereby specific miRNAs are loaded into MVBs for secretion; nor is it known how specificity is achieved in apoptotic bodies and shedding microvesicles.

miRNA –protein complexes

Several reports suggest that a substantial fraction of extracellular miRNA is not encapsulated within vesicles but is stabilized by association with proteins. Wang et al., showed that miRNAs secreted by A549 and HepG2 cells associate with RNA binding protein nucleophosmin (NPM1), a multifunctional histone binding protein known to be involved in a number of processes including the nuclear export of the ribosome (Wang et al., 2011). Arroyo et al., applied differential centrifugation and size exclusion chromatography to show that the majority of plasma miRNAs (~90%) are present as Ago2-miRNA complexes and not contained within vesicles. They further showed that these miRNAs become susceptible to degradation following proteinase-K treatment of plasma (Arroyo et al., 2011). Similar observations were made by Turchinovich et al., who showed that the majority of miRNAs found in human plasma, as well as those secreted from the MCF7 breast cancer cell line, are associated with Ago2 but exist in a form that is < 300 kDa (Turchinovich et al., 2011). The authors suggested that the high proportion of miRNA-Ago may represent by-products of dead cells, since Ago-miRNA complexes within cells are known to be extremely stable. However, Ago2 is also present within exosomes (Gibbings et al., 2009; Zhang et al., 2010b) and it may be that some of the Ago2-RNA complexes identified derive from vesicles, potentially damaged during purification. Another study has shown that specific miRNAs are complexed to high-density lipoprotein

(HDL) in serum, and this also protects miRNAs from degradation and mediates transport into recipient cells (Vickers et al., 2011).

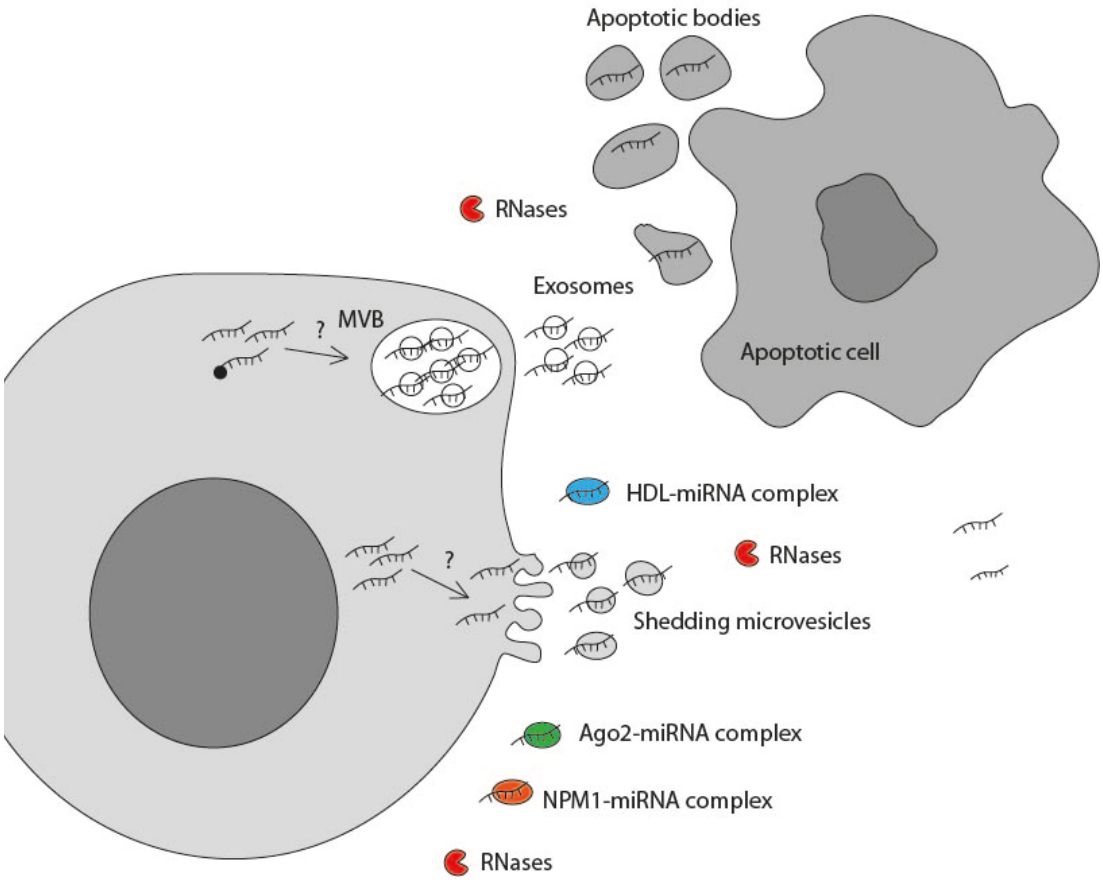

Figure 1.5 Extracellular miRNAs: vesicles and protein complexes.
Extracellular miRNAs are protected from degradation by RNases through encapsulation within exosomes, shedding microvesicles and apoptotic cells. They have also been identified in smaller molecular weight complexes bound to Ago2 or NPM1 proteins or HDL (Hoy and Buck, 2012).

The mechanisms controlling which export/import pathways are active in a cell are unknown. However, it has been reported that exosome release is blocked by inhibiting neutral sphingomyelinase 2 (nSMase2), an enzyme involved in ceramide biosynthesis (Kosaka et al., 2010b). Interestingly, inhibition of nSMase 2 actually increases the export of miRNAs by HDL (Vickers et al., 2011), suggesting distinct mechanisms and/or competition in the export pathways. Further research is required to understand the mechanisms dictating specificity in secretion and uptake pathways. Nonetheless, the capacity to mimic and exploit these natural RNA transport vehicles, whether they be vesicles or protein co-factors, has exciting implications for therapeutic RNA delivery (Alvarez-Erviti et al., 2011).

1.4.2 Diagnostic potential of miRNAs

Given the tissue-specific expression of miRNAs, differential expression in disease, and their presence in blood, extensive interest has been directed towards development of miRNA-based diagnostics. Tissue injury appears to be one pathological state where differential expression of specific miRNAs can be detected in blood. Wang et al., demonstrated that the liver-specific miRNA, miR-122, is elevated 500-fold in mouse plasma following liver injury by acetaminophen overdose (Wang et al., 2009). Others have also reported increases in miR-122 levels in human serum following liver damage induced by acetaminophen (Starkey Lewis et al., 2011) or hepatitis B infection (Zhang et al., 2010a). Differential expression of extracellular miRNAs is also associated with acute myocardial infarction (AMI). Cheng et al., reported a 200-fold increase in the level of miR-1 in serum in rat serum at 6 hours after acute myocardial infarction (AMI) (Cheng et al., 2010). They also observed a significant increase in miR-1 levels in serum taken from human patients within 24 hours of AMI. Whether miR-122 and miR-1 are released during cell death and/or there is specificity in the secretion of these miRNAs is unknown. Both of these miRNAs are highly abundant and tissue-specific (Liang et al., 2007); miR-1 in cardiac muscle and miR-122 in hepatocytes. These features may reflect their utility as biomarkers, where a high signal-to-noise must be obtained within an environment where the noise could derive from the many cell types and tissues releasing or secreting miRNAs (Hunter et al., 2008).

Beyond tissue injury, numerous reports have detailed miRNA changes in serum or plasma associated with different cancers, reviewed in (Cortez et al., 2011). As a proof-of-concept that tumour-associated miRNAs can enter circulation, Mitchell et al., used a mouse xenograph model with human prostate cancer cells expressing human-specific miRNAs (miR-629* and miR-660) to demonstrate that these tumour-derived miRNAs are detected in mouse plasma (Mitchell et al., 2008). They also reported an increase expression of miR-141 (46-fold on average) in serum of patients with prostate cancer and reported 60% sensitivity and 100% specificity in detecting individuals with cancer. Ironically, miR-141 in human plasma was first reported in association with pregnancy: this miRNA is enriched in the placenta, increases in maternal plasma with gestational age and drops off significantly by 24 hours post delivery (Chim et al., 2008). Although technically prostate cancer and pregnancy would not be examined in the same individual, these examples highlight a problem in overlapping miRNA "biomarkers". Further understanding of the mechanism of miRNAs release or secretion by cells will help realise the full potential of these molecules as biomarkers.

1.5 Hypothesis and objectives of this thesis

It is estimated that *S.mansoni* affects more than 80 million people worldwide with mortality rate of around 130,000 per year (van der Werf et al., 2003). The infection leads to accumulation of the parasite eggs in the liver and consequently liver fibrosis and portal hypertension.

Diagnosis of schistosome infection is crucial for patient management, evaluation of treatment efficiency, monitoring of disease transmission and success of control strategies. Currently used diagnostic technics have a number of drawbacks. Microscopic techniques such as Kato-Katz or ether-concentration offer poor sensitivity in detecting low-intensity infections (for example, in children), are unable to detect pre-patent or single sex infection and fail to detect infection in individuals where eggs are trapped in tissues and not excreted. Available antibody-based assays are useful for diagnosis in some cases (e.g. foreign travellers) but they cannot differentiate past and active infection and can also cross-react with antigens from

other helminths. These assays therefore do not offer a definitive diagnosis in schistosome-endemic areas.

Further, liver fibrosis caused by various insults, including infection with *S.mansoni,* is an important health problems. There is no treatment for hepatic fibrosis/cirrhosis other than transplantation highlighting the importance of investigating the molecular basis of fibrogenesis towards developing better diagnostic and therapeutic tools.

miRNAs have been shown to be altered upon disease process including liver fibrosis and are present in body fluids in a stable form, suggesting that they can be used as novel diagnostic biomarkers. Moreover, their functional implication in the fibrogenesis indicates that they have a potential to be used as new therapeutic strategies for the treatment of liver fibrosis.

Given the health burden of *S.mansoni* infection and associated liver fibrosis we reasoned that it is important to understand the role of miRNA in the *S.mansoni* infection. We hypothesized that miRNAs:

i) are altered in the liver and serum upon *S.mansoni* infection
ii) play a role in progression and resolution of liver fibrosis.

The study presented in this thesis aimed to:

1) Examine the profile of host miRNA during *S.mansoni* infection in the liver and explore the potential of miRNA inhibitors in treatment of liver fibrosis.
2) Based on the profile in liver, select miRNA candidates that might represent serum biomarkers
3) Investigate the small RNA profile in serum upon *S.mansoni* infection and examine the diagnostic potential of additional circulating small RNAs.

Chapter 2: **Materials and Methods**

2.1 Animals

For miRNA array analysis of liver and Illumina sequencing of serum in experiment 1, 8-10 week old C57BL/6 mice were left uninfected or infected percutaneously with ~180 *S. mansoni* cercariae, weighed regularly, and euthanized 7 weeks post infection. For the 12-week time course, and Illumina sequencing of serum in experiment 2, 8-10 week old C57BL/6 mice were left uninfected or infected percutaneously with ~80 cercariae (this dose was specifically selected to minimise animal loss at later time points), weighed regularly and euthanized at 4, 6, 8 and 12 weeks post infection.

For the *in vivo* inhibition of miRNAs experiment 1 and 2, 8-10 week old C57BL/6 mice were left uninfected and were injected intravenously with PBS, Negative Inhibitor, miR-122 Inhibitor or miR-199-3p Inhibitor at 30mg/kg (experiment 1) or 60mg/kg dose (experiment 2) (100ul volume), as detailed in Chapter 3, section 3.3.3. For the *in vivo* inhibition of miRNAs experiment 3, 8-10 week old C57BL/6 mice were left uninfected or infected percutaneously with ~60 *S. mansoni* cercariae, and treated with either PBS, Negative Inhibitor, miR-122 Inhibitor or miR-199-3p Inhibitor at 50mg/kg as specified in the result section (Chapter 3, section 3.3.4). All mice were weighed regularly, and examined for any adverse effects.

For characterisation of tRNA-derived fragments, 8-10 week old C57BL/6 uninfected mice were used.

All mice were maintained under specific pathogen free conditions at the University of Edinburgh Animal Facilities. Animal experiments were conducted under a Project License granted by the Home Office (United Kingdom), reference 60/4104, in accordance with local guidelines and approved by the Ethical Review Committee of the University of Edinburgh.

2.2 *S.mansoni* infection in mice

S.mansoni cercariae were shed from infected *Biomphalaria glabrata* snails. 30-40 snails were transferred to a beaker containing pond water and left under a heat lamp for 50 min. After this time the snails were returned to their tanks and the pond water was poured to a 50 ml tube. A 200 µl sample of cercariae was placed on the gridded petri dish and an equal volume of Lugol's iodine solution was added. The cercariae were counted under a dissection microscope and an average of three samples was taken. Female 8-10 weeks old C57BL/6 mice were anesthetised with a mix of medatomidine (dormitory) and ketamine (vetalar) diluted in PBS (0.25 ml domitor and 0.19 ml vetalar mixed in 2.6 ml PBS (Sigma), injected 0.01 ml/g). The hair from the abdomen area was removed with clippers and wiped with water to remove hair. The animals were placed on the pre-warmed heat pad to help maintain body temperature during the procedure and a 1cm diameter stainless steel ring was secured over the shaved region of the abdomen with tape. 200 µl of cercarial water containing an appropriate amount of cercariae was placed into the ring and further 200 µl of pond water as added on the top. The animals were left for 30 min to allowed cercarial penetration. After this time the remaining water was removed from the animals and the animals were revived with atipamezol (antidesan) diluted in PBS (0.04 ml antidesan diluted in 0.96 ml PBS (Sigma), injected subcutaneously, 0.1ml per animal). Following infection animals were monitored and weighed regularly.

2.3 Intravenous tail vein injections

miRNA Inhibitors of miR-122, miR-199a-3p, and Negative Inhibitor- *C.elegans* cel-miR-67 were synthesised by ThermoFisher. These synthetic oligonucleotided are cholesterol conjugated to facilitate delivery to the liver. Further details regarding the structure of these molecules were not shared by ThermoFisher.

In experiment 1: female 8-10 weeks old C57BL/6 mice were injected intravenously via tail vein with 30 mg/kg of miR-122 Inhibitor (n=3) or cel-miR-67 (Negative Inhibitor –NI) (n=3) or with PBS (n=3) on day 1 and day 3 and livers were harvested on days 4 and 8 as outlined in Fig 3.5 A.

In experiment 2, female 8-10 weeks old C57BL/6 mice mice (n=3) were i.v. injected twice weekly (Monday and Thursday) with 50mg/kg dose of Inhibitors (miR-122 Inhibitor, miR-199a-3p Inhibitor. Negative Inhibitor) or PBS and tissue harvest was performed on week 4 (24h post last injection) as depicted in Fig 3.6A.

In experiment 3: female 8-10 week old C57/Bl6 mice were infected with ~60 cercariae or left uninfected (Day 0). Infected mice were divided into 4 experimental groups which on days 21, 28 and 35 post infection were injected intravenously with: Group 1 (iPBS) animals- 200µl of PBS, Group 2 (iNI): 60mg/kg of NI, Group 3 (i miR-122): 60 mg/kg of miR-122 Inhibitor, Group 4 (i miR-199-3p): 60mg/kg of miR-199a-3p Inhibitor. Uninfected animals were injected with 200 µl of PBS (nPBS). Liver tissues were harvested on day 49 post infection. Initially the harvest was planned for day 56, however as two of Group 3 mice died the experiment was terminated and organs were harvested on day 49 post infection. Experimental outline provided in Fig 3.7 A.

2.4 Collection of mouse blood, serum and plasma

Whole blood was drawn from mice by cardiac puncture. The needle was removed before emptying the syringe to avoid haemolysis. For serum, blood was collected to Eppendorf tubes and was allowed to sit for 1h at RT to clot. For plasma, blood was collected to EDTA containing tubes (BD Vacutainer K2EDTA), and kept on ice prior to further processing. Both serum and plasma were separated by centrifugation at 2500g for 15 min at 4°C, and the supernatants were collected into a new tubes and spun at 10,000g for 1 min to remove remaining cells. The resultant supernatants was transferred into new tubes and stored at –20°C prior to RNA extraction.

2.5 *S.mansoni* egg count

Harvested livers were weighed and digested in 4% potassium hydroxide buffer per gram of liver at 37°C overnight. 100 µl of liver digest was pipetted onto a gridded petri dish, eggs were counted and the number of eggs per gram (epg) of liver tissue was calculated.

2.6 Masson's trichrome staining of liver tissue

Paraffin embedded liver sections were stained with Masson's trichrome at the University of Edinburgh, Histology Service, QMRI. Briefly, slides were deparaffinized and rehydrated through xylene and gradient alcohol: 100% ethanol, 90% ethanol, 80% ethanol, 70% ethanol, 50% ethanol, and washed in deionized water. Slides were then transferred to 1% (v/v) picric acid for 30s and washed under running tap water to remove yellow colour from the sections. Slides were stained in Hematoxylin solution for 10-20 s and washed in running tap water. Next, slides were placed in Biebrich Scarlet-Acid Fuchsin for 3 min, rinsed in deionized water for 10s and placed in 50% Phosphomolybdic /50% Phosphotungstic acid solution for 5-10 min. Slides were stained in Aniline Blue solution for 5 min, rinsed briefly in distilled water and placed in 1% acetic acid solution for 2-5 min. Samples were dehydrated and mounted.

2.7 Human serum samples

2.7.1 Serum tRNA characterisation analysis

Human venous blood samples were obtained from healthy volunteers working at the University of Edinburgh, Ashworth Laboratories, King's Buildings. Blood was collected to RNnase free eppendor tubes or EDTA contained tubes (BD Vacutainer K2EDTA) and serum and plasma was separated as described in section 2.3 of this chapter. Written consent was obtained from each individual.

2.7.2 S.mansoni biomarker analysis

Samples kindly obtained form Laboratory of Dr F. Mutapi – The University of Edinburgh, and Laboratory of Prof. D. Dunne – Cambridge University

Human samples were obtained from schistosome endemic areas in Zimbabwe and Uganda. Chiredzi (Zimbabwe) participants were comprised of five 'egg positive' individuals with an average egg per gram in stool (epg) = 108, range: 39-277 and nine 'egg-negative' individuals. According to the WHO's classification, Zimbabwe has high to moderate levels of *S. haemobium* infection (prevalence ranging from 10%

to greater than 70%) but low *S. mansoni* prevalence (less than 10%). The study group included in this investigation was part of a larger study on the molecular immunoepidemiology of human schistosomiasis and had not been included in the National Schistosome Control Programme and therefore had not received treatment for schistosomiasis or other helminth infections. After collection of all samples, all participants were offered anti-helminthic treatment with the recommended dose of praziquantel (40 mg/kg of body weight). Pidda (Uganda) participants comprised twenty individuals infected with *S. mansoni* with an average epg=1117 (range: 105-4030) and ten egg-negative individuals. The study group included in this investigation were part of a larger study carried out in Butiaba village, adjacent to Lake Albert, Masindi district, Uganda (Kabatereine et al., 1999). The cohort had moderate to high *S. mansoni* infection intensities and prevalence of 91%. After collection of stool and serum samples all the study participants, irrespective of the infection status, received 2 doses of praziquantel, 40 mg/kg of body weight, 6 weeks apart. Efficacy of chemotherapy was assessed 6 weeks after each treatment.

For the human serum samples collected in Chiredzi, permission to conduct the work in this province was obtained from the Provincial Medical Director. Ethical approval was received from the Medical Research Council of Zimbabwe (MRCZ). Only compliant participants were recruited into the study and they were free to drop out at any point during the study. At the beginning of the study, participants and their parents/guardians (in case of children) had the aims and procedures of the project explained fully in the local language, Shona, and oral consent (as was customary) was obtained from participants and parents/guardian before parasitology and blood samples were obtained. For the samples collected in Pidda, ethical clearance was obtained from the Uganda National Council of Science and Technology (ethics committee for Vector Control Division, Ugandan Ministry of Health). The aims and procedures were explained to the local community at the start of the study and oral consent was obtained from all adults and from the parents/legal guardians of all children under 15 who were willing to participate. Oral informed consent was obtained because of the high levels of illiteracy and cultural reasons, approved by the MRCZ or ethics committee for Vector Control Division, Ugandan Ministry of

Health. Upon oral consent participants were enrolled in the study with a written record of their name, age, sex and case number, this served as both the record of oral consent and enrolment record.

2.8 Parasitology and human serum sample collection and processing- biomarker analysis

Analysis carried out by Dr Norman Nausch (Laboratory of Dr F. Mutapi) and Frances Jones (Laboratory of Prof. D. Dunne)

Participants in the Zimbabwe study were checked for both urogenital and intestinal schistosomiasis and for inclusion in this analysis had to be free of any soil-transmitted helminths and also free of *S. haematobium* infection to avoid cross reactivity between different helminth parasites. For the analysis of urogenital schistosome infection (*S. haematobium)* participants submitted three urine and three stool samples (over four consecutive days). 10 ml of each sample received was processed on the day of collection by a urine filtration method (Mott, 1983). Stool samples were prepared and examined on the day of collection using the Kato-Katz faecal smear for detection of *S. mansoni* eggs and soil transmitted helminths (Katz et al., 1972). A single slide for microscopic examination was prepared from each urine and stool sample. Serum was prepared from 10ml venous blood collected from study participants, frozen at -20°C and afterwards stored at -80°C. Samples were transported frozen to Edinburgh and stored at -80°C prior to serological assays. Participants in the Ugandan study had duplicate 50 mg Kato-Katz slides prepared from 3 consecutive stool samples for detection of *S. mansoni* eggs, expressed as mean epg. Serum was prepared from 10ml venous blood samples, frozen at -20°C and transported to Cambridge for storage at -80°C prior to serological assays.

2.9 Mouse Serum RNA extraction

For the 12-week time course experiment and tRNA characterisation experiments, total RNA was extracted from serum (or plasma) using the miRVana PARIS extraction kit (Ambion), according to the manufacturer's protocol. In brief, 100µl of serum (or plasma) was thawed on ice, mixed with an equal volume of 2x Denaturing

Solution and kept on ice for 10 min. Samples were extracted with an equal volume of acid-phenol chloroform, vortexed for 30s and centrifuged for 10 min at 10,000 g at RT. The aqueous phase was mixed with 1.25 volumes of 100% ethanol and added to the mirVana PARIS column. The column was washed and RNA eluted in 100µl of 0.1 mM EDTA. RNA samples were stored at –20°C prior to further analysis. Extracted RNA was quantified by Qubit (Invitrogen).

2.10 Human Serum RNA extraction

For the tRNA characteristic experiments, total serum (or plasma) RNA was extracted using miRVana PARIS extraction kit (Ambion), according to the manufacturer's protocol. For the biomarker analysis experiments, due to small volumes and low amounts of RNA in available human serum samples the extraction protocol was adjusted to result in more concentrated RNA. To do this, 50μl of serum was thawed on ice, mixed with 50μl of ddH_2O and 100μl of 2x Denaturing Solution (as supplied in the miRVana Paris kit) and kept on ice for 10 min. Samples were spiked with 10fmoles of a synthetic RNA, Spike1: 5'-UGCUGAAUGCGUAGCUAUAAGC-3' (IDT) and extracted with an equal volume of acid-phenol chloroform, vortexed for 30s and centrifuged for 10 min at 10,000g at RT. The aqueous phase was mixed with 1/10 volume of 3M sodium acetate, 10μg of GlycoBlue (Ambion) and an equal volume of isopropanol. Samples were allowed to precipitate overnight at –20°C and were then centrifuged at >10,000g at 4°C. Pellets were washed twice with 75% ethanol, air-dried and then resuspended in 25μl of 0.1mM EDTA. The total RNA concentration was below the limit of detection based on Qubit (Invitrogen).

2.11 Mouse tissue and cells RNA extraction

Liver, spleen, heart, kidney, lung tissue was immersed in RNA Later Solution (Ambion) overnight at 4˚C prior to extraction. Blood RBC and PBMCs were separated using Ficoll-Paque Preminum (GE Healthcare) according to the manufacturer protocol. RNA was extracted using TRIzol Reagent (Invitrogen) according to the manufacturer's protocol. RNA was quantified by NanoDrop and

integrity assessed by 10% PAGE or Bioanalyzer 2100. All RNA samples used in the microarray analysis had RIN > 8.

2.12 Reverse Transcription & PCR

2.12.1 miRNA & tRNA fragments

In the biomarker analysis experiments, for reverse transcription of mouse serum samples, a fixed amount of extracted RNA (1.5 ng) was used as an input and 0.1 fmoles of a synthetic RNA, Spike2 5'-CGTATCGAGTGATGTCACGTA-3, was added at the RT step for normalization. For human serum samples, when the total RNA concentration was below the detection limit, a fixed volume of RNA (5 μl), corresponding to 10μl of extracted serum, was used as the input and Spike1 5'-TGCTGAATGCGTAGCTATAAGC-3' (added at the time of purification) was used for normalization. In tRNA characterisation studies a fixed volume of RNA (5 μl) corresponding to 5 μl of extracted serum was used as the input and cel-miR-39 synthetic RNA, added at the time of purification was used for normalization. For reverse transcription of RNA extracted from liver, 200ng of total RNA was used in each reaction. Reverse transcription reactions were performed using the miScript System (Qiagen) according to the manufacturer's protocol (Fig. 2.1), containing 0.5uL of miScript Reverse Transcriptase Mix, 2uL of 5x miScript RT Buffer, and appropriate amounts of RNase-free water and RNA in a total volume of 10μ. Samples were incubated for 60 min at 37ºC followed by 5 min at 95ºC and were kept at –20°C before proceeding to PCR.

PCR was carried out with SYBR green real-time PCR assays (Qiagen) and miScript primers to detect mouse and human miRNAs or tRNA fragments, according to the manufacturer's protocol (Qiagen) (Fig. 2.1). 0.5ul of cDNA (1:10 dilution) were used per sample in a total reaction volume of 5uL. The temperature profile used was as follows: pre-denaturation 15 min at 95°C and then 45 cycles of denaturation 15s at 94°C, annealing 30s at 55°C, elongation 30s at 70°C. Fluorescence data collection was performed at the end of each annealing step. All samples were tested in duplicates and nuclease free water was used as a non template control. Primers for *S. mansoni*-specific miRNAs, tRNA halves and the synthetic spikes were used at

200nM final concentration and were purchased from Invitrogen. Primers sequences are present in the Table 2.1. Primers for mouse and human miRNA were purchased from Qiagen. Data was collected on a Light Cycler 480 System (Roche). Two technical replicates were carried out for each biological replicate. Nuclease free water was used as a non-template control.

2.12.2 mRNA

SYBR green real-time PCR assays for the detection of mRNAs were performed using Light Cycler System (Roche) and 384-Well Reaction Plates (Roche). Primers for mRNA detection were designed using the Universal Probe Library Assay Design Center Roche software (available at (http://www.roche-applied-science.com) and purchased from Invitrogen. Primers sequences are present in Table 2.2. Reactions were performed using SYBR Green System (Roche) according to the manufacturer protocol. 0.5ul of cDNA (1:10 dilution) were used per sample in a total reaction volume of 5uL.

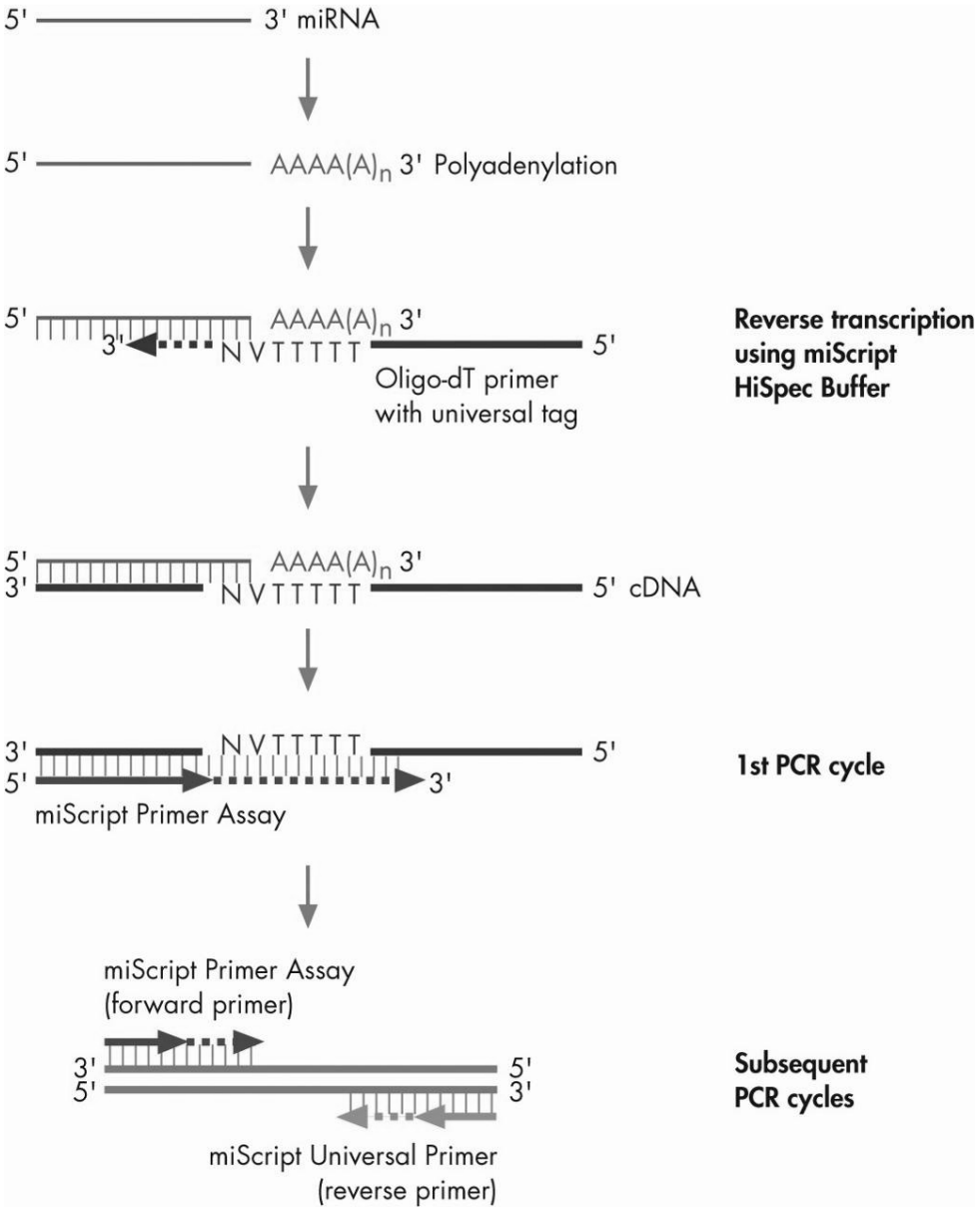

Figure 2.1 miScript qRT-PCR system.
During the reverse transcription step, RNA is polyadenylated by poly(A) polymerase and reverse transcribed by reverse transcriptase with oligo-dT primer which have a 3' degenerate anchor and a universal tag sequence on the 5' end allowing amplification of mature miRNA in the qPCR step. Generated cDNA is used as a template for qPCR using miScript Primer Assay and SYBR Green PCR Master Mix. The figure is from: http://www.qiagen.com/gb/resources/resourcedetail?id=7954ef25-3a39-4b0a-a27e-42689dbb4f5f&lang=en.

Table 2.1 List of miRNA primers.

Name	Sequence
miR-277	5'-TAAATGCATTTTCTGGCCCG-3'
miR-2162-3p	5'-TATTATGCAACGTTTCACTCT-3'
miR-3479-3p	5'-TATTGCACTAACCTTCGCCTTG-3'
bantam	5'- TGAGATCGCGATTAAAGCTGGT-3'
miR-2a-3p	5'-TCACAGCCAGTATTGATGAAC-3'
miR-71a-3p	5'- TGAAAGACGATGGTAGTGAGAT-3'
sma-miR-n1	5'-AACTCAGTGGCCTATCGGT-3'
sma-miR-n2	5'-TCAGCTGTGTTCATGTCTTCGA-3'
sma-miR-n3	5'- TGGCGCTTAGTAGAATGTCACCG-3'
5'tRNA^{Gly}(GCC)	5'-GCATTGGTGGTTCAGTGGTA-3'
3'tRNA^{Gly}(GCC)	5'-GATTCCCCGGCCAATG-3'
Spike1	5'-TGCTGAATGCGTAGCTATAAGC-3'
Spike2	5'-CGTATCGAGTGATGTCACGTA-3'
cel-miR-39	5'-TCACCGGGTGTAAATCAGC-3'
miR-21	5'- TAGCTTATCAGACTGATGTTGA-3'
miR-16	5'-TAGCAGCACGTAAATATTGGCG-3'
let-7a	5'-TGAGGTAGTAGGTTGTATAGTT-3'
miR-122	5'-TGGAGTGTGACAATGGTGTTTG-3'
miR-199-3p	5'-ACAGTAGTCTGCACATTGGTTA-3'
miR-199-5p	5'-CCCAGTGTTCAGACTACCTGTTC-3'
miR-210	5'-CTGTGCGTGTGACAGCGGCTGA-3'
miR-192	5'-CTGACCTATGAATTGACAGCC-3'
miR-194	5'-TGTAACAGCAACTCCATGTGGA-3'
miR-151-5p	5'-TCGAGGAGCTCACAGTCTAGT-3'
miR-365	5'-TAATGCCCCTAAAAATCCTTAT-3'
miR-9	5'-TCTTTGGTTATCTAGCTGTATGA-3'
miR-214	5'-ACAGCAGGCACAGACAGGCAGT-3'
miR-744	5'-TGCGGGGCTAGGGCTAACAGCA-3'

Table 2.2 List of mRNA primers.

Name	Sequence
ACTA2 F	5'-CTCTCTTCCAGCCATCTTTCAT-3'
ACTA2 R	5'-TATAGGTGGTTTCGTGGATGC-3'
COL1A2 F	5'-TGAAGTGGGTCTTCCAGGTC-3'
COL1A2 R	5'-GACCAGGCTCACCAACAAGT-3'
COL3A1 F	5'-GTCCACGAGGTGACAAAGGT-3'
COL3A1 R	5'-GATGCCCACTTGTTCCATCT-3'
MMP13 F	5'-ATCCTGGCCACCTTCTTCTT-3'
MMP13 R	5'-TTTCTCGGAGCCTGTCAACT-3'
MMP2 F	5'-TTTTTGTGCCCAAAGAAAGG-3'
MMP2 R	5'-GCCCTCCTAAGCCAGTCTCT-3'
TIMP1 F	5'-CGGAAATTTGCACATCAGTG-3'
TIMP1 R	5'-GTAGTCCTCAGAGCCCACGA-3'
TIMP2 F	5'-GACATCGAGGACCCGTAAGA-3'
TIMP2 R	5'-TGTCCCTCCAGACCCACTAC-3'
MMP9 F	5'-CACCACCACAACTGAACCAC-3'
MMP9 R	5'-CTCAGAAGAGCCCGCAGTAG-3'
FBN1 F	5'-GGACGGAAAGAACTGTGAAGAT-3'
FBN1 R	5'-ACACATTCCGTTTAGGCACA-3'
GAPDH F	5'-AGCCACATCGCTCAGACAC-3'
GAPDH R	5'-GCCCAATACGACCAAATCC -3'

The temperature profile used was as follows: pre-denaturation 5 min at 95°C and then 45 cycles of denaturation for 10s at 95°C, annealing 10s at 60°C, elongation 10s at 72°C. Fluorescence data collection was performed at the end of each elongation step. All samples were tested in duplicates and nuclease free water was used as a non-template control.

2.12.3 Generation of standard curve.

Synthetic single-stranded RNA oligonucleotides corresponding to the exact mature miRNA sequence for miR-16, miR-39, miR-21, miR-122 and miR-199-3p and tRNA halves: 5' $tRNA^{Gly}$(GCC) and 3' $tRNA^{Gly}$(GCC) were purchased from IDT. Synthetic RNAs were reverse transcribed using miScript System (Qiagen) and standard curves were generated for each miRNA/tRNA using dilution series of known input amount of the synthetic. The Ct values obtained was plotted against the logarithm of input number of copies of the synthetic molecule and a line was fitted, where Ct= a (Log copy number)+b (standard curve equation). The standard curves are shown in Appendix 1.

2.12.4 qRT-PCR Data Analysis

For analysis of miRNAs in liver samples, the relative fold change between naïve and infected samples was calculated using the $2^{-\Delta\Delta Ct}$ method (Livak and Schmittgen, 2001), normalized to miR-16. For serum miRNA data analysis, Ct values were "median-normalized" to synthetic RNA spike oligos as described previously (Mitchell et al., 2008): relative change was calculated as 2^{-Ctn}, where Ctn stands for normalized Ct values. For miRNA serum biomarker work, the sequences of used spike ins Spike 1 and Spike 2, did not match any known miRNA in miRBase and the primers for detecting these did not yield signals in serum by qRT-PCR, indicating that they do not cross-hybridize with mouse or human small RNAs. For tRNA quantification, cel-miR-39 spike in was used for normalisation purposes.

For analysis of host miRNA and tRNAs, fold change was calculated as the ratio of the relative change value of the sample compared to an average of the relative change values of naïve/uninfected samples. At each time point (4, 6, 8, 12 weeks

post infection), the calculated fold changes of each sample were plotted as naïve and infected. For parasite miRNA, the fold changes for all naive samples were plotted together – 'background' and fold change data for infected samples were plotted separately for each time point. For the cumulative analysis of miRNAs, the arithmetic mean of fold changes for miR-277, miR-3479-3p and bantam were used. For absolute quantification of miRNAs or tRNAs levels, Ct values were "median-normalized" to synthetic RNA spike oligos as described previously (Mitchell et al., 2008) and the copy number was calculated using Ctn= a (Log copy number)+b standard curve equation.

Statistical analysis of qRT-PCR data and receiver operator characteristic (ROC) curve analysis was performed with GraphPad Prism (Version 6) software. Two-way ANOVA followed by a Sidak multiple comparison test was used to calculate statistical differences for the mouse miRNA/tRNA halves time course data from serum and liver. For the parasite miRNA serum time course, one-way ANOVA followed by Holm-Sidak multiple comparison was used. For analysis of the human serum samples, the Mann-Whitney test was used and p-values of <0.05 were considered statistically significant.

2.13 miRNA Array

Samples were provided by Dr Rachel Lundie. Experimental work was carried out by Dr. Amy H. Buck, analysis were carried out by Mr Thorsten Forster. Dr Amy H Buck provided the protocol.

For the array analysis, 1 μg of total RNA was labelled using the Hy3 power labeling kit (Exiqon) and hybridized to codelink slides printed with the miRCury 8.1 probe set as described elsewhere (Ruckerl et al., 2012). Hybridization and washing were carried out following the manufacturer's protocols (Exiqon). Background signal was subtracted from foreground signal and data were transformed to log-2 scale. Between-array normalization was carried out using global array percentiles (matching median of each array); triplicate probes were represented by the median for each array. Empirical Bayes moderated t statistic (eBayes) was used to test the

null hypothesis of "no differential expression" between uninfected (n = 3) and infected (n=3) liver samples. Since this array was only used as a filter for further validation, the p values were not adjusted for multiple testing. The Exiqon 8.1 arrays contained 384 probes specific for mouse miRNAs.

2.14 Illumina Sequencing

For small RNA sequencing in experiment 1, total RNA was extracted from serum of 8 pooled *S. mansoni*-infected mice (Wk 7, 180 cercariae) and 8 uninfected age matched controls (400μl total volume) according to the miRVana PARIS protocol (as described above). The small RNAs were size selected by 15% PAGE and prepared according to the Illumina small RNA Sample Preparation Kit version 1.5 and sequenced on the GAIIX (Fig. 2.2.)For small RNA sequencing in experiment 2, total RNA was extracted from serum of 3 pooled *S. mansoni* infected mice (Wk 8, 80 cercariae) and 3 uninfected age matched controls (300μl total volume) was extracted according to the miRVana PARIS protocol. The library was prepared according to the TruSeq Small RNA protocol (without size-selecting small RNA) and sequenced on the HiSeq2 (Fig. 2.3). Both protocols are designed to enrich for RNA molecules with 5'-phosphate and a 3'-hydroxyl group. On that note, most RNA turnover and hydrolysis products generally carry a 5' hydroxyl group and a 2',3' cyclic phosphate or 2' or 3' monophosphate and these would not be present in the generated cDNA libraries.

Analysis were carried by Dr Alasdair Ivens and Dr Amy H. Buck. Dr Amy H Buck provided the protocol.

Raw reads were obtained in fastq format and 3' adapters trimmed using cutadapt, requiring at least a 6 bp match to the adapter sequence and a quality threshold of 20. Only reads that contained the adapter were retained; reads were subsequently collapsed on primary fasta sequence and those present in only one copy within a sample were discarded. Trimmed, collapsed reads ≥17 bp were then aligned to mouse (MM9) or *S. mansoni* genomes (V5.0) using BOWTIE version 0.12.5, requiring a perfect match to the full length of the sequence. Reads that mapped to

either genome were then BLASTN aligned against the RFAM database [BLASTN parameters: -max_target_seqs 1 -outfmt '6 std qseq sseq' -task blastn -word_size 6 -dust no] and categorized according to matches to Rfam class (e.g. rRNA, tRNA, etc.). Mouse reads without rfam similarities (other than miRNAs) were aligned to mature miRNAs in miRBase version 19. Some trimmed miRNA reads aligned to more than one family member: the assignment of these ambiguous reads is designated with "x" in Appendix 6. RNAs that aligned to the *S. mansoni* genome and did not show RFAM similarities were passed to mirDeep2.0.0.5 using platyhelminth miRNAs from miRBase 19 as guides (Appendix 7).

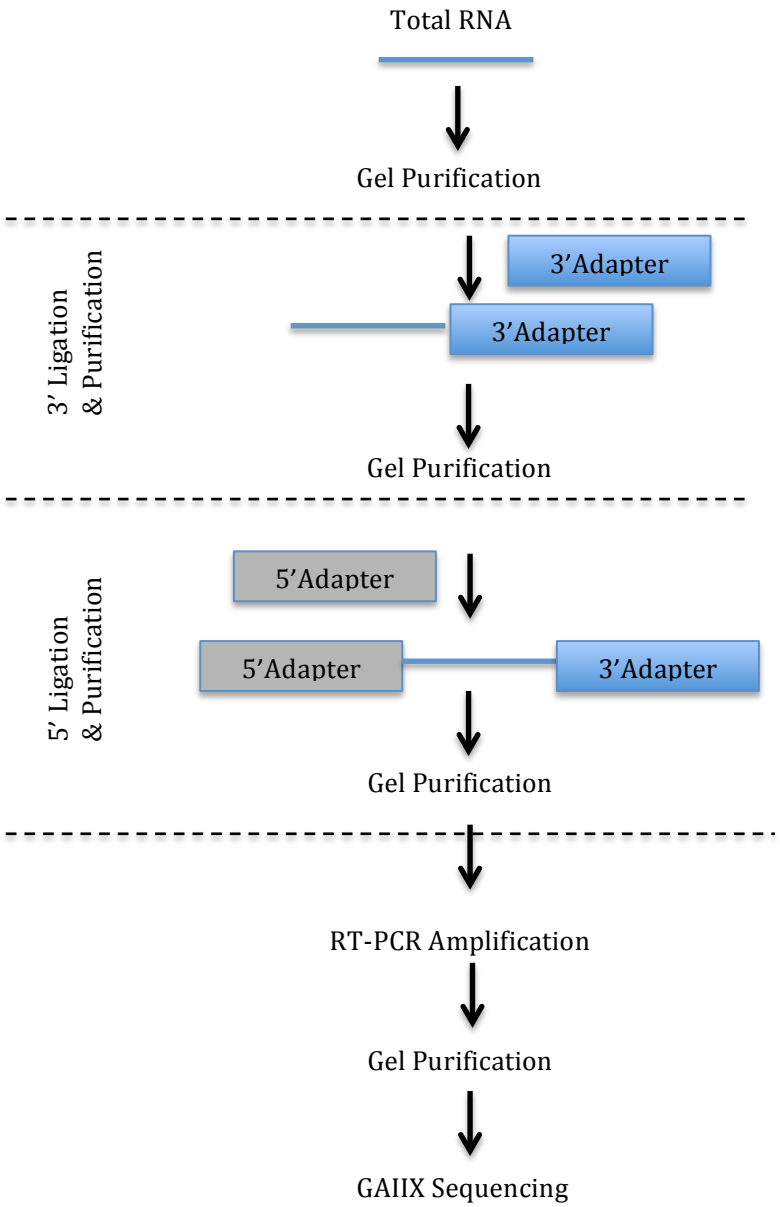

Figure 2.2 cDNA library preparation using Illumina small RNA Sample Preparation Kit version 1.5.
For small RNA sequencing in experiment 1, total RNA was extracted from serum. The small RNAs were size selected by 15% PAGE and prepared according to the Illumina small RNA Sample Preparation Kit version 1.5 and sequenced on the GAIIX. Figure was modified from: http://support.illumina.com/downloads/truseq_small_rna_sample_preparation_guide_15004197.html.

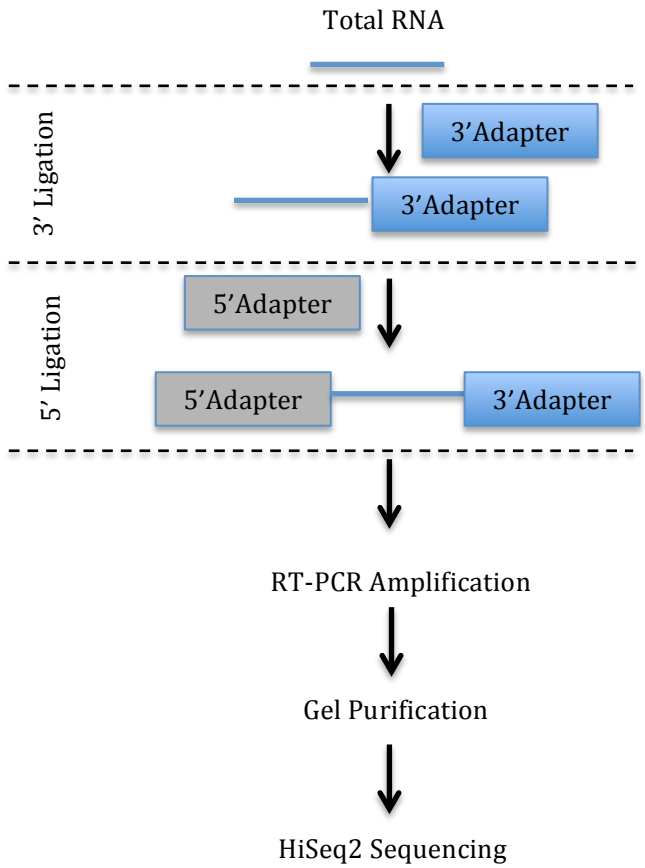

Figure 2.3 cDNA library preparation using Illumina TruSeq Small RNA Sample Preparation Kit.
For small RNA sequencing in experiment 2, total RNA was extracted from serum. The library was prepared according to the TruSeq Small RNA protocol (without size-selecting small RNA) and sequenced on the HiSeq2. Figure was modified from: http://support.illumina.com/downloads/truseq_small_rna_sample_preparation_guide_15004197.html

2.15 Northern Blotting

2.15.1 Buffers and solutions

10x TBE Buffer (Tris-borate-EDTA): 109g Tris base, Boric acid 55.6g, 50 ml of 500 mM of EDTA, adjust the volume to 1L with ddH_2O (Milliporesystem (>18 MΩ cm)).

15% TBE-UREA gel: 6ml concentrate reagent (SequaGel, National diagnostics), 3ml dilute reagent (Sequa gel, National diagnostics), 0.5 ml 10x TBE, 0.5 ml ddH_2O, 100µl of 10% ammonium persulfate (APS) (Sigma) and 4µl Tetramethylethylenediamine (TEMED) (Sigma)

2x loading dye: 8M urea (Sigma), 5 mM EDTA (Promega), 0.05% bromophenol blue (Sigma), 0.05% xylene cyanol (Sigma).

Cross-linking Solution: 245µl of 12.5M 1-methylimidazole, 9ml of ddH_2O, adjust pH to 8, 0.753g EDC, adjust the volume to 25ml using ddH_2O (Milliporesystem (>18 MΩ cm)).

Wash Buffer 1 (2x SSC, 0.1% SDS): 100 ml 20x SSC (Biosciences), 10 ml 10% SDS (Sigma), and 890 ml ddH_2O (Milliporesystem (>18 MΩ cm)). SSC -sodium chloride-sodium citrate buffer; SDS -sodium dodecyl sulfate.

Wash Buffer 2 (1x SSC, 0.1% SDS): 50 ml 20x SSC (Biosciences), 10 ml 10% SDS (Sigma), and 940 ml ddH_2O (Milliporesystem (>18 MΩ cm)).

Wash Buffer 3 (0.1x SSC, 0.1% SDS): 5 ml 20x SSC (Biosciences), 10 ml 10% SDS (Sigma), and 985 ml ddH_2O (Milliporesystem (>18 MΩ cm))

Stripping Buffer (0.1% SDS): 5 ml 10% SDS and 495 ml ddH_2O. (Milliporesystem (>18 MΩ cm))

2.15.2 5' end labeling of probes and RNA marker & northern blotting

Synthetic oligonucleotides were purchased from Invitrogen and 5'-end labelled using [γ-32P]-dATP (Perkin Elmer) and T4 Kinase Kit (Life Technologies) according to the manufacturer protocol Fig. 2.4. 20 μM of the oligonucleotide was used in each reaction. The sequences were the reverse complements to miR-16 (5'-CGCCAATATTTACGTGCTGCTA-3'), $tRNA^{Gly}$(GCC): $tRNA^{Gly}$5' (5'-TACC ACTGAACCACCAATGC-3'), $tRNA^{Gly}$3' (5'-TGCATTGGCCGGGAATCGAA-3'). The probes were purified using microSpinTM G-25 columns (GE Healthcare) and 30μl of 3mM EDTA was added. The probes were stored at -20°C. Decade™ Marker RNA System (Life Technologies) was used to produce radiolabeled RNA molecular weight markers. The labeled RNA marker was mixed with 20μl loading buffer and stored at -20°C. The required volume of RNA marker was heated at 95°C for 5 min before use.

Extracted RNA was separated on the 15% denaturing polyacrylamide gel and transferred onto a nylon membrane (Hybond N) (GE Healthcare, Fisher Scientific) (0.5% TBE, 80V, 1h, 4°C). Chemical RNA cross-linking was carried out as described in (Pall and Hamilton, 2008) at 50°C for 2hours and the membrane was pre-hybridised in the Perfect HybPlus Hybridisation buffer (Sigma) for 30 min at 42°C. 10μl of the ^{32}P-labeled probe (approx. 0.08mBq) was added to the hybridisation buffer and incubated over-night at 42°C in hybridisation oven. The membrane was washed for 10 min with pre-warmed to 42°C buffers: Wash Buffer 1, Wash Buffer 2 and Wash Buffer 3. The membrane was sealed and exposed for 24 to 48 in the phosphoimager (Molecular Dynamics, LabX, USA). The screen was scanned using a Typhoon Trio variable mode imager (GE Healthcare). The membrane was stripped using Stripping Buffer and re-exposed in phosphoimager before re-hybridisation with a new probe.

2.16 3'- end labelling

31-mer synthetic RNA oligonucleotides complementary to $tRNA^{Gly}$(GCC) halves: 5' $tRNA^{Gly}$(GCC) half: 5'-GCAUUGGUGGUUCAGUGGUAGAAU UCUCGCC-3' and 3' $tRNA^{Gly}$(GCC) half 5'-GGAGGCCCGGGUUCGAUU CCCGGCCAAUGCA-3' were purchased from IDT. Serum RNA and synthetic RNA was 3' end labelled using T4 RNA Ligase (Life Technologies) and [32P]pCp (Perking Elmer) according to the manufacturers protocols Fig. 2.4. With this method RNA with 3' hydroxyl group can be labeled.

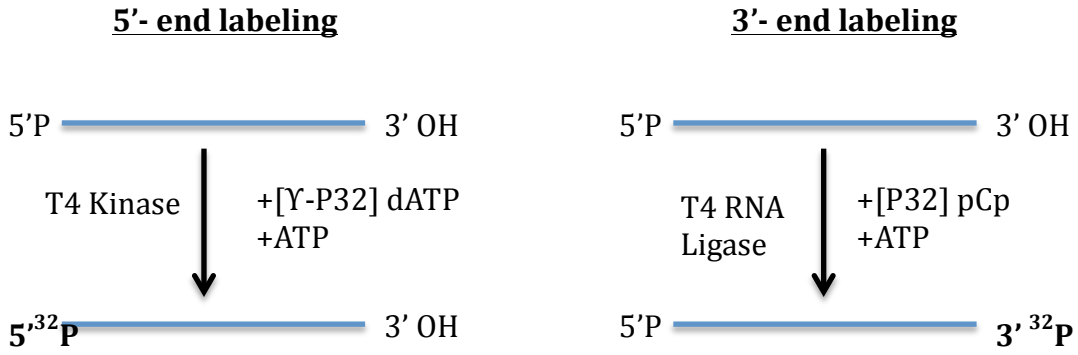

Figure 2.4 3'- and 5' –end radioactive labelling of RNA.

2.17 Protease and detergent treatment

Mouse serum (100µl) was treated with Triton X100 (Sigma-Aldrich) (0.5% final concentration) for 30 min at 37°C or Proteinase K (Promega) (25µg) for 1h at 55°C and/or RNase A (Invitrogen) (0.1mg) for 5min at 37°C. Total mouse RNA was then extracted using miRVANA Paris Kit according to the manufacturer protocol without addition of spike-ins. Extracted RNA was ^{32}P-pCp 3' end labelled and resolved on the 15% PAGE or used for northern hybridisation with a probe complementary to 5' end of $tRNA^{Gly}$(GCC).

2.18 Ultracentrifugation

Serum (1ml) was diluted into 2ml of PBS solution and gently mixed. Samples were centrifuged in the 5ml polyallomer tubes (Beckman) at 38,600xg for 70 min at 4 °C in a swing-bucket rotor (70.1Ti Backman). The supernatant was removed to a new eppendorf tube and volume was measured and the pellet was resuspended in 200ul PBS and transferred to a new eppendorf tube. 100ul of supernatant (corresponding to ~30ul of serum) and a volume of resuspended pellet corresponding to 30ul of serum were used for RNA isolation using miRVana Paris kit. cel-miR-39 spike in was added at the extraction step to allow normalisation.

2.19 Size exclusion chromatography

Calibration of the column was performed by Dr James Hewitson.

Mouse serum was subjected to Superdex 200 10/300 GL (GE Healthcare) chromatography column (Table 2.3). The column was equilibrated with 30ml of PBS solution at 0.5mL/min at room temperature. 800ul of serum was injected onto the column and eluted with PBS at 0.5ml/min at room temperature. A total of 30 fractions of 1ml each were collected. 100ul of each fraction was used for RNA extraction. Protein molecular weight standards included: thyroglobulin (669 kDa), ferritin (440 kDa), aldolase (158 kDa), conalbumin (75 kDa), ovalbumine (44 kDa). Calibration standards were prepared by plotting elution time (min) against logarithm of molecular weight (Table 2.4, Fig 2.5).

Table 2.3 Properties of Superdex 200 10/300 GL column.

Column properties Superdex 200 10/300 GL	
Column height	30cm
Column Vo	8ml
Column Vt	24ml
Separation range	10-600kDa
Exclusion limit	1300kDa
Flow Rate	0.5 ml/min
Matrix	Composite of cross-linked agarose and dextran
Particle size	13 µm

Table 2.4 Elution volume, elution time and Kav value for used protein molecular standards.

STANDARDS	Mw (kDa)	log(Mw)	Elution time min	Elution volume mL	Kav
thyroglobulin	669	2.83	18.69	9.35	0.085
ferritin	440	2.64	21.07	10.54	0.159
aldolase	158	2.20	25.97	12.99	0.312
conalbumin	75	1.88	28.76	14.38	0.399
ovalbumin	44	1.64	30.8	15.4	0.463

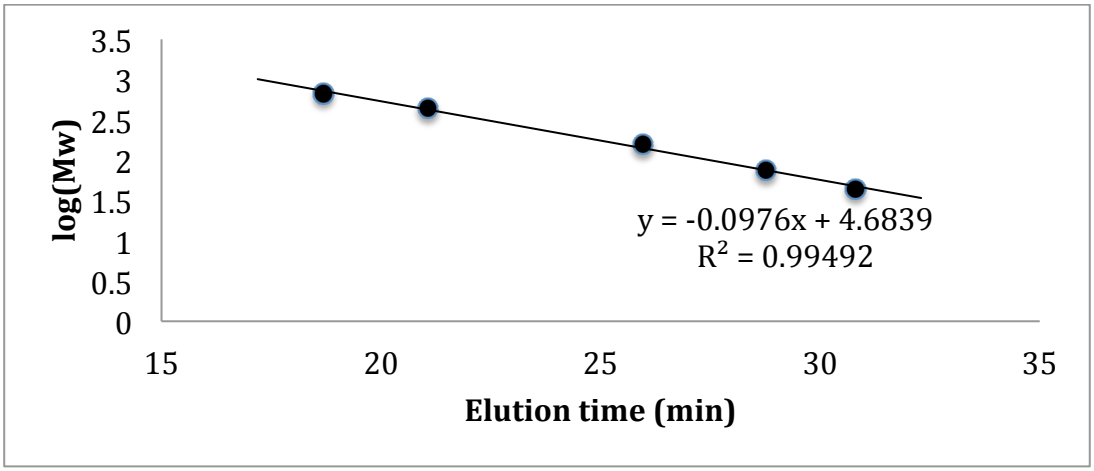

Figure 2.5 Standard curve for the protein molecular standards

Chapter 3: **Expression and functional interrogation of host- miRNAs upon *Schistosoma mansoni* infection**

3.1 INTRODUCTION

Schistosomiasis is a chronic disease caused by blood flukes of the genus *Schistosoma* that affects more than 200 million people worldwide and is second only to malaria as the most important lethal human parasitic disease in tropical and subtropical regions. Schistosomiasis is predominantly caused by hepatic *S.mansoni* and urogenital *S.haematobium* (WHO, 2013a). It is estimated that the mortality rates due to haematemesis (*S.mansoni*) and renal failure (*S.haematobium*) are around 130,000 and 150,000 per year respectively (van der Werf et al., 2003). An adult pair of *S.mansoni* resides within the mesenteric veins of the host where a mature female parasite releases ~300 eggs per day (Wynn et al., 2004). More than 50% of the eggs are carried by the blood-flow to the liver where they become trapped (Wynn et al., 2004) thus, the liver is the key organ of *S.mansoni* pathology (Pearce and MacDonald, 2002). The host immune response induced by the presence of the egg antigens in the liver leads to formation of granulomatous lesions, fibrosis and portal hypertension (Booth et al., 2004; de Jesus et al., 2004; Wynn et al., 2004).

Liver fibrosis is associated with significant changes in the extracellular matrix (ECM) composition which is a result of increased synthesis of collagens and simultaneous decreased activity of ECM-degrading matrix metalloproteinases (MMPs) and overexpression of their inhibitors - tissue inhibitors of matrix metalloproteinases TIMPs (Arthur, 2000; Friedman, 2008; Sato et al., 2003). Hepatic stellate cells (HSCs) are the main producer of ECM components and are thought to be the key cell type responsible for fibrogenesis. Upon liver injury, HSCs undergo activation or transdifferentiation from quiescent to a “myofibroblast-like” phenotype (aHSCs) and migrate to the site of tissue repair where they secrete excessive ECM components such as collagen, elastin, and fibronectin as well as enzymes involved in ECM remodelling: MMPs and TIMPs. Activated HSCs express myogenic markers (α smooth muscle actin (α-SMA or ACTA2), c-myb, myocyte enhancer factor-2 (MEF-2)) of which α-SMA is the most reliable marker of HSCs activation as it is not

expressed by any other liver cell type in either normal or injured liver (Friedman, 2008). The ECM components are known to play a role in the development of liver fibrosis, including fibrosis induced by *S.mansoni* (Bartley et al., 2006; Chang et al., 2006; Kresina et al., 1994). The balance between MMPs and their inhibitors TIMPs play a significant role in the ECM remodelling, and therefore, fibrosis progression and resolution. HSCs are a source of MMP2, MMP9, MMP13, TIMP1 and TIMP2 (Friedman, 2008). Studies in mouse models of *S.mansoni* infection revealed that aHSCs are involved in the formation of the periovular granulomas (Barbosa Junior Ade et al., 1993; Boloukhere et al., 1993; Chang et al., 2006). It has been shown that HSCs isolated from mice infected with *S.japonicum* express significantly higher levels of α-SMA, collagen type I and TIMP-1 and that *S.japonicum* egg or their soluble egg antigens (SEA) are able to activate HSCs to their myofibroblast-like phenotype via overexpression of cannabinoid receptor 1 (CB1) in HSCs (Wang et al., 2014). In contrast, it has been shown that the eggs of *S.japonicum* or *S.mansoni* eggs can reverse the phenotype of the cultured HSC cell line (LX2) cells from activated to the quiescent state (Anthony et al., 2010; Anthony et al., 2013).

miRNAs are a class of naturally occurring small non-coding RNA produced from animal, plant and viral genomes (Bartel, 2009). They are incorporated into the RNA-induced silencing complex (RISC) and function by binding to messenger RNAs (mRNAs) and inhibiting translation and/or causing mRNA destabilization (Fabian et al., 2009). A single miRNA can directly or indirectly regulate hundreds of genes within complex regulatory networks. Depending on the genes they target, miRNAs have diverse functions inside cells, from regulation of developmental programming to viral-host interactions (Mendell and Olson, 2012; Sullivan and Ganem, 2005; Xiao and Rajewsky, 2009). A number of studies have demonstrated that miRNA inhibitors or mimics can act as novel therapeutic agents in different disease contexts (reviewed in (Broderick and Zamore, 2011; Stenvang and Kauppinen, 2008; van Rooij et al., 2012; Wang and Wu, 2009)).

miRNAs have been shown to be altered in liver disease, such as hepatitis B (HBV) and hepatitis C (HCV) infections (Liu et al., 2011; Pfeffer and Baumert, 2010), alcohol liver disease (ALD) (McDaniel et al., 2014), non-alcoholic fatty liver disease (NAFLD) (Gori et al., 2014), liver fibrosis (Vettori et al., 2012) and hepatocellular

carcinoma (HCC) (Borel et al., 2012). Several studies have shown differential expression of miRNAs during the activation of HSCs including miR-15/16 (regulation of proliferation and apoptosis in aHSCs), miR-19b, -29, -146a, -150, -194, -195 (inhibition of HSCs activation and fibrosis), miR-21, -27, -181b (increased HSCs proliferation), miR-29b (suppression of collage type I), reviewed in (Guo et al., 2014).

While this work was underway, two recent reports have detailed host miRNA expression profiles in the liver of BALB/c mice following *S.japonicum* infection. Specifically, Han et al., reported an alteration in expression of 11 miRNAs (fold change>4): miR-494, miR-98, miR-5107, miR-365, miR-3962, miR-466f, miR-466h-5p, miR-466f-5p, miR-2861, miR-568 and miR-290-5p at 10 days post *S.japonicum* infection (Han et al., 2013). In the paper by Cai et al., the authors demonstrated that 89 miRNAs were dysregulated upon *S.japonicum* infection, of which 6 miRNAs were down-regulated, during the time-course of infection (15, 30, 45 days post infection). The expression of miRNAs at 15 days post infection did not change dramatically; however, several miRNAs including miR-155, miR-223, miR-142-3p, miR-146b, miR-15b, miR-126-5p were significantly altered at 30 days post infection. It has been shown that miRNAs previously associated with hepatic fibrosis, such as miR-34c and miRNAs derived from the miR-199/214 cluster were up-regulated at 45 days post infection (Cai et al., 2013). To date however, there is no data on the expression profile of miRNAs in the host liver in *S.mansoni* infection nor have any functional studies been carried out to reveal miRNAs role in the development of *Schistosoma*–induced liver fibrosis.

Given the health burden of *S.mansoni* infection and associated liver fibrosis we reasoned that it is important to understand the role of miRNA in the *S.mansoni* infection and explore the potential of using miRNA inhibitors in treatment of liver fibrosis.

In this chapter, we determine the profile of miRNAs altered in the liver upon *S. mansoni* infection, select miRNA candidates to be examined as potential serum biomarkers and examine the potential of miR-199-3p inhibitor as an anti-fibrotic agent.

3.2 SPECIFIC AIMS

1. To investigate the profile of host miRNAs in the liver upon *S.mansoni* infection.
2. To examine the effect of synthetic miRNA inhibitors in the *in vivo* setting.
3. To investigate the therapeutic potential of miR-199-3p in *S.mansoni* induced fibrosis using synthetic antimiRs.

3.3 RESULTS

3.3.1 *Specific host miRNAs are significantly altered in the liver of mice at 7 weeks post S.mansoni infection.*

miRNAs are dysregulated in most disease contexts and play important roles in mediating how cells respond to insult and infection (reviewed in (Mendell and Olson, 2012)). In order to identify miRNAs associated with *S. mansoni*-induced liver pathology, we first compared expression profiles of miRNAs in livers of naïve mice or mice that were infected with *S.mansoni* at a high dose (~180 cercariae) using miRNA array technology (miRCury 8.1 containing 384 probes specific for the mouse miRNAs probe set). Tissues were collected at 7 weeks post infection, at which time substantial hepatomegaly and granulomas were observed (Fig.3.1). A total of 33 mouse miRNAs were differentially expressed: 26 miRNAs were up-regulated and 7 miRNAs were down-regulated in infected mice, based on a fold change cut-off of ≥ 2 and p value cut off <0.05 (Table 3.1, Fig 3.2). The miRNAs that displayed the largest differential expression included miR-199a and miR-214, which are known to be altered in liver fibrosis caused by hepatitis C infection or induced by carbon tetrachloride (Iizuka et al., 2012; Murakami et al., 2011). Among the down-regulated miRNAs is the liver-enriched miR-122, which is dysregulated during hepatitis C infection, acetaminophen overdose and hepatocellular carcinoma and is involved in lipid metabolism (Girard et al., 2008; Hu et al., 2012).

A B

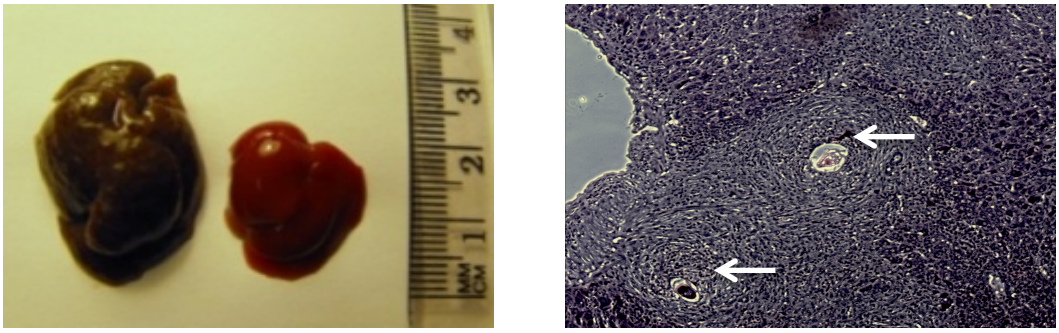

Figure 3.1 *S.mansoni* liver pathology.
8 week old C57/Bl6 mice were infected with ~180 cerc. or left uninfected, after 7 weeks livers were harvested. A) Left: picture of a liver from a C57/Bl6 mice infected with *S.mansoni* (~180 cerc. Wk7), Right- liver of uninfected age-matched C57/Bl6 mouse. B) Masson's Trichrome staining of a liver section. Arrows indicate *S.mansoni* 's eggs.

Table 3.1 miRNAs that are dysregulated in the liver upon *S.mansoni* infection as determined by microarray analysis (p<0.05, Fold change ≥2).
8 weeks old C57/Bl6 mice were infected with ~180 cerc (n=3) or left uninfected (n=3), After 7 weeks livers were harvested and samples were collected for RNA extraction. For the microarray analysis, 1 μg of total RNA for each mice (infected n=3, uninfected n=3) was labelled using the Hy3 power labeling kit (Exiqon) and hybridized to codelink slides printed with the miRCury 8.1 containing 384 probes specific for the mouse miRNAs probe set. miRNA that displayed ≥2-fold change, p-value<0.05 are displayed in the table. + indicates miRNA not conserved between mice in humans. Bold represents miRNA selected for qRT-PCR validation.

Name	P value	FC
mmu-miR-199b*/miR-199a-5p	**0.0002**	**10.1**
mmu-miR-199a-3p/mmu-miR-199b	**0.0001**	**6.4**
mmu-miR-744	**0.0002**	**5.3**
+mmu-miR-292-5p	0.0121	5.1
mmu-miR-214	**0.0001**	**4.6**
mmu-miR-210	**0.0001**	**3.9**
+mmu-miR-541	0.0467	3.8
mmu-miR-21	**0.0023**	**3.5**
mmu-miR-15b	0.0018	3.2
mmu-miR-181a	0.0004	3.1
mmu-miR-503	0.0002	3.0
mmu-miR-689	0.0008	3.0
mmu-miR-34a	0.0018	2.9
mmu-miR-497	0.0021	2.8
mmu-miR-21*	0.0012	2.8
mmu-miR-330*	0.0033	2.8
mmu-miR-322	0.0011	2.7
mmu-miR-500	0.0008	2.6
mmu-miR-146b	0.0041	2.5
mmu-miR-155	0.0008	2.4
mmu-miR-501-5p	0.0077	2.3
mmu-miR-143	0.0021	2.3
mmu-miR-342-3p	0.0072	2.3
mmu-miR-145	0.0019	2.3
mmu-miR-147	0.0090	2.2
mmu-miR-335-5p	0.0183	2.0
mmu-miR-151-5p	**0.0241**	**-12.9**
mmu-miR-9	**0.0309**	**-2.3**
mmu-miR-365	**0.0074**	**-2.2**
mmu-miR-192	**0.0064**	**-2.2**
mmu-miR-194	**0.0243**	**-2.0**
mmu-miR-122	**0.0289**	**-2.0**

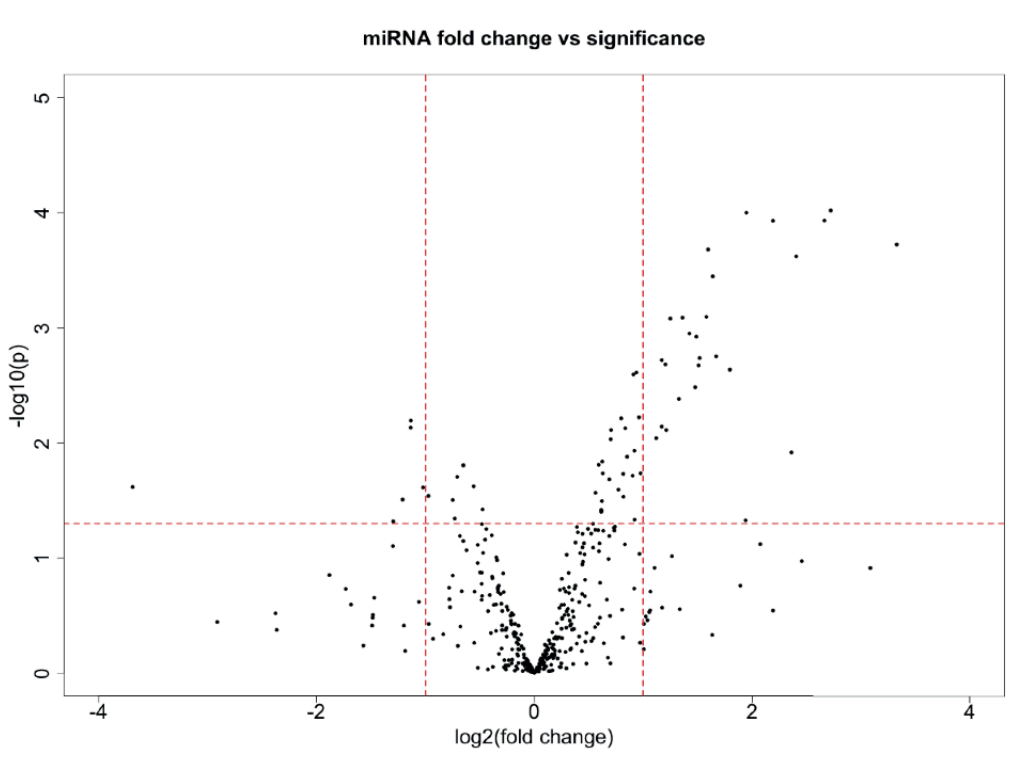

Figure 3.2 Volcano plot of miRNA microarray data comparing miRNA levels in *S. mansoni* infected versus naive mice.
8 weeks old C57/Bl6 mice were infected with ~180 cerc. (n=3) or left uninfected (n=3), After 7 weeks the livers were harvested and samples were collected for RNA extraction. For the microarray analysis, 1 μg of total RNA was labelled using the Hy3 power labeling kit (Exiqon) and hybridized to codelink slides printed with the miRCury 8.1 containing 384 probes specific for mouse miRNAs. Hybridization and washing were carried out following the manufacturer's protocols (Exiqon). The p values were not adjusted for multiple testing. Volcano plot shows fold changes (log2 values) and probability values (log10) for individual miRNAs expressed in the liver of *S.mansoni*-infected mice in comparison with uninfected controls. The horizontal line indicates a p-value cut-off of 0.05 and vertical lines indicate two-fold change thresholds.

For validation of the microarray results, the miRNAs that displayed the largest fold change and are perfectly conserved in mouse and humans were quantified by qRT-PCR and normalized to miR-16 (a total of 6 up-regulated miRNAs and 6 down-regulated miRNAs were examined). Mouse miRNAs that are not conserved in humans were not included in the analysis due to their irrelevance in human infection. The relative fold change between naïve and infected samples was calculated using the $2^{-\Delta\Delta Ct}$ method (Livak and Schmittgen, 2001). To apply this method the efficiency of the primers has to be determined, since corrections should be applied if the efficiencies are not close to 100% (Pfaffl, 2001). As all the primers used here were purchased from Qiagen standard curves were generated for 4 miRNAs as an example. The average Ct values were plotted versus logarithm of input copy number and the slope was calculated for each primer. The amplification efficiency (E value) determined as E= (10(-1/slope)-1)*100% was calculated. Slopes between -3.9 and -3.1 correspond to amplification efficiencies between 90% and 110%. The tested primers showed efficiency between 90 and 105% (Appendix 1). Consistent with the array results, there was an increase in miR-199a-5p, miR-199a-3p, miR-214, miR-21, miR-210, and a reduction of miR-192, miR-194, miR-365, miR-122 and miR-151 in the liver tissue of *S.mansoni* infected mice as compared to naïve mice; miR-9 and miR-744 did not display differential expression and were not analysed further (Figure 3.3).

3.3.2 Changes in the expression of miR-199/214, miR-21, miR-210, miR-122, miR-192, miR-194 and miR-365 in the liver correlate with the progression of S.mansoni infection

Approximately 5-6 weeks after *S. mansoni* infection, mature female parasites produce eggs, some of which are carried by the blood-flow to the liver where they become trapped (Pearce and MacDonald, 2002). The host immune response induced by the presence of the egg antigens leads to the formation of granulomatous lesions, which are composed of immune cells and collagen fibres (Wynn et al., 2004). Between weeks 6 and 12, female parasites continue to produce ~ 300 eggs per day (Moore and Sandground, 1956), resulting in an increase in the number of granulomas in the liver and the development of fibrosis (Pearce and MacDonald, 2002). Hence we hypothesized that the expression of miRNAs in the liver upon *S.mansoni* infection will correlate with the development of liver fibrosis. In order to examine the

expression of miRNAs during the time course of *S.mansoni* infection the levels of the 10 miRNAs validated to be differentially expressed at 7 weeks post infection (Figure 3.3) were next examined by qRT-PCR at 4, 6, 8 and 12 weeks post infection. Lower dose of ~80 cerc. was used to reduce pathology-induced death at later time points. All data from infected mice were compared to age-matched naive mice. To account for differences in RNA extraction or qRT-PCR efficiency, the data were normalised to miR-16, which displayed stable expression in the liver during infection, as normalised to U6 snRNA (Appendix 2). Of the 10 miRNAs examined, all except miR-365 and miR-151 were differentially expressed between naïve and infected mice by 6-8 weeks post infection (Fig. 3.4 C, Appendix 3). This timing correlated with the deposition of eggs in the liver, which were detected by 6 weeks post infection and increased by 8 and 12 weeks post infection (Fig. 3.4 A, B). miR-199a-5p was found to be the most over-expressed, with a 5.5 fold increase at 12 weeks post infection as compared to the control group. miR-192 was down-regulated at 4, 8 and 12 weeks post infection, whereas miR-194 and miR-122 were down-regulated at 8 and 12 weeks post infection. The miRNA fold change difference between data presented in Fig 3.3 and Fig 3.4 is due to the infection dose. Our results suggest that these cellular miRNAs represent tissue biomarkers of the infection that may play a role in the development and progression of liver fibrosis induced by *S. mansoni* egg deposition.

3.3.3 In vivo use of synthetic antimiRs leads to a successful inhibition of miRNAs in the liver

miR-199a-3p is highly abundant in the liver (Hou et al., 2011). The growing body of evidence suggest the involvement of this miRNA in liver disease. It has been shown that miR-199a-3p up-regulation correlates with the progression of liver fibrosis in the CCL4 –induced mouse liver fibrosis model as well as in patients with chronic hepatitis C (Murakami et al., 2011); (Ogawa et al., 2012). Further, in human hepatic stellate cell line LX2, the overexpression of miR-199a-3p causes up-regulation of TIMP-1, COL1A1 and MMP-13 mRNA (Iizuka et al., 2012). In order to study the role of miR-199a-3p in liver fibrosis induced by *S.mansoni* infection we tested the use of synthetic miRNA inhibitors through a collaboration with ThermoFisher to examine the *in vivo* inhibition of miR-199a-3p in the liver.

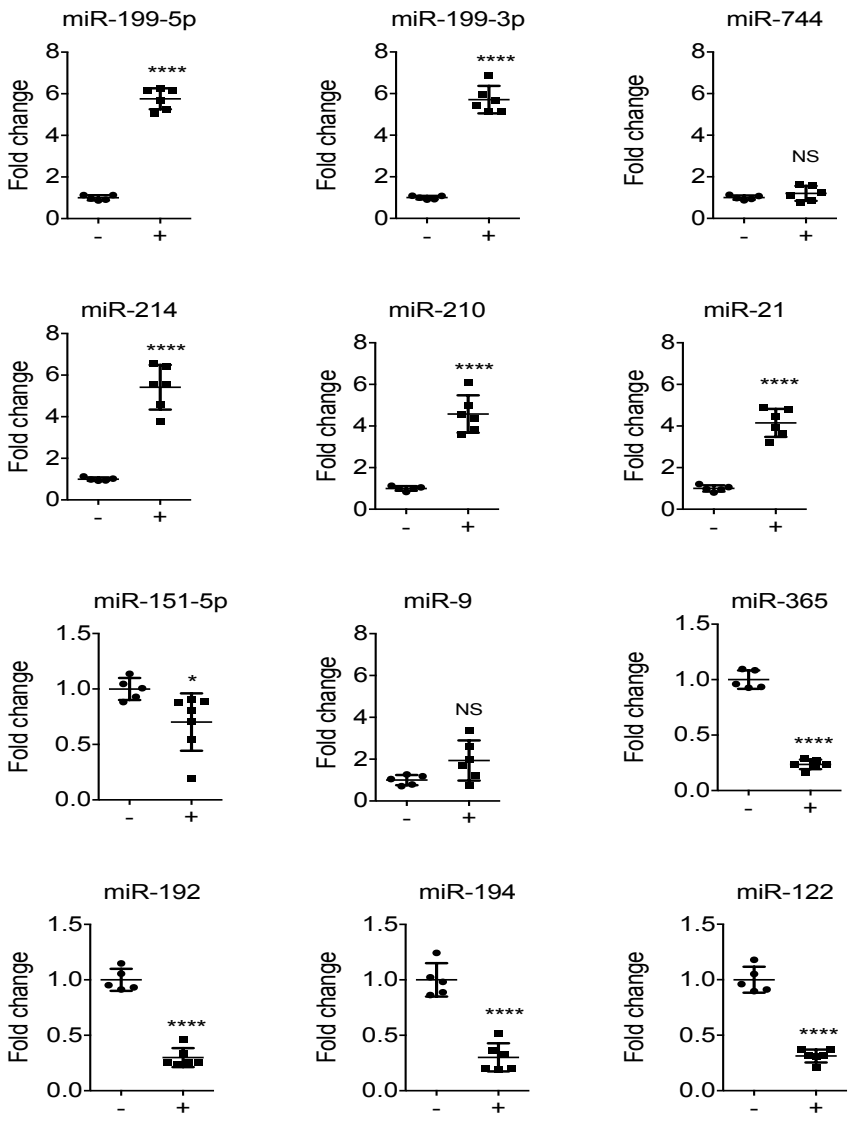

Figure 3.3 Validation of microarray data.
8 week old C57/Bl6 mice were infected (indicated with "+") with ~180 cerc. (n=6) or left uninfected (indicated with "-") (n=5). After 7 weeks post infection. livers were harvested and samples were collected for RNA extraction. miRNAs were quantified by qRT-PCR, normalized to miR-16 and fold changes were calculated as the ratio of values from infected versus naïve mice. Expression of 10 out of 12 tested miRNA showed to be in agreement with microarray data. (*p<0.05, **p<0.01, ***p<0.001, ****p<0.0001, t-test).

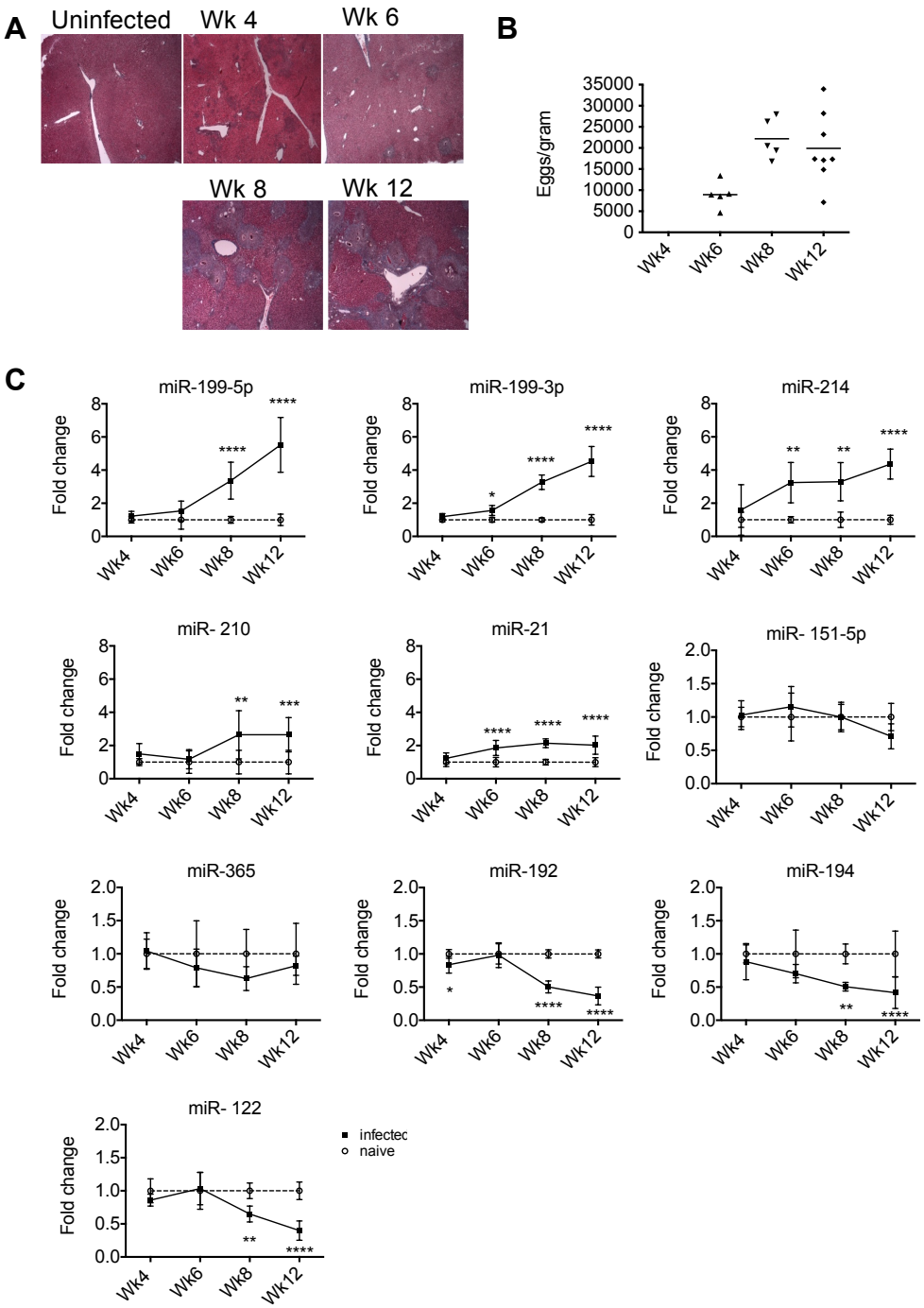

Figure 3.4 Differential expression of host miRNAs in the livers of mice at 4-12 weeks post infection with *S. mansoni*.

8-10 week old C57BL/6 mice were left uninfected or infected percutaneously with ~80 cercariae and euthanized at 4, 6, 8 and 12 weeks post infection-wk4. A) Liver pathology with Masson's Trichrome showing purple staining of collagen fibers within *S.mansoni* granulomas. B) *S. mansoni* liver egg count. C) Differential expression of host miRNAs in the liver. miRNAs were quantified by qRT-PCR, normalized to miR-16 and fold changes calculated as the ratio of values from infected versus naïve mice (*p<0.05, **p<0.01, ***p<0.001, ****p<0.0001, Two-way ANOVA, Sidak multiple comparison test). Wk4: infected n=8, naïve n=8, Wk6: infected n=5, naïve n=8, Wk8: infected n=5, naïve n=8 , Wk12: infected n=8 naïve n=8.

In the preliminary experiments we examined whether the synthetic miRNA inhibitors synthetized by ThermoFisher could effectively inhibit miRNAs in the liver. As miR-122 is one of the first miRNA that has been successfully inhibited in the liver we have used the synthetic miR-122 inhibitor as a control to demonstrate the effectives of the synthetic miRNA inhibitors. Injections with PBS and *C.elegans* cel-miR-67 (Negative Inhibitor –NI) were used as negative controls. In the first experiment mice (n=3) were injected intravenously with a miR-122 Inhibitor at a relatively low dose (30 mg/kg) on day 1 and day 3 and livers were harvested on days 4 and 8 as outlined in Fig 3.5 A. Mice were examined daily and no adverse effects of the treatment were observed. Liver miR-122 levels were measured using qRT-PCR and normalised to endogenous miR-16. Treatment of mice with a miR-122 Inhibitor lead to ~140 fold decrease in levels of endogenous miR-122 on day 4 and ~95 fold on day 8 (Fig 3.5 B,C), as compared to treatment with Negative Inhibitor (NI). To assess the effect of the miRNA inhibition the levels of two miR-122 validated target genes NDRG3 and BCKDK were measured using qRT-PCR and normalised to GAPDH. As shown in Fig 3.5 D and F, treatment of mice with a miR-122 Inhibitor did not affect the levels of miR-122 targets, presumably due to low dose. Thus, it was decided to increase the dose of miRNA inhibitor.

In the second experiment, mice (n=3) were treated twice weekly (Monday and Thursday) with 50mg/kg dose of Inhibitors and tissue harvest was performed on week 4 (24h post last injection) as depicted in Fig 3.6A. During this experiment, one of the mice treated with miR-122 Inhibitor died shortly post injection due to air embolism. Other animals did not display any side effects, although some bruising of the tail vein was observed due to frequent injections. As shown in Fig 3.6 B, treatment with miR-122 Inhibitor on day 28 resulted in ~2600 fold reduction of the endogenous level of miR-122 as compared to treatment with negative inhibitor (NI) with no change in miR-19a9-3p levels, whereas treatment with miR-199a-3p Inhibitor caused ~600 fold decrease in miR-199a-3p levels, without change in miR-122 levels Fig 3.6 C. As in the first experiment, levels of NDRG3 and BCKDK mRNA have been measured. As shown in Fig 3.6 D and E, the levels of both miRNA-122 targets were significantly up-regulated post miR-122 inhibition.

3.3.4 In vivo inhibition of miR-199-3p in the liver of S.mansoni infected mice alters the expression of several fibrosis related genes

Having determined that inhibition was potent over 28 day time course, we next used the synthetic miRNA inhibitors to block miR-199a-3p and miR-122 during *S.mansoni* infection (experiment 3). Although miR-122 is already down-regulated upon *S.mansoni* infection the use of miR-122 Inhibitor serves here as an additional control. Specifically, we expect no change in the level of miR-122 upon miR-199a-3p inhibition. On day 0, 8 week old C57/Bl6 mice were infected with ~60 cercariae or left uninfected. Infected mice were divided into 4 experimental groups which on days 21, 28 and 35 post infection were injected intravenously with: Group 1 (iPBS) animals- 200µl of PBS, Group 2 (iNI): 60mg/kg of NI, Group 3 (i miR-122): 60 mg/kg of miR-122 Inhibitor, Group 4 (i miR-199-3p): 60mg/kg of miR-199a-3p Inhibitor. After the consultation with the University Veterinary surgeon, it was decided to reduce the injection frequency from twice to once per week, and increase the dose from 50 mg/kg to 60 mg/kg to ensure effectives of the treatment. Uninfected animals were injected with 200 µl of PBS (nPBS). Liver tissues were harvested on day 49 post infection. Initially the harvest was planned for day 56, however as two of Group 3 mice died the experiment was terminated and organs were harvested on day 49 post infection.

Several fibrosis related genes have been shown to be up-regulated upon *Schisosoma* infection. Bartley et al., demonstrated that expression of HSCs activation marker α-SMA peaks at 6-10 weeks post infection and COL1A1 at week 8 post infection in mouse model of *S.japonicum*. Further, it has been show that levels of MMPs peak at 8 weeks post *S.mansoni* infection in mice, which coincides with the peak of the host immune response (Takahashi et al., 1980). We have shown that miR-199a-3p is significantly up-regulated at 6 weeks post *S.mansoni* infection and continue to increase during the 12 week time course. Studies in human hepatic stellate cell line LX2 showed that the overexpression of miR-199a-3p cause up-regulation of fibrosis related genes such as: TIMP-1, COL1A1 and MMP-13 mRNA (Iizuka et al., 2012). This led to a hypothesis that upon *S.mansoni* infection miR-199a-3p promotes development of liver fibrosis by indirect up-regulation of pro-fibrotic genes such as COL1A1, TIMPs, α-SMA and down-regulation of anti-fibrotic genes such as MMPs.

Therefore, with the inhibition of miR-199a-3p upon *S.mansoni* infection we expected a decrease in expression of HSCs activation marker α-SMA, as well as down-regulation of TIMPs, ECM components such as collagen type I and III and fibrylin, and an increase in levels of MMPs, thus reduction of fibrosis.

As the intensity of *S.mansoni* infection has an effect on the liver pathology, in order to show the effect of the treatment with miRNA inhibitors on liver fibrosis it is important to ensure equal intensity of *S.mansoni* infection. As shown in Fig 3.7 B the level of parasite eggs per gram of liver tissue was uniform among the infected groups with an average egg/g of 31950 ±14003 across all groups combined. Two of the iNI mice were uninfected and were removed from analysis. One of the miR-199a-3p Inhibitor injected mice displayed a high levels of eggs in the liver (77250 egg/g). Liver miRNA levels were measured by qRT-PCR and normalised to endogenous miR-16. miRNA fold changes were calculated versus uninfected mice (nPBS). As shown in Fig 3.7 C miR-199a-3p was 4.8, 5.3 and 6.3 fold up-regulated upon *S.mansoni* infection in iPBS, iNI and i miR-122 groups which is in agreement with our previous results (Fig 3.3). Upon treatment with miR-199a-3p Inhibitor we observe ~200 fold decrease in miR-199-3p level as compered to normal *S.mansoni* infection (iPBS), or 37 fold decrease as compared to the level in the liver of uninfected mice (nPBS). The levels of miR-122 decreased 2.2, 1.8, 1.9 fold upon *S.mansoni* infection in iPBS, iNI and i miR-199a-3p groups respectively. As expected, further inhibition (~1000 fold, compared to nPBS) was observed upon treatment with miR-122 Inhibitor (Fig 3.7 D).

miRNA incorporated in the RISC complex bind to the 3' UTR of target mRNAs leading to inhibition of translation and/or destabilisation of the target transcript (Fabian and Sonenberg, 2012). This in turn, alters expression of downstream genes within a pathway, indicating that altered miRNA expression level might have a direct and indirect impact on signalling pathways. To assess the effect of miR-199a-3p inhibition upon *S.mansoni* infection on fibrosis the levels of known fibrosis-related genes: ACTA2 (α-SMA), collagen type I and III (COL1A2, COL3A1), fibrilin (FBN1), matrix metalloproteinases (MMP2, MMP9, MMP13), tissue inhibitors of matrix metalloproteinases (TIMP1, TIMP2) were quantified using qRT-PCR. Genes

were normalised to GAPDH and fold changes were calculated as a ratio of values from infected versus naïve mice.

As expected, the expression of ACTA2, COL1, COL3, MMP2, MMP9, MMP13, TIMP1, FBN1, were significantly up-regulated upon *S.mansoni* infection (iPBS). Upon miR-199a-3p inhibition the levels of ACTA2, COL1, COL3, MMP2, MMP9, MMP13, TIMP1 decreased significantly as compared to iNI or iPBS controls (Fig. 3.8). MMPs and their inhibitors (TIMPs) play an important role in collagen degradation and their imbalance can contribute to liver fibrosis. As shown in Fig. 3.8 and Appendix 4, upon *S.mansoni* infection (iPBS) both MMPs and TIMP1 are up-regulated with TIMP1 levels exceeding levels of MMPs (TIMP1/MMP13- ~2 fch) as compared to nPBS. The inhibition of miR-199a-3p leads to down regulation of both MMPs (~3 fch) and TIMP1 (~6 fch) and shifts the imbalance between MMPs and TIMPs (TIMP1/MMP13 ~0.9 fold). This data provides insight into the involvement of the miR-199-3p in the activation of hepatic stellate cells and extracellular matrix (ECM) accumulation and regulation during hepatic fibrosis induced by *S.mansoni* infection. Specifically, it shows that inhibition of miR-199a-3p leads to reduction in level of collagen type I and III mRNAs, reduction in ACTA2 (α-SMA) level, thus inactivation/clearance of aHSC, and a change in the MMPs:TIMPs balance in favour of MMPs potentially leading to fibrosis regression. Further experiments will be necessary to expand our knowledge of the involvement of this miRNA in the process of progression and resolution of fibrosis.

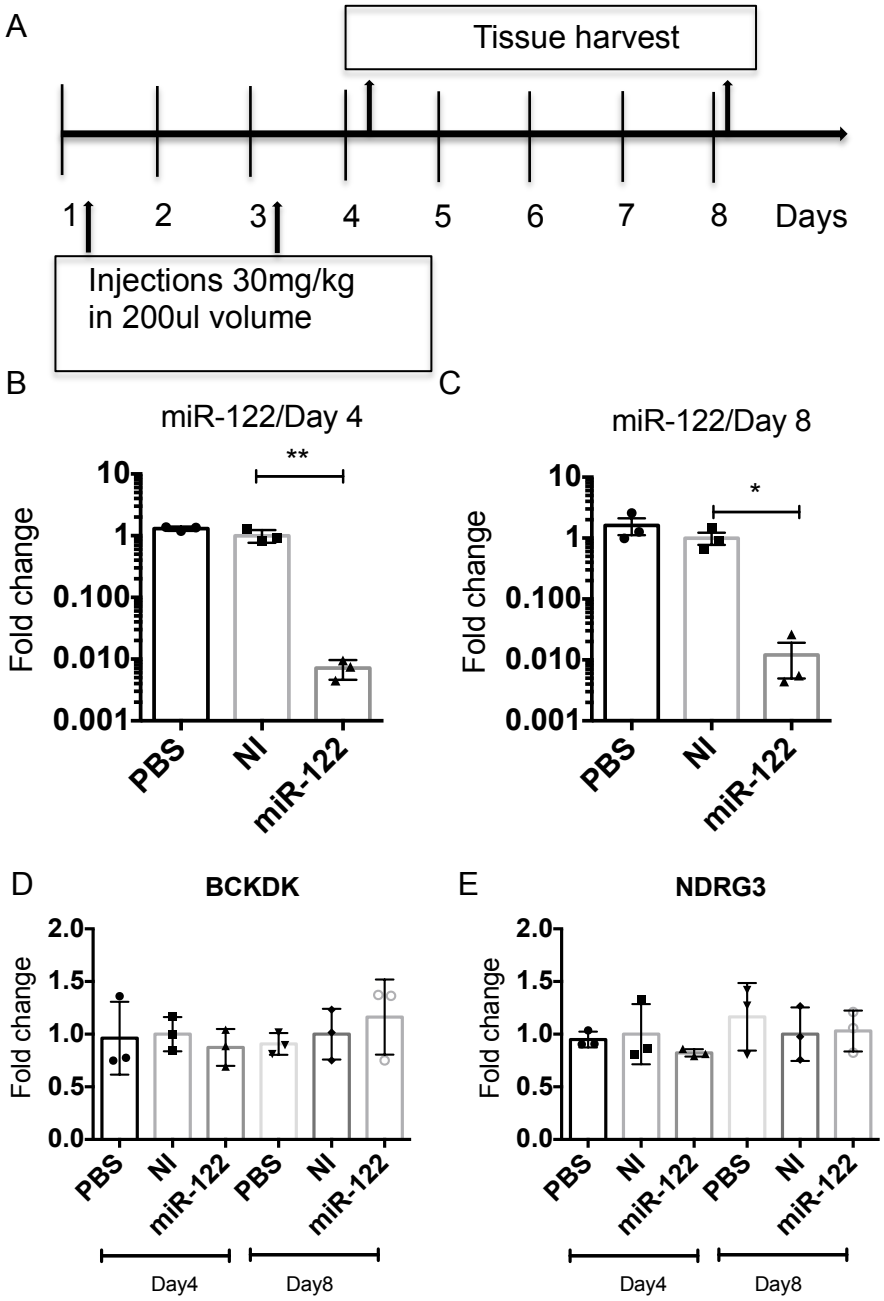

Figure 3.5 Inhibition of miR-122 in the liver.
A) Experimental outline. B) Expression of miR-122 in the liver of naïve mice treated with PBS, Negative Inhibitor and miR-122 Inhibitor on Day 4 C) Day 8 post infection. D) Expression of miR-122 target –BCKDK. E) Expression of miR-122 target –NDRG3. (n_{PBS} =3, n_{NI} =3, $n_{miR\text{-}122}$ =3). miRNAs were quantified by qRT-PCR, normalized to miR-16 and fold changes calculated versus NI. mRNAs were quantified by qRT-PCR, normalized to GAPDH and fold changes calculated versus NI (*p<0.05, **p<0.01, ***p<0.001, ****p<0.0001).

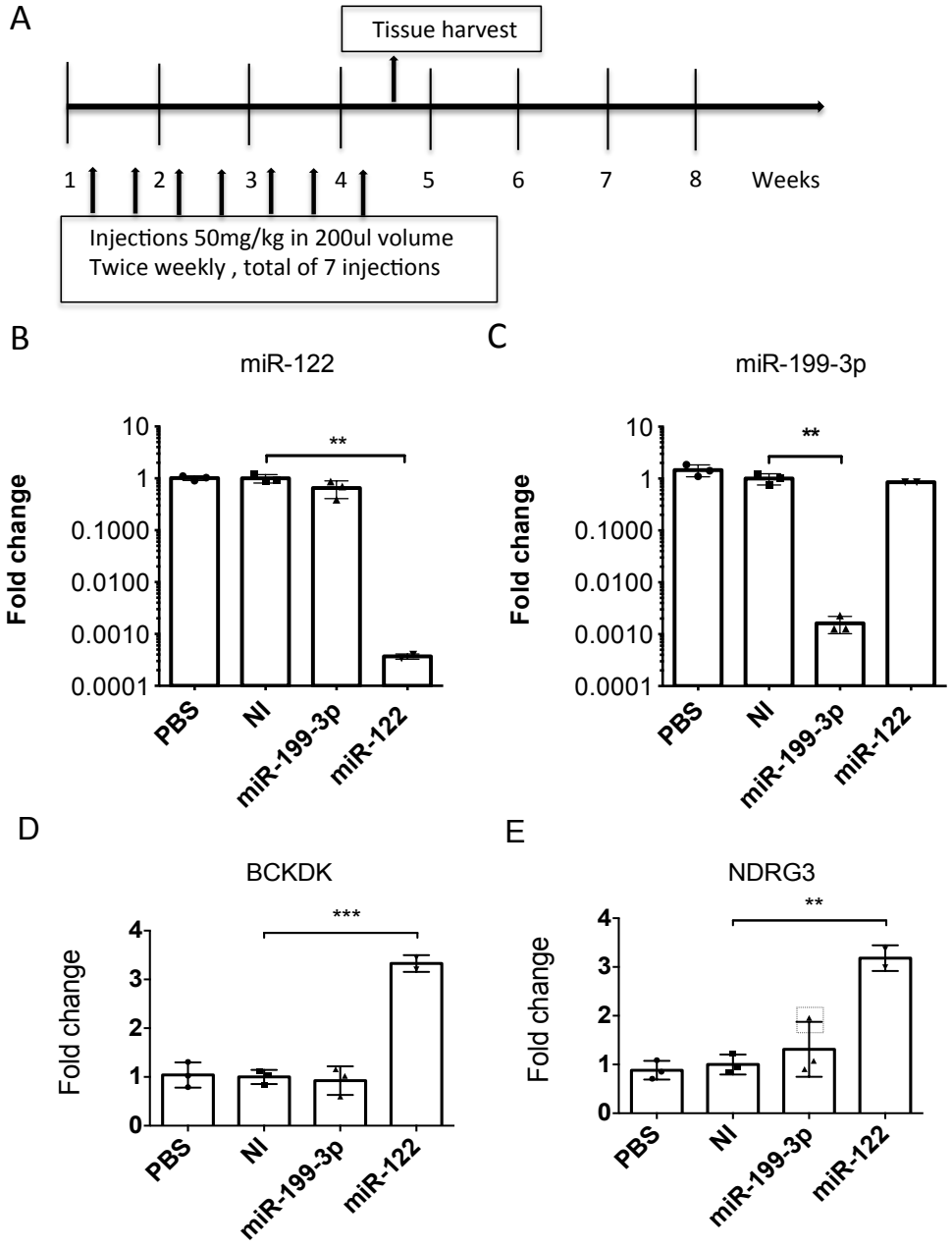

Figure 3.6 Inhibition of miR-122 and miR-199-3p in the liver.
A) Experimental outline. B) Expression of miR-122 and C) miR-199-3p in the liver of naïve mice treated with PBS, Negative Inhibitor, miR-199-3p Inhibitor and miR-122 Inhibitor. D) Expression of miR-122 target –BCKDK. E) Expression of miR-122 target –NDRG3 ($n_{PBS}=3$, $n_{NI}=3$, $n_{miR\text{-}122}=2$, $n_{miR\text{-}199\text{-}3p}=3$). miRNAs were quantified by qRT-PCR, normalized to miR-16 and fold changes calculated versus NI. mRNAs were quantified by qRT-PCR, normalized to GAPDH and fold changes calculated versus NI. (*p<0.05, **p<0.01, ***p<0.001, ****p<0.0001).

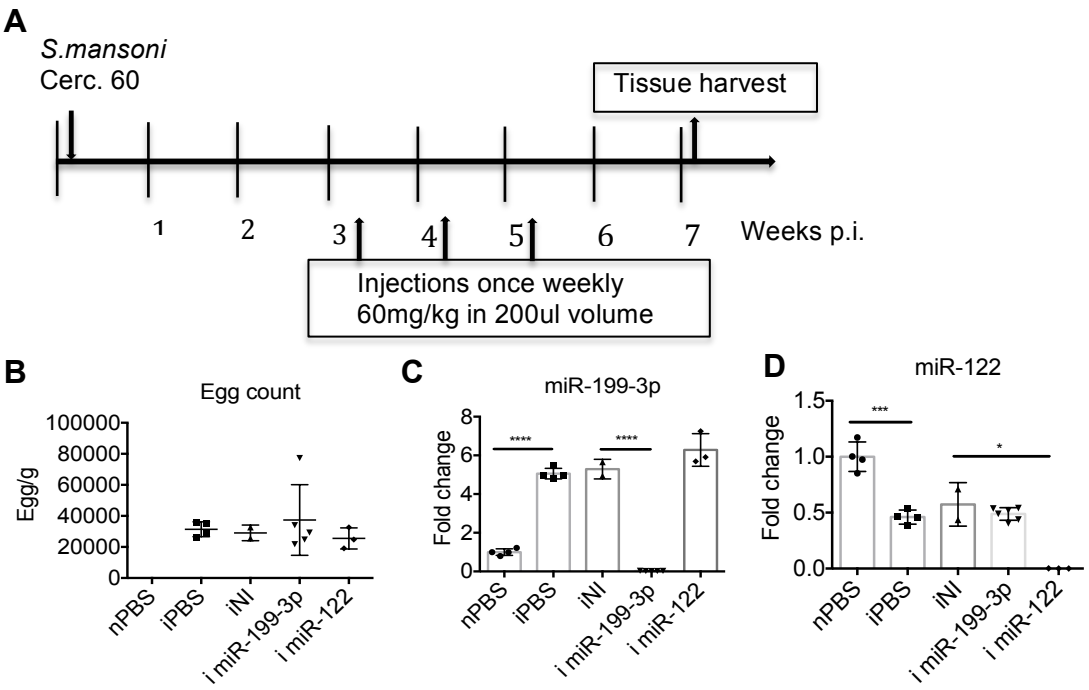

Figure 3.7 Inhibition of miR-199-3p in the liver upon *S.mansoni* infection.
A) Experimental outline. B) *S.mansoni* egg count in liver tissue. C) Expression of miR-199-3p in the liver of naïve (nPBS) and *S.mansoni* infected mice treated with PBS (iPBS), Negative Inhibitor, miR-199-3p Inhibitor and miR-122 Inhibitor. D) Expression of miR-122 in the liver of naïve and *S.mansoni* infected mice treated with PBS, Negative Inhibitor, miR-199-3p Inhibitor and miR-122 Inhibitor ($n_{nPBS}=4$, $n_{iPBS}=4$, $n_{iNI}=2$, $n_{I\ miR\text{-}122}=3$, $n_{I\ miR\text{-}199\text{-}3p}=5$). miRNAs were quantified by qRT-PCR, normalized to miR-16 and fold changes calculated versus nPBS (*p<0.05, **p<0.01, ***p<0.001, ****p<0.0001).

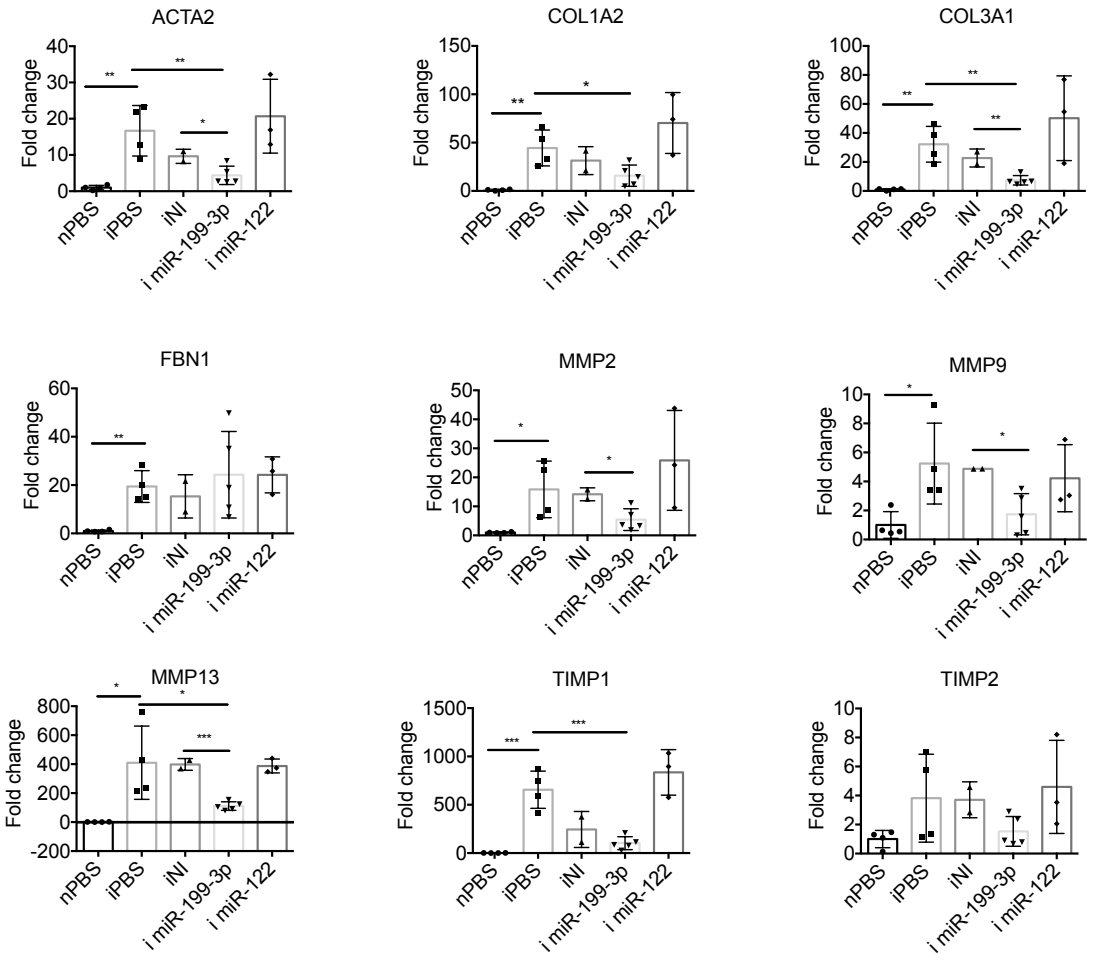

Figure 3.8 Expression profile of fibrosis-related genes in the liver of *S.mansoni* infected mice upon miR-199-3p inhibition.
S.mansoni infected mice were treated with PBS, Negative Inhibitor, miR-199-3p Inhibitor and miR-122 Inhibitor. Seven weeks post infection genes were quantified by qRT-PCR, normalized to GAPDH and fold changes calculated versus nPBS (*p<0.05, **p<0.01, ***p<0.001, ****p<0.0001).

3.4 SUMMARY

- 33 miRNAs are dysregulated in the liver upon *S.mansoni* infection (>2 fold change, $p<0.05$)
- miRNAs dysregulated in the liver correlate with the progression of the disease
- Intravenous administration of synthetic miRNA inhibitors leads to their inhibition in liver
- *In vivo* inhibition of miR-199-3p in the liver leads to decrease in mRNA levels of: ACTA2, COL1A2, COL3A1, MMP2, MMP9, MMP13 and TIMP1

3.5 DISCUSSION

The first objective of this chapter was to identify host miRNAs that might be involved in liver pathology associated with *S. mansoni* infection. We have shown for the first time that miRNAs are differentially expressed in the liver upon *S.mansoni* infection and correlate with the development of liver fibrosis induced by *S.mansoni* infection. On this note, it is important to mention that liver fibrogenesis upon *S.mansoni* infection is a complex process involving both resident liver cells as well as infiltrating immune cells and it is yet to be determined the exact mechanism of miRNAs dysregualation and role. Moreover, identification and validation of appropriate reference genes for normalisation of qRT-PCR expression of miRNA is crucial for data validity. Several miRNA expression studies have shown the use of miRNA, e.g. miR-16 or other small RNAs (U6 snRNA , RNU44 or RNU48) as reference genes to normalize qRT-PCR expression data for miRNAs in tissues (Mattie et al., 2006; Shell et al., 2007; Youssef et al., 2011). Here, we have selected miR-16 as a normalizer based on its unchanged expression in the liver upon *S.mansoni* infection (as normalised to U6 snRNA). An alternative to this approach could be the use of a panel of invariant miRNAs. Available programs such as NormFinder (available at: http://moma.dk/normfinder-software)(Andersen et al., 2004) and GeNorm (available at: http://medgen.ugent.be/~jvdesomp/genorm/) (Mestdagh et al., 2009) can aid analysis of data to select the best candidates.

Among the miRNAs that displayed the highest fold change were: miR-199a-3p, miR-199a-5p and miR-214, miR-21 and miR-210 (up-regulated) and miR-122, miR-192 and miR-194 (down-regulated). Interestingly, our results do not overlap with those

reported by Han et al., who examined changes in host miRNA levels in the liver of BALB/c mice during *S. japonicum* infection (Han et al., 2013). They reported alteration of 11 miRNAs (fold change>4): miR-494, miR-98, miR-5107, miR-365, miR-3962, miR-466f, miR-466h-5p, miR-466f-5p, miR-2861, miR-568 and miR-290-5p at 10 days post infection. None of these miRNAs were altered in liver of *S.mansoni* infected mice at 7 weeks post infection. We assume this may be due to the different time points used in the studies. Indeed, it is likely that the host miRNA changes we observe are primarily related to the liver pathology and/or the immune response initiated by the parasite eggs trapped in the liver, rather than the initial host immune response to the schistosomula. A recent report by Cai et al., showed up-regulation of miR-199/214 cluster (co-transcribed from a conserved antisense intronic transcript at the dynamin3 (*Dnm3*) locus (Loebel et al., 2005)), miR-21 and miR-210 in the liver at 45 days post *S. japonicum* infection in BALB/c mice, confirming our results and hypothesis that these miRNAs might play a role in the development of liver pathology (Cai et al., 2013).

Several miRNAs we identified as differentially expressed are already known to be associated with fibrosis or liver disease in other contexts (Chen, 2009; Girard et al., 2008; Hu et al., 2012; Jiang et al., 2010).

miR-21 is known to be up-regulated in fibrosis of liver, kidney and lung (Chau et al., 2012; Liu et al., 2010; Zhang et al., 2013). In a recent publication by Zhang et al., it was shown that the up-regulation of miR-21 in the liver occurs primarily in the activated HSC and the inhibition of miR-21 leads to the down-regulation of HSC activation marker α-SMA and COL1A1 mRNA. The authors demonstrated that miR-21 maintains its high levels by employing a miRNA-21/Programmed cell death protein 4/Activation Protein-1 (miR-21/PDCD4/AP-1) feedback loop. Further, miR-21 can amplify the TGF-β1/SMAD2/3 pathway by degrading its anti-fibrotic target SMAD7. These results suggest that miR-21 is an important player in HSC activation and fibrosis of the liver (Zhang et al., 2013) and its up-regulation upon *S.mansoni* infection is likely to be pro-fibrotic.

We have shown that increased levels of miR-210 correlate with the factors associated with development of liver fibrosis induced by *S.mansoni* infection. It is known that HIF1a and HIF2a regulate miR-210 under hypoxia conditions (Camps et al., 2008;

Huang et al., 2010; Zhang et al., 2009). Interestingly, HIF1a is up-regulated in inflammatory cells and hepatocytes surrounding granulomas upon *S.mansoni* infection (Araujo et al., 2010) which could explain the up-regulation of miR-210. A number of miR-210 targets have been linked to angiogenesis, stem cell differentiation and cell cycle regulation reviewed in (Chan et al., 2012; Huang and Zuo, 2014). These might also play a role in *S.mansoni* infection.

miR-122 is a liver specific miRNA constituting around 70% of all miRNAs in hepatocytes (Lagos-Quintana *et al.,* 2002). Studies have shown an important role of this miRNA in cholesterol and fatty-acid metabolism in the liver (Esau et al., 2006; Krützfeldt et al., 2005), in human hepatocellular carcinoma (HCC) (Gramantieri *et al*., 2007) and in hepatitis C virus (HCV) infection (Jopling *et al*., 2005; Lanford *et al*., 2010). Further, Li et al., reported that miR-122 inhibits HSCs activation and proliferation and plays a role in negatively regulating collagen maturation by targeting P4HA1, which encodes a component of prolyl 4-hydroxylase, an enzyme that is involved in collagen post-transcriptional modification (maturation). This suggests that the down-regulation of miR-122 upon *S.mansoni* infection contributes to development of liver fibrosis (Li et al., 2013). Thus, a targeted delivery of miR-122 mimic may be a novel therapeutic approach for treatment of liver fibrosis.

We have shown that miRNAs derived from the miR-199/214 cluster are up-regulated upon *S.mansoni* infection. A growing body of evidence suggest the involvement of these miRNAs in the fibrotic processes in various tissues. It has been shown that miR-199a-3p up-regulation correlates with the progression of liver fibrosis in the CCL4–induced mouse liver fibrosis model as well as in patients with chronic hepatitis C (Murakami et al., 2011; Ogawa et al., 2012) and both miR-199a-5p and miR-199a-3p are up-regulated in bile duct ligation mouse model of liver fibrosis (Kanda et al., 2010). In the human HSC cell line LX2, the overexpression of miR-199a-3p causes up-regulation of TIMP1, COL1A1 and MMP13 mRNA (Iizuka et al., 2012). The role of miR-214-5p was recently explored by Izuka et al., who showed the up-regulation of this miRNA upon fibrosis in mice and humans with chronic hepatitis C infection. Further, the overexpression of miR-214-5p in LX2 increases the levels of MMP2, MMP9, α-SMA (ACTA2) and TGF-β1 mRNA (Iizuka et al., 2012). Lino Cardenas et al., reported that miR-199a-5p is up-regulated in the myofibroblasts of the injured

lung in bleomycin-treated mice and fibroblastic foci of idiopathic pulmonary fibrosis patients where it mediates profibrotic cytokine transforming growth factor beta 1 TGFβ-induced down-regulation of caveolin1 (CAV1) expression. Further, the authors also compared the expression of miRNAs in the mouse models of kidney, liver and lung fibrosis, showing that both miR-199-3p and 199-5p were up-regulated (Lino Cardenas et al., 2013). These results suggest the importance of miR-199/214 cluster role in biology of HSCs and liver fibrosis.

Although studies in different models of fibrosis or liver disease provide important insights, the functional role of miRNAs in the pathology induced by *S. mansoni* infection remains to be determined. Hence, one of the objectives of this chapter was to evaluate the role of miRNAs, specifically miR-199a-3p, in liver fibrosis induced by *S.mansoni* infection. *In vitro* studies of miRNAs provide important insight into miRNAs role, specifically; they can be used to determine miRNA targets and the physiological effect of overexpression or inhibition of miRNAs in the cell of interest. However, due to the complexity of interactions between cells within the tissue, the miRNA phenotype *in vitro* might differ from what is happening *in vivo*. Further, miRNAs function through multiple gene targets and the combine effect of a miRNA on its targets determines the functionality of this miRNA. Thus, the combination of both *in vitro* and *in vivo* approaches is needed to show the relevance of miRNAs and reveal the mechanism in which they contribute to certain phenotype. Here to examine the combined effect (phenotype) of miRNA manipulation on the entire organ we employed *in vivo* inhibition of miR-199a-3p in the liver using synthetic antimiRs. The antimiRs we used were synthetized by ThermoFisher and are cholesterol-conjugated oligonucleotides with sequence complementary to the full mature miR-199a-3p. We demonstrated the ability of miR-199a-3p antimiRs to inhibit the endogenous levels of miR-199a-3p in the liver of naïve mice or those infected with *S.mansoni*. As this is the first *in vivo* study on the role of miR-199a-3p in liver fibrosis we focused on the genes known to be altered during liver fibrosis such as: marker of HSCs activation Acta2/α-SMA, extracellular matrix components [(ECM); collagen type I and III (COL1A2, COL3A1), fibrillin (FBN1)], matrix metalloproteinases (gelatinases MMP2, MMP9 and collagenase MMP13) and tissue inhibitors of metalloproteinases (TIMP1, TIMP2).

In the liver, HSCs are considered to be the main producer of ECM proteins and have been shown to be involved in liver fibrosis upon *S.mansoni* and *S.japonicum* infections (Barbosa Junior Ade et al., 1993; Chang et al., 2006). Upon liver injury, quiescent HSCs undergo activation to a "myofibroblast-like" phenotype (activated HSCs), characterised by *de novo* expression of ACTA2 (α-SAM), and secrete collagen type I and III, MMPs and TIMPs (Iredale, 2003). Here we have shown that upon *S.mansoni* infection (7 weeks post infection) the activation marker of HSCs, ACTA2 (α-SMA) as well as COL1A2, COL3A1, are up-regulated. This is in agreement with work carried out by Bartley et al., in mouse model of *S.japonicum*. The authors showed the peak up-regulation of α-SMA at 6-10 weeks post infection and COL1A1 at week 8 post infection. Moreover, the authors used *in situ* localisation to show that activated HSCs are present mainly in the periphery of the *S.japonicum* egg granuloma and co-localise with collagen type I mRNA (Bartley et al., 2006). Work carried in the Buck Lab in parallel with my study led to the observation that *S.mansoni* granulomas are composed of cells expressing miR-199a-3p (Appendix 5). Importantly, we have shown that the inhibition of miR-199a-3p during *S.mansoni* infection leads to down regulation of ACTA2 (α-SMA), COL1 and COL3. Together these results suggest that miR-199a-3p inhibition results in inactivation or elimination of activated HSCs and consequently reduction in collagen levels. Indeed, clearance of aHSCs by apoptosis (Iredale et al., 1998), senescence (Krizhanovsky et al., 2008) or reversion to quiescent phenotype (Kisseleva et al., 2012; Troeger et al., 2012) is thought to be a key step in the fibrosis regression.

The imbalance between levels of MMPs and their inhibitors, TIMPs, is thought to play a key role in progression and resolution of liver fibrosis. We have shown that MMP-2, MMP-9, MMP-13 and TIMP-1 are up-regulated upon *S.mansoni* infection at 7 weeks with the clear dominance of TIMP-1 levels over MMPs. This is in agreement with Vaillant et al., (2001) and Singh et al., (2004) who showed the expression of MMPs and TIMPs in liver of mice infected with ~25 *S.mansoni* cercariae. Specifically, Vaillant et al., showed that the levels of MMP-13 increases by week 6 and MMP-2, -3, -9, -12 increase by week 9 post infection, TIMP-1 mRNA increase was observed at 6 weeks post infection and continued to rise through week 12, whereas TIMP-2 was significantly elevated at week 9 and then decreased by week 12 (Vaillant et al., 2001). Singh et al., (2004), showed that MMP-9, MMP-13 and TIMP-

1 increase at 7 weeks, and MMP-2 and TIMP-2 at 8 weeks post infection (Singh et al., 2004a). The treatment of mice with miR-199a-3p inhibitor resulted in the down regulation of levels of both MMPs and TIMP-1, presumably due in part to the inactivation/clearance of aHSC, and a shift in the MMPs:TIMPs ratio towards MMPs, which is known to favour matrix degradation. Interestingly, treatment with praziquantal showed similar effects on the change in balance between MMPs and TIMPs during resorption of *S.mansoni* egg-induced fibrosis in mice (Singh et al., 2004b).

Madala et al., showed that upon *S.mansoni* infection, mice-deficient in MMP-12 display higher level of MMP-2 and MMP-13 expression which results in reduction of liver fibrosis levels, suggesting that MMP-12 acts as an inducer of fibrosis by limiting the expression of MMP-2 and MMP-13 (Madala et al., 2010). Thus, it would be of interest to investigate the effect of the miR-199a-3p inhibition on MMP-12 levels and whether the reduction off MMP-2 and MMP-13 mRNA levels observed upon miR-199a-3p inhibition is due to an increase in MMP-12 levels.

Excitingly, the gene expression analysis carried out here revealed three factors that could influence fibrosis regression upon inhibition of miR-199-3p: reduced level of collagen type I and III mRNAs, reduction in ACTA2 (α-SMA) level, thus inactivation/clearance of aHSC, and a change in the MMPs:TIMPs balance in favour of MMPs. Further studies are necessary to confirm these observations, which were not possible due to time constrains of this PhD project, which focused more on the diagnostic potential of miRNAs (Chapters 4 and 5). Histological analysis of liver sections combined with hydroxyproline (or a similar) assay would be worthwhile to assess collagen levels during infection and confirm the effect of miR-199a-3p inhibition. The analysis of enzymatic activity of MMPs could be assessed by zymography. In addition, assessing the levels of liver enzymes such as ALT and AST could provide information on hepatic function. Such analysis would provide a more in-depth understanding of the "phenotypic effect" of miR-199a-3p inhibition upon *S.mansoni* infection.

Immune response is thought to play an important role in development of liver fibrosis in *S.mansoni* infection, with IL-13 being the dominant Th2 cytokine responsible for development of liver fibrosis (Pearce and MacDonald, 2002). Fallon et al., showed

that infection of mice deficient in IL-13 results in lower level of collagen and enhances survival (Fallon et al., 2000). IL-13 directly induces synthesis of collagen type I, III and V in fibroblasts and has been shown to stimulate collagen synthesis in HSCs (Wynn et al., 2004). In HSCs, IL-13 which binds to IL-13Rα1 activates JAK/STAT6 signalling pathway leading to liver fibrosis (de Jesus et al., 2004). IL-13Rα2 is a negative regulator of IL-13 and was showed to reduce the volume of granulomas in the liver and reduction of liver fibrosis (Mentink-Kane et al., 2004). Thus, it would be interesting to evaluate whether the antifibrotic effect of miR-199a-3p inhibition is IL-13- dependant, providing and important insight to our understanding of *S.mansoni* induced liver fibrosis and miR-199a-3p function.

Further studies are necessary to provide in-depth understanding of the mechanism by which miR-199a-3p influence the activation status of HSC and ECM components synthesis. One hypothesis is that miR-199a-3p modulates the HSCs phenotype by targeting genes involved in these processes within the HSC. *In vitro* studies using primary HSCs or human HSC cell lines such as LX1, LX2 or TWYN-4 with inhibition and overexpression of miR-199a-3p would be one approach to study miR-199a-3p targets. One such study, in HSC cell line LX2, showed that the overexpression of miR-199a-3p cause up-regulation of TIMP1, COL1A1 and MMP13 mRNA (Iizuka et al., 2012) which is in line with our *in vivo* data.

In summary, we have shown that changes in level of miRNAs in the liver upon *S. mansoni* infection correlates with the progression of *S.mansoni* infection. Excitingly, we have shown that inhibition of miR-199a-3p in the liver upon *S.mansoni* infection results in the reduced level of collagen and a shift in MMPs:TIMPs balance towards the former. This is presumably due to clearance or reversion of HSCs phenotype from "myofibroblast-like" to an inactivated state, therefore suggesting the therapeutic potential of miR-199a-3p inhibition in the treatment of liver fibrosis.

Chapter 4: **The potential of miRNAs in diagnosis of *S.mansoni* infection.**

4.1 INTRODUCTION

Diagnosis of schistosome infection is crucial for patient management, evaluation of treatment efficiency, monitoring of disease transmission and success of control strategies, as recommended by the World Health Organization (WHO, 2002). In the field, *S. mansoni* and other intestinal schistosomes are currently diagnosed through the detection of the parasite eggs in stool specimens using microscopic techniques such as Kato-Katz or ether-concentration (Glinz et al., 2010). While these techniques are relatively simple, inexpensive and specific, their major drawbacks include poor sensitivity in detecting low-intensity infections, their inability to detect pre-patent or single sex infection and their failure to detect infection in individuals where eggs are trapped in tissues and not excreted (Stothard et al., 2011). Available antibody-based assays are useful for diagnosis in some cases (e.g. foreign travellers) but they cannot differentiate past and active infection and can also cross-react with antigens from other helminths (Doenhoff et al., 2004). These assays therefore do not offer a definitive diagnosis in schistosome-endemic areas. Recent studies have shown success with point-of-care tests for *Schistosoma* circulating cathodic and anodic antigens (CCA and CAA, respectively) in serum and urine, which decrease rapidly after chemotherapy (Coulibaly et al., 2013; Shane et al., 2011; Sousa-Figueiredo et al., 2013; Stothard et al., 2011; van Dam et al., 1996; van Lieshout et al., 1993) and these are now being further developed for use in the field (van Dam et al., 2013). Detection of schistosome DNA in urine and stool samples or plasma by the polymerase chain reaction (PCR) method is another strategy for routine diagnosis of infection that has shown promising results (Enk et al., 2012; Ibironke et al., 2011; Lodh et al., 2013; Pontes et al., 2003a; Wichmann et al., 2009).

miRNAs have diverse functions inside cells, from regulation of developmental programming to viral-host interactions (Mendell and Olson, 2012;

Sullivan and Ganem, 2005; Xiao and Rajewsky, 2009). In the last 5 years, reports have shown that miRNAs circulate in serum in a cell-free form and many cell types secrete miRNAs through encapsulation within exosomes or in association with specific proteins (Mitchell et al., 2008; Valadi et al., 2007). These extracellular RNAs have been shown to be extremely stable in body fluids (Chen et al., 2008b; Mitchell et al., 2008). They have received extensive attention for their promise as biomarkers of disease, including cancer (Etheridge et al., 2011; Kosaka et al., 2010a; Weiland et al., 2012a). Extracellular miRNAs have also been shown to be altered in human serum and/or plasma in infection settings, including Hepatitis C and Hepatitis B infections (Li et al., 2010; Shrivastava et al., 2013) as well as during pulmonary tuberculosis (Qi et al., 2012).

Analyses of small RNA content in bodily fluids has been largely directed toward host miRNAs, given the precedence for their differential expression in disease and tissue-specific expression (Calin and Croce, 2006). However, an increasing number of reports suggest that other classes of small RNAs play unforeseen roles in gene regulation, including snoRNAs and tRNAs (Tuck and Tollervey, 2011), which are also present in body fluids. For example, Semenov et al., showed that 3' end fragments of rRNAs and tRNAs are detectable in human milk, although the functional relevance of this is not yet known (Semenov et al., 2004). Appaiah et al., reported upregulation of U6 RNA in the sera of cancer patients (Appaiah et al., 2011); ironically this study was originally focused on miRNA content and analysis of U6 expression was included for purposes of normalization. It is possible, therefore, that various small RNAs exist in an extracellular form that may be of diagnostic or biological interest.

Interestingly, it has been shown that exogenous miRNA derived from bacteria, fungi and plants are present in human plasma (Semenov et al., 2012; Wang et al., 2012b). It seems possible therefore that various pathogens, including helminths, could also secrete RNA. Parasitic helminths are animals that encode an average of 50-200 miRNAs, many of these are highly conserved while some can arise in specific lineages (Britton, 2014). et al., have shown that in *S.mansoni*, of 112 miRNAs

identified 12% are conserved in other flatworms and 64% are unique to *S.mansoni* (Marco et al., 2013).

In this chapter, we explore the serum RNA profile in search for *S.mansoni* biomarkers. We demonstrate that rRNA, tRNA and miRNAs of host and parasite origin are present in serum. Importantly, we show that parasite-derived miRNAs can serve as biomarkers of *S.mansoni* infection.

4.2 SPECIFIC AIMS

1. To examine diagnostic potential of miR-199/214, miR-21, miR-210, miR-192, miR-194 and miR-122 as serum biomarkers of infection.
2. To investigate small RNA serum profile in naïve and *S.mansoni* infected mice and select additional biomarker candidates for further analysis.
3. To determine the serum abundance profile of parasite-derived miRNAs during the time course of *S.mansoni* infection.
4. To investigate diagnostic potential of parasite-derived miRNAs in the human *S.mansoni* endemic population.
5. To determine sensitivity and specificity of the proposed diagnostic test.

4.3 RESULTS

4.3.1 miR-199/214, miR-21 and miR-210 are up-regulated in mouse serum at 12 weeks post S.mansoni infection

Several studies have shown that liver-specific miRNAs are detectable in serum and can be used as biomarkers in liver disease. In line with this we examined whether the murine miRNAs that are altered in liver tissue are similarly altered in serum during *S. mansoni* infection. qRT-PCR was used to measure miRNA levels in the serum of mice infected with *S.mansoni* over a 12 week time course. The methodology of miRNA analysis in body fluids is not well standardized, and it is still not clear which small RNAs are appropriate for normalization (Hoy and Buck, 2012; Scholer et al., 2010; Weiland et al., 2012b). Here we used a constant amount of total RNA in the reverse transcription reaction. To account for any variation in qRT-PCR efficiency due to contaminants, miRNA levels were normalized to a

synthetic RNA oligo ("spike-in") that was included at the reverse-transcription step. The ratio of miRNA levels in infected versus age-matched naïve mice was quantified at each time point and plotted as fold change (Fig. 4.1). Compared to the analysis of liver samples (Chapter 3), there is more variation in the serum miRNA levels between biological replicates. As shown in Fig. 4.1, the levels of miR-192, miR-194 and miR-122 in serum do not change between 4-12 weeks post infection, whereas five of the miRNAs that are up-regulated in the liver are also significantly elevated in serum at 12 weeks post infection ($p<0.05$), ranging from 2.6 fold (miR-21) to 4.7 fold (miR-214) (Appendix 3). These five host miRNAs represent potential serum biomarkers of *S. mansoni* infection. However, since their levels do not change until 12 weeks post infection in mice, they may only be useful in cases of more advanced liver pathology.

4.3.2 Expression of miR-199/214, miR-21 and miR-210 fails to discriminate S.mansoni infected and uninfected individuals.

Having selected 5 host miRNAs candidates that were up-regulated at 12 weeks post infection as potential biomarkers of *S.mansoni* we extended our analysis to human patients. Serum samples from two field sites were examined: an area of high infection in the Piida community, Butiaba, which is situated on the shore of Lake Albert in Uganda (*S.mansoni* prevalence is 72% (Dunne et al., 2006; Kabatereine et al., 2004; Naus et al., 2003)) and an area of low infection in the Chiredzi community of Zimbabwe where *S.mansoni* is endemic with ~70% (67.9-74%) prevalence in school age children (Mduluza et al., 2009; Mutapi et al., 2002).

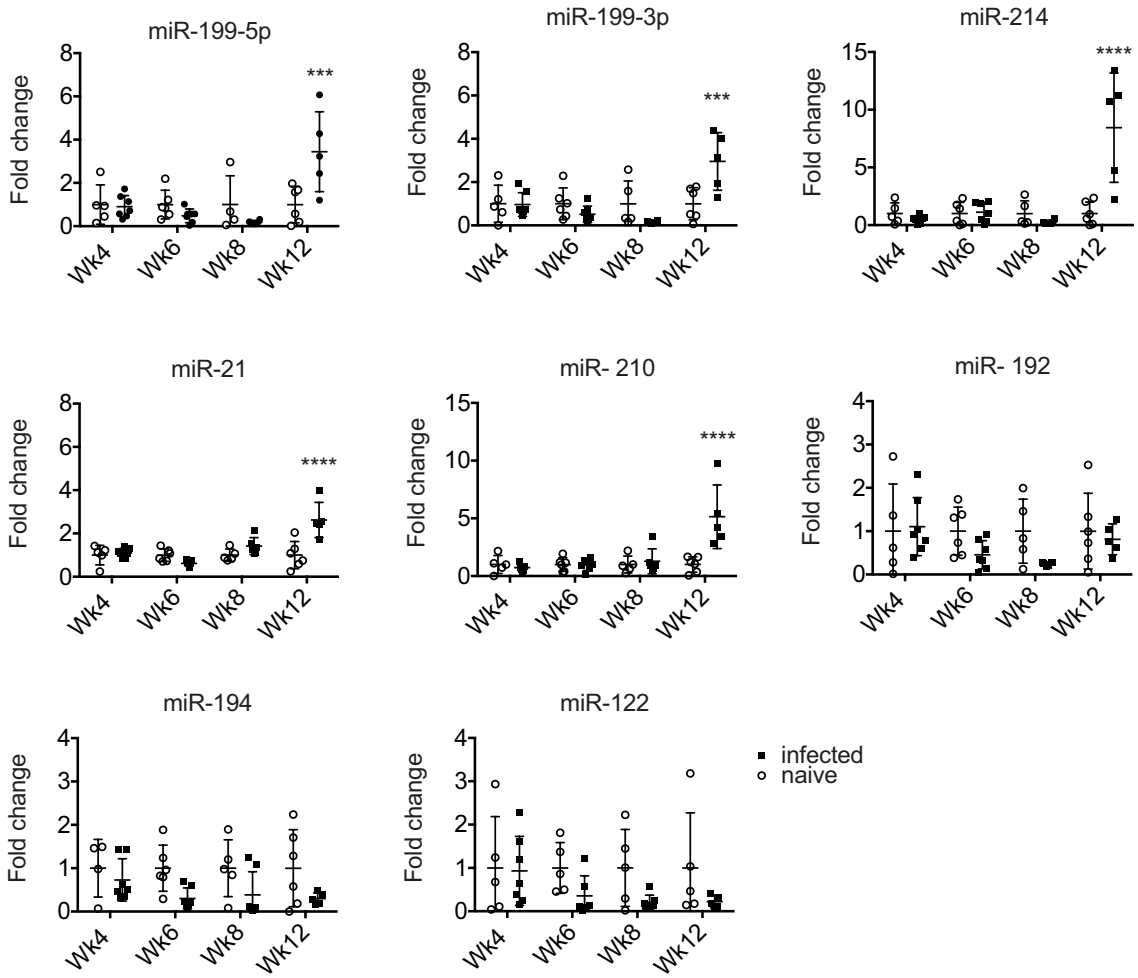

Figure 4.1 Differential abundance of host miRNAs in mouse serum during *S. mansoni* infection.

8-10 week old C57BL/6 mice were left uninfected or infected percutaneously with ~80 cercariae and euthanized at 4, 6, 8 and 12 weeks post infection. miRNAs were quantified by qRT-PCR and normalized to a synthetic RNA spike-in. Each symbol represents data from one individual mouse. Fold changes are defined as the ratio of abundance in infected versus naïve serum; the signal from naïve was set as 1. (***p<0.001, ****p<0.0001, Two-way ANOVA, Sidak multiple comparison test). Data represents 1 experiment. Wk4: infected n=6, naïve n=5, Wk6: infected n=6, naïve n=6, Wk8: infected n=5, naïve n=5, Wk12: infected n=5, naïve n=6).

The high infection samples were collected from mixed-age participants from Piida diagnosed as *S.mansoni* infected, termed 'egg positive' (n=20, epg=1117) and compared to volunteers from the same community with undetectable parasite eggs (n=10) in the stool, termed 'egg-negative'. The low infection samples were collected from children in Chiredzi diagnosed with *S. mansoni* (n=5, epg=108) and compared to age matched participants with undetectable eggs (n=10) by standard stool examination methods. The samples were non-randomly selected based on the infection intensity, sex and age. Demographic data of individuals are provided in Table 4.1 and Table 4.2.

Table 4.1 Piida study cohort.

Characteristic	Egg-negative (n=10)	Egg-positive (n=20)
Age (range)	33.1 (17-48)	24.2 (7-56)
Sex (F/M)	5/5	9/11
S.mansoni status (epg&range)	0	1117 (105-4030)

Table 4.2 Chiredzi study cohort.

Characteristic	Egg-negative (n=9)	Egg-positive (n=5)
Age (range)	10.67 (8-11)	10 (9-11)
Sex (M/F)	6/3	2/3
S.mansoni status (epg&range)	0	108 (39-207)

The data obtained by qRT-PCR have been median normalised to the synthetic spike-in. The fold change was calculated as described in (Chapter 2: Materials and Methods (2.9.4)). The 5 host miRNAs (miR-21, miR-199a-3p, miR-199a-5p, miR-210, miR-214) were detectable in human serum with variable abundance. Unfortunately, these miRNAs did not discriminate between 'egg-positive' and 'egg-negative' participants (Fig. 4.2).

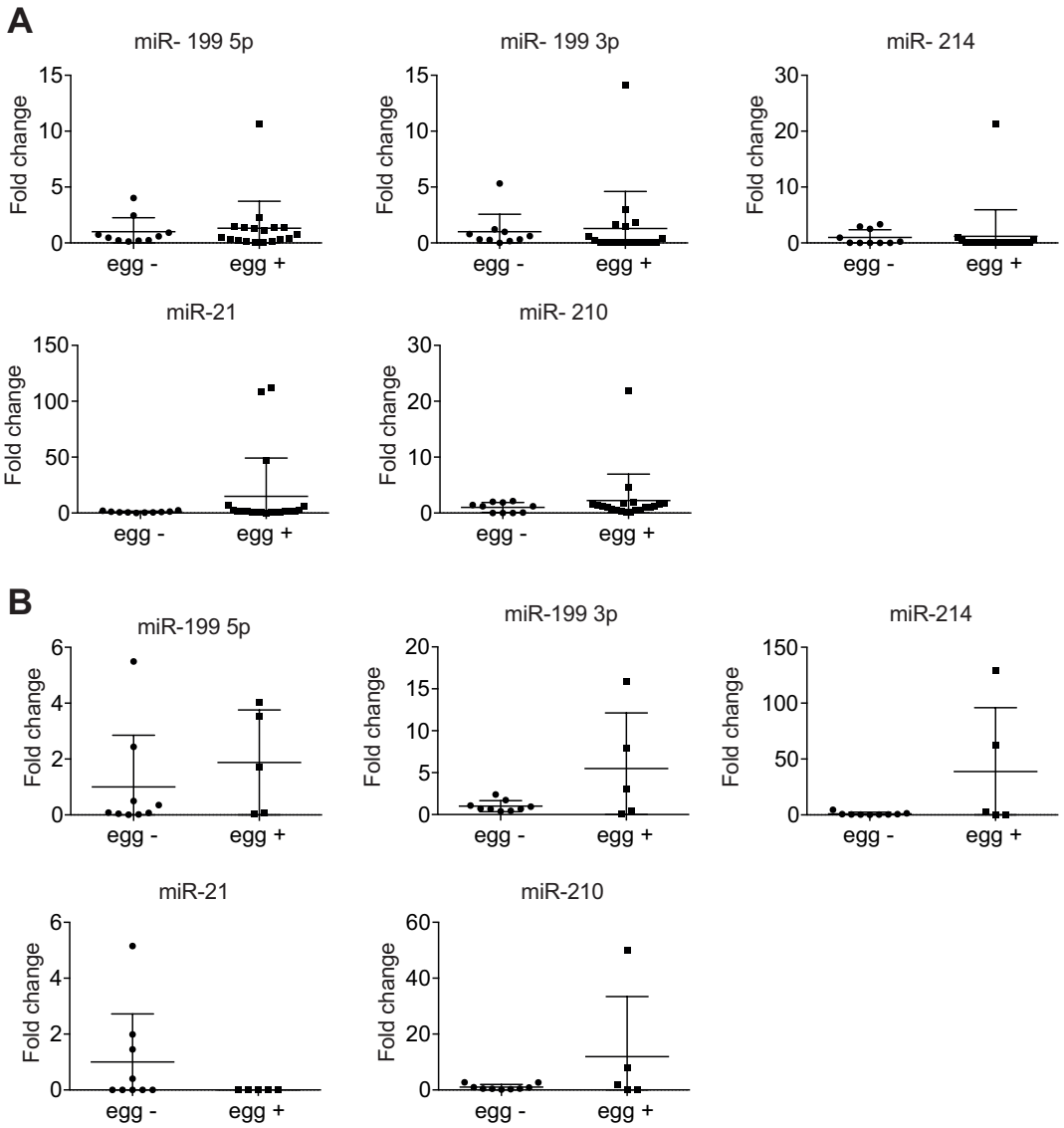

Figure 4.2 Abundance of host miRNAs in serum of *S. mansoni* egg-positive and egg-negative individuals.

Venous blood was collected from individuals from Piida and Chiredzi and serum was obtained by centrifugation. *S.mansoni* infection status was determined using the Kato-Katz faecal smear method. Serum RNA was extracted using miRVANA Paris kit. miRNAs were quantified by qRT-PCR, normalized to a synthetic RNA oligo "spike-in" and fold changes were calculated as the ratio of infected to uninfected individuals. Piida: panel A, Chiredzi: panel B. Mann-Whitney test was used and p-values of <0.05 was considered significant.

4.3.3 The RNA content of mouse serum is dominated by small RNAs

To investigate the distribution of small RNA populations of serum, total serum RNA was ^{32}P pCp 3' end labelled and analysed on a 10% denaturing polyacrylamide gel. With this approach only fragments with 3' hydroxyl group can be labelled. As shown in Fig 4.3, mouse serum contains small RNA species in size ranging from 18-100 nt including a population of ~22 nt characteristic of most miRNAs. Surprisingly, the most abundant RNA species are 30-35nt in length. To characterize these small RNAs, total RNA from serum of naïve mice or mice infected with *S.mansoni* were sequenced using the Illumina platform (Fig 4.4). For small RNA sequencing in experiment 1, total RNA was extracted from serum of 8 pooled *S.mansoni*-infected mice (Wk. 7, 180 cercariae) and 8 uninfected age matched controls (400μl total volume) according to the miRVana PARIS protocol (as described in Materials and Methods). The small RNAs were size selected by 15% PAGE and prepared according to the Illumina small RNA Sample Preparation Kit version 1.5 and sequenced on the GAIIX. For small RNA sequencing in experiment 2, total RNA was extracted from serum of 3 pooled *S.mansoni* infected mice (Wk 8, 80 cercariae) and 3 uninfected age matched controls (300μl total volume) according to the miRVana PARIS protocol. The library was prepared according to the TruSeq Small RNA protocol (without size-selecting small RNA) and sequenced on the HiSeq2. We have specifically chosen to examine the small RNA population in those two infection conditions. By looking at the serum RNA profile of mice infected with 180 cercariae ("super-infection") we aimed to maximise the chance of finding altered small RNAs, whereas an infection with 80 cerecarie, provides insight into a more "natural" infection. Although examining the small RNA profile during the whole time course of infection would be of benefit, we have chosen a time point that coincides with a peak of Th2 response, substantial granulomas and liver fibrosis. Further, two different library preparation protocols and sequencing platforms have been used to minimise ligation and sequencing associated bias.

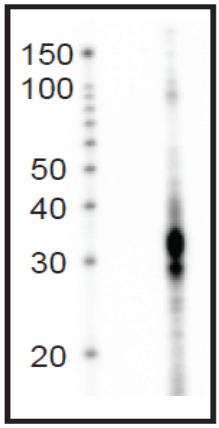

Figure 4.3 ^{32}P pCp labelled total mouse serum RNA (125ng) separated on 10% PAGE. Total naïve C57/Bl6 mouse serum RNA was extracted using miRVana PARIS kit. Approximately 125ng of RNA was labeled with ^{32}P pCp and separated on a 10% PAGE.

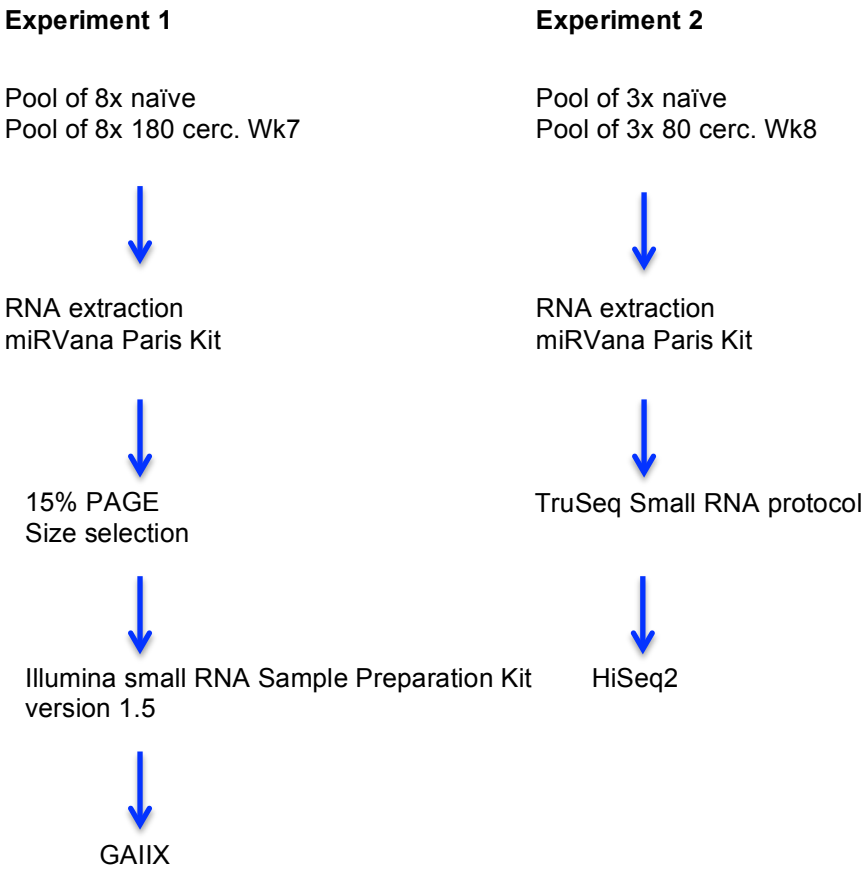

Figure 4.4 Mouse serum deep sequencing- experimental outline.

In both experiments, the majority of small RNA reads aligned to the mouse genome (ranging from 64-70%, Table 4.4). Approximately 30% of sequence reads did not align to either mouse or *S.mansoni* genome. These sequences are presumably of bacterial origin and were not analysed further. A small percentage of reads unambiguously aligned to the *S. mansoni* genome in infected mice (0.04 - 0.14%); <0.01% of reads mapped to the *S. mansoni* genome in naïve samples. Only 1 – 6% of the reads that mapped to the mouse genome were miRNAs (Table 4.3, listed in Appendix 6). The majority of reads in all samples were 29-33nt fragments derived from tRNAs: 92-98% of the reads that mapped to the mouse genome and 42-100% of reads that mapped to the *S. mansoni* draft genome (Table 4.3).

4.3.4 RNA deep sequencing reveals the presence of parasite-specific miRNAs in sera of S.mansoni infection but not control mice

A total of 78 and 225 mature miRNAs are known to be encoded by the trematodes *S.japonicum* and *S.mansoni*, respectively (de Souza Gomes et al., 2011; Kozomara and Griffiths-Jones, 2011; Marco et al., 2013; Wang et al., 2010; Xue et al., 2008), and further miRNAs have been predicted (de Souza Gomes et al., 2011). Analysis of the reads that mapped to the *S. mansoni* draft genome using the miRdeep2 program (Friedlander et al., 2012) identified at least 11 miRNAs from infected samples: 8 of these were positively identified based on identity to known miRNAs in *S. mansoni* and/or S.*japonicum* (Table 4.4) (Wang et al., 2010; Xue et al., 2008) and 3 are predicted by miRdeep (here named sma-miR-n1, sma-miR-n2 and sma-miR-n3). The predicted stem-loop structures for the putative pre-miRNAs are shown in Fig. 4.5; since the depth of coverage of *S. mansoni* reads in this study was very low and reads did not map to both arms of the hairpin, these can not yet be considered prototypical miRNAs. However, sma-miR-n3 shares a seed site with *Schmidtea mediterranea* miR-2160 and was annotated as sma-miR-8437 in a study of *S. mansoni* miRNAs published recently (Marco et al., 2013). Additional analysis of the datasets allowing 1 mismatch to the *S. mansoni* draft genome identified one further miRNA from infected but not naïve serum: miR-277, which is identical to miR-277 in *S.japonicum* and *Echinococcus granulosus* but has a C→T mutation at position 17 in relation to

the *S. mansoni* draft genome (Table 4.4). Other reads from infected samples that aligned are detailed in Appendix 7. It is possible that some of these less abundant sequences derive from real miRNAs but the coverage in these studies is not sufficient to conclude this.

Table 4.3 Small RNA classification in serum of naïve and infected mice.

	Illumina Small RNA		TruSeq	
	Naïve	Infected 7 weeks 180 cercariae	Naïve	Infected 8 weeks 80 cercariae
Trimmed reads	19,992,215	19,687,439	5,360,110	6,975,834
Mouse genome match	12,864,294	12,771,443	3,786,803	4,621,905
Unambiguous	**12,841,090(64.2%)**	**12,430,681 (63.1%)**	**3,779,361 (70.5%)**	**4,613,742 (66.1%)**
rRNA	6493 (0.05%)	51173 (0.4%)	377 (0.01%)	6499 (0.14%)
tRNA	12,615,823 (98.2%)	11,464,782 (92.2%)	3,736,007 (98.9%)	4,409,765 (95.6%)
other rfam	7579 (0.06%)	14563 (0.012%)	514 (0.014%)	1758 (0.04%)
miRNA	128,222(1.0%)	772,150 (6.2%)	36,615 (1.0%)	158,069 (3.4%)
Uncharacterized	82973 (0.6%)	128013 (1%)	5848 (0.16%)	37651 (0.8%)
S.mansoni genome match				
Unambiguous	**1,683 (<0.01%)**	**27,347(0.14%)**	**529 (<0.01%)**	**2,914 (0.04%)**
rRNA	272 (16.2%)	2828 (10.3%)	0	182 (6.2%)
tRNA	1,236 (73.4%)	20,191 (73.8%)	529 (100%)	1,231 (42%)
other rfam	52 (3.1%)	117 (0.4%)	0	22 (0.75%)
miRNA	2 (0.12%)	148 (0.54%)[1]	0	25 (0.9%)
Uncharacterized	121 (7.2%)	4,063 (15%)	0	1,454 (49.9%)

[1]This does not include 42 reads identical to sja-miR-277 that contain 1 nucleotide mismatch to *S. mansoni* draft genome.

Table 4.4 Parasite-miRNAs in serum of mice infected with *S. mansoni* identified by deep-sequencing.

Name	miRNA sequence (5'-3')	Precursor Location	Reads[2]
sja-miR-277[1]	UAAAUGCAUUUUCUGG**C**CCGUA	Inferred from sja-miR-277 in miRBase	42
sma-bantam	UGAGAUCGCGAUUAAAGCUGGU	S_mansoni.SC_0137:369450..369509:+	37
sja-miR-2162-3p	UAUUAUGCAACGUUUCACUCU	S_mansoni.SC_0049:36195..36251:+	29
sma-miR-3479-3p	UAUUGCACUAACCUUCGCCUUG	S_mansoni.Chr_4.unplaced.SC_0032:1561293..1561349:-	16
sma-miR-10-5p	AACCCUGUAGACCCGAGUUUGG	S_mansoni.Chr_4:19959278..19959336:-	4
sma-miR-2a-3p	UCACAGCCAGUAUUGAUGAAC	S_mansoni.Chr_W:22875762..22875816:+	3
sma-let-7-3p	CAUACAACCGACUGGCUUUCC	S_mansoni.Chr_7:5118795..5118860:+	2
sma-miR-71a-3p	UGAAAGACGAUGGUAGUGAGAU	S_mansoni.Chr_W:22875670..22875724:+	2
sma-miR-n1	AACUCAGUGGCCUAUCGGU	S_mansoni.Chr_1:18109172..18109229:-	9
sma-miR-n2	UCAGCUGUGUUCAUGUCUUCGA	S_mansoni.SC_0170:285549..285631:-	66
sma-miR-n3 (sma-miR-8437)	UGGCGCUUAGUAGAAUGUCACCG	S_mansoni.Chr_3:22962153..22962218:+	7

[1]The nucleotide which does not match the *S. mansoni* draft genome is shown in bold; [2]Reads in combined infected samples (compared to a combined total of 930,209 mouse miRNAs in the same samples, Appendix 6).

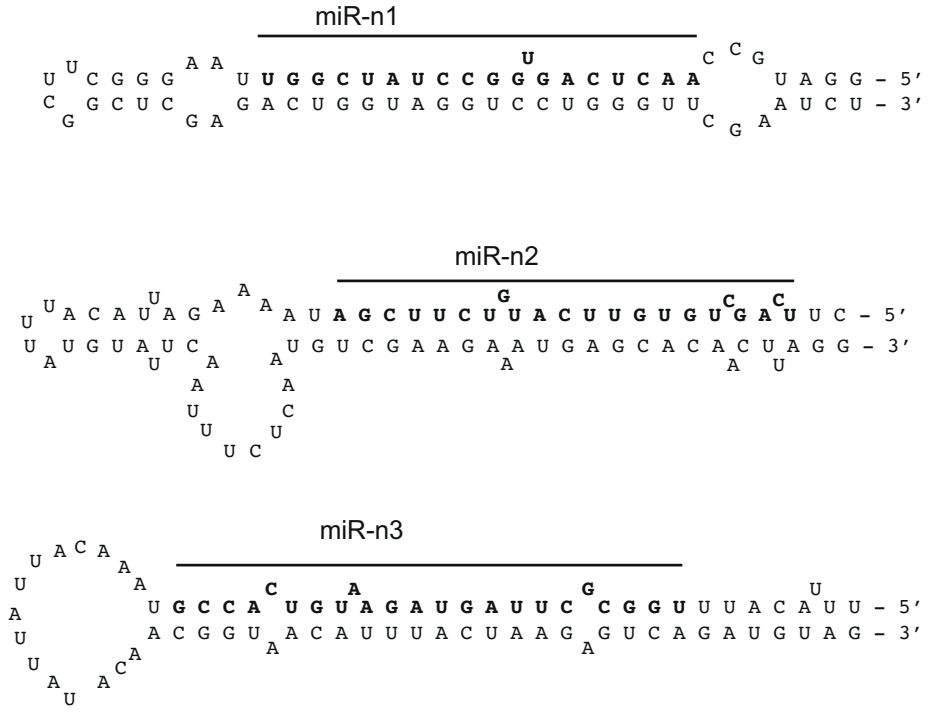

Figure 4.5 Predicted stem-loop structures of the *S. mansoni* miRNAs identified in this study. The mature sequence that was identified in serum is shown in bold.

4.3.5 S.mansoni-specific miRNAs are present in mouse serum as early as 8 weeks post infection

Using a deep-sequencing approach we identified 11 parasite-derived miRNAs in serum of *S.mansoni* infected mice. To determine their kinetic profile in serum during *S. mansoni* infection, qRT-PCR analysis was carried out as described above, using primers specific for 9 of the 11 parasite miRNAs. The other 2 miRNAs, sma-miR-10-5p and sma-let-7-3p, were excluded from analysis because they are highly similar to homologous mouse miRNAs that are present at > 100 fold higher read frequencies (Appendix 6). Importantly, most miRNAs in helminth parasites have evolved after the last common ancestor with their vertebrate hosts and are therefore distinguishable in sequence, however several miRNAs are perfectly conserved across animals or highly similar in sequence (Kozomara and Griffiths-Jones, 2011). Several of the parasite-specific probes showed a signal in the serum of naïve mice (background), which is presumably due to cross-hybridization with endogenous small RNAs. In cases where no signal was observed in naïve mice, the maximum cycle value of 50 was set as background for the purpose of calculating signal over noise (which we interchange here with "fold change"). Six of the nine parasite miRNA probes tested (miR-277, bantam, miR-3479-3p, miR-2a-3p, miR-n1, miR-n2) showed a statistically significant signal over noise at 8 or 12 weeks post infection (Fig. 4.6 $p<0.05$); the three miRNAs that were not reliably detected (miR-n3, miR-71a-3p, miR-2162-3p) were not analysed further. The average signal over noise ratios for each probe during the time course of infection are provided in Appendix 8 and range from 4.2 to > 3,000.

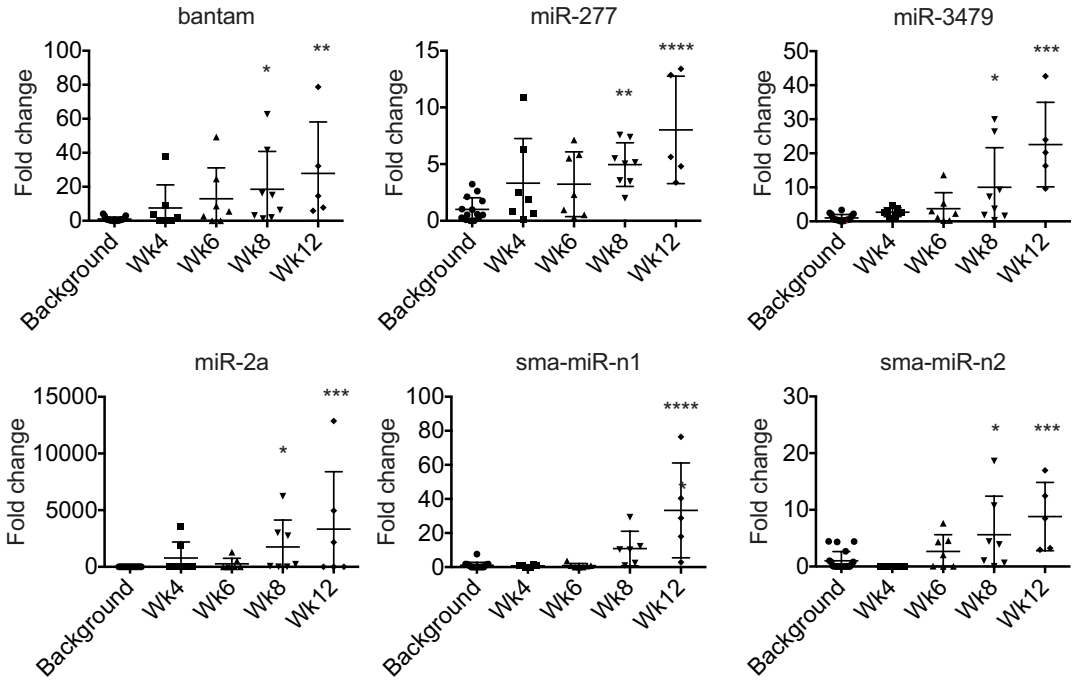

Figure 4.6 Detection of parasite-derived miRNAs in mouse serum during *S. mansoni* infection.

8-10 week old C57BL/6 mice were left uninfected or infected percutaneously with ~80 cercariae and euthanized at 4, 6, 8 and 12 weeks post infection. miRNAs were quantified by qRT-PCR, normalized to a synthetic RNA spike-in and signal over noise calculated as the ratio of abundance in infected serum compared to the background abundance level detected in naïve serum, which represents the noise in the assay likely derived from cross-hybridization with endogenous small RNAs. One-way ANOVA followed by Holm-Sidak multiple comparison (*p<0.05, **p<0.01, ***p<0.001, ****p<0.0001).

4.3.6 Three S. mansoni miRNAs are detected in human serum and distinguish egg-negative from egg-positive individuals

Based on the results described above (4.3.5), we extended the analyses of parasite derived-miRNAs to human patients from an area of high infection in the Piida community of Uganda and an area of low infection in the Chiredzi community of Zimbabwe. The signal over noise was calculated (as described in Materials and Methods (2.9.4)) using synthetic spike-ins for normalization. Unlike host miRNAs, three out of the six parasite miRNAs (bantam, miR-277 and miR-3479-3p) displayed a significant signal over noise level in the serum of *S. mansoni* infected individuals 'egg-positive' from both high (Fig. 4.7A) and low (Fig. 4.7B) infection endemic areas, compared to the 'egg-negative' participants from the same communities ($p<0.05$, Mann – Whitney test). miR-n1, miR-n2 and miR-2a-3p were below the detection limit (Ct=50) in both 'egg-positive' and 'egg-negative' samples (not shown).

Receiver Operating Characteristic (ROC) curve analysis were used to assess the specificity, sensitivity and accuracy of a *S.mansoni* diagnostic test where a single parasite-miRNA was used to discriminate between infected and uninfected individuals. Data presented using ROC curves show that the single parasite miRNA discriminated between *S. mansoni* 'egg-negative' and 'egg-positive' with an area under the curve (AUC) of 0.785, 0.790, 0.768 for bantam, miR-277 and miR-3479-3p, respectively, in the individuals from Uganda (Fig. 4.7A) and 0.889, 0.933, 0.911 in the individuals from Zimbabwe (Fig. 4.7B). Using optimal cut-off points (highest sensitivity and specificity pair), this translates to detection of *S. mansoni* infected individuals with specificity/sensitivity of 80%/60%, 80%/70% and 80%/60 in the patients from Uganda (Fig. 4.7 A) and specificity/sensitivity of 100%/60% 89%/80% and 89%/80% respectively in the patients from Zimbabwe (Fig. 4.7 B). When combining the data for all three of the miRNAs into a cumulative value, the AUC increased to 0.845 and 0.933 for each cohort of participants. This resulted in improved specificity/sensitivity in detection for samples from Uganda (80%/90%) using a fold change cut-off of 1.189 (Fig. 4.8). This approach is very similar to a

recent report that uses a "miRNA score" based on cumulative normalized signals of miRNAs (Goren et al., 2012). Analysis of our data based on cumulative fold change or "miRNA score" yields very similar results (Fig 4.9). These results show that combining data for bantam, miR-277 and miR-3479-3p may improve sensitivity of *S. mansoni* diagnosis compared to analysis of individual miRNAs.

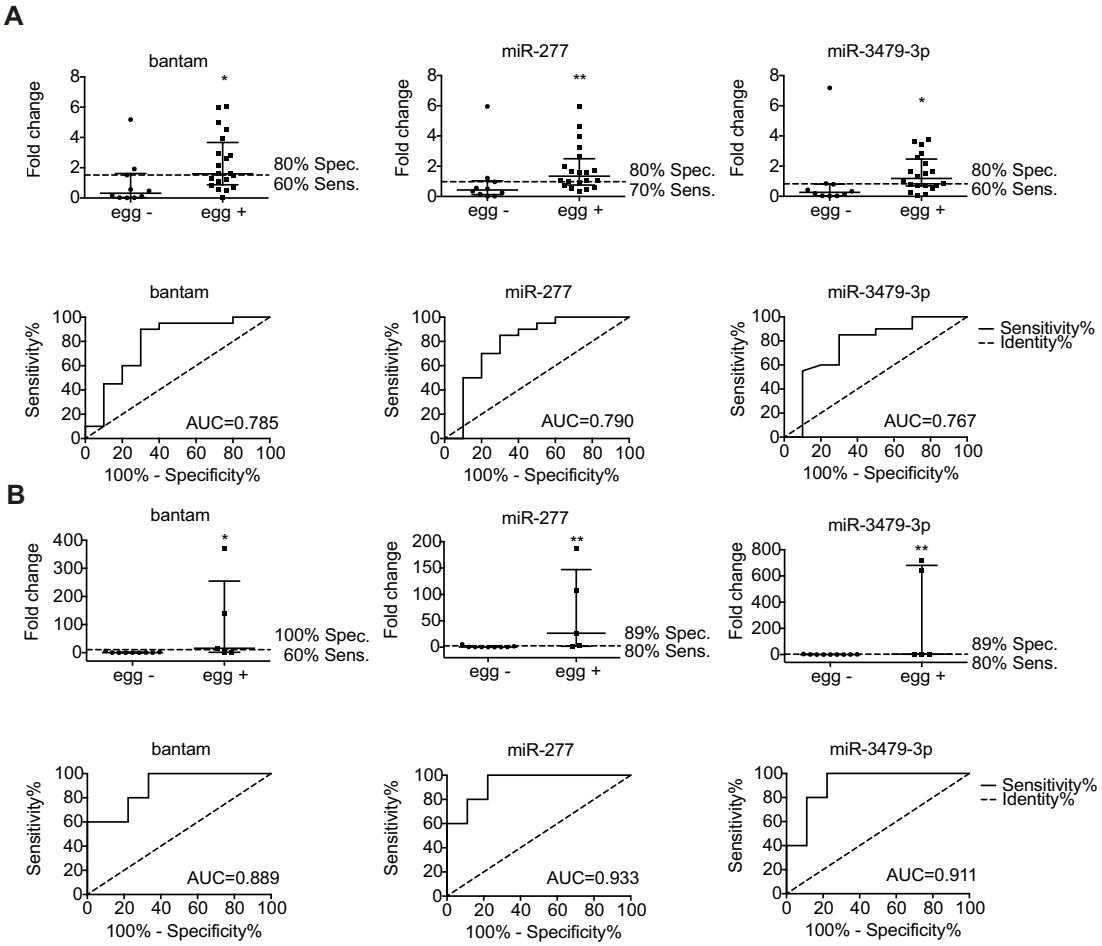

Figure 4.7 Discrimination between the *S. mansoni* infected and uninfected individuals using parasite-specific miRNA detection.

Venous blood was collected from individuals from Piida and Chiredzi and serum was obtained by centrifugation. *S.mansoni* infection status was determined using the Kato-Katz faecal smear method. Serum RNA was extracted using miRVANA Paris kit. miRNAs were quantified by qRT-PCR, normalized to a synthetic RNA oligo "spike-in" and fold changes were calculated as the ratio of infected to uninfected individuals (median with interquartile range indicated).Piida: panel A, Chiredzi: panel B. Man-Whitney test (*p<0.05, **p<0.01). Specificity and sensitivity and ROC curves with AUC are indicated.

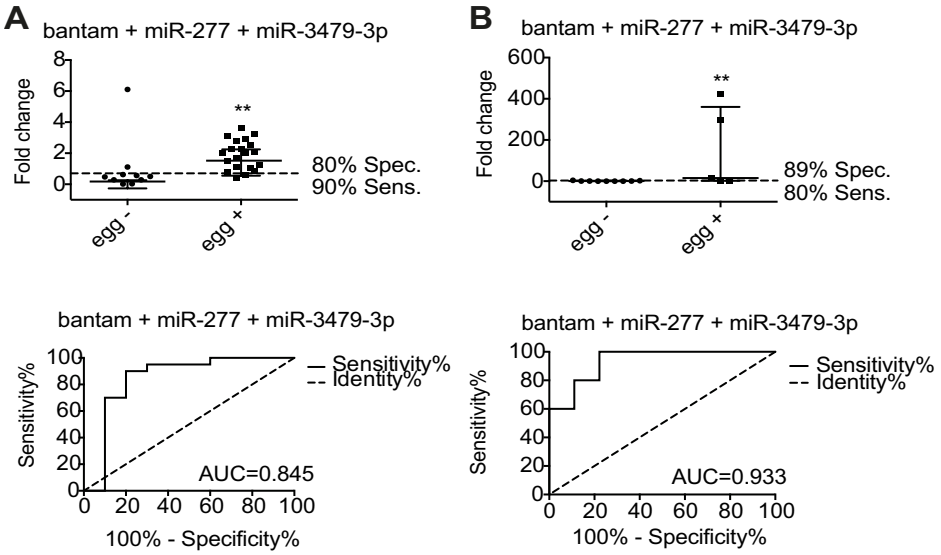

Figure 4.8 Discrimination between the *S. mansoni* infected and uninfected individuals using the combined data for 3 parasite miRNAs.

Venous blood was collected from individuals from Piida and Chiredzi and serum was obtained by centrifugation. *S.mansoni* infection status was determined using the Kato-Katz faecal smear method. Serum RNA was extracted using miRVANA Paris kit. miRNAs were quantified by qRT-PCR, normalized to a synthetic RNA oligo "spike-in" and fold changes were calculated as the ratio of infected to uninfected individuals (median with interquartile range indicated). Obtained fold changes for bantam, miR-277and miR-3479-3p were combined (arithmetic mean) into one cumulative fold change and plotted on the graph.Piida: panel A, Chiredzi: panel B. Man-Whitney test (**p<0.01). Specificity and sensitivity and ROC curves with AUC are indicated.

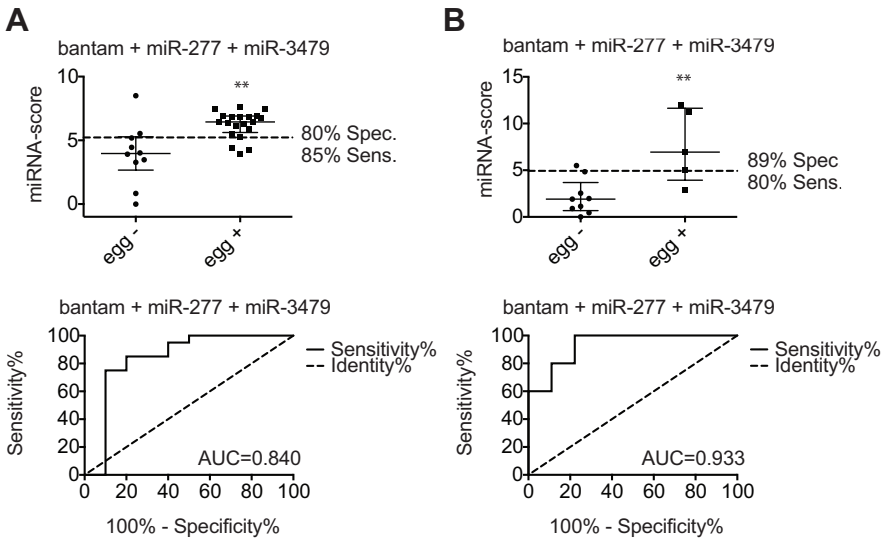

Figure 4.9 Discrimination between the *S. mansoni* infected and uninfected patients using the miRNA-score.

Venous blood was collected from individuals from Piida and Chiredzi and serum was obtained by centrifugation. *S.mansoni* infection status was determined using the Kato-Katz faecal smear method. Serum RNA was extracted using miRVANA Paris kit. miRNAs were quantified by qRT-PCR, normalized to a synthetic RNA oligo "spike-in" and miRNA-score was calculated as described by (Goren et al., 2012). Piida- panel A, Chiredzi- panel B. Man-Whitney test (**$p<0.01$). Specificity and sensitivity and ROC curves with AUC are indicated.

4.4 SUMMARY

- miR-miR-199/214, miR-21 and miR-210 are up-regulated in mouse serum at 12 weeks post *S.mansoni* infection.
- miR-miR-199/214, miR-21 and miR-210 fail to discriminate 'egg-positive' and 'egg-negative' individuals.
- The RNA content of serum that can be labelled with pCp is dominated by small RNAs: miRNAs, tRNAs, rRNAs.
- 11 parasite derived miRNAs were identified to be present in sera of infected mice.
- miR-277, bantam, miR-3479-3p, miR-2a-3p, miR-n1, miR-n2 showed a statistically significant signal over noise at 8 or 12 weeks post infection.
- miR-277, bantam, miR-3479-3p displayed a significant signal over noise level in the serum of *S. mansoni* infected individuals.
- The single parasite miRNAs (bantam, miR-277 and miR-3479-3p) discriminated between *S. mansoni* 'egg-negative' and 'egg-positive' individuals with specificity/sensitivity of 80%/60%, 80%/70% and 80%/60 in the patients from Uganda and 100%/60% 89%/80% and 89%/80% respectively in the patients from Zimbabwe.
- Combining data for bantam, miR-277 and miR-3479-3p improve sensitivity of *S. mansoni* diagnosis compared to analysis of individual miRNAs (Uganda data).

4.5 DISCUSSION

S.mansoni infection leads to hepatic inflammation, portal hypertension, splenomegaly, upper gastrointestinal tract varices, peri-portal (Symmer's) fibrosis (Gryseels et al., 2006) making early diagnosis essential for patient management. The recent evidence that miRNAs can be released into the circulation from mammalian cells and tissues has stimulated extensive interest in the potential use of these molecules as biomarkers (Etheridge et al., 2011; Kosaka et al., 2010a; Weiland et al., 2012b). miRNA-based diagnostics are being developed for a number of diseases and although qRT-PCR is the most common detection method at present, there is

extensive interest in improving and diversifying detection technologies, which may provide more field-friendly tools. Since miRNAs have been shown to be extremely stable in body fluids (Chen et al., 2008b; Li et al., 2011b; Mitchell et al., 2008), we anticipate that these nucleic acids could be particularly useful as diagnostics in field settings where collection and storage conditions can be difficult to control. Thus, the main aim of this chapter was to develop miRNA-based biomarkers of *S.mansoni* infection.

A number of reports have demonstrated an increase in miR-122 and miR-192 in plasma or serum during viral infection as well as chemically induced liver disease (Starkey Lewis et al., 2012; Zhang et al., 2010a). He et al., showed that levels of miR-223, miR-122 and miR34a were elevated and miR-199a-3p, miR-199a-5p and miR-146b were decreased in serum at 6 weeks post upon S.*japonicum* infection in BALB/c mice with miR-223 levels decreasing post praziquantel (PZQ) treatment (He et al., 2013). However, according to our analysis, although miR-192, miR-122 and miR-194 were down-regulated in the liver during infection, their levels in mouse serum did not change significantly. In contrast, the miRNAs up-regulated in the liver (miR-199a-3p, miR-199a-5p, miR-21, miR-214 and miR-210) showed significantly higher levels in mouse serum at 12 weeks post infection, suggesting that these miRNA could represent a marker of advance *S.mansoni* pathology. Unfortunately, when we examined the expression of miR-199a-3p, miR-199a-5p, miR-21, miR-214 and miR-210 in individuals from *S.mansoni* endemic areas, these failed to differentiate *S.mansoni* infected from uninfected humans.

Our alternative strategy, in search for miRNA candidate biomarkers was to examine the small RNA population of serum using a deep-sequencing approach. This approach allows quantification of known miRNAs and discovery of new small RNA sequences. Unlike most of the available reports, our bioinformatics analysis showed that only a small percentage of reads that mapped to mouse genome are miRNAs. Interestingly, the majority of reads were 29-33nt fragments derived from tRNAs: 92-98% of the reads that mapped to the mouse genome and 42-100% of reads that mapped to the *S. mansoni* draft genome. It is important to note, however, that due to

the sequence similarity of the tRNAs between species, we cannot at this point definitively determine the organism from which they derive. One could argue that this could be due to random degradation or contamination with cellular material during library construction. However, if this was a case we might also expect to see an enrichment in rRNA fragments which is not the case. Further analysis of the tRNA population in serum is discussed in Chapter 5 of this thesis.

We found that miRNAs derived from the helminth parasite *S.mansoni* are present in infected mouse and human serum. The fact that they are not present in the serum of uninfected mice offers advantages over endogenous miRNAs as biomarkers of infection which differential abundance can derive from multiple cells and can be attributed to unrelated conditions. Specifically, we found 9 known miRNAs and at least 2 novel putative miRNAs derived from *S. mansoni* that are present in the serum of infected mice. The read counts of some of these are very low (between 2-66 reads as compared to 89,415 reads for most abundant miRNAs -miR-122) and will require further validation with better coverage. However, we show that three of these miRNAs (bantam, miR-277, mirR-3479-3p) can be detected in human serum from schistosome endemic areas. Notably, a study published recently identified 5 miRNAs derived from *S.japonicum* in the plasma of infected rabbits and 3 of these are identical or homologous to those identified here: bantam, miR-3479-3p and miR-10-5p (Cheng et al., 2013), providing independent validation for the presence of trematode miRNAs in the serum of infected animals.

It is intriguing to think that the existence of these miRNAs outside the parasite has a function. Given the short size of miRNAs and the fact that they do not require perfect complementarity with their targets, one could predict hundreds of possible targets in the host. Interestingly, Xue et al., showed that three of the miRNAs that we find in serum (sja-bantam, sja-miR-71 and sja-let-7) are expressed during all the stages of parasite development but are enriched in the cercariae, suggesting that they may be important during the initial stages of schistosome infection (Xue et al., 2008). The bantam miRNA has been implicated in regulating organ growth in response to

environmental conditions in *Drosophila* as well as *C.elegans* (Brennecke et al., 2003; Schaedel et al., 2012) but functional homologues of bantam do not exist in mammals.

This work extends an area of research detailing "foreign" small RNAs in body fluids. Zhang et al., recently reported that the plant miRNA, miR-168a, is present in human and animal serum and demonstrated that this derives from a rice diet (Zhang et al., 2012). Wang et al., showed that a wide range of exogenous RNAs can be found in human plasma, including small RNAs derived from bacteria and fungi (Wang et al., 2012b). From our results it is not yet clear whether the miRNAs identified in serum are actively secreted from the parasite and how they are stabilized, since serum contains high amounts of RNases (Blank and Dekker, 1981; Kamm and Smith, 1972). From the time course analysis presented here, schistosome-derived small RNAs were reliably detected in serum by 8 weeks post infection, after deposition of the eggs in the liver. However, further *in vitro* and *in vivo* studies would be required to determine whether these RNAs in circulation are derived from the eggs and/or adult worms; this is relevant to diagnostic applications, for example the capacity to detect pre-patent infection.

An ideal biomarker should: i) have 100% sensitivity and specificity, ii) have an ability to diagnose the disease at the early time point, which in case of *S.mansoni* infection should be prior to parasite egg secretion, iii) have minimal and predictable inter-individual variability, iv) be minimally invasive, v) and its measurement should be robust, rapid, simple, accurate and inexpensive. Importantly, we have shown here that parasite-derived miRNAs can be detected in human serum by qRT-PCR and can distinguish 'egg-negative' from 'egg-positive' individuals in areas of both low and high infection intensity. By combining data for miR-277, miR-3479-3p and bantam we detected infection with a sensitivity of 80-90% and specificity of 80-89%. We anticipate that this may be improved further by optimizing RNA isolation protocols, probe design and more robust methods for normalizing the data. Since one of the main requirements for diagnosis of schistosomiasis is the development of more sensitive assay it is of great importance to examine the performance of the parasite-derived miRNAs against the "gold standard" Kato-Katz assay, which offers 100%

specificity. The performance of our parasite-derived miRNAs test is comparable to the PCR technique for detection of *S.mansoni* DNA in human faeces published by (Pontes et al., 2003b). The authors showed that sensitivity and specificity of their PCR test was 97% and 88% as compared to the Kato-Katz (79% and 100%). Further, it is of importance to examine the abundance of parasite-derived miRNAs in serum upon infection with other *Schistosoma* species and other helminths to further evaluate their specificity.

Further improvements and standardisation of the methodology of analysis of circulating miRNAs are also necessary before they can be applied in the hospital or field settings. Firstly, it is important to unify the method of blood collection and processing into serum and plasma as the preparation process, specifically centrifugation, affects the amount of contaminating cellular RNA. This is especially problematic in plasma samples (Duttagupta et al., 2011; McDonald et al., 2011). For this reason we used serum rather than plasma samples in our studies. Moreover, as miRNAs are present in red blood cells (Chen et al., 2008a; McDonald et al., 2011) the degree of haemolysis also affects the miRNA profile in serum or plasma. It seems that not all miRNAs are affected by haemolysis, it has been shown that miR-16 and miR-15a levels increase in the haemolysed sample whereas miR-122 expression remains unchanged (McDonald et al., 2011).

Secondly, it is crucial to unify the RNA extraction process, RT method, qRT-PCR and normalisation. As shown by MacDonald et al., assay imprecision (imprecision under the same operating conditions over a short interval of time, imprecision within and between laboratories) significantly affect the reproducibility of miRNA measurements, with the highest intra-assay imprecision being due to RNA extraction step. The authors suggest that longer incubation of serum with the denaturing solution when using the column-based extraction protocols (miRVANA) or use of liquid-liquid extraction protocols (TRIzol LS) can decrease assays' imprecision. Thus, it is important to further improve the available extraction methods and introduce a set of controls, such as inter-assay controls or extraction efficiency controls. Additionally, studies focused on revealing the origin of circulating miRNAs

have shown two populations of miRNAs: those associated with protein complexes and those encapsulated in vesicles (Arroyo *et al*., 2011; Turchinovich *et al*., 2011; K. Wang *et al*., 2010). This finding needs to be taken into account when using these molecules as biomarkers since the stability of miRNAs in serum and the efficiency of their extraction may vary if they are present in different complexes. Further work on how and when the miRNAs are secreted to the extracellular environment is necessary to realise their potential as diagnostic biomarkers.

The main limitation of parasite derived miRNA detection in serum appears to be cross-hybridization of the probes with endogenous small RNAs, which influences the signal to noise ratios. In particular, we report the finding that the majority of small RNAs in mouse serum are derived from tRNAs, consistent with a recent study (Dhahbi et al., 2013). It is possible that depletion of these tRNAs prior to qRT-PCR may improve the specificity or sensitivity of miRNA detection; this requires further investigation. In addition, one of the parasite-derived miRNAs identified by sequencing, miR-2162-3p could not be validated by qRT-PCR, likely owing to its low GC content (33%). Optimization of probe design for the parasite-derived miRNAs may also greatly increase their diagnostic utility in larger scale studies in human patients.

The methodology of analysis of miRNAs in body fluids is not unified and it is still not clear which small RNAs are appropriate for normalisation (Hoy and Buck, 2012; Scholer et al., 2010; Weiland et al., 2012b). To overcome these challenges, in cases when quantification of RNA was possible, we used a constant amount of total RNA as an input to the reverse transcription reaction. To account for any variation in qRT-PCR efficiency due to contaminants, miRNA levels were normalized to a synthetic RNA oligo ("spike-in") that was included at the reverse-transcription step. When RNA levels were below the detection limit, we used a constant volume in the reverse transcription reaction and included a synthetic RNA oligo ("spike-in") at the extraction step to account for variability in purification procedure and amplification efficiency. Obtained Ct values were "median-normalized" to synthetic RNA spike-in as described previously (Mitchell et al., 2008): relative change was calculated as 2^{-Ctn},

where Ctn stands for normalized Ct values. The caveat of using a spiked miRNA as a normaliser is a limited ability to control for the internal variations of the overall serum miRNA expression levels between individuals which is especially important when working with host-derived miRNAs. An alternative to this approach could be the use of a panel of invariant miRNAs. This requires profiling miRNAs under both conditions (uninfected and infected) using microarray, or deep sequencing followed by selection of a miRNA panel and further validation by qRT-PCR. Available programs such as NormFinder (available at: http://moma.dk/normfinder-software)(Andersen et al., 2004) and GeNorm (available at: http://medgen.ugent.be/~jvdesomp/genorm/) (Mestdagh et al., 2009) can aid analysis of data to select the best candidates. This approach proved to be successful in determining tissue/cell normalisers; however, to date, the determination of reliable, invariant miRNAs in body fluids is still a challenge.

The work presented here was performed on a relatively small number of individuals. Following further optimization of the extraction methods and probe design to minimize cross hybridization and sensitivity, larger studies will be important to assess the full potential of the proposed miRNA biomarkers, including positive and negative predictive values in comparison to existing techniques. It will also be of interest to determine the origin of these parasite-derived miRNAs, examine their abundance levels in response to treatment and or upon infections with other helminths.

In summary we have shown that host miRNAs are altered in mouse serum at 12 weeks post *S.mansoni* infection, but fail to distinguish between "egg-positive" and "egg–negative" individuals. Importantly, we have shown that parasite-derived miRNAs are present in mouse and human serum and can be used in diagnosis of *S.mansoni* infection. We anticipate that the parasite miRNAs in serum could complement or transform existing diagnostic strategies and may serve as a platform for detecting a range of helminth infections.

Chapter 5: **Characterization of tRNA halves in serum**

5.1 INTRODUCTION

Mature transfer RNAs (tRNAs) are ~75 nt long non-coding RNAs and function as amino acid adaptor molecules during the process of decoding mRNA into protein. A secondary structure of a properly folded tRNA resembles a cloverleaf, with three stem loops (D loop, T loop and an anticodon-loop) Fig. 5.1 (Giege et al., 2012). In humans up to 506 genes encode 49 different tRNAs (Lowe and Eddy, 1997). The tRNA genes are transcribed by RNA polymerase III (RNA Pol III) (White, 2011). The 5' - leader and 3'- trailer sequences are removed from the primary transcript (pre-tRNA) by endoribunuclease P (RNase P) and endonuclease Z (RNase Z, ELAC1/2 in human), respectively. If the pre-tRNA contains introns it undergoes splicing (Phizicky and Hopper, 2010; Robertson et al., 1972; Schiffer et al., 2002; Walker and Engelke, 2006). The 3'CCA acceptor is then added by tRNA nucleotidyl transferase (Xiong and Steitz, 2006). The possession of the 3'CCA is required for tRNA participation in translation as it is through the 3'CCA that a tRNA can be aminoacylated (charged). The tRNA undergoes multiple post-transcriptional modification events that are important for its structure, stability and function (Motorin and Helm, 2010; Phizicky and Hopper, 2010). For their adaptor function, tRNAs are aminoacetylated, each by one of the 20 different aminoacyl-tRNA synthetases (aaRSs) and exported form the nucleus by Exportin-T (XPOT) to become an adaptor molecule for translation (Lund and Dahlberg, 1998). tRNAs are one of the most stable RNAs and one of the most abundant RNA transcripts in the cell, accounting for around 15% of the total RNAs (Li and Zhou, 2009). Recent studies suggest their functions and/or regulation may extend beyond a role in translation. In particular, multiple tRNA cleavage pathways have been described in response to stress and the roles of generated tRNA fragments have been suggested.

5.1.1 tRNA fragments: their biogenesis and biological role

The tRNA fragments identified to date are divided in the literature into two classes: i) fragments ~35nt long that are generated by the cleavage within the anticodon-loop, named as "tRNA halves" and ii) shorter fragments 13-30 nt long that are generated by cleavage of the mature or pre-tRNA, named as tRNA-derived fragments (tRFs), specifically: 5'tRFs, 3'CCA tRFs, 3' U tRFs, 5' leader-exon tRFs (Fig. 5.1). Although the role of tRNA halves and tRNA-derived fragments are not fully understood, accumulating evidence suggests that these small RNAs play roles in regulation of gene expression, potentially in relation to stress responses.

tRNA halves

tRNA halves, also known as stress-induced small RNAs or short tiRNAs, are 30-35nt long. They are generated by endonucleolytic cleavage of tRNA which occurs within the anticodon-loop in response to oxidative stress, hypoxia or apoptotic inducers, although they were also observed in unstressed conditions (Emara et al., 2010; Nowacka et al., 2013; Thompson et al., 2008; Yamasaki et al., 2009). It has been shown that the majority of tRNA halves lack the 5' leader sequence, 3' trailer sequences or introns showing that they originating from the mature tRNA. The 3'tRNA halves have also been shown to contain the 3'CCA sequence, further supporting the idea that these are derived from the full length, mature tRNA (Fu et al., 2009; Nowacka et al., 2013). The tRNA halves were described for the first time in *Tetrahymena thermophilia* in (Lee and Collins, 2005) and since then, they have been identified under various stress conditions in bacteria - *Streptomyces coelicolor* (Haiser et al., 2008), fungi - *Aspergillus fumigatus* (Jochl et al., 2008), yeast - *Saccharomyces cerevisiae* (Thompson and Parker, 2009), parasites - *Trypanosoma cruzi* (Garcia-Silva et al., 2010) and *Giardia lamblia* (Li et al., 2008), plants – *Arabidopsis thaliana* (Hsieh et al., 2010) and human cells (Yamasaki et al., 2009). In yeast, the tRNA cleavage is catalysed by Rny1 and in mammals by angiogenin. Although mammalian cells contain a homolog of Rny1, named RNASET2, it does not induce tRNA cleavage during oxidative stress (Fu et al., 2009; Thompson and Parker, 2009; Yamasaki et al., 2009). Rny1 belongs to RNase T2 family and is

predicted to leave 5' hydroxyl and 2'-3' cyclic phosphate groups. It has been shown that Rny1 promotes cell death in response to oxidative stress, which is independent of tRNA cleavage (Thompson and Parker, 2009). Angiogenin (ANG) is a member of the RNase A family that is known to be a key angiogenic factor (Fett et al., 1985) and is predicted to leave 5' hydroxyl and 2'-3' cyclic phosphate groups (Rybak and Vallee, 1988). Under normal conditions Rny1 is sequestered in vacuoles and during oxidative stress it exits from the vacuoles and move into the cytoplasm. ANG is bound to ribonuclease/angiogenin inhibitor 1 (RNH1) and is released to cytoplasm under stress conditions (Thompson and Parker, 2009; Yamasaki et al., 2009). Both enzymes have limited specificity, with tRNA cleavage occurring at multiple positions within anticodon loop. Interestingly, certain tRNAs such as $tRNA^{Asp}$(GTC), $tRNA^{Gly}$(GCC), $tRNA^{Val}$(ACC) can be methylated by DNA methyltransferase 2 (DNMT2) which protects them from this cleavage (Schaefer et al., 2010). Two different cleavage phenomena have been described: in *T.thermophilia* and *S. coelicolor* the generation of tRNA halves is global, affecting all tRNAs, and correlates with codon usage (Haiser et al., 2008; Lee and Collins, 2005; Schaefer et al., 2010), whereas in *T.crusi* and *A. thaliana* it has been shown that generation of tRNA halves affects a small subset of tRNAs and there is no correlation with the number of tRNA genes or the codon usage (Garcia-Silva et al., 2010; Hsieh et al., 2010). Further, it seems that the stability of generated tRNA halves relates to the stress conditions. For example, tRNA halves in *T.thermophilia* are generated under cold shock but not heat shock (Andersen and Collins, 2012). Franzen et al., reported that 88.9% of reads that mapped to tRNA are derived from 3' end of tRNA in *T.cruzi* under normal conditions (Franzen et al., 2011), whereas under stress conditions, the majority of derived tRNA fragments are 5' tRNA halves, of which 90% are derived from $tRNA^{Asp}$(GCU), $tRNA^{Glu}$(CUC), $tRNA^{Glu}$(UUC) (Garcia-Silva et al., 2010).

Since tRNAs are key elements of translation process, it has been suggested that tRNA cleavage would reduce the pool of functional tRNAs in the cell, thereby negatively effecting protein synthesis. Indeed, it has been shown that the translation inhibition correlates with the extent of the tRNA cleavage by angiogenin (Saxena et al., 1992). However, several factors argue against this. Firstly, only a small

proportion of tRNAs are cleaved, such that the level of full- length tRNA molecules is unlikely to be largely affected. Secondly, the tRNA halves have been shown to be highly stable in some cases, and their levels are likely to be regulated in some way since there is specificity in which fragments are most abundant (Haiser et al., 2008; Jochl et al., 2008; Kawaji et al., 2008; Saikia et al., 2012). In addition, it has been shown that stress induced 5' tRNA halves are able to inhibit translation in mammalian cells and *A.thaliana* (Emara et al., 2010; Nowacka et al., 2013) Moreover, it has been reported that certain 5' tRNA halves are able to displace translation initiation factors (eIF4E/G/A) from mRNA which result in formation of stress granules (Ivanov et al., 2011). Durdevic et al., reported that tRNA halves bind to Dicer-2 in *Drosophila* subjected to heat shock, which contributes to the reduction of siRNA pathway function. This is further enhanced in the DNMT2 mutant flies suggesting the involvement of DNMT2 in tRNA stability and correct function of siRNA pathway (Durdevic et al., 2013).

tRNA-derived fragments

5' tRFs are products of a cleavage near or within the D loop of tRNA (Fig. 5.1). Their size ranges from 19-26nt and they lack 5' leader sequence suggesting that similarly to 5' tRNA halves they originate from the mature tRNA. With an exception of 5' tRFs observed in *T. thermophilia*, their abundance levels do not correlate with the number of tRNA genes copies or codon usage (Couvillion et al., 2010). Further, in many species, 5' tRFs originate predominantly from a single isotype tRNA, e.g. the majority of 19nt long 5'tRFs found in the roots of *A. thaliana* originate from $tRNA^{Gly}$ (Hsieh et al., 2009), most of 5' tRFs found in rice (20-22nt long) correspond to 5' end of $tRNA^{Ala}$ (Chen et al., 2011b) and the majority of archeon *Haloferax volcanii* 5'tRF 26nt) come from $tRNA^{Val}$ (Gebetsberger et al., 2012). Studies in HeLa cells suggested that the production of 19 nt long 5' tRFs is Dicer dependent and that 5'tRFs associate weakly with Argonaute (Ago) proteins (Cole et al., 2009). However, Dicer-independent 5' tRF (23 nt long) generation has been shown in yeast (Buhler et al., 2008). It has been shown that 5' tRF derived from $tRNA^{Val}$ in *H. volcanii* bind directly to the small ribosomal subunit *in vivo* and *in vitro* affecting protein synthesis

under stress conditions (Gebetsberger et al., 2012). Like tRNA halves, the 5'tRFs have been shown to inhibit translation. Sobala et al., showed that three out of four tested 5'tRFs have an ability to inhibit translation, and implicated the presence of a "GG" dinucleotide at the 3' end of the molecule in this process. However, other motifs are likely to be involved. Further work is needed to reveal the mechanism by which 5'tRFs affect translation (Sobala and Hutvagner, 2013).

3'CCA tRFs are formed by cleavage of a mature, charged tRNA near or within the T loop (Fig. 5.1) and are 13-22 nt long. It has been shown that 3'CCA tRFs are generated in some cases by Dicer, but not exclusively (Haussecker et al., 2010; Kawaji et al., 2008; Yeung et al., 2009). Angiogenin and other RNase A family enzymes have been proposed for the Dicer-independent cleavage (Sobala and Hutvagner, 2013). The 3' CCA tRFs that are cleaved by Dicer were shown to associate with the RNAi machinery and some of the tRFs exhibited gene silencing properties. Specifically, they were shown to associate with Argonaute (Ago1-4) and have a modest silencing ability (Haussecker et al., 2010). Interestingly, it has also been shown that 3'CCA tRFs are involved in defence against viral infections. Yeung et al., showed that the 18nt long 3' CCA tRFs originating from $tRNA^{Lys}$ is associated with Ago2 and Dicer and have moderate gene silencing activity in a luciferase reporter assay (Yeung et al., 2009). This tRNA is known to be used by viral reverse transcriptases as a primer for the initiation of reverse transcription and DNA synthesis, but any mechanistic link with its RNAi functions is not yet clear.

The 3' U tRFs correspond to the 3' trailer of pre-tRNAs, such that the 5' end is generated by RNase Z cleavage. These have been observed in vertebrates and archaea (Haussecker et al., 2010; Heyer et al., 2012; Lee et al., 2009b; Liao et al., 2010). They are localised in the cytoplasm (Liao et al., 2010), which suggest either they are generated in the nucleus and rapidly exported (they have not been observed in the nucleus) or generation in cytoplasm by 3' tRNases. Indeed, it has been shown that in human cancer cells a 3' U tRF derived from pre-$tRNA^{Ser}$(TGA) named tRF-1001 is generated in the cytoplasm by tRNA 3' endonuclease ELAC2 (Lee et al., 2009b). Two other classes of tRFs have been recently reported. sitRNAs (tRFs ~

46nt long) that are generated by the cleavage of the mature tRNAs anticodon left arm have been identified in *G.lamblia* as a result of stress (Li et al., 2008). Hanada et al., recently reported that loss of mammalian RNA kinase CLP1, results in an accumulation of tRF originating from pre-$tRNA^{Tyr}$. These tRFs are 41-46 nt long and contain 5' leader followed by 5'exon tRFs and are not generated by angiogenin (Hanada et al., 2013).

In summary, in last 5 years development of new generation sequencing technologies led to discovery of novel small ncRNAs, including tRNA-derived fragments. It emerged that some of these ncRNAs, such as miRNAs have important biological functions and have a potential to be used as novel diagnostic and therapeutic tools. Research to date suggest that tRNA halves and tRFs present in cells are product of a specific cleavage events and are biologically relevant. Here we characterise tRNA – derived fragments of ~29-33 nt long, that circulate in mouse serum, and investigate their diagnostic potential.

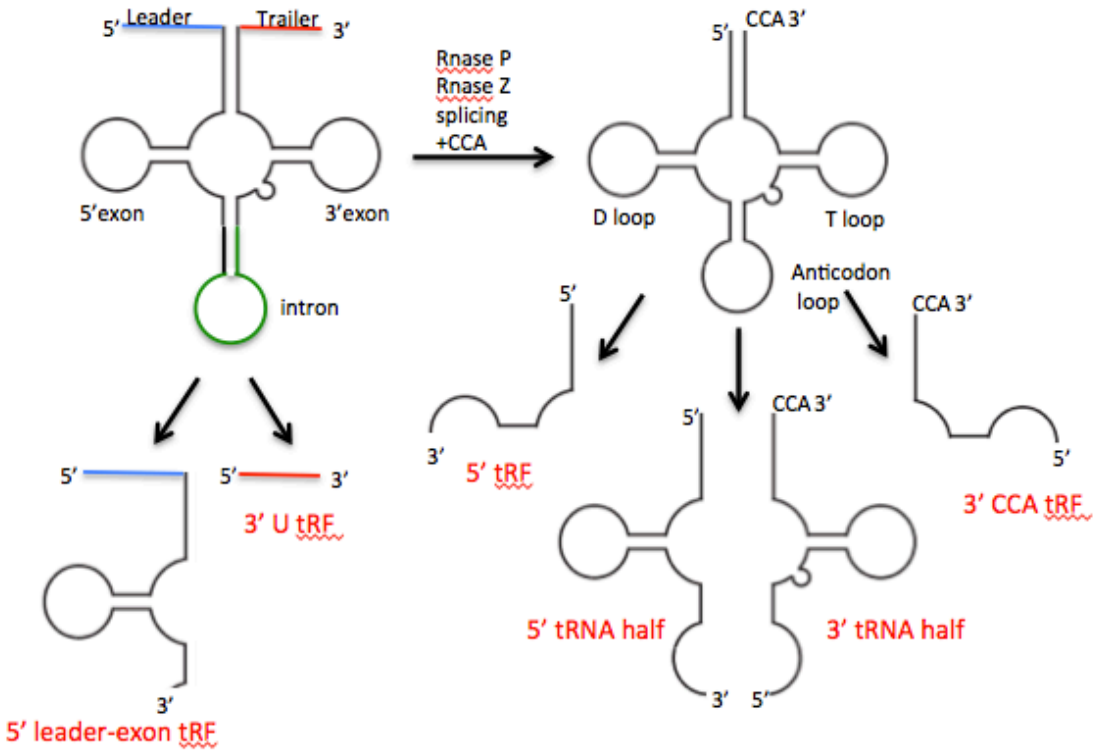

Figure 5.1 Processing of tRNA and tRNA- derived fragments.
Pre-tRNA is processed by RNase P, RNase Z to remove the 5'leader (blue) and 3'trailer (red), the introns, if present (green) are removed by splicing endonuclease and the CCA is added. Pre-tRNA and mature tRNA can give rise to smaller tRNA fragments. Depending on their origin we can differentiate: 5′ leader-exon tRF, 3′ U tRF, 5′ tRF, 3′ CCA tRF, 5′ and 3′ tRNA halves

5.2 SPECIFIC AIMS

1. To characterise tRNA halves present in serum: tRNA abundance and stability.
2. To investigate diagnostic potential of 5' $tRNA^{Gly}$(GCC) and 3' $tRNA^{Gly}$(GCC) halves in *S.mansoni* infection

5.3 RESULTS

5.3.1 tRNA fragments of 29-33nt dominate the small RNA population in serum and are products of specific cleavage events near the anti-codon loop

Our analysis of tRNA fragments in mouse serum showed that approximately 94% of reads of 29-33nt long correspond to five of tRNA genes: $tRNA^{Gly}$(GCC), $tRNA^{Glu}$(CTC), $tRNA^{Glu}$(TTC), $tRNA^{His}$(GTG) and $tRNA^{Ala}$(TGC). These are present in multiple copies in the genome so we cannot definitively determine their origin. The majority of reads were fragments derived from $tRNA^{Gly}$(GCC), accounting for over 80% of the tRNA reads (Table 4.3). Of the top five most abundant tRNAs identified in our datasets, over 99% of reads mapped to the 5' end of tRNA (Table 5.1) and ranged in size from 29-31nt. Further, from the distribution of reads we infer that full length tRNA is cleaved within the anti-codon loop at more than one site. Fig. 5.2 shows the most dominant cleavage sites.

Table 5.1 Percentage of sequencing reads that mapped to tRNA halves.

tRNA	Percentage of reads that mapped to tRNA		
	Total	5'half	3'half
$tRNA^{Gly}$(GCC)	80.28	99.96	0.04
$tRNA^{Glu}$(CTC	10.06	99.99	0.01
$tRNA^{Ala}$(TGC)	0.50	99.52	0.48
$tRNA^{Glu}$(TTC)	2.76	95.25	4.75
$tRNA^{His}$(GTG)	0.47	85.61	14.39

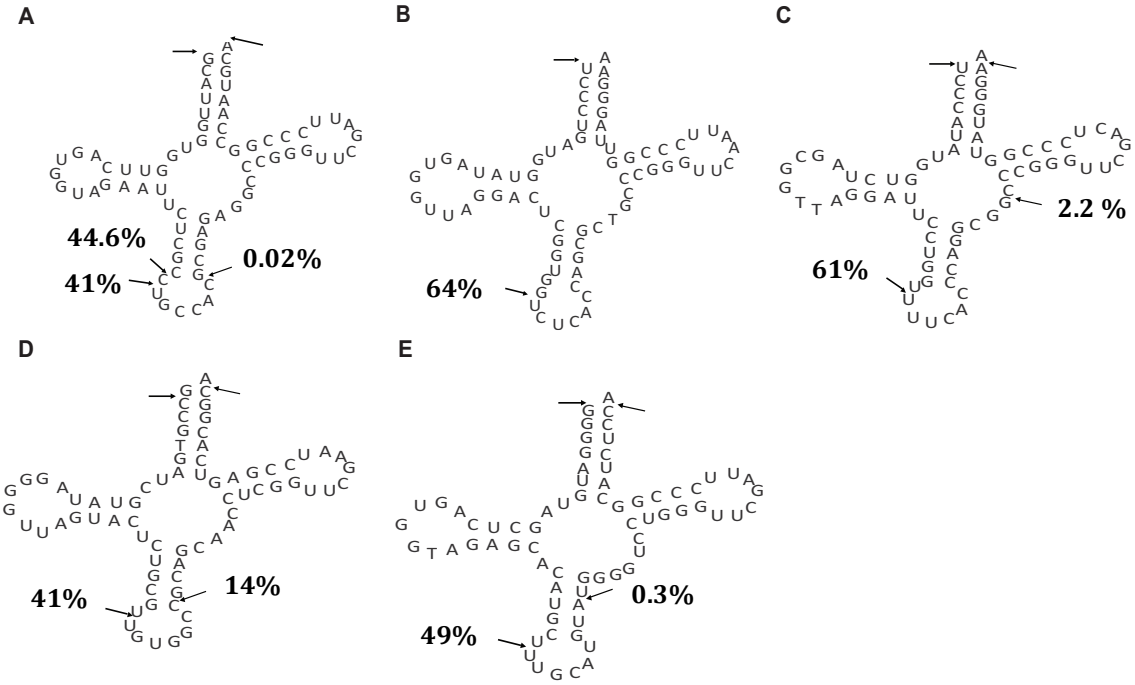

Figure 5.2 Cleavage sites of tRNAs.
Secondary structure of A) $tRNA^{Gly}$(GCC), B) $tRNA^{Glu}$(CTC), C) $tRNA^{Glu}$(TTC), D) $tRNA^{His}$(GTG) and E) $tRNA^{Ala}$(TGC). Black solid arrows represent the most dominant tRNA cleavage sites (percentage indicated) as determined by sequencing data.

5.3.2 High levels of 5' fragment of tRNA^{Gly} are present in serum

To assess the levels of tRNA-derived fragments in serum, tRNA^{Gly}(GCC) in comparison to miR-122, miR-16 and miR-21 were measured in mouse serum using qRT-PCR using miScript protocol. To determine the proportion of tRNA^{Gly}(GCC)-derived fragments, 18nt and 15nt long primers corresponding to the 5' and 3' end of tRNA^{Gly}(GCC) respectively were designed (Fig 5.3 A). To allow simultaneous quantification of tRNAs and miRNAs, the tRNA primers where designed to have melting temperature (Tm) of ~60°C. The absolute copy numbers were calculated from the standard curves generated for the serial 10 fold dilutions of the synthetic RNA standards of known concentration (standard curves present in Apendix 1). As shown in Fig 5.3 B, sequences containing 5' and 3' portion of tRNA^{Gly}(GCC) are present is mouse serum. The 5' tRNA^{Gly}(GCC) derived fragments are highly abundant (~5.6 x 10^6 copies/µl of serum), showing ~20 fold higher level than miR-16 and ~100 fold higher than 3'tRNA^{Gly}(GCC) derived fragments. To examine whether any of the signal for the tRNA fragments could derive from the full length molecule, total mouse serum RNA was resolved on the 15% PAGE gel (Fig 5.3 C) and three RNA size fractions were excised (10-25nt, 25-50nt and 50-100nt). The RNA was then extracted and the levels of 5' tRNA^{Gly}(GCC), 3' tRNA^{Gly}(GCC) quantified by qRT-PCR (Fig 5.3 D). The 3' portion of tRNA^{Gly}(GCC) was present in all three fractions at a relatively similar level (lowest in the 10-25nt (10^2 copies/ng of RNA loaded) and highest in 25-50nt ($1.5x10^3$ copies/ng of RNA loaded). The 5' tRNA^{Gly}(GCC) levels varied substantially between fractions with the highest in the 25-50nt fraction ($2.1x10^5$ copies/ng of RNA loaded) and similar levels, comparable to the 3' tRNA^{Gly}(GCC) fragments in the remaining two fractions. This demonstrates that full length, tRNA halves and smaller tRF-like fragments are present in serum. Therefore, detection of tRNA^{Gly}(GCC) by qRT-PCR without the size selection reflects the quantity of both full length and tRNA-derived fragments present in serum and needs to be taken into account with the analysis of 3'-end containing fragments. As 5' tRNA^{Gly}(GCC) fragments are predominantly derived from the 25-50nt fraction

we concluded that qRT-PCR quantification without size selection is an appropriate method for 5' tRNA half detection.

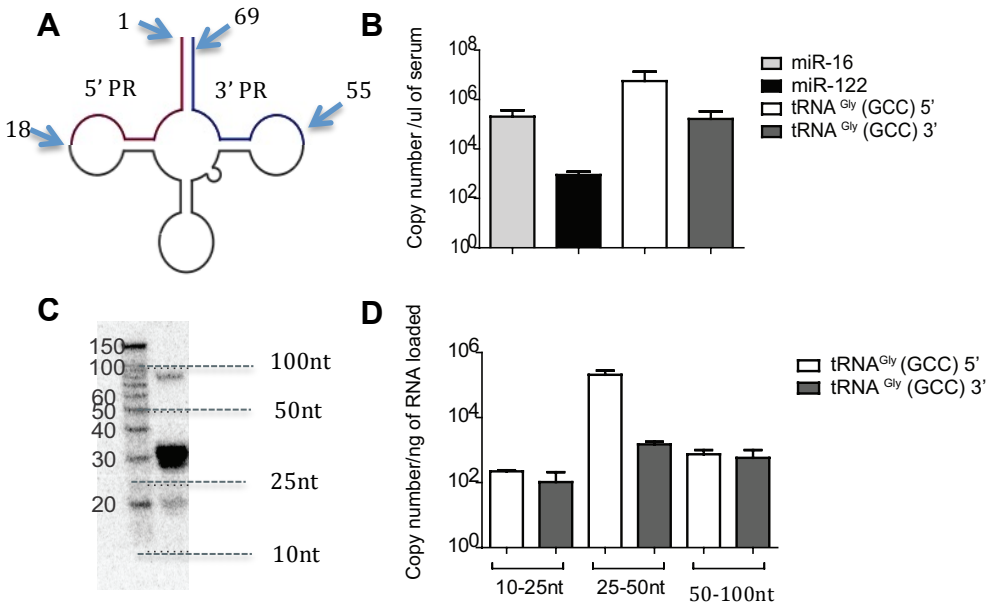

Figure 5.3 Quantification of tRNA^{Gly} (GCC) halves in mouse serum.
A) Position of the PCR primers are indicated with arrows. B) Total serum RNA was extracted from 100ul of serum and miR-16, miR-122, tRNA^{Gly} (GCC) fragments were quantified by qRT-PCR (5' and 3' primers were used as shown) and normalized to a synthetic RNA oligo "spike-in". Absolute copy numbers were calculated using standard curves generated for the serial 10 fold dilutions of the synthetic RNA standards of known concentration (standard curves present in Apendix1). D) Total serum RNA was extracted from 100ul of mouse serum, resolved on the 15% PAGE and three RNA size selected faction were excised (10-25nt, 25-50nt and 50-100nt) as shown on the cartoon C) RNA was purified from the excised fraction and D) the levels of 5' tRNA^{Gly}(GCC), 3' tRNA^{Gly}(GCC) were quantified by qRT-PCR and normalized to a synthetic RNA oligo "spike-in".

5.3.3 $tRNA^{Gly}$ halves are detected in mouse tissue and are the primary form of $tRNA^{Gly}$ in serum of mouse

As detailed above, previous studies have shown that tRNA halves are present in tissues and cells and are generated upon stress condition (Haiser et al., 2008; Jochl et al., 2008; Lee and Collins, 2005; Thompson and Parker, 2009; Yamasaki et al., 2009). In order to examine the origin of the tRNA halves we observe in serum we carried out northern blot hybridization experiments to assess their levels in mouse tissues (lung, spleen, heart, kidney and liver) compared to mouse and human serum and plasma. Extracted RNA was resolved on a 15% PAGE gel and probed for 3' and 5' $tRNA^{Gly}$(GCC) and miR-16. To investigate whether the tRNA fragments originate directly from cells present in circulation, RNA was extracted from blood cells separated using density gradient centrifugation into two fractions: peripheral blood mononuclear cells (PBMC) and the remaining cells: red blood cells (RBC) and polymorphonuclear cells (PMNs). We observed the presence of $tRNA^{Gly}$(GCC) halves in lung, heart, kidney and liver and lower expression in the spleen which suggests that tRNA halves present in serum could originate from these tissues (Fig 5.4). In order to rule out that tRNA halves present in serum are a result of blood clotting we examined the presence of tRNA halves in both serum and plasma. We detected both 3' and 5' $tRNA^{Gly}$(GCC) halves as well as a trace of full length tRNA in mouse serum and plasma but human serum and plasma we detected only 5' $tRNA^{Gly}$(GCC) halves and a trace of full length tRNA $tRNA^{Gly}$(GCC) (Fig 5.4). This is likely due to the fact that, in general, we do extract significantly less RNA from human serum/plasma (compared to mouse, based on measurement of endogenous miRNAs) such that we are likely operating at the limit of detection. In PBMC and RBC+PMNs, a probe for 3' end and 5' end of $tRNA^{Gly}$(GCC) detected the full length tRNA (Fig 5.4). A band of ~20 nt was detected with the probes complementary to 3' and 5' $tRNA^{Gly}$(GCC) in all mouse tissues and body fluids (3' $tRNA^{Gly}$(GCC)-derived product of this size were not present in blood cells) (Fig 5.4). This further confirms the presence of tRNA-derived fragments of this size.

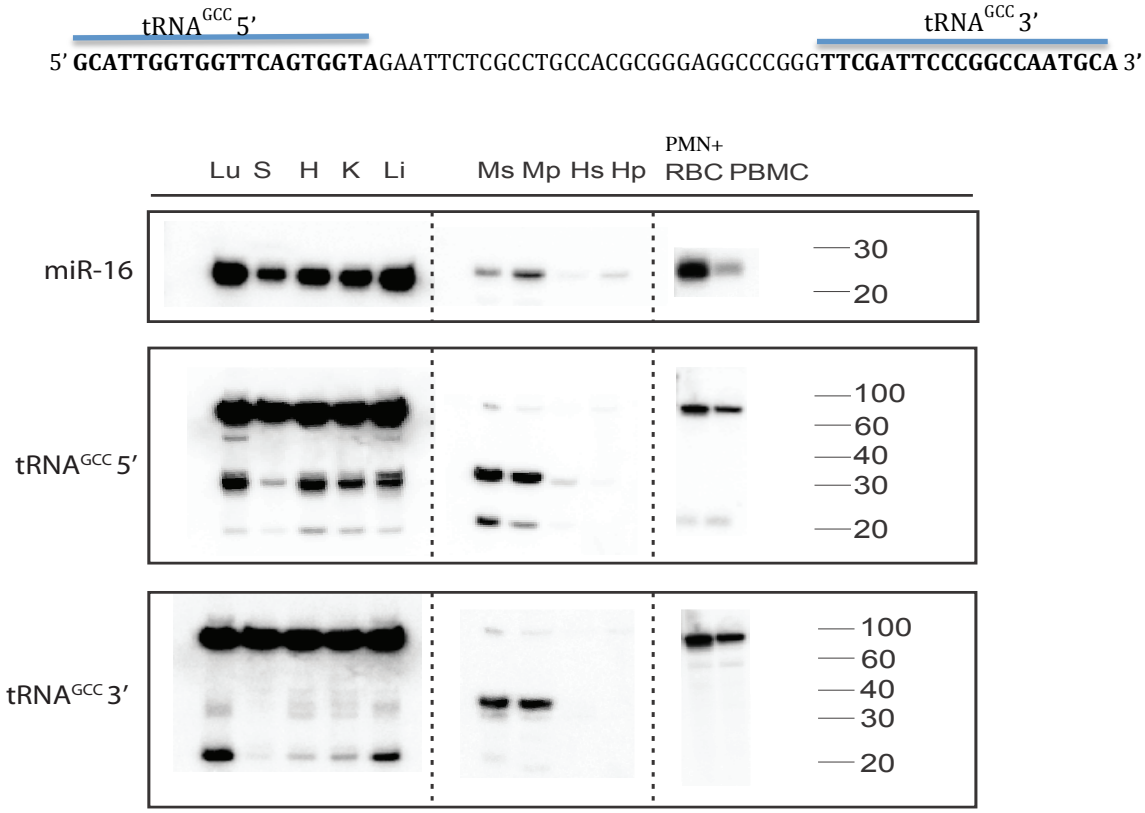

Figure 5.4 Distribution of tRNA^{Gly} (GCC) in tissues, blood cells, serum and plasma. Northern blots containing RNA from mouse tissues (3µg), mouse PBMC cells, RBC+PMN cells (100ng), serum and plasma of mouse and human (RNA extracted from 300ul) hybridized with ^{32}P-labelled miRNA-16, tRNA^{Gly} 3' and 5' probes (positions of the tRNA probes are shown). Abb.; S-spleen, H-heart, K- kidney, Lu- lung, Li-liver, RBC- red blood cells, PMNs-polymorphonuclear cells and PBMC-peripheral blood mononuclear cells, Ms/Mp- mouse serum/plasma, Hs/Hp- human serum/plasma.

5.3.4 Serum tRNA halves are protected against RNase activity by protein complexes rather than vesicles

Serum and plasma are rich in highly stable RNases: the concentrations of RNases in human blood are estimated at several hundred ng/mL, and can be elevated in cancer patients (Blank and Dekker, 1981; Kamm and Smith, 1972). Consistent with this, Tsui et al., showed that synthetic RNA is degraded in less than 5 seconds when incubated with human plasma, yet RNA present in serum and plasma are stable for many hours (Tsui et al., 2002). We hypothesized that tRNA halves present in serum are protected against serum enzymatic activity.

To investigate that, at first, we examined whether serum enzymatic activity can degrade unprotected tRNA halves. We incubated ^{32}P pCp 3'-end labelled synthetic tRNA 31-mer oligonucleotides designed for the 3' and 5' tRNA^{Gly}(GCC) halves for 5 min at 37°C with 1µl of mouse serum, RNase A (0.1mg) or serum pre-treated with RNase Inhibitor (Fig 5.5A). We showed that incubation with both serum and RNase A but not serum pre-treated with RNase Inhibitor can degrade the synthetic tRNA halves (Fig 5.5B), suggesting that tRNA fragments present in circulation are protected against serum enzymatic activity. Recent studies have shown that miRNAs present in circulation are protected against serum enzymatic activity by ribonucleoprotein complexes or encapsulation in vesicles (Arroyo et al., 2011; Turchinovich et al., 2011; Vickers et al., 2011; Wang et al., 2011). To investigate whether serum tRNA halves are protected by protein complexes or vesicles, mouse serum (100µl) was treated with Triton X100 (0.5% final concentration) for 30 min at 37°C or Proteinase K (25µg) for 1h at 55°C and/or RNase A (0.1mg) for 5min at 37°C. Total mouse RNA was extracted, ^{32}P-pCp 3' end labelled and resolved on the 15% PAGE (Fig 5.5C) or used for northern hybridisation with a probe complementary to 5' end of tRNA^{Gly}(GCC) (Fig 5.5D). As shown in Fig. 5.5 C treatment with Proteinase K but not Triton X100 made tRNA halves susceptible to enzymatic digestion leading to the conclusion that tRNA halves present in serum are protected by association by protein rather than encapsulation within vesicles. The addition of RNase A to serum did not affect the stability of serum tRNA halves.

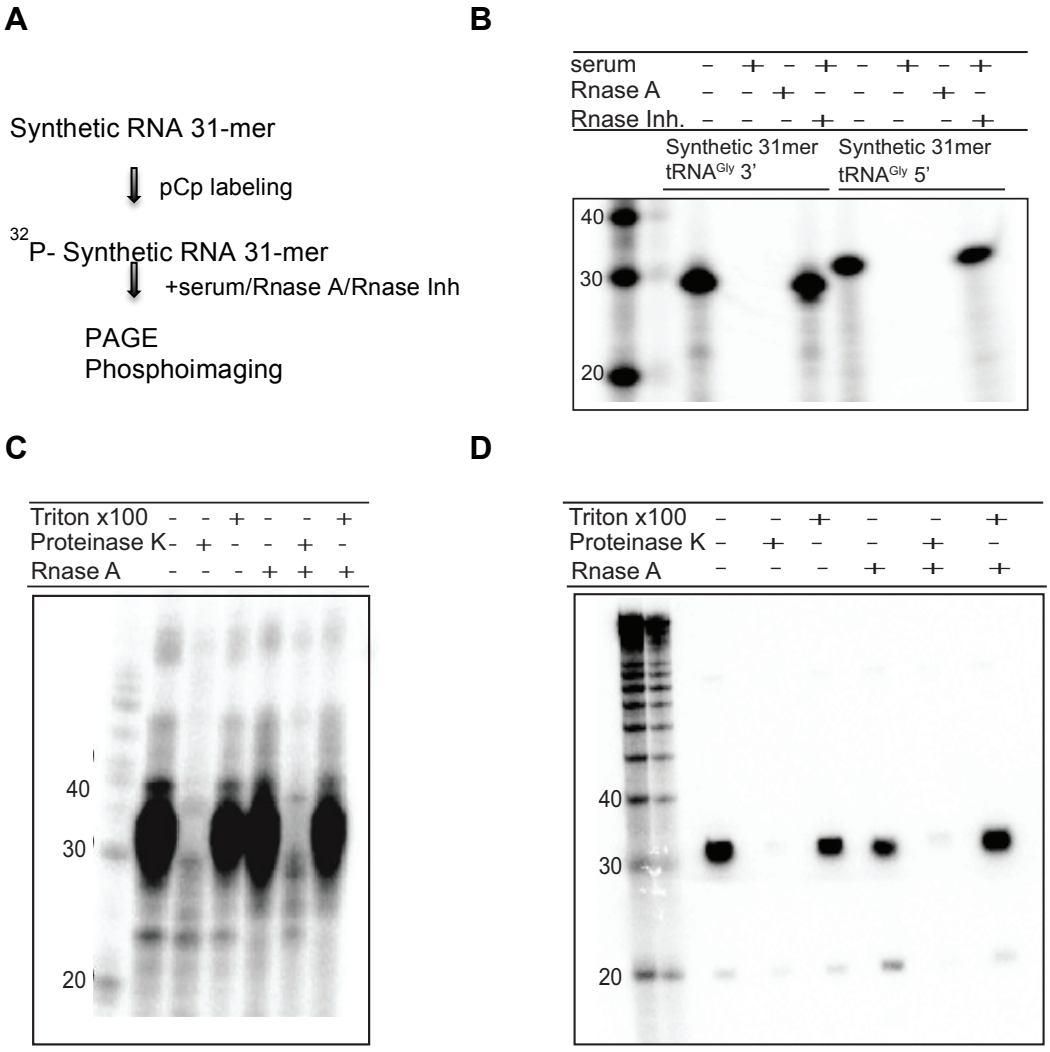

Figure 5.5. Proteinase-sensitive complexes protect tRNA^{Gly}(GCC) halves from serum enzymatic activity.
^{32}P-pCp 3'- end labeled synthetic tRNA 31-mer oligonucleotides designed for the 3' and 5' tRNA^{Gly}(GCC) halves were incubated with serum, Rnase A or serum pre-treated with Rnase Inhibitor B) and resolved on the 15% PAGE. C) 100µl of mouse serum was treated prior to extraction with Triton X-100 (0.5% final concentration) or Proteinase K (25µg) and/or RNase A (0.1mg). Total RNA was extracted, C) ^{32}P-pCp 3' end labeled and resolved on the 15% PAGE or used for D) northern hybridization with a probe (20nt long) complementary to 5' end of tRNA^{Gly}(GCC).

This was confirmed by northern blot hybridisation using 5' $tRNA^{Gly}$(GCC) probe (20 nt long) (Fig. 5.5D). The investigation of the protection of 3' $tRNA^{Gly}$(GCC) was impossible due to its low level in serum and limited sensitivity of northern blotting.

To further confirm that the tRNA fragments are not encapsulated within vesicles, a pool of mouse serum and human serum obtained from three healthy individuals were ultracentrifuged according to the protocol described previously by (Arroyo et al., 2011). In their paper Arroyo et al., demonstrated that in serum and plasma the majority of miRNAs co-fraction with protein complexes rather than vesicles. Specifically they showed that miR-21 and miR-16 appeared to be protected by association with proteins whereas let-7a was protected by vesicle encapsulation (Arroyo et al., 2011). miR-16, miR-21, let-7a, 5' RNA^{Gly}(GCC) and 3' $tRNA^{Gly}$(GCC) were quantified by qRT-PCR and their relative expression was calculated using ΔΔCt method. A synthetic RNA oligo complementary to cel-miR-39 was included at the extraction step and used as a normaliser. As shown in Fig 5.6 A, B miR-16 and miR-21 are mainly present in the vesicle-depleted supernatant (~95% and ~65% in mouse and human serum, respectively) and let-7a is present in the vesicle-enriched pellet (~53% and ~90% in mouse and human serum respectively). 5' RNA^{Gly}(GCC) halves are almost exclusively present in the vesicle-depleted supernatant fraction of human and mouse serum (70% and >99% respectively), which confirms our previous results that they are protected by protein complexes rather than vesicles. The mechanism of 3' $tRNA^{Gly}$(GCC) halves protection remains inconclusive (association with vesicles in the human serum but not in the mouse serum).

5.3.5 tRNA fragments have a size-exclusion chromatography profile consistent with non-vesicle complexes and distant from those of miRNA-protein complexes.

The presence of RNA^{Gly}(GCC) halves in the vesicle-depleted supernatant post centrifugation might be due to the incomplete recovery of vesicles, or an effect of vesicle rupture (due to high force condition of the ultracentrifugation). To further

examine the association of tRNA halves with proteins we employed size exclusion chromatography (SEC) that separates molecules in solution based on their size.

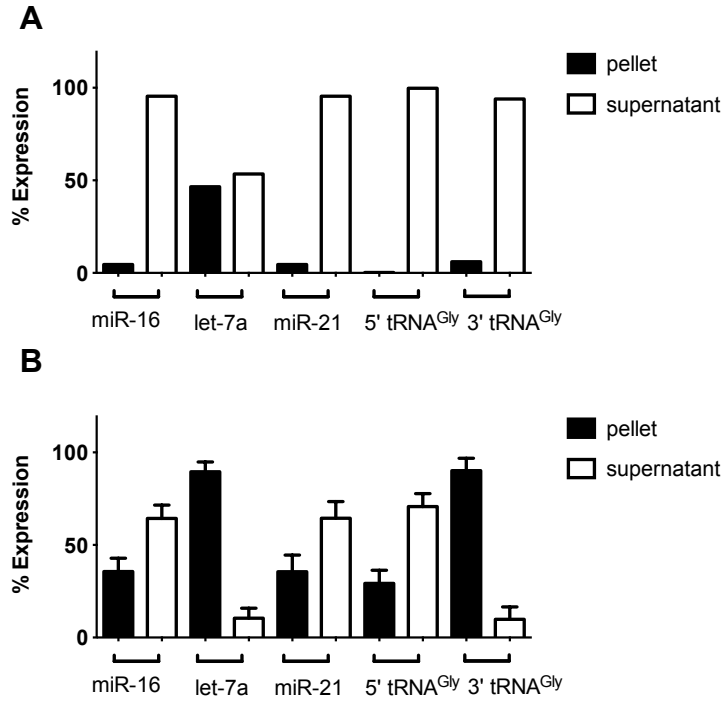

Figure 5.6 Serum 5' $tRNA^{Gly}$ (GCC) are present in a vesicle-depleted supernatant post ultracentrifugation.
Circulating vesicles were purified from A) a pool of 3 mouse serum samples and B) serum samples from human donors (n=3) by ultracentrifugation according to (Arroyo et al., 2011). Levels of miR-16, miR-7a, miR-21, 5' $tRNA^{Gly}$ (GCC) and 3' $tRNA^{Gly}$ (GCC) were quantified by qRT-PCR and normalized to a synthetic RNA oligo "spike-in". Black bars represent vesicle-rich pellet, white bars represent vesicle-depleted supernatant.

Two separate experiments were carried out in which 800µl of mouse serum was injected onto a Superdex 200 10/300 GL column and eluted with PBS solution at room temperature and a total of 30 1ml fractions were collected. Total RNA was extracted from obtained fractions and miR-16, miR-21, let-7a, 5' RNA^{Gly}(GCC) and 3' $tRNA^{Gly}$(GCC) were quantified by qRT-PCR. Their relative expression was calculated using the ΔΔCt method. In order to enable tRNA and miRNA quantification a synthetic RNA oligo complementary to cel-miR-39 was included at the extraction step. The presence of 5' $tRNA^{Gly}$(GCC) in the fractions was also confirmed by northern blot hybridization (Fig 5.7A).

Based on the miRNA and tRNA expression examined by qRT-PCR, the small RNAs eluted in three distinct sizes: Pool I- fraction 3-4, Pool II- fraction 9-10 and Pool III- fraction 11-12 (Fig 5.7 C, D). Using protein molecular standard curves (Fig 2.1) we determined that Pool I contains protein complexes of >800kDa and vesicles (elution time: 14-18min), Pool II contains protein complexes of ~ 60-220kDa (elution time: 24-28 min), and Pool III contains smaller protein complexes of ~50kDa (30-34 min). The full length tRNA of 75nt and tRNA half of 30nt have molecular weights of ~25kDa and ~10kDa respectively which would also have a size impact on the total molecular weight of the protein complexes in each Pool. As shown in Fig 5.7 B, 5'$tRNA^{Gly}$(GCC) halves (size confirmed by northern blotting (Fig 5.7 A)) were primarily present in Pool III . 3' $tRNA^{Gly}$(GCC) fragments and/or full length tRNA $tRNA^{Gly}$(GCC) were present mainly in Pool I (~80%) and only 20% in Pool III. miRNA were present in Pool I and II, specifically, let-7a dominated in Pool I, miR-21 in Pool II and miR-16 was evenly distributed in both Pool I and II (Fig 5.7 C), which is in agreement with data published in (Arroyo et al., 2011). This shows that the size exclusion profile of 5' $tRNA^{Gly}$(GCC) in the serum differs from those of miRNAs, and suggest that tRNA halves are protected by a protein of ~40 kDa. As shown previously it is impossible to differentiate between full length tRNA and tRNA-derived fragments by qRT-PCR without RNA size fractionation. With the detection of 3' $tRNA^{Gly}$(GCC) by northern blotting failing presumably due to low levels of 3' $tRNA^{Gly}$(GCC) in serum and limited sensitivity of northern blotting it is difficult to conclude on mechanism of 3' $tRNA^{Gly}$(GCC) protection.

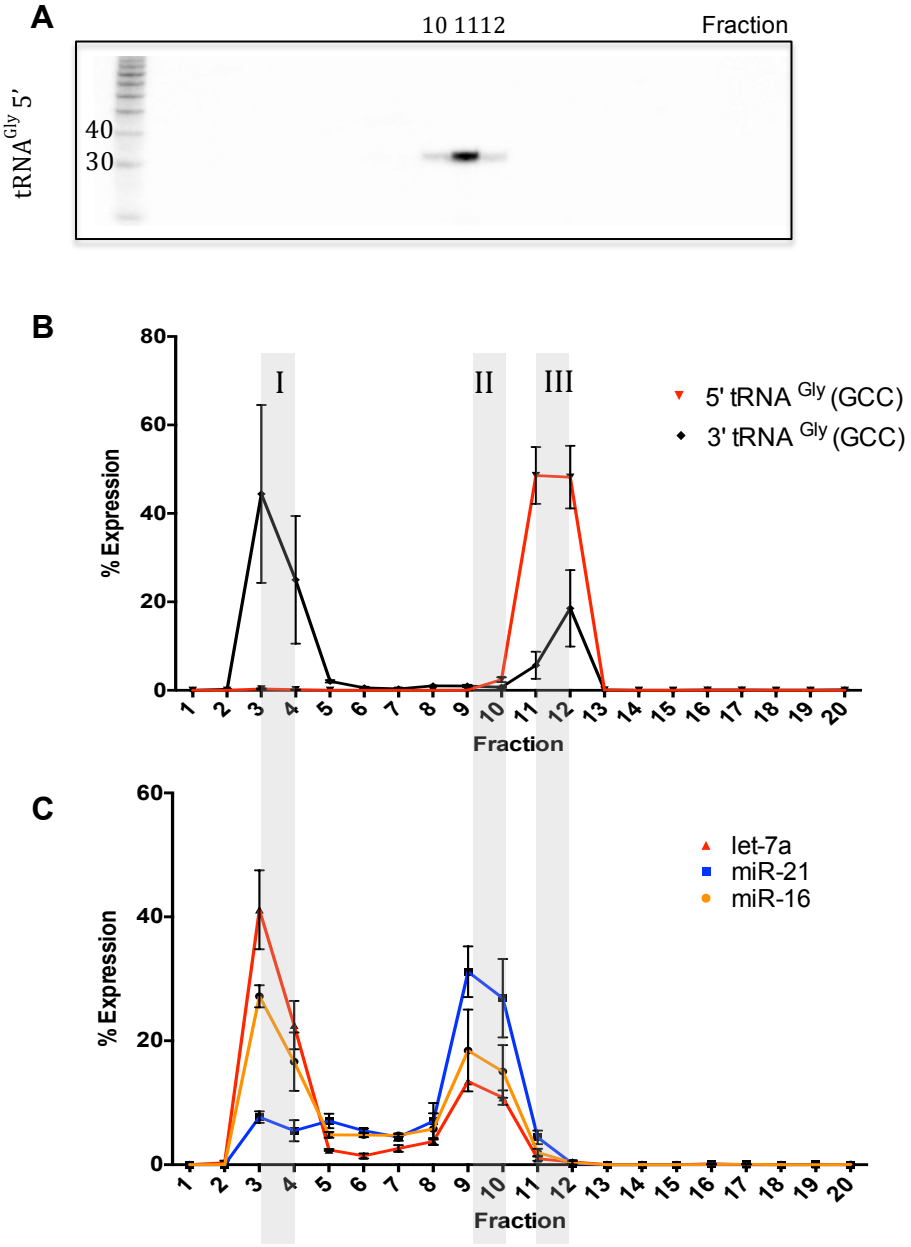

Figure 5.7 Size Exclusion Chromatography (SEC) profile of tRNA^{Gly}(GCC) halves in serum.

The mouse serum sample (800µl) was fractioned on a Superdex 200 10/300 GL column. Total RNA was extracted from obtained fractions (first 20). A) Presence of 5' tRNA^{Gly}(GCC) halves were confirmed by northern blot hybridization. Levels of B) 5' tRNA^{Gly}(GCC) and 3' tRNA^{Gly}(GCC) and C) miR-16, miR-21, let-7a were quantified by qRT-PCR and normalized to a synthetic RNA oligo "spike-in" Sera used in B and C come from different mouse serum pools. SEC experiments were conducted on consecutive days.

5.3.6 tRNAGly expression does not change upon S.mansoni infection

$tRNA^{Gly}$ halves are dominant small RNA molecules present in mouse serum. It has been shown that tRNA halves are produced during stress conditions in various cells and their levels in serum change with age and calorie restriction (Dhahbi et al., 2013). It has been shown that *S.mansoni* infection leads to alteration in oxidative status in the liver as well as other organs such as kidney, heart and brain. In the liver, the oxidative stress is related to the presence of granulomas and immune cells which are strongly associated with the production of reactive oxygen species and oxidative damage (de Oliveira et al., 2013).

Thus, we hypothesized that the expression of tRNA halves in serum could be altered, reflecting the oxidative damage in the liver and other tissues and therefore have a potential as an indirect biomarker of *S.mansoni* infection. To examine whether tRNA halves can be used as serum biomarker of *S.mansoni* infection, the levels of 3' $tRNA^{Gly}$(GCC) and 5' $tRNA^{Gly}$(GCC) were measured in serum during the time course of infection by qRT-PCR. Levels of tRNA were normalized to a synthetic RNA oligo ("spike-in") that was included at the reverse-transcription step. As shown in Fig 5.8, the level of $tRNA^{Gly}$(GCC) halves do not change significantly during the *S.mansoni* infection. Presence of 3' $tRNA^{Gly}$(GCC) half in serum shows an insignificant increase during the time course of infection.

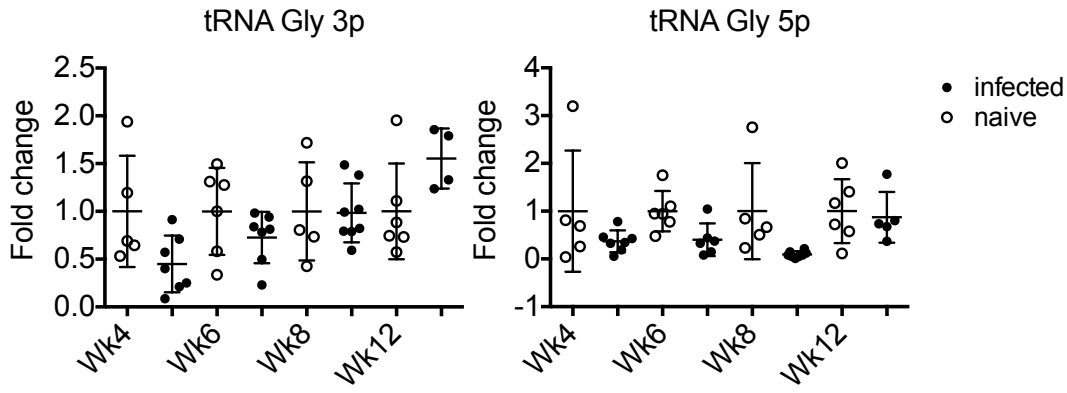

Figure 5.8 Differential abundance of tRNA Gly (GCC) halves in mouse serum during *S. mansoni* infection.
8-10 week old C57BL/6 mice were left uninfected or infected percutaneously with ~80 cercariae and euthanized at 4, 6, 8 and 12 weeks post infection. 5' RNA^{Gly}(GCC) and 3' $tRNA^{Gly}$(GCC) were quantified by qRT-PCR and normalized to a synthetic RNA spike-in. Each symbol represents data from one individual mouse. Fold changes are defined as the ratio of abundance in infected versus naïve serum; the signal from naïve was set as 1. (***p<0.001, ****p<0.0001, Two-way ANOVA, Sidak multiple comparison test). Data represents 1 experiment. Wk4: infected n=6, naïve n=5, Wk6: infected n=6, naïve n=6, Wk8: infected n=5, naïve n=5, Wk12: infected n=5, naïve n=6).

5.4 SUMMARY

- Fragments derived from $tRNA^{Gly}$(GCC), $tRNA^{Glu}$(CTC), $tRNA^{Glu}$(TTC), $tRNA^{His}$(GTG) and $tRNA^{Ala}$(TGC) account for 94% of all tRNA reads in mouse serum.
- tRNA halves are present in tissues, serum and plasma but not in blood cells.
- 5' $tRNA^{Gly}$(GCC) halves are protected by association with protein and are distinct in their size profile compared to miRNAs.
- $tRNA^{Gly}$(GCC) halves are not altered in serum upon *S.mansoni* infection.

5.5 DISCUSSION

As shown in Chapter 4, the deep-sequencing of mouse serum revealed the presence of tRNA-derived fragments. The aim of this chapter was to characterise this tRNA population in serum and explore their biomarker potential. It is important to mention that at the time of carrying out the work presented in this chapter (starting in 2010) there was no published data on the nature of tRNA halves in serum. Since then, a paper by Dhahbi et al., was published (May 2013) that confirms some of our findings. Thus, in this section we will discuss our results and where appropriate compare them to those published by (Dhahbi et al., 2013).

Our analysis of deep-sequencing data revealed that tRNA fragments 29-33nt long, here named as 'tRNA halves', dominate the serum RNAome in mice. Of all tRNA-derived fragments the majority derive from five tRNAs: $tRNA^{Gly}$(GCC), $tRNA^{Glu}$(CTC), $tRNA^{Glu}$(TTC), $tRNA^{His}$(GTG) and $tRNA^{Ala}$(TGC) of which 80% is derived from one specific tRNA: $tRNA^{Gly}$(GCC). This suggests that the presence of tRNA fragments in serum is not due to degradation (in that case a distribution of reads for all tRNAs in serum would reflect those in the cells) but rather there is specificity in what is secreted and/or stabilized in serum.

Further analysis of the distribution of reads in our study suggests that the tRNA halves are a product of a specific cleavage event, which occurs within the anti-codon

loop. Cleavage of full length tRNA under stress conditions was described previously in *Tetrahymena thermophilia* (Lee and Collins, 2005), bacteria (Haiser et al., 2008), fungi (Jochl et al., 2008), *Saccharomyces cerevisiae* (Thompson and Parker, 2009) and human cells (Yamasaki et al., 2009). It has been shown that in mammalian cells a secreted, 14-kDa member of the pancreatic RNase superfamily - angiogenin cleaves the full length tRNAs creating these tRNA halves leaving 5' hydroxyl and 2'-3' cyclic phosphate groups (Rybak and Vallee, 1988). Regarding the origin and biogenesis of tRNA halves in serum one can ask a number of fundamental questions: where does cleavage reaction occurs: i) does the cleavage occur in cells and fragments are then secreted, in that case what is the mechanism of secretion? or ii) does cleavage of full length tRNA occur in serum? In this case, what enzyme is responsible for this, perhaps angiogenin?

In attempt to investigate whether tRNA halves present in serum are derived from tissues or blood cells we employed northern blot hybridisation and qRT-PCR quantification. Unlike Dhahbi et al., we were able to detect the full length tRNA fragments of ~70nt long, and smaller fragments of ~20nt in serum. However, their levels in serum are much lower than tRNA halves (Fig 5.3 & 5.4). The fact that a full length tRNA is present in serum, suggests that the tRNA fragments could be generated in serum. The fact that angiogenin is present in normal human serum at a concentration of 60–480 ng/ml could support this possibility (Shapiro et al., 1987; Shimoyama et al., 1996), however, based on the fact that i) angiogenin is predicted to leave 5' hydroxyl and 2'-3' cyclic phosphate groups (Rybak and Vallee, 1988) and ii) only RNA fragments with 5' phosphate and 3' hydroxyl group can be detected using our deep-sequencing approach, it is unlikely that the fragments we identified by sequencing are a product of angiogening cleavage. Dhahbi et al., have shown that 5' $tRNA^{Gly}$(GCC) are concentrated in hematopoietic and lymphoid tissues (spleen, lymph nodes, foetal liver, leucocytes, thymus and bone marrow) and only present in other tissues (heart, brain, kidney, testes, liver) at very low levels suggesting that they might originate from blood cells. Our results, however, show that 5' $tRNA^{Gly}$(GCC) halves are present in lung, heart, kidney and liver and at lower levels in the spleen. Moreover, they are not present in purified PBMCs and RBC+PMNs.

Thus, our results are more consistent with a model where, if secreted as already processed halves, these do not originate from blood cells but could come from non-blood tissues. Further work needs to be carried out to investigate this.

Deep-sequencing data confirmed by northern blotting and qRT-PCR show a clear bias in the abundance of 5' versus 3' products of tRNA, indicating specificity in the mechanism of stabilization of these products following cleavage. RNA molecules have been identified in vesicles and specific small RNAs are enriched in vesicles in relation to the pool of intracellular small RNA (Pigati et al., 2010; Valadi et al., 2007; Villarroya-Beltri et al., 2013). Several reports suggest, however, that a substantial fraction of miRNAs are not encapsulated within vesicles but are stabilized from RNase digestion by association with proteins (Arroyo et al., 2011; Turchinovich et al., 2011; Vickers et al., 2011; Wang et al., 2011). Studies of intracellular tRNA halves showed that 5' $tRNA^{Ala}$ can directly or indirectly interact with several proteins such as: TDP-43, Vigilin, YB-1, eIF4E, eIF4G, CAPRINI1, Argonaute-2, PABP1 and FXR1 which are involved in mRNA metabolism (Ivanov et al., 2011). Our findings suggest that tRNA halves (5' $tRNA^{Gly}$(GCC)) are protected against serum RNase activity by protein complexes rather than vesicles which is in agreement with (Dhahbi et al., 2013). Specifically, we have shown that 5' $tRNA^{Gly}$(GCC) halves are destabilised by Proteinase K digestion of serum and are present in the vesicle-depleted fraction post ultracentrifugation. Further, by employing size exclusion chromatography, we have shown that the majority of 5' $tRNA^{Gly}$(GCC) halves is not present in the vesicle rich/large protein fraction. Interestingly, the size exclusion profile of 5' $tRNA^{Gly}$(GCC) in the serum differs from that of miRNAs, which suggest that 5' tRNA halves are not protected by Argonaute protein which typically have a molecular weight of ~100 kDa (Ender and Meister, 2010) but a smaller protein (~40kDa). This differs from results presented by Dhahbi et al., who used molecular weight cut-off filters rather than SEC, and showed that 5' $tRNA^{Gly}$(GCC) and 5' $tRNA^{Val}$(CAC) halves are a part of a 100-300kDa complex (Dhahbi et al., 2013). Based on our data, 3' $tRNA^{Gly}$(GCC) was present mainly in the vesicle/large protein complexes fraction. Further work would need to be carried out

to determine which proteins and/or other factors complex with tRNA halves in the extracellular space, which might provide insights on their roles.

To do that there is a need for increasing the resolution and separation range of SEC in order to better differentiate between Pool II (miRNA rich fraction) and Pool III (tRNA-rich fraction). Alternatively the fractions could be further separated by anion exchange chromatography. More resolved fractions could then be subjected to Mass Spectrometry to identify the proteins present.

Dhahbi et al., demonstrated that the levels of 5' tRNA fragments change with age in mice and that calorie restrictions prevents these changes, suggesting that they are subject to physiological conditions (Dhahbi et al., 2013). We measured the levels of $tRNA^{Gly}$(GCC) halves in mouse serum upon oxidative stresses caused by *S. mansoni* infection. We showed that their levels do not change and that they cannot serve as biomarker of this infection. As mentioned in Chapter 4, the methodology of miRNA analysis in body fluids is not well standardized, and it is still not clear which small RNAs are appropriate for normalization (Hoy and Buck, 2012; Scholer et al., 2010; Weiland et al., 2012b). With tRNA halves being stable, present at > 10 fold higher copy number than known miRNAs, and unchanged upon *S.mansoni* infection, it would be of interest to determine whether they could be used as endogenous normaliser.

It is exciting to think that tRNA halves present in serum might be functional. To date, several studies have shown the role of intercellular tRNA halves produced during a stress response. During stress cells protect themselves by down-regulating transcription and translation of several 'houskeeping' genes and simultaneous up-regulating genes important for cell survival. Phosphorylation of eukaryotic translation initiation factor 2α (eIF2α) plays a profound role in translation inhibition and assembly of stress granules. Yamasaki et al., have shown that both angiogenin and 5' tRNA halves generated by angiogenin inhibit modestly global protein synthesis in cultured cells (Yamasaki et al., 2009). It has been shown that 5' but not 3' tRNA halves bind to YB-1 and promote assembly of stress granules, which is independent of phospho-eIF2α (Emara et al., 2010; Ivanov et al., 2011). The

mechanism of protein synthesis inhibition by certain tRNA halves ($tRNA^{Ala}$, $tRNA^{Cys}$) involves displacing eIF4G/eIF4A from mRNA and eIF4F from the m7G cap (Ivanov et al., 2011). A recently published paper has shown that 5'$tRNA^{Glu}$ (CTC) halves generated in human airway epithelial cells infected with respiratory syncytial virus (RSV) promotes viral replication. The authors have shown that 5' $tRNA^{Glu}$ (CTC) halves exhibit *trans*-silencing capacity that is distinct from those of miRNA and siRNAs by designing a series of *in vitro* experiments using a sensor plasmid harbouring a reverse complementary sequence of 5' $tRNA^{Glu}$(CTC) halves in the 3'-untranslated region of the firefly luciferase gene (Wang et al., 2013). It has been shown that *S.mansoni* infection leads to alteration in oxidative status in the liver as well as other organs such as kidney, heart and brain. In the liver, the oxidative stress is related to the presence of granulomas and immune cells, which are strongly associated with the production of reactive oxygen species and oxidative damage (de Oliveira et al., 2013).

Chapter 6: **Concluding Remarks and Future Directions**

6.1 Rational and objectives of this thesis

Schistosomiasis is second to malaria as as the most important parasitic infection in the world in terms of economic and public health impact. It has been estimated that 200 million people are infected worldwide of which more than 40% are affected by *S.mansoni* (Steinmann et al., 2006; WHO, 2013a). Diagnosis of schistosome infection is crucial for patient management, evaluation of treatment efficacy, monitoring of disease transmission and success of control strategies; however, currently used techniques have a number of drawbacks, hence the importance of developing better diagnostic methods of schistosomiasis have been emphasized by the WHO (WHO, 2008, 2013b). The chronic pathology of *S.mansoni* infection is characterized by granulomatous inflammation around the parasite egg, portal hypertension, splenomegaly, gastrointestinal varices and liver fibrosis (Gryseels et al. 2006). Liver fibrosis itself, regardless of the causative insult, is a major global health issue. Despite the huge progress the research has made in improving our understanding of the process of fibrogenesis, apart for the removal of the causative agent, which is impossible in some cases, there is no treatment for hepatic fibrosis/cirrhosis other than liver transplantation at the end stage of liver failure. There is also a lack of good markers for differentiating between early stages of fibrosis and for significant liver fibrosis that could replace currently used liver biopsies.

The development of novel therapeutics and diagnostics requires a greater understanding of the systemic, cellular and molecular processes in the liver during the progression and resolution of fibrosis. One class of non-coding RNAs, miRNAs, have been recognised to play vital roles in disease processes including fibrogenesis. The fact that these molecules are present in body fluids in a remarkably stable form and that their expression is altered in the disease sparked extensive interest in the use of miRNAs as biomarkers of disease. The therapeutic potential of miRNA is also now widely recognised and many miRNAs have been identified as potential targets for development of treatment for liver fibrosis. Several pre-clinical studies have been

conducted to develop miRNA-based therapeutics and test their efficacy in various animal models of disease. With recent successes of the phase 1 and 2 clinical trials for miRNA therapeutics for treatment of hepatitis C and lung cancer, it is expected that miRNAs will become an important therapeutic tool in the near future.

Given the health burden of *S.mansoni* infection and associated liver fibrosis this thesis examined the role of miRNAs in the *S.mansoni* infection with the emphasis on development of novel RNA-based diagnostics of *S.mansoni* infection and exploring the potential of miRNA-based therapeutics for the treatment of liver fibrosis.

The study presented in this thesis aimed to:

- Examine the profile of miRNAs upon *S.mansoni* infection and select miRNA candidates that have potential to be used as novel biomarkers and therapeutic agents.
- Investigate the role of miRNAs in progression and resolution of liver fibrosis induced upon *S.mansoni* infection and examine the potential of miRNA inhibitors in the treatment of liver fibrosis.
- Investigate the RNA profile in serum upon *S.mansoni* infection and examine the diagnostic potential of circulating miRNAs.

6.2 Conclusions

At the time of carrying out the work presented in this thesis there was no published data on the profile of host miRNAs in the liver upon *S.mansoni* infection, thus the first aim was to examine the expression of miRNAs in the liver upon infection. We demonstrated that a set of miRNAs are altered in the liver of infected compared to naïve mice, among which were miRNAs that have previously been linked to liver disease. This provides the framework for further studies of the function of these miRNAs in this infection. Moreover, some of the miRNAs we identified, for example miR-21 and miR-199/214, have been reported to be up-regulated in liver fibrosis induced by different insults and thus could serve as targets for the development of general antifibrotic therapeutic, rather than being disease specific. This opens an exciting avenue for further studies in the area of fibrogenesis and drug development.

The second aim of this thesis was to investigate the role of miRNAs in the progression and resolution of liver fibrosis induced upon *S.mansoni* infection and examine the potential of miRNA inhibitors in the treatment of liver fibrosis. One of the miRNAs that we identified to be dysregulated, miR-199a-3p, is the third most abundant miRNA in the liver (Hou et al., 2011) and has previously been shown to be up-regulated upon liver fibrosis (Murakami et al., 2011; Ogawa et al., 2012). The over-expression of this miRNA leads to up-regulation of fibrosis – related genes such as TIMP-1, COL1A1, MMP-13 in HSCs *in vitro* (Iizuka et al., 2012). We therefore investigated whether the inhibition of this miRNA has an antifibrotic effect *in vivo*. The advantage of examining the functionality *in vivo* is that we can examine the effect of treatment in the living subject, on the entire organ, which is composed of multiple cell types that work together. The main caveats to this approach are i) not knowing which cell types uptake the drug, without performing isolation of cells and ii) more difficult, as compared to in vitro studies, investigation of exact mechanism of the tested molecules.

We have shown that systemic administration of miR-199a-3p inhibitor upon *S.mansoni* infection results in changes of fibrosis-related genes on the mRNA level in such a way that it indicates an indirect antifibrotic effect. From the previous literature it seems that miR-199a-3p plays a role in hepatic stellate cell activation and extracellular matrix synthesis and degradation, which are key in the progression and resolution of liver fibrosis. These data provide a starting point for further research, showing the importance of this miRNA in fibrogenesis and the potential of a miR-199a-3p antagonist in the treatment of liver fibrosis. Although this thesis was focused on *S.mansoni* infection, further work on the therapeutic potential of miR-199a-3p should be carried out in different models of liver fibrosis such as cholestatic (bile duct ligation) or toxic (using carbon tetrachloride) models of liver injury as these closely reflect human liver fibrosis caused by different aetiologies. It is necessary to confirm the effect of miR-199a-3p inhibition on fibrosis - related genes on a protein level and seek out the molecular mechanism of miR-199a-3p action, specifically, examining the targets of miR-199a-3p in HSCs. With the systemic delivery of miRNA agents it is of a great importance to determine the effect of miR-199a-3p inhibition in other then liver tissues and examine the potential occurrence of unwanted immune response. *In vitro* studies using human primary HSCs and human precision liver slices would

provide essential information of the effect of miR-199a-3p inhibition in humans and would be key to further the drug discovery process to the clinical stage.

The third aim of this study was to examine the small RNA profile in serum in search for diagnostic biomarkers of *S.mansoni* infection and liver pathology. We have shown that several classes of small non-coding RNAs are present in the serum of mice and that tRNA-derived fragments, specifically 5' tRNA halves originating form $tRNA^{Gly}$(GCC) are the most abundant small ncRNA. Chapter 5 provided a characterisation of tRNA halves, revealing that they are products of a specific cleavage event within the anticodon loop and are protected against serum RNase activity by protein association that is distinct in size from the complexes containing miRNAs. Further we have shown that the expression of $tRNA^{Gly}$(GCC) halves do not change upon *S.mansoni* infection. With lack of endogenous normalisation control for analysis of miRNAs in serum it is important to examine whether these molecules would be suitable for this purpose. Of importance is the fact that Dhahbi et al., have shown that the expression of 5' $tRNA^{Gly}$(GCC) increases with age which needs to be taken in account in assessing the utility of tRNA fragments as internal controls (Dhahbi et al., 2013).

We have examined the diagnostic potential of host-miRNAs that were altered in the liver upon *S.mansoni* infection. This involved overcoming of challenges of analysis of miRNAs in body fluids, such as lack of endogenous controls or unified methodology of data analysis. The levels of the five tested host-miRNAs that were up-regulated in the liver, were elevated in mice serum in the late stage of infection but failed to differentiate between infected and uninfected human individual. These host miRNAs therefore do not show an advantage over currently used diagnostic techniques, which are able to detect the infection at earlier time points. However they might represent a marker of advanced liver disease. To confirm this they should be examined across different liver disease models, ideally in humans, where measurements of liver function and pathophysiology are available to allow conclusions to be drawn. Moreover, although the literature provides examples of active secretion of miRNAs to the extracellular space, in the case of five tested miRNAs it seems that these miRNAs passively leaked from broken cells.

Importantly, we have found for the first time that parasite-derived miRNAs are present in circulation during *S.mansoni* infection as early as 8 weeks post infection, which correlates with the timing of egg secretion. Three of these miRNAs, specifically miR-277, miR-3479-3p and bantam, can differentiate infected from uninfected individuals with good sensitivity and specificity. Parasite-derived miRNAs offer a diagnostic advantage over host-derived miRNAs since the latter can be altered in serum due to various unrelated conditions. Moreover, it is anticipated that parasite-derived miRNAs could be used as diagnostic tool for other parasitic infections of man and animals. Future work in the area of *S.mansoni* diagnosis should be focused on: i) the optimisation of the qRT-PCR assay for the detection of miR-277, miR-3479-3p and bantam to improve the specificity and sensitivity of the assay, ii) validation in the large group of participants, including single and co-infections with parasitic worm of the genus *Schistosoma* and others, iii) and examining the effect of PZQ treatment on their expression.

Although it is exciting to think that parasite-derived miRNAs might have a function in the host, the fact that they are expressed at very low levels and that mammals lack a mechanism for RNA amplification, it is not clear whether these would be functional.

6.3 Future directions

The findings presented in this thesis provide: i) a background for further studies of the role of miRNAs in *S.mansoni* infection, ii) a base for the development of parasite-derived miRNA assays for diagnosis of *S.mansoni* and other parasitic infections, iii) insight into the therapeutic potential of miR-199a-3p antagonists for the treatment of liver fibrosis and a base for further mechanistic studies in this area, iv) a foundation for further characterisation of tRNA halves and their function. Thus, providing a number of potentially interesting avenues of research. Among the questions yet to be answered are:

Questions regarding host miRNAs:

- What is the mechanism of dysregulation of host-miRNAs in the liver upon *S.mansoni* infection?
- Can the parasite itself influence host-miRNA expression for its benefit?

- What are the functions of host miRNAs altered in the liver upon *S.mansoni* infection?
- What is the role of miR-199a-3p in HSCs activation? What are the targets of miR-199a-3p that mediate HSCs activation and ECM synthesis?

Parasite-derived miRNAs:

- What is the origin of parasite-derived miRNAs in serum? Do they originate from immature or mature worms or the egg? Having in mind the importance of diagnosis of the pre-patent infection, can we identify miRNAs that are specific to the schisotosmulum?
- What is the mechanism of secretion of parasite-derived miRNAs?
- Do parasite-derived miRNAs have a function in the host?
- What is the half-life of parasite-miRNAs in serum? Do the levels of parasite-miRNAs is serum decrease after the PZQ treatment?

Regarding tRNA halves:

- How are the tRNA halves observed in serum produced and what is the mechanism underlying their export to circulation?
- Which proteins associate with tRNA halves in circulation?
- What is the function of extracellular tRNA halves and other tRNA-derived fragments?

Chapter 7: **Appendices**

Appendix 1

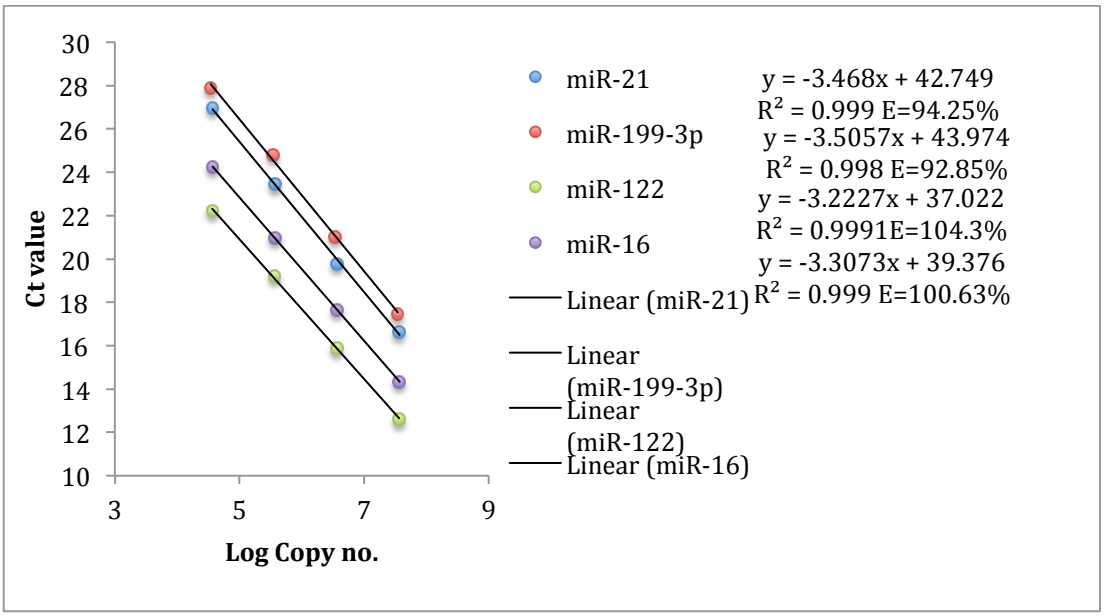

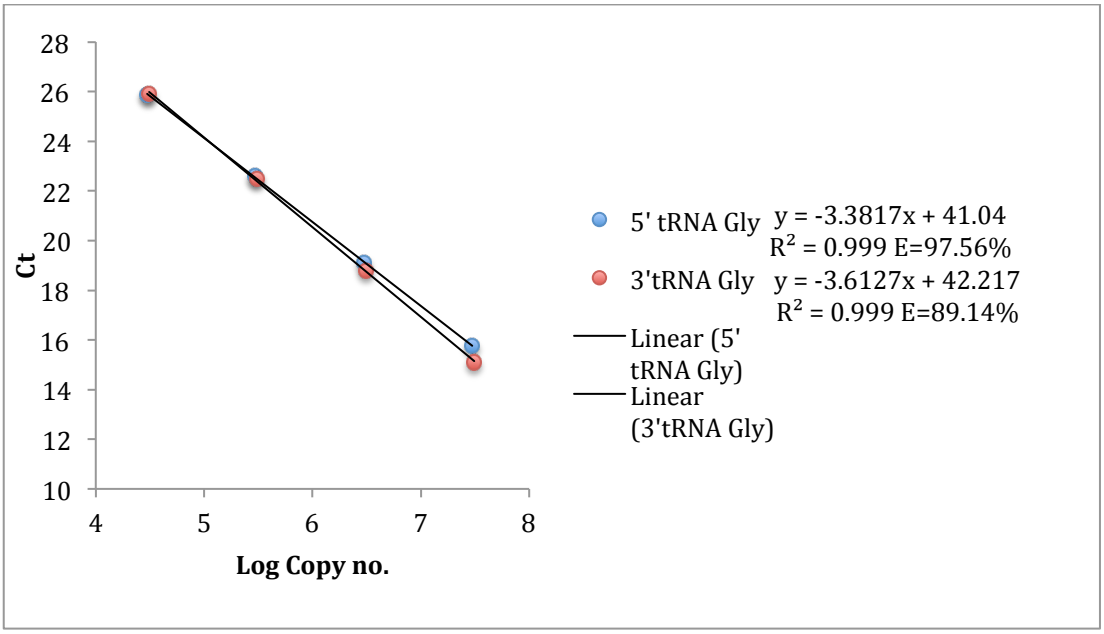

Appendix 1. Standard curves for miRNAs (top) and tRNA^{Gly} (GCC) halves (bottom).

Appendix 2

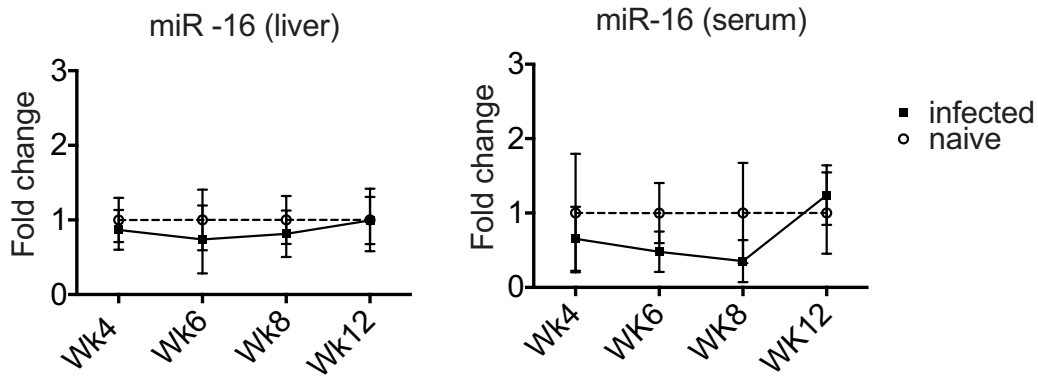

Appendix 2. Expression of miR-16 in the liver and serum during the time course of *S. mansoni* infection.
miRNAs were quantified by qRT-PCR, normalised to U6 snRNA (liver) or synthetic RNA spike-in (serum) and fold change was calculated as infected to naïve ratio. ($P<0.05$, two-way ANOVA followed by Sidak multiple-comparison test).

Appendix 3

Appendix 3. Expression of miRNAs in the liver and serum during the time course of *S.mansoni* infection.
8-10 week old C57BL/6 mice were left uninfected or infected percutaneously with ~80 cercariae and euthanized at 4, 6, 8 and 12 weeks post infection. miRNAs were quantified by qRT-PCR and normalized to a synthetic RNA spike-in (serum) or miR-16 (liver). Fold changes are defined as the ratio of abundance in infected versus naïve serum; the signal from naïve was set as 1. (***p<0.001, ****p<0.0001, Two-way ANOVA, Sidak multiple comparison test

ttest		Liver Fold change	ANOVA	Serum Fold Change	ANOVA
miR-199-5p	Wk4	1.2247	ns	0.9013	ns
	Wk6	1.5344	ns	0.4812	ns
	Wk8	3.3633	****	0.1861	ns
	W12	5.5222	****	3.4435	***
miR-199-3p	Wk4	1.1878	ns	0.9632	ns
	Wk6	1.5647	*	0.5151	ns
	Wk8	3.268	****	0.1358	ns
	W12	4.5223	****	2.955	***
miR-214	Wk4	1.5937	ns	0.50634	ns
	Wk6	3.2422	**	1.11909	ns
	Wk8	3.2945	**	0.24445	ns
	Wk12	4.3588	****	8.44836	****
mir-210	Wk4	1.4978	ns	0.7285	ns
	Wk6	1.1733	ns	0.979	ns
	Wk8	2.6473	**	1.2762	ns
	Wk12	2.6489	***	5.1376	****
miR-21	Wk4	1.2287	ns	1.1002	ns
	Wk6	1.857	****	0.6199	ns
	Wk8	2.1401	****	1.4159	ns
	Wk12	2.0253	****	2.6236	****
miR-122	Wk4	0.8596	ns	0.9307	ns
	Wk6	1.0334	ns	0.355	ns
	Wk8	0.6497	**	0.2035	ns
	Wk12	0.3984	****	0.2208	ns
miR-192	Wk4	0.8381	*	1.1054	ns
	Wk6	0.9809	ns	0.4546	ns
	Wk8	0.5028	****	0.2483	ns
	Wk12	0.3654	****	0.8122	ns
miR-194	Wk4	0.8826	ns	0.7292	ns
	Wk6	0.702	ns	0.3032	ns
	Wk8	0.5063	**	0.3854	ns
	Wk12	0.4155	****	0.2992	ns
miR-365	Wk4	1.0425	ns	0.6283	ns
	Wk6	0.7892	ns	0.3603	ns
	Wk8	0.6271	ns	0.2132	ns
	Wk12	0.8208	ns	1.199	ns

Appendix 4

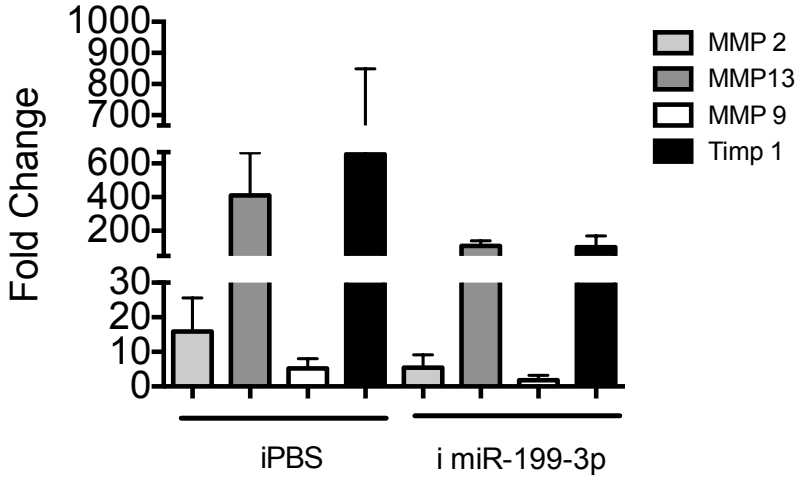

Appendix 4. Expression profile of MMPs and TIMP1 in the liver of *S.mansoni* infected mice upon miR-199a-3p inhibition.

MMP2, MMP13, MMP9 and TIMP1 genes were quantified by qRT-PCR, normalized to GAPDH and fold changes calculated versus nPBS. (*p<0.05, **p<0.01, ***p<0.001, ****p<0.0001).

Appendix 5

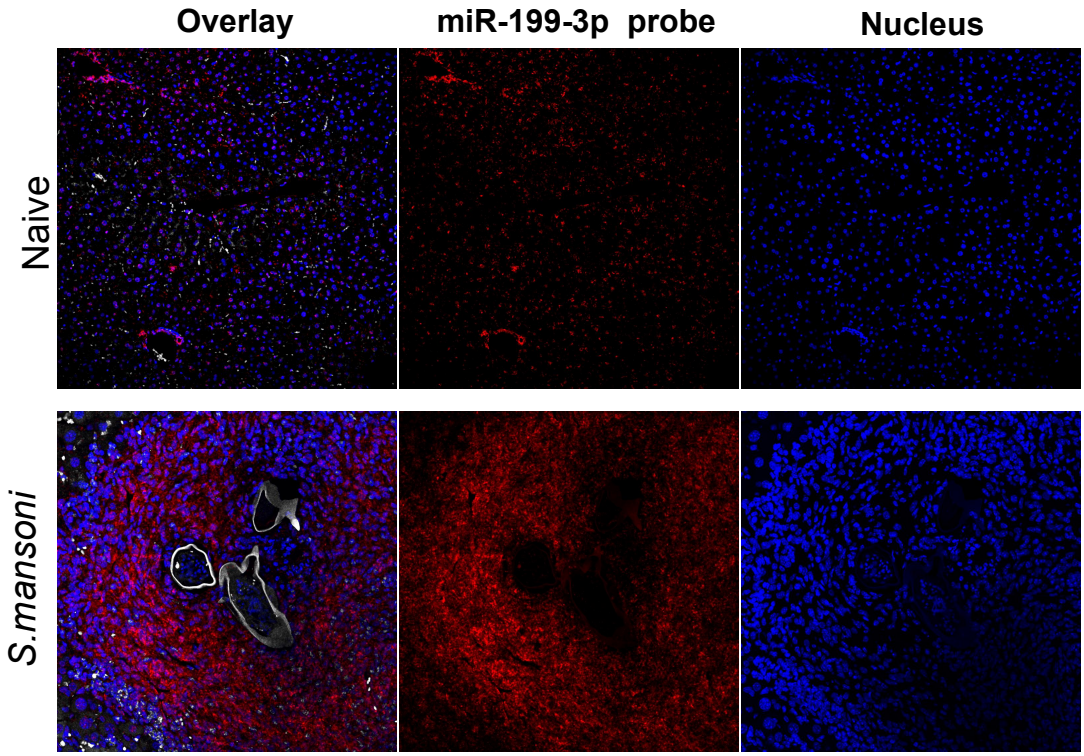

Appendix 5. ***In situ*** **detection of DIG-labelled probes against miR-199a-3p in liver of naïve and** ***S.mansoni*** **(80 cerc.) infected mice at 8 weeks post infection.**
miR-199a-3p signal (red) and nuclear DAPI signal (blue). *Figure provided by Dr. Jess Borger.*

Appendix 6

Appendix 6. Tabulated mouse miRNA reads identified in serum of naïve and infected mice.

The "X" denotes the miRNAs who were assigned reads that could have derived from one of multiple miRNA family members (e.g. in the case of shortened reads).

miRNA	Experiment 1		Experiment 2			Ambiguous
	Naïve	Infected	Naïve	Infected	Total	
mmu-miR-99b-5p	516	717	85	101	1419	
mmu-miR-99b-3p	0	0	3	6	9	
mmu-miR-99a-5p	137	86	132	825	1180	
mmu-miR-98-5p	6	2	8	14	30	
mmu-miR-98-3p	0	4	0	0	4	
mmu-miR-96-5p	0	0	9	7	16	
mmu-miR-93-5p	67	205	2323	3064	5659	
mmu-miR-93-3p	0	0	4	18	22	
mmu-miR-92b-3p	2	73	4	4	83	
mmu-miR-92a-3p	53	348	969	1043	2413	
mmu-miR-9-5p	0	0	7	0	7	
mmu-miR-9-3p	0	0	0	2	2	
mmu-miR-879-5p	0	0	0	4	4	
mmu-miR-877-3p	0	0	0	2	2	
mmu-miR-874-3p	0	2	0	57	59	
mmu-miR-872-5p	0	3	11	63	77	
mmu-miR-872-3p	0	0	0	26	26	
mmu-miR-802-5p	0	0	2	68	70	
mmu-miR-802-3p	3	0	0	26	29	
mmu-miR-7a-5p	0	10	6	12	28	
mmu-miR-7a-1-3p	0	0	3	32	35	
mmu-miR-744-5p	3	50	1645	1244	2942	
mmu-miR-708-5p	0	0	8	8	16	
mmu-miR-702-3p	0	2	0	0	2	
mmu-miR-701-5p	0	0	0	3	3	
mmu-miR-700-5p	0	0	0	6	6	
mmu-miR-700-3p	0	0	3	8	11	
mmu-miR-676-5p	0	2	3	4	9	
mmu-miR-676-3p	8	68	2	46	124	
mmu-miR-674-5p	0	0	2	122	124	
mmu-miR-674-3p	0	0	2	50	52	
mmu-miR-672-5p	0	0	6	8	14	
mmu-miR-671-5p	0	0	3	30	33	
mmu-miR-671-3p	0	7	7	9	23	
mmu-miR-669c-5p	0	0	21	12	33	
mmu-miR-669a-5p	0	2	0	2	4	
mmu-miR-669a-3p	0	0	0	2	2	X
mmu-miR-667-3p	0	0	0	5	5	
mmu-miR-665-3p	0	0	0	34	34	

miRNA	Experiment 1		Experiment 2			Ambiguous
	Naïve	Infected	Naïve	Infected	Total	
mmu-miR-654-3p	0	0	4	3	7	
mmu-miR-6538	0	2	0	0	2	
mmu-miR-652-3p	0	7	27	125	159	
mmu-miR-6240	0	3	0	0	3	
mmu-miR-615-3p	0	2	0	0	2	
mmu-miR-598-3p	0	0	7	4	11	
mmu-miR-582-5p	0	0	2	3	5	
mmu-miR-582-3p	0	0	0	2	2	
mmu-miR-574-3p	7	8	86	300	401	
mmu-miR-543-3p	0	0	4	9	13	
mmu-miR-542-5p	0	0	6	6	12	
mmu-miR-542-3p	0	0	30	31	61	
mmu-miR-541-5p	69	41	138	56	304	
mmu-miR-540-3p	0	0	0	2	2	
mmu-miR-532-5p	2	6	403	176	587	
mmu-miR-532-3p	0	2	0	14	16	
mmu-miR-5120	0	0	2	0	2	
mmu-miR-511-3p	0	2	0	80	82	
mmu-miR-5109	0	24	0	8	32	
mmu-miR-5107-5p	0	2	0	0	2	
mmu-miR-5105	0	0	0	2	2	
mmu-miR-5100	0	0	0	19	19	
mmu-miR-505-3p	0	0	0	2	2	
mmu-miR-503-5p	0	0	2	42	44	
mmu-miR-503-3p	0	3	11	4	18	
mmu-miR-501-5p	0	0	0	4	4	
mmu-miR-501-3p	8	46	15	93	162	
mmu-miR-500-3p	0	0	15	515	530	
mmu-miR-499-5p	0	0	0	5	5	
mmu-miR-497-5p	0	0	5	146	151	
mmu-miR-495-3p	0	0	0	4	4	
mmu-miR-494-3p	0	0	0	15	15	
mmu-miR-486-3p	10	18	113	159	300	
mmu-miR-485-3p	0	0	0	9	9	
mmu-miR-484	12	35	44	629	720	
mmu-miR-483-5p	0	0	0	2	2	
mmu-miR-467a-5p	0	0	0	5	5	
mmu-miR-455-5p	0	0	4	0	4	
mmu-miR-451a	378	492	5688	37762	44320	
mmu-miR-450a-5p	0	0	5	0	5	
mmu-miR-450a-2-3p	0	0	0	2	2	
mmu-miR-434-5p	4	3	2	9	18	
mmu-miR-434-3p	8	9	9	42	68	
mmu-miR-433-3p	0	0	0	4	4	
mmu-miR-431-5p	2	2	0	0	4	
mmu-miR-429-3p	0	4	14	63	81	

miRNA	Experiment 1		Experiment 2			Ambiguous
	Naïve	Infected	Naïve	Infected	Total	
mmu-miR-425-5p	39	285	45	1599	1968	
mmu-miR-425-3p	0	0	4	27	31	
mmu-miR-423-5p	269	2697	58	772	3796	
mmu-miR-423-3p	14	180	43	1179	1416	
mmu-miR-421-3p	0	2	0	17	19	
mmu-miR-411-5p	0	0	6	6	12	
mmu-miR-411-3p	0	0	4	0	4	
mmu-miR-410-3p	5	8	0	17	30	
mmu-miR-409-3p	3	0	9	27	39	
mmu-miR-382-5p	0	0	54	18	72	
mmu-miR-381-3p	0	6	89	49	144	
mmu-miR-380-5p	0	0	2	0	2	
mmu-miR-380-3p	0	0	0	10	10	
mmu-miR-379-5p	11	8	79	57	155	
mmu-miR-378d	0	0	12	18	30	
mmu-miR-378b	0	0	2	2	4	
mmu-miR-378a-5p	0	0	8	70	78	
mmu-miR-378a-3p	48	90	3779	2633	6550	X
mmu-miR-377-3p	0	0	5	49	54	
mmu-miR-376c-3p	0	0	0	2	2	
mmu-miR-376b-5p	0	0	2	8	10	
mmu-miR-376b-3p	0	0	0	32	32	
mmu-miR-376a-3p	0	0	0	2	2	
mmu-miR-375-3p	7	39	698	100	844	
mmu-miR-374b-5p	14	7	13	76	110	X
mmu-miR-370-3p	0	2	0	0	2	
mmu-miR-369-5p	0	0	0	4	4	
mmu-miR-369-3p	0	0	3	24	27	
mmu-miR-365-3p	0	3	2	57	62	
mmu-miR-363-3p	2	2	0	17	21	
mmu-miR-362-5p	0	0	7	14	21	
mmu-miR-362-3p	0	0	3	91	94	
mmu-miR-361-5p	2	16	8	263	289	
mmu-miR-361-3p	0	3	6	4	13	
mmu-miR-351-5p	24	32	2	12	70	
mmu-miR-351-3p	0	0	0	2	2	
mmu-miR-350-3p	0	0	0	57	57	
mmu-miR-34c-5p	0	14	69	41	124	
mmu-miR-34c-3p	0	0	0	2	2	
mmu-miR-34b-3p	0	0	2	3	5	
mmu-miR-34a-5p	0	0	7	274	281	
mmu-miR-345-5p	0	0	0	6	6	
mmu-miR-345-3p	0	0	0	9	9	
mmu-miR-344d-3p	0	2	3	4	9	
mmu-miR-342-5p	0	2	0	15	17	
mmu-miR-342-3p	9	51	7	437	504	

miRNA	Experiment 1		Experiment 2			Ambiguous
	Naïve	Infected	Naïve	Infected	Total	
mmu-miR-340-5p	18	16	7	65	106	
mmu-miR-340-3p	0	0	2	0	2	
mmu-miR-339-5p	0	4	15	656	675	
mmu-miR-339-3p	0	2	11	176	189	
mmu-miR-338-5p	0	0	15	28	43	
mmu-miR-335-5p	0	3	0	138	141	
mmu-miR-335-3p	0	0	0	4	4	
mmu-miR-331-5p	0	0	10	2	12	
mmu-miR-330-3p	0	0	14	76	90	
mmu-miR-33-5p	0	0	9	270	279	
mmu-miR-33-3p	0	0	0	5	5	
mmu-miR-328-3p	7	33	29	370	439	
mmu-miR-326-3p	3	2	4	61	70	
mmu-miR-324-5p	0	0	0	29	29	
mmu-miR-322-5p	0	0	4	123	127	
mmu-miR-322-3p	3	6	0	6	15	
mmu-miR-320-3p	4	57	43	810	914	
mmu-miR-32-5p	0	0	4	213	217	
mmu-miR-3107-5p	11723	68425	4696	2750	87594	X
mmu-miR-3107-3p	0	7	29	33	69	X
mmu-miR-3105-5p	0	0	0	2	2	
mmu-miR-3105-3p	0	0	0	2	2	
mmu-miR-3102-3p	0	0	0	3	3	
mmu-miR-30e-5p	82	207	135	1707	2131	
mmu-miR-30e-3p	19	10	145	18	192	
mmu-miR-30d-5p	377	2002	834	3649	6862	
mmu-miR-30d-3p	0	2	14	4	20	
mmu-miR-30c-5p	16	8	77	1823	1924	
mmu-miR-30b-5p	14	13	56	470	553	X
mmu-miR-30b-3p	0	2	0	0	2	
mmu-miR-30a-5p	1833	9179	2878	5625	19515	
mmu-miR-30a-3p	11	31	975	98	1115	
mmu-miR-3074-5p	0	0	0	4	4	
mmu-miR-3066-5p	0	0	2	0	2	
mmu-miR-3058-5p	0	0	0	2	2	
mmu-miR-3058-3p	0	2	0	0	2	
mmu-miR-3057-5p	0	0	15	6	21	
mmu-miR-301b-3p	0	0	2	4	6	
mmu-miR-301a-3p	3	8	14	36	61	
mmu-miR-300-3p	6	23	6	67	102	
mmu-miR-29c-3p	2	13	72	4970	5057	
mmu-miR-29b-3p	0	0	60	681	741	
mmu-miR-29a-5p	0	0	0	11	11	
mmu-miR-29a-3p	31	127	363	18883	19404	
mmu-miR-299a-3p	0	0	13	23	36	
mmu-miR-298-5p	0	2	0	0	2	

miRNA	Experiment 1		Experiment 2			Ambiguous
	Naïve	Infected	Naïve	Infected	Total	
mmu-miR-296-5p	0	0	0	50	50	
mmu-miR-296-3p	0	2	25	31	58	
mmu-miR-28a-5p	0	0	7	44	51	
mmu-miR-28a-3p	2	4	328	115	449	
mmu-miR-27b-5p	0	0	0	7	7	
mmu-miR-27b-3p	734	1997	247	4225	7203	
mmu-miR-27a-5p	0	0	0	14	14	
mmu-miR-27a-3p	33	120	1553	4746	6452	X
mmu-miR-26b-5p	10	3	6	54	73	
mmu-miR-26a-5p	282	235	59	298	874	
mmu-miR-25-3p	278	888	22328	5329	28823	
mmu-miR-24-3p	140	381	652	25987	27160	
mmu-miR-24-2-5p	0	14	14	134	162	
mmu-miR-24-1-5p	0	0	0	2	2	
mmu-miR-23b-3p	5	0	214	219	438	
mmu-miR-23a-5p	0	0	0	9	9	
mmu-miR-23a-3p	60	158	2091	5490	7799	X
mmu-miR-224-5p	0	0	0	2	2	
mmu-miR-223-5p	0	0	0	3	3	
mmu-miR-223-3p	5	9	22	727	763	
mmu-miR-222-5p	0	2	0	0	2	
mmu-miR-222-3p	3	7	39	980	1029	
mmu-miR-221-3p	12	46	1136	3373	4567	
mmu-miR-22-5p	0	0	3	269	272	
mmu-miR-22-3p	837	4642	1041	24343	30863	
mmu-miR-21a-5p	117	1021	34554	83163	118855	
mmu-miR-21a-3p	16	165	0	306	487	
mmu-miR-219-5p	0	0	0	10	10	
mmu-miR-218-5p	0	0	2	10	12	
mmu-miR-216a-5p	0	0	0	4	4	
mmu-miR-215-5p	4	17	1089	504	1614	
mmu-miR-215-3p	0	0	9	2	11	
mmu-miR-214-5p	0	0	2	7	9	
mmu-miR-214-3p	0	0	0	8	8	
mmu-miR-212-3p	0	2	0	35	37	
mmu-miR-210-3p	0	27	25	2479	2531	
mmu-miR-20b-5p	0	0	5	42	47	
mmu-miR-20a-5p	0	4	36	499	539	
mmu-miR-208b-3p	0	2	0	10	12	
mmu-miR-208a-3p	0	0	9	227	236	
mmu-miR-206-3p	2	0	4	15	21	
mmu-miR-205-5p	3	0	8	54	65	
mmu-miR-204-5p	16	4	2	2	24	
mmu-miR-203-5p	0	0	14	0	14	
mmu-miR-203-3p	0	6	38	122	166	
mmu-miR-200c-3p	0	4	208	53	265	

miRNA	Experiment 1		Experiment 2			Ambiguous
	Naïve	Infected	Naïve	Infected	Total	
mmu-miR-200b-5p	0	0	0	10	10	
mmu-miR-200b-3p	0	0	181	129	310	
mmu-miR-200a-5p	0	0	18	3	21	
mmu-miR-200a-3p	16	50	34	320	420	
mmu-miR-1a-3p	71	16	123	473	683	
mmu-miR-1a-1-5p	0	0	3	4	7	
mmu-miR-19b-3p	0	5	617	1519	2141	
mmu-miR-19a-3p	0	0	274	432	706	
mmu-miR-199b-5p	0	0	0	2	2	
mmu-miR-199a-5p	0	3	7	25	35	
mmu-miR-199a-3p	43	44	22	587	696	X
mmu-miR-1983	0	0	0	17	17	
mmu-miR-1981-5p	4	6	66	28	104	
mmu-miR-1981-3p	0	0	2	0	2	
mmu-miR-196b-5p	0	0	12	11	23	
mmu-miR-196a-5p	0	0	7	0	7	
mmu-miR-1968-5p	0	0	0	2	2	
mmu-miR-1965	0	0	0	2	2	
mmu-miR-1964-5p	0	0	0	7	7	
mmu-miR-1964-3p	0	11	11	8	30	
mmu-miR-1960	0	2	0	0	2	
mmu-miR-195a-5p	22	3	0	11	36	
mmu-miR-195a-3p	0	0	2	0	2	
mmu-miR-1955-3p	0	0	0	2	2	
mmu-miR-1943-5p	0	16	3	21	40	
mmu-miR-1943-3p	0	0	0	2	2	
mmu-miR-194-5p	3	10	67	4293	4373	
mmu-miR-193b-3p	0	0	8	99	107	
mmu-miR-193a-5p	0	0	5	116	121	
mmu-miR-193a-3p	0	0	2	276	278	
mmu-miR-1930-5p	0	0	0	3	3	
mmu-miR-192-5p	436	2884	2683	10675	16678	
mmu-miR-192-3p	0	0	0	72	72	
mmu-miR-191-5p	450	2509	394	1792	5145	
mmu-miR-191-3p	0	4	2	10	16	
mmu-miR-18a-5p	0	0	25	326	351	
mmu-miR-18a-3p	0	2	0	11	13	
mmu-miR-188-5p	0	0	0	16	16	
mmu-miR-187-5p	0	0	0	2	2	
mmu-miR-187-3p	0	0	0	5	5	
mmu-miR-186-5p	85	169	476	147	877	
mmu-miR-185-5p	0	8	30	1601	1639	
mmu-miR-185-3p	0	0	0	3	3	
mmu-miR-184-3p	6	11	9	6	32	
mmu-miR-183-5p	0	2	208	16	226	
mmu-miR-182-5p	7	64	467	33	571	

miRNA	Experiment 1		Experiment 2			Ambiguous
	Naïve	Infected	Naïve	Infected	Total	
mmu-miR-181d-5p	5	14	60	64	143	
mmu-miR-181c-5p	12	34	7	27	80	
mmu-miR-181c-3p	0	0	15	9	24	
mmu-miR-181b-5p	6	14	146	133	299	
mmu-miR-181a-5p	172	407	217	694	1490	
mmu-miR-181a-1-3p	0	0	23	4	27	
mmu-miR-17-5p	0	0	78	878	956	
mmu-miR-17-3p	0	2	0	8	10	
mmu-miR-16-5p	1535	2945	1810	22432	28722	
mmu-miR-16-2-3p	0	3	2	16	21	
mmu-miR-16-1-3p	0	3	3	3	9	
mmu-miR-15b-5p	0	6	35	1140	1181	
mmu-miR-15b-3p	2	9	20	192	223	
mmu-miR-15a-5p	19	37	55	2136	2247	
mmu-miR-15a-3p	7	15	0	40	62	
mmu-miR-155-5p	0	0	2	34	36	
mmu-miR-154-5p	0	0	2	10	12	
mmu-miR-154-3p	0	0	0	8	8	
mmu-miR-152-3p	2	8	52	1620	1682	
mmu-miR-151-5p	6	14	17	65	102	
mmu-miR-151-3p	60	270	859	251	1440	
mmu-miR-150-5p	26	92	43	595	756	
mmu-miR-150-3p	0	3	14	26	43	
mmu-miR-149-5p	4	2	0	12	18	
mmu-miR-148b-5p	0	3	6	8	17	
mmu-miR-148b-3p	10	21	98	1456	1585	
mmu-miR-148a-5p	9	68	43	32	152	
mmu-miR-148a-3p	365	1176	6260	14510	22311	
mmu-miR-147-3p	0	0	0	11	11	
mmu-miR-146b-5p	14	18	6	8	46	
mmu-miR-146a-5p	537	2385	255	1374	4551	
mmu-miR-145a-5p	0	0	21	444	465	
mmu-miR-145a-3p	0	4	14	8	26	
mmu-miR-144-5p	2	2	445	12	461	
mmu-miR-144-3p	99	243	454	12938	13734	
mmu-miR-143-5p	0	0	5	2	7	
mmu-miR-143-3p	1707	1721	5687	1580	10695	
mmu-miR-142-5p	41	119	16	346	522	
mmu-miR-142-3p	0	0	19	93	112	
mmu-miR-141-3p	42	264	22	98	426	
mmu-miR-140-5p	0	0	25	124	149	
mmu-miR-140-3p	2	7	311	467	787	
mmu-miR-139-5p	8	8	3	155	174	
mmu-miR-139-3p	0	0	0	3	3	
mmu-miR-138-5p	0	0	0	7	7	
mmu-miR-137-5p	0	0	0	2	2	

miRNA	Experiment 1		Experiment 2			Ambiguous
	Naïve	Infected	Naïve	Infected	Total	
mmu-miR-137-3p	0	0	0	41	41	
mmu-miR-136-5p	0	0	2	12	14	
mmu-miR-136-3p	0	0	2	3	5	
mmu-miR-135b-5p	0	0	14	6	20	
mmu-miR-134-5p	0	0	19	95	114	
mmu-miR-133a-3p	4	0	9	42	55	
mmu-miR-132-5p	0	0	0	2	2	
mmu-miR-132-3p	0	0	92	158	250	
mmu-miR-130b-5p	0	0	2	4	6	
mmu-miR-130b-3p	2	29	40	699	770	
mmu-miR-130a-3p	45	165	145	6375	6730	
mmu-miR-1306-5p	0	0	0	8	8	
mmu-miR-1306-3p	0	0	0	2	2	
mmu-miR-129-5p	0	0	14	4	18	
mmu-miR-129-2-3p	0	2	0	0	2	
mmu-miR-128-3p	5	46	2	176	229	
mmu-miR-128-2-5p	0	0	2	0	2	
mmu-miR-127-5p	0	0	2	8	10	
mmu-miR-127-3p	32	14	68	31	145	
mmu-miR-126-5p	34	125	100	417	676	
mmu-miR-126-3p	2	8	120	1392	1522	
mmu-miR-125b-5p	9	10	107	183	309	
mmu-miR-125b-2-3p	7	15	16	38	76	
mmu-miR-125b-1-3p	0	2	0	3	5	
mmu-miR-125a-5p	94	232	31	180	537	
mmu-miR-125a-3p	0	2	10	11	23	
mmu-miR-1249-3p	0	0	0	3	3	
mmu-miR-1247-5p	0	0	0	6	6	
mmu-miR-122-5p	2892	16730	2963	72685	95270	
mmu-miR-122-3p	0	0	0	235	235	
mmu-miR-1198-5p	4	25	44	101	174	
mmu-miR-10b-5p	3270	11869	1237	318	16694	
mmu-miR-10b-3p	0	0	0	2	2	
mmu-miR-10a-5p	4929	14490	972	599	20990	
mmu-miR-10a-3p	0	0	25	28	53	
mmu-miR-107-3p	0	0	2	4	6	
mmu-miR-106b-5p	2	2	417	4599	5020	
mmu-miR-106b-3p	13	12	188	52	265	
mmu-miR-106a-5p	0	0	0	32	32	
mmu-miR-103-3p	207	1861	146	1946	4160	X
mmu-miR-103-2-5p	0	0	0	2	2	
mmu-miR-101b-3p	2	8	987	2280	3277	
mmu-miR-101a-5p	0	0	0	6	6	
mmu-miR-101a-3p	5	3	515	309	832	
mmu-miR-100-5p	167	123	147	111	548	
mmu-let-7i-5p	115	270	639	1394	2418	

miRNA	Experiment 1		Experiment 2			Ambiguous
	Naïve	Infected	Naïve	Infected	Total	
mmu-let-7i-3p	0	0	0	96	96	
mmu-let-7g-5p	42	57	594	1095	1788	
mmu-let-7g-3p	0	0	0	2	2	
mmu-let-7f-5p	98	209	157	281	745	
mmu-let-7f-1-3p	0	2	0	2	4	
mmu-let-7e-5p	0	0	11	17	28	
mmu-let-7e-3p	0	0	2	2	4	
mmu-let-7d-5p	0	7	10	360	377	
mmu-let-7d-3p	13	60	119	565	757	
mmu-let-7c-5p	271	152	714	510	1647	
mmu-let-7b-5p	39	58	880	904	1881	
mmu-let-7b-3p	0	0	0	10	10	
mmu-let-7a-5p	24	60	478	241	803	X
mmu-let-7a-1-3p	0	0	12	30	42	

Appendix 7

Appendix 7.txt available on the CD or at:

http://www.plosntds.org/article/info%3Adoi%2F10.1371%2Fjournal.pntd.0002701#s5

Appendix 7. Prediction of known or novel *S. mansoni* miRNAs in mouse serum based on miRdeep2.
This table shows all predictions (only predictions with a miRdeep2 score >0 are included in the text). Read assignments are: uninfected experiment 1 (R1N), infected experiment 1 (R1I), uninfected experiment 2 (607), infected experiment 2 (608 or 609). The number of reads in that sample is listed after the "x".

Appendix 8

Appendix 8. Relative expression of parasite miRNAs in serum during the time course of *S.mansoni* infection, based on qRT-PCR analysis, normalized to values in naïve mice.
8-10 week old C57BL/6 mice were left uninfected or infected percutaneously with ~80 cercariae and euthanized at 4, 6, 8 and 12 weeks post infection. miRNAs were quantified by qRT-PCR, normalized to a synthetic RNA spike-in and signal over noise calculated as the ratio of abundance in infected serum compared to the background abundance level detected in naïve serum, which represents the noise in the assay likely derived from cross-hybridization with endogenous small RNAs. One-way ANOVA followed by Holm-Sidak multiple comparison (*p<0.05, **p<0.01, ***p<0.001, ****p<0.0001).

miRNA		Background	Wk4	Wk6	Wk8	Wk12
bantam	Mean	1	7.51	13	18.55	27.85
	Std. Deviation	1.23	13.64	18.13	22.21	30.28
	Holm-Sidak's test		ns	ns	*	**
miR-277	Mean	1	3.32	3.23	4.96	8.02
	Std. Deviation	1.04	3.94	2.86	1.93	4.74
	Holm-Sidak's test		ns	ns	**	****
miR-3479	Mean	1	2.69	3.71	10.02	22.58
	Std. Deviation	1.02	1.28	4.73	11.62	12.42
	Holm-Sidak's test		ns	ns	*	***
miR-2a	Mean	1	780.50	262.60	1755	3334
	Std. Deviation	2.46	1412	497.8	2379	5061
	Holm-Sidak's test		ns	ns	*	***
miR-n1	Mean	1	0.74	0.87	10.88	33.29
	Std. Deviation	1.81	0.62	1.29	10.13	27.82
	Holm-Sidak's test		ns	ns	ns	****
miR-n2	Mean	1	0.01	2.67	5.62	8.81
	Std. Deviation	1.65	0.03	2.95	6.79	6.02
	Holm-Sidak's test		ns	ns	*	***
miR-n3	Mean	1	11.89	12.02	14.83	3.76
	Std. Deviation	1.57	8.97	13.45	24.66	6.05
	Holm-Sidak's test		ns	ns	ns	ns
miR-71	Mean	1	0.13	0.17	10.95	2.77
	Std. Deviation	2.96	0.14	0.15	28.82	3.73
	Holm-Sidak's test		ns	ns	ns	ns
miR-2162	Mean	1	4.05	0.49	9.23	1.45
	Std. Deviation	1.52	8.7	0.43	22.38	1.40
	Holm-Sidak's test		ns	ns	ns	ns

Appendix 9

Appendix 9. Parasite-Derived MicroRNAs in Host Serum As Novel Biomarkers of Helminth Infection.

Anna M. Hoy, Rachel J. Lundie, Alasdair Ivens, Juan F. Quintana, Norman Nausch, Thorsten Forster, Frances Jones, Narcis B. Kabatereine, David W. Dunne, Francisca Mutapi, Andrew S. MacDonald, Amy H. Buck

PLoS Negl Trop Dis 8(2): e2701. doi:10.1371/journal.pntd.0002701

Available at: http://www.plosntds.org/article/info%3Adoi%2F10.1371%2Fjournal.pntd.0002701

OPEN ACCESS Freely available online

PLOS | NEGLECTED TROPICAL DISEASES

Parasite-Derived MicroRNAs in Host Serum As Novel Biomarkers of Helminth Infection

Anna M. Hoy[1], Rachel J. Lundie[2], Alasdair Ivens[1], Juan F. Quintana[1], Norman Nausch[1], Thorsten Forster[3], Frances Jones[4], Narcis B. Kabatereine[5], David W. Dunne[4], Francisca Mutapi[1], Andrew S. MacDonald[1,6], Amy H. Buck[1]*

1 Centre for Immunity, Infection and Evolution, Ashworth Laboratories, University of Edinburgh, Edinburgh, United Kingdom, **2** The Walter and Eliza Hall Institute of Medical Research, Parkville, Victoria, Australia, **3** Division of Pathway Medicine, The University of Edinburgh, Edinburgh, United Kingdom, **4** Department of Pathology, University of Cambridge, Cambridge, United Kingdom, **5** Vector Control Division, Ministry of Health, Kampala, Uganda, **6** Manchester Collaborative Centre for Inflammation Research, The University of Manchester, Manchester, United Kingdom

Abstract

Background: MicroRNAs (miRNAs) are a class of short non-coding RNA that play important roles in disease processes in animals and are present in a highly stable cell-free form in body fluids. Here, we examine the capacity of host and parasite miRNAs to serve as tissue or serum biomarkers of *Schistosoma mansoni* infection.

Methods/Principal Findings: We used Exiqon miRNA microarrays to profile miRNA expression in the livers of mice infected with *S. mansoni* at 7 weeks post-infection. Thirty-three mouse miRNAs were differentially expressed in infected compared to naïve mice (>2 fold change, $p<0.05$) including miR-199a-3p, miR-199a-5p, miR-214 and miR-21, which have previously been associated with liver fibrosis in other settings. Five of the mouse miRNAs were also significantly elevated in serum by twelve weeks post-infection. Sequencing of small RNAs from serum confirmed the presence of these miRNAs and further revealed eleven parasite-derived miRNAs that were detectable by eight weeks post infection. Analysis of host and parasite miRNA abundance by qRT-PCR was extended to serum of patients from low and high infection sites in Zimbabwe and Uganda. The host-derived miRNAs failed to distinguish uninfected from infected individuals. However, analysis of three of the parasite-derived miRNAs (miR-277, miR-3479-3p and bantam) could detect infected individuals from low and high infection intensity sites with specificity/sensitivity values of 89%/80% and 80%/90%, respectively.

Conclusions: This work identifies parasite-derived miRNAs as novel markers of *S. mansoni* infection in both mice and humans, with the potential to be used with existing techniques to improve *S. mansoni* diagnosis. In contrast, although host miRNAs are differentially expressed in the liver during infection their abundance levels in serum are variable in human patients and may be useful in cases of extreme pathology but likely hold limited value for detecting prevalence of infection.

Citation: Hoy AM, Lundie RJ, Ivens A, Quintana JF, Nausch N, et al. (2014) Parasite-Derived MicroRNAs in Host Serum As Novel Biomarkers of Helminth Infection. PLoS Negl Trop Dis 8(2): e2701. doi:10.1371/journal.pntd.0002701

Editor: William Evan Secor, Centers for Disease Control and Prevention, Atlanta, United States of America

Received July 4, 2013; **Accepted** January 3, 2014; **Published** February 20, 2014

Funding: This work was supported by a NERC studentship (http://www.nerc.ac.uk/) to AMH, funding by the Thrasher Research Fund (https://www.thrasherresearch.org) to FM and NN, a MRC SNCF to AsM (G0701437) and a Wellcome Trust RCDF to AHB (097394/Z/11/Z). The funders had no role in study design, data collection and analysis, decision to publish, or preparation of the manuscript.

Competing Interests: The authors have declared that no competing interests exist.

* E-mail: a.buck@ed.ac.uk

Introduction

Helminths are parasitic worms that infect a third of the world's population and cause a diverse range of health consequences leading to significant social and economical burdens [1,2]. Schistosomiasis is a chronic disease caused by blood flukes of the genus *Schistosoma* that affects more than 200 million people worldwide and is second only to malaria as the most important lethal human parasitic disease in tropical and subtropical regions. Schistosomiasis is predominantly caused by hepatic *S. mansoni* and urogenital *S. haematobium* [3]. It is estimated that the mortality rates due to haematemesis (*S. mansoni*) and renal failure (*S. haematobium*) are around 130,000 and 150,000 per year respectively [4]. In addition, schistosomiasis is associated with anaemia, diarrhoea, under nutrition, chronic pain and exercise intolerance, which are estimated to contribute to 0.02 0.15 disability-adjusted life-years (DALY) [5].

Diagnosis of schistosome infection is crucial for patient management, evaluation of treatment efficiency, monitoring of disease transmission and success of control strategies, as recommended by the World Health Organization [6]. In the field, *S. mansoni* and other intestinal schistosomes are currently diagnosed through the detection of the parasite eggs in stool specimens using microscopic techniques such as Kato-Katz or ether-concentration [7]. While these techniques are relatively simple, inexpensive and specific, their major drawbacks include poor sensitivity in detecting low-intensity infections (for example, in children), their inability to detect pre-patent or single sex infection and their failure to detect infection in individuals where eggs are trapped in tissues and not excreted [8]. Available antibody-based assays are useful for diagnosis in some cases (e.g. foreign travellers) but they cannot differentiate past and active infection and can also cross-react with antigens from other

Author Summary

Schistosomiasis is a chronic disease caused by blood flukes that affects over 200 million people worldwide, of which 90% live in Sub-Saharan Africa. In the field setting schistosomiasis caused by *S. mansoni* is diagnosed by detection of parasite eggs in stool samples using microscopic techniques. Here we investigate the potential of microRNAs (miRNAs), a class of short noncoding RNAs, to act as biomarkers of *S. mansoni* infection. We have identified a specific subset of murine miRNAs whose expression is significantly altered in the liver between 6–12 weeks post infection. However their abundance in serum is not significantly different between naïve and *S. mansoni*-infected mice until twelve weeks post infection and they do not display consistent differential abundance in the serum of infected versus uninfected humans. In contrast, three parasite-derived miRNAs (miR-277, bantam and miR-3479-3p) were detected in the serum of infected mice and human patients and the combined detection of these miRNAs could distinguish *S. mansoni* infected from uninfected individuals from low and high infection intensity areas with 89%/80% or 80%/90% specificity/sensitivity, respectively. These results demonstrate that miRNAs of parasite origin are a new class of serum biomarker for detecting *S. mansoni* and likely other helminth infections.

helminths [9]. These assays therefore do not offer a definitive diagnosis in schistosome-endemic areas. Recent studies have shown success with point-of-care tests for Schistosoma circulating cathodic and anodic antigens (CCA and CAA, respectively) in serum and urine, which decrease rapidly after chemotherapy [8,10,11,12,13,14] and these are now being further developed for use in the field [15]. Detection of schistosome DNA in urine and stool samples or plasma by the polymerase chain reaction (PCR) method is another strategy for routine diagnosis of infection that has shown promising results [16,17,18,19,20]. Here we examine whether microRNAs (miRNAs), which are extremely stable in serum and detectable by quantitative reverse transcription PCR (qRT-PCR) could provide an additional diagnostic tool for *S. mansoni* infection.

miRNAs are a class of naturally occurring small non-coding RNA produced from animal, plant and viral genomes [21]. They are incorporated into the RNA-induced silencing complex (RISC) and function by binding to messenger RNAs (mRNAs) and inhibiting translation and/or causing mRNA destabilization [22]. Depending on the genes they target, miRNAs have diverse functions inside cells, from regulation of developmental programming to viral-host interactions [23,24,25]. In the last 5 years, reports have shown that miRNAs circulate in serum in a cell-free form and many cell types secrete miRNAs through encapsulation within exosomes or in association with specific proteins [26,27]. These extracellular RNAs have been implicated in cell-to-cell communication in a range of systems [28,29], and have been shown to be extremely stable in body fluids [27,30]. They have received extensive attention for their promise as biomarkers of disease, including cancer [31,32,33]. Extracellular miRNAs have also been shown to be altered in human serum and/or plasma in infection settings, including hepatitis C and hepatitis B infections [34,35] as well as during pulmonary tuberculosis [36]. A recent report has also identified miRNAs derived from rice in human serum [37], sparking interest in foreign RNA in body fluids and its diagnostic potential.

Here we investigate the potential of miRNAs to act as tissue and serum biomarkers of experimental mouse and natural human *S. mansoni* infection. We demonstrate that several host miRNAs are dysregulated in the liver of mice during *S. mansoni* infection, but do not serve as reliable serum biomarkers of infection in humans. In contrast, we identify at least three parasite-derived miRNAs in the serum of mice infected with *S. mansoni* that are also detected in human patients and can distinguish 'egg-negative' from 'egg-positive' individuals with high specificity and sensitivity. We anticipate that parasite-derived miRNAs may provide a general platform for specific and non-invasive detection of active helminth infection.

Methods

Animals and *S. mansoni* infection

For miRNA array analysis of liver and Illumina sequencing of serum in experiment 1, 8 10 week old C57BL/6 mice were left uninfected or infected percutaneously with ~180 *S. mansoni* cercariae, weighed regularly, and euthanized 7 weeks post infection. For the 12-week time course, 8 10 week old C57BL/6 mice were left uninfected or infected percutaneously with ~80 cercariae, weighed regularly, and euthanized at 4, 6, 8 and 12 weeks post infection.

Collection of blood and serum

Whole blood was drawn from mice by cardiac puncture. The needle was removed before emptying the syringe to avoid haemolysis and blood was allowed to sit for 1 h at RT to clot. Serum was separated by centrifugation at 2500 g for 15 min at 4°C, and the supernatant was collected into a new tube and spun at 10,000 g for 1 min to remove remaining cells. The resultant supernatant was transferred into a new tube and stored at −20°C prior to RNA extraction.

Human serum samples

Human serum was screened retrospectively from samples obtained from schistosome endemic areas in Zimbabwe and Uganda. The study group included in this investigation (Zimbabwe) was part of a larger study on the molecular immunoepidemiology of human schistosomiasis (carried out between November 1999 and March 2000) and had not been included in the National Schistosome Control Programme and therefore had not received treatment for schistosomiasis or other helminth infections. After collection of all samples, all participants were offered anti-helminthic treatment with the recommended dose of praziquantel (40 mg/kg of body weight). The selection of samples for screening here was based on availability of sufficient serum for miRNA analysis, and comprised five 'egg positive' individuals with an average egg per gram in stool (epg) = 108, range: 39-277 and nine 'egg-negative' individuals (Table 1). According to the WHO's classification, Zimbabwe has high to moderate levels of *S. haemobium* infection (prevalence ranging from 10% to greater than 70%) but low *S. mansoni* prevalence (less than 10%). The selection of serum for screening from Piida (Uganda) participants was based on availability of sufficient material and comprised twenty individuals infected with *S. mansoni* with an average epg = 1117 (range: 105-4030) and ten egg-negative individuals. The study group included in this investigation were part of a larger study carried out in Butiaba village, adjacent to Lake Albert, Masindi district, Uganda in 1996, described further in [38]. The cohort had moderate to high *S. mansoni* infection intensities and prevalence of 91%. After collection of stool and serum samples all the study participants, irrespective of the infection status, received 2 doses of praziquantel, 40 mg/kg of body weight, 6

Table 1. Top miRNAs dysregulated in the liver at 7 weeks post *S. mansoni* infection as determined by microarray analysis and showing results obtained by qRT-PCR (microarray: $p<0.05$, Fold change ≥ 2, qRT-PCR: t-test).

Up regulated miRNA				
miRNA	**P value**	**Log2 (*S.mansoni* infected/Naïve ratio)**	**PCR Fold Change**	**PCR P value**
miR-199-5p	0.0002	10.1	5.76	<0.0001
miR-199-3p	0.0001	6.4	5.7	<0.0001
miR-744	0.0002	5.3	1.2	NS
miR-214	0.0001	4.6	5.42	<0.0001
miR-210	0.0001	3.9	4.58	0.0001
miR-21	0.002	3.5	4.15	<0.0001
Down regulated miRNA				
miRNA	**P value**	**Log2 (*S.mansoni* infected/Naïve ratio)**	**PCR Fold Change**	**PCR P value**
miR-151-5p	0.024	−12.9	−1.42	0.0359
miR-9	0.031	−2.3	1.9	NS
miR-365	0.007	−2.2	−4.24	<0.0001
miR-192	0.006	−2.2	−3.35	<0.0001
miR-194	0.024	−2.0	−3.32	<0.0001
miR-122	0.028	−2.0	−3.2	<0.0001

doi:10.1371/journal.pntd.0002701.t001

weeks apart. Efficacy of chemotherapy was assessed 6 weeks after each treatment.

Ethics statement

Animal experiments were conducted under a Project License granted by the Home Office (United Kingdom), reference 60/4104, in accordance with local guidelines and approved by the Ethical Review Committee of the University of Edinburgh.

For the human serum samples collected in Chiredzi, permission to conduct the work in this province was obtained from the Provincial Medical Director. Ethical approval was received from the Medical Research Council of Zimbabwe (MRCZ). Only compliant participants were recruited into the study and they were free to drop out at any point during the study. At the beginning of the study, participants and their parents/guardians (in case of children) had the aims and procedures of the project explained fully in the local language, Shona, and oral consent (as was customary) was obtained from participants and parents/guardian before parasitology and blood samples were obtained. For the samples collected in Piida, ethical clearance was obtained from the Uganda National Council of Science and Technology (ethics committee for Vector Control Division, Ugandan Ministry of Health). The aims and procedures were explained to the local community at the start of the study and oral consent was obtained from all adults and from the parents/legal guardians of all children under 15 who were willing to participate. Due to cultural reasons and low levels of literacy, oral consent is deemed acceptable by the Ugandan Ministry of Health and was approved by the Uganda National Council of Science and Technology. Upon oral consent participants were enrolled in the study with a written record of their name, age, sex and case number, this served as both the record of oral consent and enrolment record.

Parasitology and serum sample collection and processing

Participants in the Zimbabwe study were checked for both urogenital and intestinal schistosomiasis and for inclusion in this analysis had to be free of any soil-transmitted helminths and also free of *S. haematobium* infection to avoid cross reactivity between different helminth parasites. For the analysis of urogenital schistosome infection (*S. haematobium*) participants submitted three urine and three stool samples (over four consecutive days). 10 ml of each sample received was processed on the day of collection by a urine filtration method [39]. Stool samples were prepared and examined on the day of collection using the Kato-Katz faecal smear for detection of *S. mansoni* eggs and soil transmitted helminths; this was carried out by trained and experienced technical staff from the National Institute of Health Research [40]. A single slide for microscopic examination was prepared from each urine and stool sample. Serum was prepared from 10 ml venous blood collected from study participants, frozen at −20°C and afterwards stored at −80°C. Samples were transported frozen to Edinburgh and stored at −80°C prior to serological assays. Participants in the Ugandan study had duplicate 50 mg Kato-Katz slides prepared from 3 consecutive stool samples for detection of *S. mansoni* eggs, expressed as mean epg; this was carried out by trained and experienced technical staff from the Vector Control division at the Ministry of Health in Uganda. Serum was prepared from 10 ml venous blood samples, frozen at −20°C and transported to Cambridge for storage at −80°C prior to serological assays.

Mouse serum RNA extraction

For the 12-week time course experiment, total RNA was extracted from serum using the miRVana PARIS extraction kit (Ambion), according to the manufacturer's protocol. In brief, 100 µl of serum was thawed on ice, mixed with an equal volume of 2× Denaturing Solution and kept on ice for 10 min. Samples were extracted with an equal volume of acid-phenol chloroform, vortexed for 30 s and centrifuged for 10 min at 10,000 g at RT. The aqueous phase was mixed with 1.25 volumes of 100% ethanol and added to the mirVana PARIS column. The column was washed and RNA eluted in 100 µl of 0.1 mM EDTA. RNA samples were stored at −20°C prior to further analysis. Extracted RNA was quantified by Qubit (Invitrogen).

Human serum RNA extraction

Due to small volumes and low amounts of RNA in available human serum samples the extraction protocol was adjusted to result in more concentrated RNA. To do this, 50 µl of serum was thawed on ice, mixed with 50 µl of ddH_2O and 100 µl of 2× Denaturing Solution (as supplied in the miRVana Paris kit) and kept on ice for 10 min. Samples were spiked with 10 fmoles of a synthetic RNA, Spike1: 5′-UGCUGAAUGCGUAGCUAUA-AGC-3′ (IDT) and extracted with an equal volume of acid-phenol chloroform, vortexed for 30 s and centrifuged for 10 min at 10,000 g at RT. The aqueous phase was mixed with 1/10 volume of 3M sodium acetate, 10 µg of GlycoBlue (Ambion) and an equal volume of isopropanol. Samples were allowed to precipitate overnight at −20°C and were then centrifuged at >10,000 g at 4°C. Pellets were washed twice with 75% ethanol, air-dried and then resuspended in 25 µl of 0.1 mM EDTA. The total RNA concentration was below the limit of detection based on Qubit (Invitrogen).

Liver RNA extraction

Liver tissue was immersed in RNA Later Solution (Ambion) overnight at 4°C prior to extraction using TRIzol Reagent (Invitrogen) according to the manufacturer's protocol. RNA was quantified by NanoDrop and integrity assessed by 10% PAGE or Bioanalyzer 2100. All RNA samples used in the microarray analysis had RIN >8.

Reverse transcription & PCR

For reverse transcription of mouse serum samples, a fixed amount of extracted RNA (1.5 ng) was used as an input and 0.1 fmoles of a synthetic RNA, Spike2: 5′-CGUAUCGAGUGAU-GUCACGUA-3′, was added at the RT step for normalization. For human serum samples, where the total RNA concentration was below the detection limit, a fixed volume of RNA (5 µl), corresponding to 10 µl of extracted serum, was used as the input and Spike1 (added at the time of purification) was used for normalization. For reverse transcription of RNA extracted from liver, 200 ng of total RNA was used in each reaction. Reverse transcription reactions were performed using the miScript System (Qiagen) according to the manufacturer's protocol. PCR was carried out with SYBR green real-time PCR assays (Qiagen) and miScript primers to detect mouse and human miRNAs, according to the manufacturer's protocol (Qiagen). Primers for *S. mansoni*-specific miRNAs and the synthetic spikes were used at 200 nM final concentration and were purchased from Invitrogen: miR-277, 5′-TAAATGCATTTTCTGGCCCG-3′, miR-2162-3p, 5′-TATTATGCAACGTTTCACTCT-3′, miR-3479-3p, 5′-TATT-GCACTAACCTTCGCCTTG-3′, bantam, 5′- TGAGATCGC-GATTAAAGCTGGT-3′, miR-2a-3p, 5′-TCACAGCCAGTAT-TGATGAAC-3′, miR-71a-3p, 5′- TGAAAGACGATGGTAGT-GAGAT-3′, sma-miR-n1, 5′-AACTCAGTGGCCTATCGGT-3′, sma-miR-n2, 5′-TCAGCTGTGTTCATGTCTTCGA-3′, sma-miR-n3, 5′- TGGCGCTTAGTAGAATGTCACCG-3′, Spike1, 5′-TGCTGAATGCGTAGCTATAAGC-3′, Spike2, 5′-CGTATCGAGTGATGTCACGTA-3′. Data were collected on a Light Cycler 480 System (Roche) with the following temperature profile: pre-denaturation 15 min at 95°C followed by 50 cycles of denaturation for 15 s at 95°C, annealing for 30 s at 55°C, elongation for 30 s at 70°C. The efficiencies of pre-optimized miScript host miRNA probes (Qiagen) were measured from standard curves and ranged between 93 100% and the efficiency of custom probes ranged from 87 97%; both displayed homogenous melting curves and amplification products of the expected size, as described in [41], which were examined here by 6% TBE PAGE (data not shown). Two technical replicates were carried out for each biological replicate. Nuclease free water was used as a non-template control.

miRNA array

For the array analysis, 1 µg of total RNA was labelled using the Hy3 power labeling kit (Exiqon) and hybridized to codelink slides printed with the miRCury 8.1 probe set as described elsewhere [42]. Hybridization and washing were carried out following the manufacturer's protocols (Exiqon). Background signal was subtracted from foreground signal and data were transformed to log-2 scale. Between-array normalization was carried out using global array percentiles (matching median of each array); triplicate probes were represented by the median for each array. Empirical Bayes moderated t statistic (eBayes) was used to test the null hypothesis of "no differential expression" between uninfected (n = 3) and infected (n = 3) liver samples. Since this array was only used as a filter for further validation, the p values were not adjusted for multiple testing. The Exiqon 8.1 arrays contained 384 probes specific for mouse miRNAs.

qRT-PCR data analysis

For analysis of miRNAs in liver samples, the relative fold change between naïve and infected samples was calculated using the $2^{-\Delta\Delta Ct}$ method [43], normalized to miR-16; values for infected mice were compared to values for age-matched naïve controls and the median value for naïve mice was set to 1 for the purpose of calculating fold change. For serum miRNA data analysis, Ct values were "median-normalized" to synthetic RNA spike oligos as described previously [27]: relative change was calculated as 2^{-Ctn}, where Ctn stands for normalized Ct values. The spike-in sequences did not match any known miRNA in miRBase and the primers for detecting these did not yield signals in serum by qRT-PCR, indicating that they do not cross-hybridize with mouse or human small RNAs (data not shown). Fold change was calculated as the ratio of the relative change value of the sample compared to an average of the relative change values of uninfected samples. For the cumulative analysis of miRNAs, the arithmetic mean of fold changes for miR-277, miR-3479-3p and bantam were used.

Statistical analysis of qRT-PCR data and receiver operator characteristic (ROC) curve analysis (95% confidence intervals) was performed with GraphPad Prism (Version 6) software. Two-way ANOVA followed by a Sidak multiple comparison test was used to calculate statistical differences for the mouse miRNA time course data from serum and liver. For the parasite miRNA serum time course, one-way ANOVA followed by Holm-Sidak multiple comparison was used. For analysis of the human serum samples, the Man-Whitney test was used and p-values of <0.05 were considered statistically significant. The measurement of miRNA levels by qRT-PCR was carried out by a trained doctoral student who was not blinded to the results of the infection status of each sample. Of the samples available for screening, none were excluded from the analysis.

Illumina sequencing

For small RNA sequencing in experiment 1, total RNA was extracted from serum of 8 pooled *S. mansoni*-infected mice (Wk 7, 180 cercariae) and 8 uninfected age matched controls (400 µl total volume) according to the miRVana PARIS protocol (as described above). The small RNAs were size selected by 15% PAGE and prepared according to the Illumina small RNA Sample Preparation Kit version 1.5 and sequenced on the GAIIX. For small RNA sequencing in experiment 2, total RNA was extracted from serum of 3 pooled *S. mansoni* infected mice (Wk 8, 80 cercariae) and 3

uninfected age matched controls (300 µl total volume) according to the miRVana PARIS protocol. The library was prepared according to the TruSeq Small RNA protocol (without size-selecting small RNA) and sequenced on the HiSeq2.

Raw reads were obtained in fastq format and 3′ adapters trimmed using cutadapt, requiring at least a 6 bp match to the adapter sequence and a quality threshold of 20. Only reads that contained the adapter were retained; reads were subsequently collapsed on primary fasta sequence and only reads present at ≥2 copies were analyzed. Trimmed, collapsed reads ≥17 bp were then aligned to mouse (MM9) or *S. mansoni* genomes (V5.0) using BOWTIE version 0.12.5, requiring a perfect match to the full length of the sequence. Reads that mapped to either genome were then BLASTN aligned against the RFAM database [BLASTN parameters: -max_target_seqs 1 -outfmt '6 std qseq sseq' -task blastn -word_size 6 -dust no] and categorized according to matches to Rfam class (e.g. rRNA, tRNA, etc.). Mouse reads without rfam similarities (other than miRNAs) were aligned to mature miRNAs in miRBase version 19. Some trimmed miRNA reads aligned to more than one family member: the assignment of these ambiguous reads is designated with "X" in Table S3. RNAs that aligned to the *S. mansoni* genome and did not show RFAM similarities were passed to mirDeep2.0.0.5 using platyhelminth miRNAs from miRBase 19 as guides (Table S4); reads mapping to known miRNAs from miRBase were identified regardless of miRdeep score, for prediction of novel miRNAs a cut-off value of 0 was used for reporting in Table 1.

Results

Specific host miRNAs are significantly dysregulated in the liver of mice at 7 weeks post *S. mansoni* infection

miRNAs are dysregulated in most disease contexts and play important roles in mediating how cells respond to insult and infection (reviewed in [44]). Approximately 4 6 weeks after *S. mansoni* infection, mature female parasites produce eggs, some of which are carried by the blood-flow to the liver where they become trapped [45]. The host immune response induced by the presence of the egg antigens leads to the formation of granulomatous lesions, which are composed of immune cells and collagen fibres [46] and result in fibrosis and associated pathology. In order to identify miRNAs associated with *S. mansoni*-induced liver pathology, and to prioritise candidates for further screening as biomarkers, we first compared expression profiles of miRNAs in livers of naïve mice or mice that were infected with *S. mansoni* at a high dose (~180 cercariae). Tissues were collected at 7 weeks post infection, at which time substantial granulomas were observed (data not shown). A total of 33 mouse miRNAs were differentially expressed: 26 miRNAs were up-regulated and 7 miRNAs were down-regulated in infected mice, based on a fold change cut-off of ≥2 and p value cut off <0.05 (Table S1, Fig. S1). The miRNAs that displayed the largest differential expression included miR-199a and miR-214, which are known to be altered in liver fibrosis caused by hepatitis C infection or induced by carbon tetrachloride [47,48]. Among the down regulated miRNAs was the liver-enriched miR-122, which is dysregulated during hepatitis C infection, acetaminophen overdose and hepatocellular carcinoma and is involved in lipid metabolism [49,50].

For validation of the microarray results, the miRNAs that displayed the largest fold change were quantified by qRT-PCR and normalized to miR-16 (a total of 6 up-regulated miRNAs and 6 down-regulated miRNAs were examined). Consistent with the array results, there was an increase in miR-199-5p, miR-199-3p, miR-214, miR-21, miR-210, and a reduction of miR-192, miR-194, miR-365, miR-122 and miR-151 in the liver tissue of *S. mansoni* infected mice as compared to naïve mice; miR-9 and miR-744 did not display differential expression and were not analysed further (Table 1). All of these miRNAs are perfectly conserved in mouse and human.

Temporal expression analysis of miR-199, miR-214, miR-21, miR-210, miR-122, miR-192 and miR-194 in the liver during *S. mansoni* infection

Between weeks 6 and 12, female parasites continue to produce ~300 eggs per day [51], resulting in an increase in the number of granulomas in the liver and the development of fibrosis [45]. For the 10 miRNAs validated to be differentially expressed at 7 weeks post infection, we next examined their temporal expression between 4 12 weeks post infection using a lower parasite dose (80 cercariae). All data from infected mice were compared to age-matched naive mice. To account for differences in RNA extraction or qRT-PCR efficiency, the data were normalised to miR-16, which displayed stable expression in the liver during infection (Fig. S2). Of the 10 miRNAs examined, all except miR-365 and miR-151 were differentially expressed between naïve and infected mice by 6 8 weeks post infection (Fig. 1, Table S2). This timing correlated with the deposition of eggs in the liver, which were detected by 6 weeks post infection and increased by 8 and 12 weeks post infection (Fig. S3). Our results suggest that these cellular miRNAs represent tissue biomarkers of infection that may play a role in the development and progression of liver fibrosis induced by *S. mansoni* egg deposition.

Temporal host miRNA dysregulation in the liver during infection is not reflected in serum

Several studies in non-helminth systems have shown that liver-derived miRNAs are detectable in serum and can be used as biomarkers in disease states [52,53,54,55,56]. We therefore examined whether the murine miRNAs that are altered in liver tissue are similarly altered in serum during *S. mansoni* infection. qRT-PCR was used to measure miRNA levels in the serum of mice infected with *S. mansoni* over the 12 week time course. The methodology of miRNA analysis in body fluids is not well standardized, and it is still not clear which small RNAs are appropriate for normalization [57,58,59,60]. Here we used a constant amount of total RNA in the reverse transcription reaction. To account for any variation in qRT-PCR efficiency due to contaminants, miRNA levels were normalized to a synthetic RNA oligo ("spike-in") that was included at the reverse-transcription step. The ratio of miRNA levels in infected versus age-matched naïve mice was quantified at each time point and plotted as fold change (Fig. 2). Compared to the analysis of liver samples, there is more variation in the serum miRNA levels between biological replicates. As shown in Fig. 2, the levels of miR-192, miR-194 and miR-122 in serum do not change between 4 12 weeks post infection, whereas five of the miRNAs that are up-regulated in the liver are also significantly elevated in serum at 12 weeks post infection ($p<0.05$), ranging from 2.6 fold (miR-21) to 4.7 fold (miR-214) (Table S2). These five host miRNAs represent potential serum biomarkers of *S. mansoni* infection. However, since their levels do not change until 12 weeks post infection in mice, they may only be useful in cases of more advanced pathology.

Small RNA sequencing reveals the presence of *S. mansoni*-derived miRNAs in the serum of infected mice

Multiple cell types release or secrete miRNAs into the circulation [59,61] and it is possible that other miRNAs, beyond

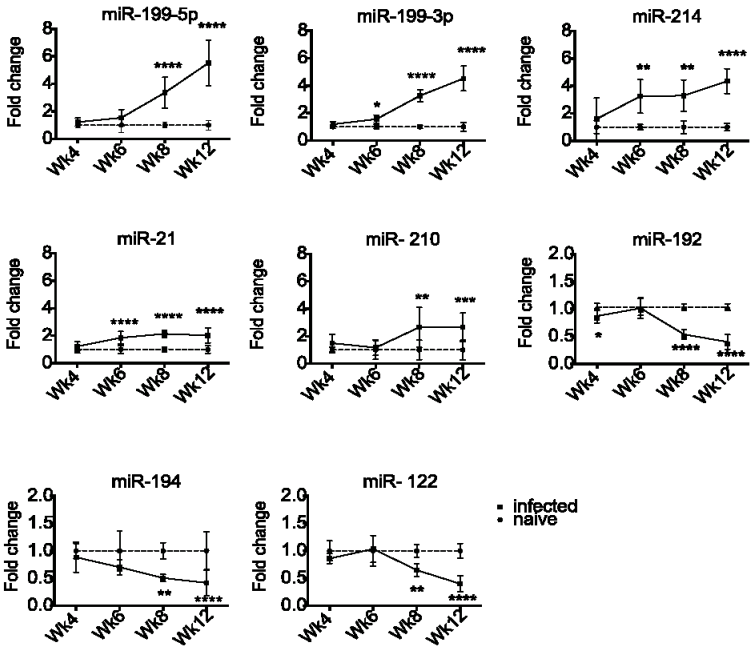

Figure 1. Differential expression of host miRNAs in the livers of mice at 4–12 weeks post infection with *S. mansoni*. miRNAs were quantified by qRT-PCR, normalized to miR-16 and fold changes calculated as the ratio of values from infected versus naïve mice (*p<0.05, **p<0.01, ***p<0.001, ****p<0.0001).
doi:10.1371/journal.pntd.0002701.g001

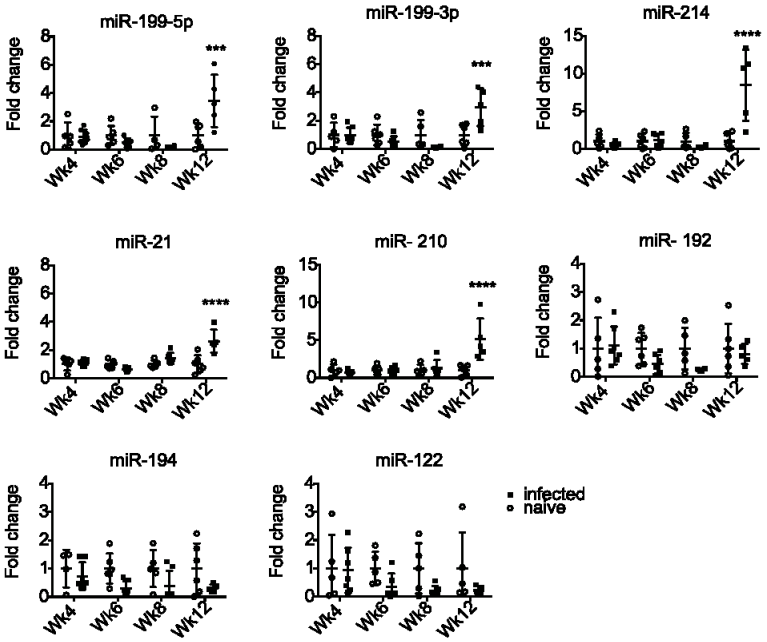

Figure 2. Differential abundance of host miRNAs in mouse serum during *S. mansoni* infection. miRNAs were quantified by qRT-PCR and normalized to a synthetic RNA spike-in. Each symbol represents data from one individual mouse. Fold changes are defined as the ratio of abundance in infected versus naïve serum; the signal from naïve was set as 1. (***p<0.001, ****p<0.0001).
doi:10.1371/journal.pntd.0002701.g002

those differentially expressed in the liver, might represent biomarkers of infection. To examine this in an unbiased fashion, small RNAs from serum of naïve mice or mice infected with *S. mansoni* were sequenced using the Illumina platform. Small RNA libraries were prepared in two independent experiments, using two different preparation methods (Methods). In both experiments, the majority of small RNA reads aligned to the mouse genome (ranging from 63 71%, Table 2). A small percentage of reads unambiguously aligned to the *S. mansoni* genome in infected mice (0.04 0.14%); <0.01% of reads mapped to the *S. mansoni* genome in naïve samples. Interestingly, the majority of reads in all samples were derived from tRNAs: 92 98% of the reads that mapped to the mouse genome and 42 100% of reads that mapped to the *S. mansoni* draft genome (Table 2). It is important to note, however, that due to the sequence similarity of the tRNAs between species and the scope for post-transcriptional editing, we cannot at this point definitively determine the organism from which these derive. Only 1 6% of the reads that mapped to the mouse genome were miRNAs (Table 2, listed in Table S3). There was no correlation between differences in host miRNA levels in naive and infected mice from the two experiments (data not shown), this could relate to the different doses, although it is not possible to derive statistical conclusions from these data due to low read numbers. A total of 78 and 29 mature miRNAs are known to be encoded by the trematodes *S. japonicum* and *S. mansoni*, respectively [62,63,64,65], and further miRNAs have been predicted [62]. Analysis of the reads that mapped to the *S. mansoni* draft genome using the miRdeep2 program [66] identified at least 11 miRNAs from infected samples: 8 of these were positively identified based on identity to known miRNAs in *S. mansoni* and/or S. *japonicum* (Table 3) [64,65] and 3 are predicted by miRdeep (here named sma-miR-n1, sma-miR-n2 and sma-miR-n3). The predicted stem-loop structures for the putative pre-miRNAs are shown in Fig. 3; since the depth of coverage of *S. mansoni* reads in this study was very low and reads did not map to both arms of the hairpin, these cannot yet be considered prototypical miRNAs. However, sma-miR-n3 shares a seed site with *Schmidtea mediterranea* miR-2160 and was annotated as sma-miR-8437 in a study of *S. mansoni* miRNAs published after submission of this manuscript [67]. Additional analysis of the datasets allowing 1 mismatch to the *S. mansoni* draft genome identified one further miRNA from infected but not naïve serum: miR-277, which is identical to miR-277 in *S. japonicum* and *Echinococcus granulosus* but has a C→T mutation at position 17 in relation to the *S. mansoni* draft genome (Table 3). Other reads from infected samples that aligned to *S. mansoni* but did not make the miRdeep2 cut-offs are provided in Table S4. It is possible that some of these less abundant sequences derive from real miRNAs but the coverage in these studies is not sufficient to determine this.

S. mansoni miRNAs are present in mouse serum as early as 8 weeks post infection

To determine the kinetic profile of parasite miRNAs in serum during *S. mansoni* infection, qRT-PCR analysis was carried out as described above, using primers specific for 9 of the 11 parasite miRNAs. The other 2 miRNAs, sma-miR-10-5p and sma-let-7-3p, were excluded from analysis because they are highly similar to homologous mouse miRNAs that are present at >100 fold higher read frequencies (Table S3). Importantly, most miRNAs in helminth parasites have evolved after the last common ancestor with their vertebrate hosts and are therefore distinguishable in sequence, however several miRNAs are perfectly conserved across animals or highly similar in sequence [63]. Several of the parasite-specific probes showed a signal in the serum of naïve mice, which is presumably due to cross-hybridization with endogenous small RNAs. In cases where no signal was observed in naïve mice, the maximum cycle value of 50 was set as background for the purpose of calculating signal over noise (which we interchange here with "fold change"). Six of the nine parasite miRNA probes tested (miR-277, bantam, miR-3479-3p, miR-2a-3p, miR-n1, miR-n2) showed a statistically significant signal over noise at 8 or 12 weeks post infection (Fig. 4, $p<0.05$); the three miRNAs that were not reliably detected (miR-n3, miR-71a-3p, miR-2162-3p) were not analysed further. The average signal over noise ratios for each probe during the time course of infection are provided in Table S5 and range from 4.2 to >3,000.

Three *S. mansoni*-derived miRNAs are detected in human serum and distinguish egg-negative from egg-positive individuals

Based on the results described above, we extended our analyses to human patients, using the 6 parasite miRNAs and 5 mouse miRNAs that displayed differential abundance in serum of infected compared to naïve mice. Serum samples from two field sites were examined: an area of high infection in the Pïida community of Uganda and an area of low infection in the Chiredzi community of Zimbabwe. The high infection samples were collected from mixed-age participants from Pïida diagnosed as *S. mansoni* infected, termed 'egg positive' and compared to volunteers from the same community with undetectable parasite eggs in the stool, termed 'egg-negative'. The low infection samples were collected from children in Chiredzi diagnosed with *S. mansoni* and compared to age matched participants with undetectable eggs by standard stool examination methods. Demographic data of individuals are provided in Tables 4 and 5. The signal over noise was calculated as described above, using synthetic spike-ins for normalization. miR-n1, miR-n2 and miR-2a-3p were below the detection limit (Ct = 50) in both 'egg-positive' and 'egg-negative' samples. The 5 host miRNAs were detectable in serum (miR-21, miR-199-3p, miR-199-5p, miR-210, miR-214) but showed variable abundance and failed to differentiate 'egg-positive' and 'egg-negative' participants (Fig. S4). In contrast, three out of the six parasite miRNAs (bantam, miR-277 and miR-3479-3p) displayed a significant signal over noise level in the serum of *S. mansoni* infected individuals 'egg-positive' from both high (Fig. 5A) and low (Fig. 5B) infection endemic areas, compared to the 'egg-negative' participants from the same communities ($p<0.05$, Mann Whitney test). Data presented using ROC curves show that the single parasite miRNAs discriminated between *S. mansoni* 'egg-negative' and 'egg-positive' with an area under the curve (AUC) of 0.785, 0.790, 0.768 for bantam, miR-277 and miR-3479-3p, respectively, in the individuals from Uganda (Fig. 5A) and 0.889, 0.933, 0.911 in the individuals from Zimbabwe (Fig. 5B). Using optimal cut-off points, this translates to detection of *S. mansoni* infected individuals with specificity/sensitivity of 80%/60%, 80%/70% and 80%/60%, in the patients from Uganda (Fig. 5A) and specificity/sensitivity of 100%/60%, 89%/80% and 89%/80% respectively in the patients from Zimbabwe (Fig. 5B). A repeated measurement of the parasite miRNA levels in the same samples displayed Pearson correlation values between 0.86 to 0.95 and comparable specificity/sensitivity values (Table S6). When combining the data for all three of the miRNAs into a cumulative value, the AUC increased to 0.845 and 0.933 for each cohort of participants. This resulted in improved specificity/sensitivity in detection for samples from Uganda (80%/90%) using a fold change cut-off of 1.189 (Fig. 6). This approach is very similar to a recent report that uses a "miRNA score" based on cumulative normalized signals of miRNAs [68]; analysis of our data based on cumulative fold change or cumulative normalized signals yields very similar results (Fig. S5). These results show that combining data for bantam,

Table 2. Small RNA classification in serum of naïve and infected mice.

	Illumina Small RNA (Experiment 1)		TruSeq (Experiment 2)	
	Naïve	Infected	Naïve	Infected
		7 weeks		8 weeks
		180 cercariae		80 cercariae
Trimmed reads	19,992,215	19,687,439	5,360,110	6,975,834
Mouse genome match	12,864,294	12,771,443	3,786,803	4,621,905
Unambiguous	**12,841,090(64.2%)**	**12,430,681 (63.1%)**	**3,779,361 (70.5%)**	**4,613,742 (66.1%)**
rRNA	6493 (0.05%)	51173 (0.4%)	377 (0.01%)	6499 (0.14%)
tRNA	12,615,823 (98.2%)	11,464,782 (92.2%)	3,736,007 (98.9%)	4,409,765 (95.6%)
other rfam	7579 (0.06%)	14563 (0.012%)	514 (0.014%)	1758 (0.04%)
miRNA	128,222(1.0%)	772,150 (6.2%)	36,615 (1.0%)	158,069 (3.4%)
Uncharacterized	82973 (0.6%)	128013 (1%)	5848 (0.16%)	37651 (0.8%)
S.mansoni genome match				
Unambiguous	**1,683 (<0.01%)**	**27,347(0.14%)**	**529 (<0.01%)**	**2,914 (0.04%)**
rRNA	272 (16.2%)	2828 (10.3%)	0	182 (6.2%)
tRNA	1,236 (73.4%)	20,191 (73.8%)	529 (100%)	1,231 (42%)
other rfam	52 (3.1%)	117 (0.4%)	0	22 (0.75%)
miRNA	2 (0.12%)	148 (0.54%)[1]	0	25 (0.9%)
Uncharacterized	121 (7.2%)	4,063 (15%)	0	1,454 (49.9%)

[1]This does not include 42 reads identical to sja-miR-277 that contain 1 nucleotide mismatch to *S. mansoni* draft genome.
doi:10.1371/journal.pntd.0002701.t002

miR-277 and miR-3479-3p may improve sensitivity of *S. mansoni* diagnosis compared to analysis of individual miRNAs.

Discussion

The recent evidence that miRNAs can be released into circulation from mammalian cells and tissues has stimulated extensive interest in the potential use of these molecules as non-invasive biomarkers [31,32,57]. MiRNA-based diagnostics are being developed for a number of diseases and although qRT-PCR is the most common detection method at present, there is extensive interest in improving and diversifying detection technologies, which may provide more field-friendly tools. Since miRNAs have been shown to be extremely stable in body fluids [27,30,69], we anticipate that these nucleic acids could be particularly useful as diagnostics in field settings where collection and storage conditions can be difficult to control. Here we find that miRNAs derived from the helminth parasite *S. mansoni* are present in infected mouse and human serum and offer advantages over endogenous miRNAs as biomarkers of infection. Specifically, we find 9 known miRNAs

Table 3. Parasite-miRNAs in serum of mice infected with *S. mansoni* identified by deep-sequencing.

Name	miRNA sequence (5′-3′)	Precursor Location	Reads[2]
sma-miR-n2	UCAGCUGUGUUCAUGUCUUCGA	S_mansoni.SC_0170:285549..285631:-	66
sja-miR-277[1]	UAAAUGCAUUUUCUGGCCCGUA	Inferred from sja-miR-277 in miRBase	42
sma-bantam	UGAGAUCGCGAUUAAAGCUGGU	S_mansoni.SC_0137:369450..369509:+	37
sja-miR-2162-3p	UAUUAUGCAACGUUUCACUCU	S_mansoni.SC_0049:36195..36251:+	29
sma-miR-3479-3p	UAUUGCACUAACCUUCGCCUUG	S_mansoni.Chr_4.unplaced.SC_0032:1561293..1561349:-	16
sma-miR-n1	AACUCAGUGGCCUAUCGGU	S_mansoni.Chr_1:18109172..18109229:-	9
sma-miR-n3	UGGCGCUUAGUAGAAUGUCACCG	S_mansoni.Chr_3:22962153..22962218:+	7
sma-miR-10-5p	AACCCUGUAGACCCGAGUUUGG	S_mansoni.Chr_4:19959278..19959336:-	4
sma-miR-2a-3p	UCACAGCCAGUAUUGAUGAAC	S_mansoni.Chr_W:22875762..22875816:+	3
sma-let-7-3p[3]	CAUACAACCGACUGGCUUUCC	S_mansoni.Chr_7:5118795..5118860:+	2
sma-miR-71a-3p	UGAAAGACGAUGGUAGUGAGAU	S_mansoni.Chr_W:22875670..22875724:+	2

[1]The nucleotide which does not match the *S. mansoni* draft genome is shown in bold;
[2]Reads in combined infected samples (compared to a combined total of 930,209 mouse miRNAs in the same samples, Table 1);
[3]The 3p arm of sma-let-7 is not annotated in mirbase.
doi:10.1371/journal.pntd.0002701.t003

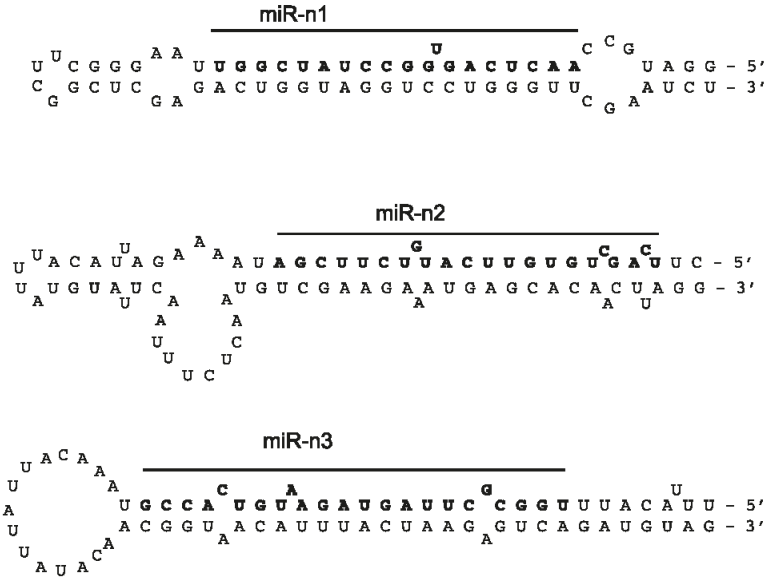

Figure 3. Predicted stem-loop structures of the *S. mansoni* miRNAs identified in this study. The mature sequence that was identified in serum is shown in bold.
doi:10.1371/journal.pntd.0002701.g003

and at least 2 novel putative miRNAs derived from *S. mansoni* that are present in the serum of infected mice. The read counts of some of these are very low (between 2 66 reads per 930,209 mouse miRNAs reads) and will require further validation with better coverage. However, we show that three of these miRNAs (bantam, miR-277, mirR-3479-3p) can be detected in human serum from schistosome endemic areas. These represent a direct marker for infection and may also provide an indirect marker for the pathology induced by infection. Notably, a study published after submission of this manuscript identified 5 miRNAs derived from *S. japonicum* in the plasma of infected rabbits and 3 of these are identical or homologous to those identified here: bantam,

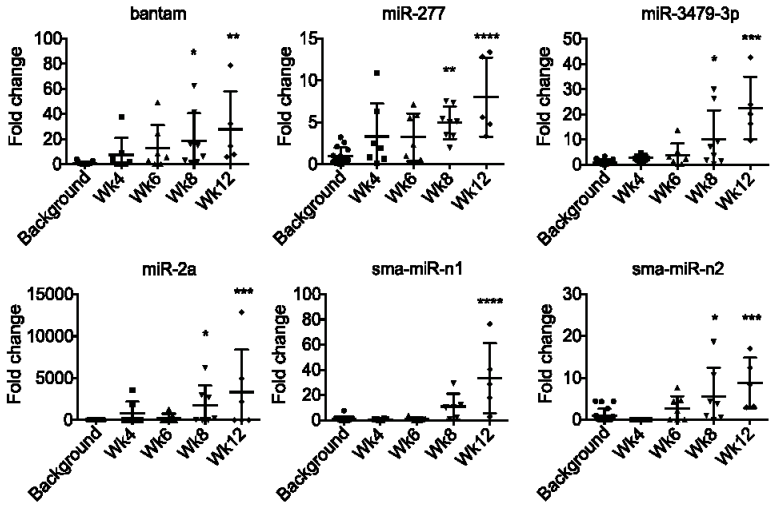

Figure 4. Detection of parasite-derived miRNAs in mouse serum during *S. mansoni* infection. miRNAs were quantified by qRT-PCR, normalized to a synthetic RNA spike-in and fold change calculated as the ratio of abundance in infected serum compared to the background abundance level detected in naïve serum, which represents the noise in the assay likely derived from cross-hybridization with endogenous small RNAs (*p<0.05, **p<0.01, ***p<0.001, ****p<0.0001).
doi:10.1371/journal.pntd.0002701.g004

Table 4. Piida study participants.

Characteristic	Egg-negative (n = 10)	Egg-positive (n = 20)
Age (range)	33.1 (17–48)	24.2 (7–56)
Sex (F/M)	5/5	9/11
S.mansoni status (epg & range)	0	1117 (105–4030)

doi:10.1371/journal.pntd.0002701.t004

Table 5. Chiredzi study participants.

Characteristic	Egg-negative (n = 9)	Egg-positive (n = 5)
Age (range)	10.67 (8–11)	10 (9–11)
Sex (M/F)	6/3	2/3
S.mansoni status (epg & range)	0	108 (39–277)

doi:10.1371/journal.pntd.0002701.t005

miR-3479-3p and miR-10-5p [70], providing independent validation for the presence of trematode miRNAs in the serum of infected animals. Here we demonstrate small RNAs derived from a helminth parasite are also present in patient serum, and provides a starting point for developing more field-friendly methods for their detection. This work also extends a burgeoning area of research detailing "foreign" small RNAs in body fluids. Zhang et al., (2012) recently reported that the plant miRNA, miR-168a, is present in human and animal serum and demonstrated that this derives from a rice diet [37]. Wang et al., (2012) recently reported

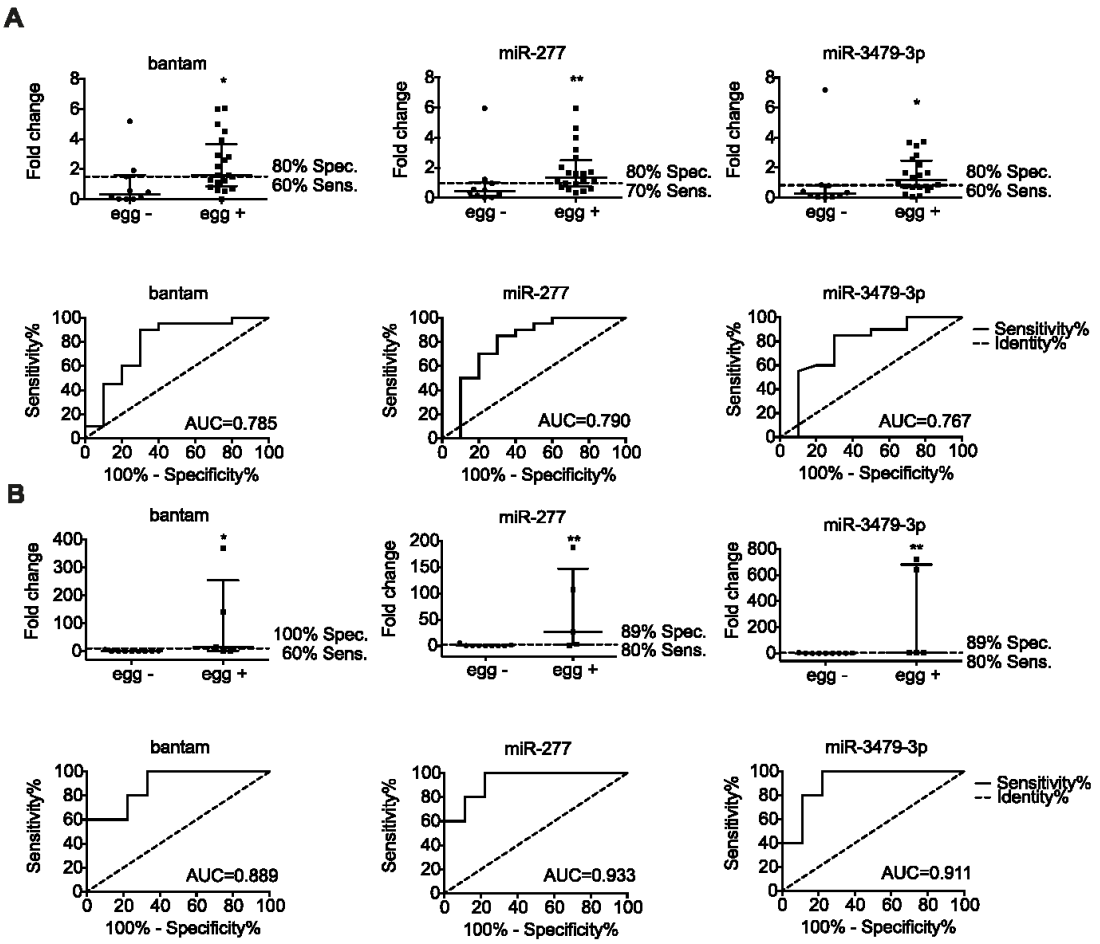

Figure 5. Discrimination between the *S. mansoni* infected and uninfected individuals using parasite-specific miRNA detection. miRNAs were quantified by qRT-PCR, normalized to a synthetic RNA spike-in and fold changes calculated as the ratio of infected to uninfected (median with interquartile range indicated). Piida- panel A, Chiredzi- panel B. Specificity and sensitivity and ROC curves with AUC are indicated. (*$p<0.05$, **$p<0.01$).

doi:10.1371/journal.pntd.0002701.g005

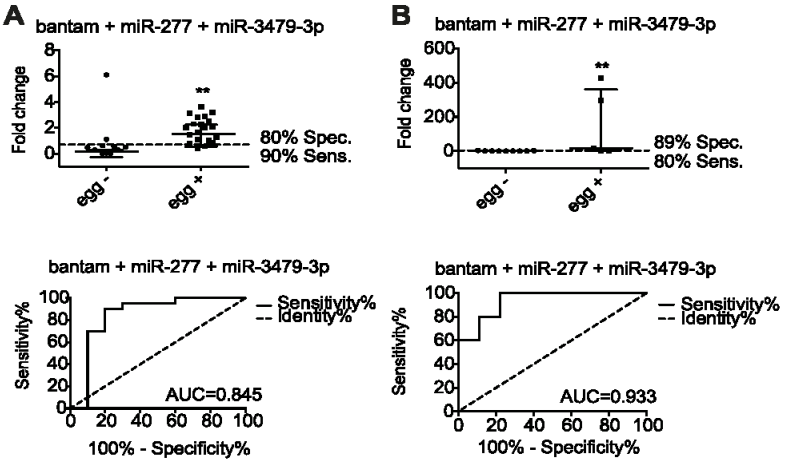

Figure 6. Discrimination between the *S. mansoni* infected and uninfected individuals using the combined data for 3 parasite miRNAs. Fold-changes (median with interquartile range indicated) and ROC curves for bantam, miR-277 and miR-3479-3p (Piida- panel A, Chiredzi- panel B) (**p<0.01).
doi:10.1371/journal.pntd.0002701.g006

that a wide range of exogenous RNAs can be found in human plasma, including small RNAs derived from bacteria and fungi [71]. From our results is not yet clear whether the miRNAs identified in serum are actively secreted from the parasite and how they are stabilized, since serum contains high amounts of RNases [72,73]. From the time course analysis presented here, schistosome-derived small RNAs were reliably detected in serum by 8 weeks post infection, after deposition of the eggs in the liver (Fig. 4 and Fig. S4). At present, we cannot determine whether these RNAs derive from the adult worms or the eggs; further *in vitro* and *in vivo* studies will shed light on this issue, which is relevant to diagnostic applications, for example the capacity to detect pre-patent infection.

It is intriguing to think that existence of these miRNAs outside the parasite has a function, but this is beyond the scope of the current analysis. Given the short size of miRNAs and the fact that they do not require perfect complementarity with their targets, one could predict hundreds of possible targets in the host. Interestingly, Xue et al. (2008) showed that three of the miRNAs that we find in serum (sja-bantam, sja-miR-71 and sja-let-7) are expressed during all the stages of parasite development but are enriched in the cercariae, suggesting that they may be important during the initial stages of schistosome infection [65]. The bantam miRNA has been implicated in regulating organ growth in response to environmental conditions in *Drosophila* as well as *C. elegans* [74,75] but functional homologues of bantam do not exist in mammals.

An initial objective in this study was to identify host miRNAs that may be involved in liver pathology associated with *S. mansoni* infection and to then determine whether these hold any diagnostic value. A number of reports have demonstrated an increase in miR-122 and miR-192 in plasma or serum upon viral infection as well as chemically induced liver disease [54,56]. However, according to our analysis, although miR-192, miR-122 and miR-194 were down-regulated in the liver during infection, their levels in serum did not change significantly (Fig. 1 2). In contrast, the miRNAs up-regulated in the liver (miR-199-3p, miR-199-5p, miR-21, miR-214 and miR-210) showed significantly higher levels in mouse serum at 12 weeks post infection (Fig. 2), however these failed to differentiate *S. mansoni* infected from uninfected humans (Fig. S4). It should be noted that in addition to significant liver disease, pulmonary and intestinal complications can also occur during *S. mansoni* infection that could also contribute to serum miRNA levels [45,76]. Related to this, a possible limitation in the use of endogenous miRNAs as biomarkers is the fact that their differential abundance in serum can derive from multiple cell types and can also be attributed to unrelated conditions [59]. Although the diagnostic value of these host miRNAs in serum is therefore not obvious, our work provides a foundation for further research into the functional role of these miRNAs in *S. mansoni* pathogenesis. Interestingly, our results do not overlap with those reported by Han et al., (2013) who examined changes in host miRNA levels in the liver of BALB/c mice during *S. japonicum* infection. We assume this may be due to the very early time point (10 days post infection) used in their study. Indeed, it is likely that the host miRNA changes we observe are primarily related to the liver pathology and/or the immune response initiated by the parasite eggs trapped in the liver, rather than the initial host immune response to the schistosomula. Several of the miRNAs we identify as differentially expressed are already known to be associated with liver fibrosis or disease in other, non-helminth, settings [49,50,77,78]. The functional role of the miRNAs in the pathology induced by *S. mansoni* infection remains to be determined. Future work in this area will shed light on the molecular basis of pathology and may offer innovative new therapeutic strategies.

Importantly, we report here that parasite-derived miRNAs can be detected in human serum and can distinguish 'egg-negative' from 'egg-positive' individuals in areas of both low and high infection intensity. By combining data for miR-277, miR-3479-3p and bantam we detected infection with a sensitivity of 80 90% and specificity of 80 89%. We anticipate that this may be improved further by optimizing isolation protocols, probe design and more robust methods for normalizing the data, for example to identify appropriate endogenous small RNAs that could be used as controls, rather than synthetic spike-ins [79]. The main limitation of miRNA detection in serum appears to be cross-hybridization of the probes with endogenous small RNAs, which influences the signal to noise ratios. In particular, we report the finding that the majority of small RNAs in mouse serum are derived from tRNAs

(Table 2), consistent with a recent study [80]. It is possible that depletion of these tRNAs prior to qRT-PCR may improve the specificity or sensitivity of miRNA detection; this requires further investigation. In addition, one of the parasite-derived miRNAs identified by sequencing, miR-2162-3p could not be validated by qRT-PCR, likely owing to its low GC content (33%). Optimization of probe design for the parasite-derived miRNAs may also greatly increase their diagnostic utility in larger scale studies in human patients. On this note, the work presented here was performed on a relatively small number of individuals. Following further optimization of the extraction methods and probe design to minimize cross hybridization and sensitivity, larger studies will be important to assess the full potential of the proposed miRNA biomarkers, including positive and negative predictive values in comparison to existing techniques. It will also be of interest to determine the origin of these parasite-derived miRNAs and examine their abundance levels in response to treatment. We anticipate that the parasite miRNAs in serum could complement or transform existing diagnostic strategies and may serve as a platform for detecting a range of helminth infections.

Supporting Information

Figure S1 Volcano plot of miRNA microarray data comparing miRNA expression levels in mice infected with *S. mansoni* compared to naive mice. The horizontal line indicates a p-value cut-off of 0.05 and vertical lines indicate fold change thresholds of 2.
(EPS)

Figure S2 Expression of miR-16 in liver and serum over the time course of *S. mansoni* infection. miRNAs were quantified by qRT-PCR, relative change was calculated as 2^{-Ct} (for liver samples) or 2^{-Ctn},(for serum samples) and fold changes were calculated as infected to naïve ratio.
(EPS)

Figure S3 *S. mansoni* egg counts in the livers of mice over the course of infection.
(EPS)

Figure S4 Abundance of host miRNAs in serum of *S. mansoni* egg-positive and egg-negative individuals. miRNAs were quantified by qRT-PCR, normalized to a synthetic RNA spike-in and fold changes calculated as the ratio of infected to uninfected individuals. Piida- panel A, Chiredzi- panel B.
(EPS)

Figure S5 Discrimination between the *S. mansoni* infected and uninfected patients using the miRNA-score. Dot plot comparing cumulative (bantam, miR-277 and miR-3479-3p) miRNA-score between *S. mansoni* egg positive and negative participants (median with interquartile range indicated) and ROC curves (Piida- panel A, Chiredzi-panel B) (**$p<0.01$).
(EPS)

Table S1 miRNAs that are dysregulated in the liver upon *S.mansoni* infection as determined by microarray analysis ($p<0.05$, fold change ≥ 2).
(DOCX)

Table S2 Relative expression of miRNAs in the liver and serum during the time course of *S.mansoni* infection based on qRT-PCR analysis, normalized to values in naïve mice.
(DOCX)

Table S3 Tabulated mouse miRNA reads identified in serum of naïve and infected mice. The "X" denotes the miRNAs who were assigned reads that could have derived from one of multiple miRNA family members (e.g. in the case of shortened reads).
(XLSX)

Table S4 Prediction of known or novel *S. mansoni* miRNAs in mouse serum based on miRdeep2. This table shows all predictions (only predictions with a miRdeep2 score >0 are included in the text). Read assignments are: uninfected experiment 1 (R1N), infected experiment 1 (R1I), uninfected experiment 2 (607), infected experiment 2 (608 or 609). The number of reads in that sample is listed after the "x".
(TXT)

Table S5 Relative expression of parasite miRNAs in serum during the time course of *S.mansoni* infection, based on qRT-PCR analysis, normalized to values in naïve mice.
(DOCX)

Table S6 miRNA detection values in Chiredzi and Uganda samples. Fold change is defined as the abundance value in each sample compared to the median of values obtained in uninfected individuals. Repeated miRNA measurements from Chiredzi samples are shown (there was not enough material to repeat measurement in Uganda samples).
(XLSX)

Table S7 Ct values obtained for qRT-PCR.
(XLSX)

Checklist S1 STARD Checklist.
(DOC)

Acknowledgments

We greatly acknowledge the help of Rinku Rajan with the mouse *S. mansoni* infections and Fabio Simbari, Nouf Laqtom, Gillian Coakley, Marissa Lear with organ harvests. We thank Sujai Kumar for processing initial sequencing data and Dan Frank and Margo Chase-Topping for helpful discussions on analysis. Schistosome life cycle stages used to infect mice for this research were supplied by the N.I.A.I.D. Schistosomiasis Resource Centre at the Biomedical Research Institute (Rockville, MD) through Contract N01-AI-30026.

The data discussed in this publication have been deposited in NCBI's Gene Expression Omnibus and are accessible through GEO Series accession number GSE 49668.

Author Contributions

Conceived and designed the experiments: AMH RJL ASM AHB. Performed the experiments: AMH RJL JFQ AHB. Analyzed the data: AMH TF AI AHB. Contributed reagents/materials/analysis tools: NN FM NBK FJ DWD. Wrote the paper: AMH AHB.

References

1. Hotez PJ, Brindley PJ, Bethony JM, King CH, Pearce EJ, et al. (2008) Helminth infections: the great neglected tropical diseases. The Journal of clinical investigation 118: 1311 1321.
2. Awasthi S, Bundy DA, Savioli L (2003) Helminthic infections. BMJ 327: 431 433.
3. Organisation WH (2013) Schistosomiasis-Fact sheet 115. WHO.
4. van der Werf MJ, de Vlas SJ, Brooker S, Looman CW, Nagelkerke NJ, et al. (2003) Quantification of clinical morbidity associated with schistosome infection in sub-Saharan Africa. Acta tropica 86: 125 139.
5. King CH, Dickman K, Tisch DJ (2005) Reassessment of the cost of chronic helmintic infection: a meta-analysis of disability-related outcomes in endemic schistosomiasis. Lancet 365: 1561 1569.
6. Organization WH (2002) Prevention and Control of Schistosomiasis and Soil Transmitted helminthiasis- Report of a WHO Expert Committee. Geneva.
7. Glinz D, Silue KD, Knopp S, Lohourignon LK, Yao KP, et al. (2010) Comparing diagnostic accuracy of Kato-Katz, Koga agar plate, ether-concentration, and FLOTAC for Schistosoma mansoni and soil-transmitted helminths. PLoS neglected tropical diseases 4: e754.

8. Stothard JR, Sousa-Figueiredo JC, Betson M, Adriko M, Arinaitwe M, et al. (2011) Schistosoma mansoni Infections in young children: when are schistosome antigens in urine, eggs in stool and antibodies to eggs first detectable? PLoS neglected tropical diseases 5: e938.
9. Doenhoff MJ, Chiodini PL, Hamilton JV (2004) Specific and sensitive diagnosis of schistosome infection: can it be done with antibodies? Trends in Parasitology 20: 35 39.
10. Shane HL, Verani JR, Abudho B, Montgomery SP, Blackstock AJ, et al. (2011) Evaluation of urine CCA assays for detection of Schistosoma mansoni infection in Western Kenya. PLoS neglected tropical diseases 5: e951.
11. van Lieshout L, De Jonge N, Mansour MM, Bassily S, Krijger FW, et al. (1993) Circulating cathodic antigen levels in serum and urine of schistosomiasis patients before and after chemotherapy with praziquantel. Transactions of the Royal Society of Tropical Medicine and Hygiene 87: 311 312.
12. van Dam GJ, Bogitsh BJ, van Zeyl RJ, Rotmans JP, Deelder AM (1996) Schistosoma mansoni: in vitro and in vivo excretion of CAA and CCA by developing schistosomula and adult worms. The Journal of parasitology 82: 557 564.
13. Coulibaly JT, N'Gbesso YK, Knopp S, N'Guessan NA, Silue KD, et al. (2013) Accuracy of urine circulating cathodic antigen test for the diagnosis of Schistosoma mansoni in preschool-aged children before and after treatment. PLoS neglected tropical diseases 7: e2109.
14. Sousa-Figueiredo JC, Betson M, Kabatereine NB, Stothard JR (2013) The urine circulating cathodic antigen (CCA) dipstick: a valid substitute for microscopy for mapping and point-of-care diagnosis of intestinal schistosomiasis. PLoS neglected tropical diseases 7: e2008.
15. van Dam GJ, de Dood CJ, Lewis M, Deelder AM, van Lieshout L, et al. (2013) A robust dry reagent lateral flow assay for diagnosis of active schistosomiasis by detection of Schistosoma circulating anodic antigen. Exp Parasitol 135: 274 282.
16. Enk MJ, Oliveira e Silva G, Rodrigues NB (2012) Diagnostic accuracy and applicability of a PCR system for the detection of Schistosoma mansoni DNA in human urine samples from an endemic area. PloS one 7: e38947.
17. Pontes LA, Oliveira MC, Katz N, Dias-Neto E, Rabello A (2003) Comparison of a polymerase chain reaction and the Kato-Katz technique for diagnosing infection with Schistosoma mansoni. The American journal of tropical medicine and hygiene 68: 652 656.
18. Wichmann D, Panning M, Quack T, Kramme S, Burchard GD, et al. (2009) Diagnosing schistosomiasis by detection of cell-free parasite DNA in human plasma. PLoS neglected tropical diseases 3: e422.
19. Lodh N, Mwansa JC, Mutengo MM, Shiff CJ (2013) Diagnosis of Schistosoma mansoni without the Stool: Detecting DNA from Filtered Urine Comparison of Three Diagnostic Tests to Detect Schistosoma mansoni Infection from Filtered Urine in Zambia. Am J Trop Med Hyg 89:46 50.
20. Ibironke OA, Phillips AE, Garba A, Lamine SM, Shiff C (2011) Diagnosis of Schistosoma haematobium by detection of specific DNA fragments from filtered urine samples. The American journal of tropical medicine and hygiene 84: 998 1001.
21. Bartel DP (2009) MicroRNAs: target recognition and regulatory functions. Cell 136: 215 233.
22. Fabian MR, Sonenberg N (2012) The mechanics of miRNA-mediated gene silencing: a look under the hood of miRISC. Nature structural & molecular biology 19: 586 593.
23. Sullivan CS, Ganem D (2005) MicroRNAs and viral infection. Molecular cell 20: 3 7.
24. Xiao C, Rajewsky K (2009) MicroRNA control in the immune system: basic principles. Cell 136: 26 36.
25. Mendell JT, Olson EN (2012) MicroRNAs in stress signaling and human disease. Cell 148: 1172 1187.
26. Valadi H, Ekstrom K, Bossios A, Sjostrand M, Lee JJ, et al. (2007) Exosome-mediated transfer of mRNAs and microRNAs is a novel mechanism of genetic exchange between cells. Nature cell biology 9: 654 659.
27. Mitchell PS, Parkin RK, Kroh EM, Fritz BR, Wyman SK, et al. (2008) Circulating microRNAs as stable blood-based markers for cancer detection. Proceedings of the National Academy of Sciences of the United States of America 105: 10513 10518.
28. Xu L, Yang BF, Ai J (2013) MicroRNA transport: a new way in cell communication. Journal of cellular physiology 228: 1713 1719.
29. Creemers EE, Tijsen AJ, Pinto YM (2012) Circulating microRNAs: novel biomarkers and extracellular communicators in cardiovascular disease? Circulation research 110: 483 495.
30. Chen X, Ba Y, Ma L, Cai X, Yin Y, et al. (2008) Characterization of microRNAs in serum: a novel class of biomarkers for diagnosis of cancer and other diseases. Cell research 18: 997 1006.
31. Etheridge A, Lee I, Hood L, Galas D, Wang K (2011) Extracellular microRNA: A new source of biomarkers. Mutation Research-Fundamental and Molecular Mechanisms of Mutagenesis 717: 85 90.
32. Kosaka N, Iguchi H, Ochiya T (2010) Circulating microRNA in body fluid: a new potential biomarker for cancer diagnosis and prognosis. Cancer Science 101: 2087 2092.
33. Weiland M, Gao XH, Zhou L, Mi QS (2012) Small RNAs have a large impact Circulating microRNAs as biomarkers for human diseases. Rna Biology 9: 850 859.
34. Shrivastava S, Petrone J, Steele R, Lauer GM, Bisceglie AM, et al. (2013) Upregulation of circulating miR-20a is correlated with hepatitis C virus mediated liver disease progression. Hepatology 58: 863 71.
35. Li LM, Hu ZB, Zhou ZX, Chen X, Liu FY, et al. (2010) Serum microRNA profiles serve as novel biomarkers for HBV infection and diagnosis of HBV-positive hepatocarcinoma. Cancer research 70: 9798 9807.
36. Qi Y, Cui L, Ge Y, Shi Z, Zhao K, et al. (2012) Altered serum microRNAs as biomarkers for the early diagnosis of pulmonary tuberculosis infection. BMC infectious diseases 12: 384.
37. Zhang L, Hou D, Chen X, Li D, Zhu L, et al. (2012) Exogenous plant MIR168a specifically targets mammalian LDLRAP1: evidence of cross-kingdom regulation by microRNA. Cell research 22: 107 126.
38. Kabatereine NB, Vennervald BJ, Ouma JH, Kemijumbi J, Butterworth AE, et al. (1999) Adult resistance to schistosomiasis mansoni: age-dependence of reinfection remains constant in communities with diverse exposure patterns. Parasitology 118 (Pt 1): 101 105.
39. Mott KE (1983) A reusable polyamide filter for diagnosis of S. haematobium infection by urine filtration. Bulletin de la Societe de pathologie exotique et de ses filiales 76: 101 104.
40. Katz N, Chaves A, Pellegrino J (1972) A simple device for quantitative stool thick-smear technique in Schistosomiasis mansoni. Revista do Instituto de Medicina Tropical de Sao Paulo 14: 397 400.
41. Buck AH, Santoyo-Lopez J, Robertson KA, Kumar DS, Reczko M, et al. (2007) Discrete clusters of virus-encoded micrornas are associated with complementary strands of the genome and the 7.2-kilobase stable intron in murine cytomegalovirus. J Virol 81: 13761 13770.
42. Ruckerl D, Jenkins SJ, Laqtom NN, Gallagher IJ, Sutherland TE, et al. (2012) Induction of IL-4Ralpha-dependent microRNAs identifies PI3K/Akt signaling as essential for IL-4-driven murine macrophage proliferation in vivo. Blood 120: 2307 2316.
43. Livak KJ, Schmittgen TD (2001) Analysis of relative gene expression data using real-time quantitative PCR and the 2(T)(−Delta Delta C) method. Methods 25: 402 408.
44. Mendell JT, Olson EN (2012) MicroRNAs in Stress Signaling and Human Disease. Cell 148: 1172 1187.
45. Pearce EJ, MacDonald AS (2002) The immunobiology of schistosomiasis. Nature reviews Immunology 2: 499 511.
46. Wynn TA, Thompson RW, Cheever AW, Mentink-Kane MM (2004) Immunopathogenesis of schistosomiasis. Immunological reviews 201: 156 167.
47. Iizuka M, Ogawa T, Enomoto M, Motoyama H, Yoshizato K, et al. (2012) Induction of microRNA-214-5p in human and rodent liver fibrosis. Fibrogenesis & tissue repair 5: 12.
48. Murakami Y, Toyoda H, Tanaka M, Kuroda M, Harada Y, et al. (2011) The progression of liver fibrosis is related with overexpression of the miR-199 and 200 families. PloS one 6: e16081.
49. Girard M, Jacquemin E, Munnich A, Lyonnet S, Henrion-Caude A (2008) miR-122, a paradigm for the role of microRNAs in the liver. Journal of hepatology 48: 648 656.
50. Hu J, Xu Y, Hao J, Wang S, Li C, et al. (2012) MiR-122 in hepatic function and liver diseases. Protein & cell 3: 364 371.
51. Moore DV, Sandground JH (1956) The relative egg producing capacity of Schistosoma mansoni and Schistosoma japonicum. The American journal of tropical medicine and hygiene 5: 831 840.
52. Waidmann O, Koberle V, Brunner F, Zeuzem S, Piiper A, et al. (2012) Serum microRNA-122 predicts survival in patients with liver cirrhosis. PloS one 7: e45652.
53. Farid WR, Pan Q, van der Meer AJ, de Ruiter PE, Ramakrishnaiah V, et al. (2012) Hepatocyte-derived microRNAs as serum biomarkers of hepatic injury and rejection after liver transplantation. Liver transplantation : official publication of the American Association for the Study of Liver Diseases and the International Liver Transplantation Society 18: 290 297.
54. Starkey Lewis PJ, Merz M, Couttet P, Grenet O, Dear J, et al. (2012) Serum microRNA biomarkers for drug-induced liver injury. Clinical pharmacology and therapeutics 92: 291 293.
55. Wang LG, Gu J (2012) Serum microRNA-29a is a promising novel marker for early detection of colorectal liver metastasis. Cancer epidemiology 36: e61 67.
56. Zhang Y, Jia Y, Zheng R, Guo Y, Wang Y, et al. (2010) Plasma microRNA-122 as a biomarker for viral-, alcohol-, and chemical-related hepatic diseases. Clinical chemistry 56: 1830 1838.
57. Weiland M, Gao XH, Zhou L, Mi QS (2012) Small RNAs have a large impact: circulating microRNAs as biomarkers for human diseases. RNA biology 9: 850 859.
58. Scholer N, Langer C, Dohner H, Buske C, Kuchenbauer F (2010) Serum microRNAs as a novel class of biomarkers: a comprehensive review of the literature. Experimental hematology 38: 1126 1130.
59. Hoy AM, Buck AH (2012) Extracellular small RNAs: what, where, why? Biochemical Society transactions 40: 886 890.
60. Benz F, Roderburg C, Vargas Cardenas D, Vucur M, Gautheron J, et al. (2013) U6 is unsuitable for normalization of serum miRNA levels in patients with sepsis or liver fibrosis. Experimental & molecular medicine 45: e42.
61. Turchinovich A, Weiz L, Burwinkel B (2012) Extracellular miRNAs: the mystery of their origin and function. Trends in biochemical sciences 37: 460 465.

62. de Souza Gomes M, Muniyappa MK, Carvalho SG, Guerra-Sa R, Spillane C (2011) Genome-wide identification of novel microRNAs and their target genes in the human parasite Schistosoma mansoni. Genomics 98: 96 111.
63. Kozomara A, Griffiths-Jones S (2011) miRBase: integrating microRNA annotation and deep-sequencing data. Nucleic acids research 39: D152 157.
64. Wang Z, Xue X, Sun J, Luo R, Xu X, et al. (2010) An "in-depth" description of the small non-coding RNA population of Schistosoma japonicum schistosomulum. PLoS neglected tropical diseases 4: e596.
65. Xue X, Sun J, Zhang Q, Wang Z, Huang Y, et al. (2008) Identification and characterization of novel microRNAs from Schistosoma japonicum. PloS one 3: e4034.
66. Friedlander MR, Mackowiak SD, Li N, Chen W, Rajewsky N (2012) miRDeep2 accurately identifies known and hundreds of novel microRNA genes in seven animal clades. Nucleic acids research 40: 37 52.
67. Marco A, Kozomara A, Hui JH, Emery AM, Rollinson D, et al. (2013) Sex-biased expression of microRNAs in Schistosoma mansoni. PLoS neglected tropical diseases 7: e2402.
68. Goren Y, Kushnir M, Zafrir B, Tabak S, Lewis BS, et al. (2012) Serum levels of microRNAs in patients with heart failure. European journal of heart failure 14: 147 154.
69. Li Y, Jiang Z, Xu L, Yao H, Guo J, et al. (2011) Stability analysis of liver cancer-related microRNAs. Acta biochimica et biophysica Sinica 43: 69 78.
70. Cheng G, Luo R, Hu C, Cao J, Jin Y (2013) Deep sequencing-based identification of pathogen-specific microRNAs in the plasma of rabbits infected with Schistosoma japonicum. Parasitology 140: 1751 1761.
71. Wang K, Li H, Yuan Y, Etheridge A, Zhou Y, et al. (2012) The complex exogenous RNA spectra in human plasma: an interface with human gut biota? PloS one 7: e51009.
72. Blank A, Dekker CA (1981) Ribonucleases of human serum, urine, cerebrospinal fluid, and leukocytes. Activity staining following electrophoresis in sodium dodecyl sulfate-polyacrylamide gels. Biochemistry 20: 2261 2267.
73. Kamm RC, Smith AG (1972) Ribonuclease activity in human plasma. Clinical biochemistry 5: 198 200.
74. Brennecke J, Hipfner DR, Stark A, Russell RB, Cohen SM (2003) bantam encodes a developmentally regulated microRNA that controls cell proliferation and regulates the proapoptotic gene hid in Drosophila. Cell 113: 25 36.
75. Schaedel ON, Gerisch B, Antebi A, Sternberg PW (2012) Hormonal signal amplification mediates environmental conditions during development and controls an irreversible commitment to adulthood. PLoS biology 10: e1001306.
76. Crosby A, Jones FM, Kolosionek E, Southwood M, Purvis I, et al. (2011) Praziquantel reverses pulmonary hypertension and vascular remodeling in murine schistosomiasis. Am J Respir Crit Care Med 184: 467 473.
77. Chen XM (2009) MicroRNA signatures in liver diseases. World journal of gastroenterology : WJG 15: 1665 1672.
78. Jiang X, Tsitsiou E, Herrick SE, Lindsay MA (2010) MicroRNAs and the regulation of fibrosis. The FEBS journal 277: 2015 2021.
79. Kang K, Peng X, Luo J, Gou D (2012) Identification of circulating miRNA biomarkers based on global quantitative real-time PCR profiling. Journal of animal science and biotechnology 3: 4.
80. Dhahbi JM, Spindler SR, Atamna H, Yamakawa A, Boffelli D, et al. (2013) 5′ tRNA halves are present as abundant complexes in serum, concentrated in blood cells, and modulated by aging and calorie restriction. BMC genomics 14: 298.

Appendix 10

Appendix 10 Extracellular small RNAs: what, where, why?

Anna M. Hoy, Amy H. Buck

Biochem Soc Trans. Aug 1, 2012; 40(Pt 4): 886–890. doi: 10.1042/BST20120019

Available at: http://www.ncbi.nlm.nih.gov/pmc/articles/PMC3433256/

Extracellular small RNAs: what, where, why?

Anna M. Hoy and Amy H. Buck[1]
Centre for Immunity, Infection and Evolution, Ashworth Laboratories, King's Buildings, University of Edinburgh, Edinburgh EH9 3YT, U.K.

Biochemical Society TRANSACTIONS

Abstract

miRNAs (microRNAs) are a class of small RNA that regulate gene expression by binding to mRNAs and modulating the precise amount of proteins that get expressed in a cell at a given time. This form of gene regulation plays an important role in developmental systems and is critical for the proper function of numerous biological pathways. Although miRNAs exert their functions inside the cell, these and other classes of RNA are found in body fluids in a cell-free form that is resistant to degradation by RNases. A broad range of cell types have also been shown to secrete miRNAs in association with components of the RISC (RNA-induced silencing complex) and/or encapsulation within vesicles, which can be taken up by other cells. In the present paper, we provide an overview of the properties of extracellular miRNAs in relation to their capacity as biomarkers, stability against degradation and mediators of cell–cell communication.

Introduction

Mandel and Métais first described the presence of extracellular nucleic acids in human plasma in 1948 [1]. The concept of extracellular RNA emerged in a different context in the 1970s, when Kolodny et al. [2,3] showed that RNA is transferred between fibroblast cells *in vitro* and Stroun et al. [4] demonstrated that highly methylated RNA is secreted by diverse cell types through a process not associated with cell death. In parallel, a range of reports in the 1960s suggested that RNA from one tissue (e.g. liver) could induce tissue-specific expression in other cell types [5], although the mechanisms surrounding this phenomenon were never described. The recent discovery of RNA encapsulation within extracellular vesicles [6] is consistent with some of these earlier studies and provides a framework for conceptualizing RNA transport in mammals. At present, however, there is little connection between secretion and uptake of RNA observed *in vitro* and the meaning of RNA in systemic circulation. In the present paper, we highlight some of the key issues surrounding the biological and medical meaning of extracellular miRNA (microRNA).

miRNA classification

Several classes of small RNA have been identified in animals, fungi and plants which play diverse roles in gene regulation and genome defence (reviewed in [7]). The defining features of a small RNA include its origin and interaction partners. In the present paper, we focus on miRNAs, which are derived from stem–loop structures located within the introns or exons of coding genes or transcribed from 'intergenic' regions of the genome. In animals, the stem–loop structures are processed by Drosha in the nucleus, followed by Dicer in the cytoplasm, resulting in a ~22 nt duplex RNA (reviewed in [8]). One strand of this duplex is incorporated into RISC (RNA-induced silencing complex), which binds to mRNAs at specific sites with base-pair complementarity to the miRNA; generally these sites are located in the 3′-UTR (untranslated region) of the mRNA [9]. The interactions of the miRNA and mRNA within RISC leads to destabilization of the mRNAs and/or inhibition of translation [9]. Currently, 1921 mature human miRNAs have been annotated in miRBase version 18 [10], each of which is predicted to target hundreds of mRNAs [9]. Given the vast scope for combinatorial regulation of targets, it is difficult to find a cellular pathway not regulated at some level by a miRNA. Indeed, the majority of protein-coding genes contain miRNA-binding sites under selective pressure [11] and misexpression of miRNAs is associated with many disease processes, encompassing all cancers, as well as metabolic, cardiovascular, neuronal and immune-related diseases [12].

miRNAs as extracellular biomarkers

The first evidence that miRNAs exist outside cells was reported by Valadi et al. [6] in 2007, who showed that exosomes secreted by mast cell lines contain both mRNA and miRNA. In parallel, several reports in 2008 demonstrated that miRNAs are present in a cell-free form in human and mouse serum [13–16]. Given the numerous associations between miRNAs and disease, their presence in blood has sparked enormous interest in using them as non-invasive biomarkers [17]. However, the actual composition of extracellular miRNAs in blood is likely to derive from a variety of cell types and factors dictating secretion of RNA are not yet known (discussed further below). Tissue injury appears to be one pathological state that leads to differential expression of specific miRNAs in blood. Wang

Key words: extracellular small RNA, microRNA (miRNA), RNA, RNA-induced silencing complex (RISC).

Abbreviations used: Ago2, Argonaute 2; AMI, acute myocardial infarction; HDL, high-density lipoprotein; HMEC-1, human microvascular endothelial cell 1; miRNA, microRNA; MVB, multivesicular body; NPM1, nucleophosmin; nSMase2, neutral sphingomyelinase 2; RISC, RNA-induced silencing complex; snRNA, small nuclear RNA; UTR, untranslated region.

[1]To whom correspondence should be addressed (email a.buck@ed.ac.uk).

Biochem. Soc. Trans. (2012) 40, 886–890; doi:10.1042/BST20120019

et al. [18] demonstrated that the liver-specific miRNA *miR-122* is elevated ~500-fold in mouse plasma following liver injury by acetaminophen overdose. Others have reported increases in *miR-122* levels in human serum following liver damage induced by acetaminophen [19] or hepatitis B infection [20]. Differential expression of extracellular miRNAs is also associated with AMI (acute myocardial infarction). Cheng et al. [21] reported a transient 200-fold increase in the level of *miR-1* in rat serum at 6 h after AMI and a similar increase in human serum taken within 24 h of AMI. Whether *miR-122* and *miR-1* are released during cell death and/or there is specificity in the secretion of these miRNAs is unknown. Both of these miRNAs are highly abundant and tissue-specific [22], which might be essential criteria for any good miRNA biomarker, since many cell types can secrete miRNAs into circulation [23].

Beyond tissue injury, miRNA changes in serum or plasma are also associated with different cancers (reviewed in [24]). Mitchell et al. [14] used a mouse xenograph model with human prostate cancer cells expressing human-specific miRNAs (*miR-629** and *miR-660*) to demonstrate that tumour-derived miRNAs enter the circulation and are detectable in plasma [14]. They also observed a 46-fold elevation in *miR-141* in the serum of patients with prostate cancer and reported 60% sensitivity and 100% specificity in detecting individuals with cancer. Ironically, *miR-141* in human plasma was first reported in association with pregnancy; this miRNA is enriched in the placenta, increases in maternal plasma with gestational age and falls off significantly 24 h after delivery [16]. Clearly, prostate cancer and pregnancy would not be examined in the same individual, but these examples highlight the complexity of using circulating miRNAs as biomarkers. Further understanding of when, where and how miRNAs are released or secreted by different cell types will guide investigations into their capacity as biomarkers.

Who else is out there?

Analyses of small RNA content in bodily fluids has been largely directed toward miRNAs, given their tissue-specific expression, the precedence for their differential expression in disease, and existing commercial interest [25]. However, other classes of small RNA have also been detected in the extracellular environment: the 3′-end fragments of rRNAs and tRNAs are detectable in human milk [26] and U6 snRNA (small nuclear RNA) is up-regulated in the sera of cancer patients [27]. It is therefore possible that various small RNAs exist in an extracellular form that may be of diagnostic or biological interest. Interestingly, studies in the 1970s suggested that much of the RNAs secreted by cells were small (sedimenting between 2.5 and 4 S) and highly methylated [4]. It is possible that miRNAs are not the only, or even the most interesting, player in the extracellular space. Existing sequence datasets from human serum and plasma suggest that miRNAs dominate the small RNA fraction (40–96% of reads), but in some cases, a significant proportion of reads map to rRNA (3–56%) or tRNA (11–51%), with <1% mapping to snoRNA (small nucleolar RNA) and snRNA [14,15,28,29]. However, in most publications, only those reads annotated as miRNAs are reported, and it should be noted that rigorous controls/standards for contamination of cellular RNA have not yet been defined. On the other hand, the extracellular environment is known to be full of RNases, and a key question in interpreting the meaning of any extracellular RNA is how and why it is stabilized.

The extracellular environment

miRNAs have been found in various body fluids, including serum, plasma, saliva, tears, urine, amniotic fluid, colostrum, breast milk, bronchial lavage, cerebrospinal fluid, peritoneal fluid, pleural fluid and seminal fluid [30]. Yet, highly stable RNases are an abundant component of these fluids; the concentrations of RNases in human serum or plasma are estimated at several hundred nanograms/ml, and can be elevated in cancer patients [31,32]. Consistent with this, Tsui et al. [33] showed that synthetic RNA is degraded in less than 5 s when incubated with human plasma, yet they found that mRNAs present in serum and plasma are stable for many hours. Further studies (before analysis of miRNAs) have confirmed this apparent RNA stability: mRNA in plasma is not degraded by RNase-A/T, RNase H or DNase [34], arguing against the possibility that it is stabilized by association with DNA [4]. A range of reports have shown similar results with miRNAs, and researchers have gone on to test the extremes of miRNA stability in serum and plasma using long periods at room temperature, freeze–thawing, exposure to boiling and different pHs [14,15,35]. These and other investigations suggest that a large component of the RNA found in fluids is extremely stable. On the other hand, pre-treatment of serum or plasma with detergents (e.g. Triton X or SDS) makes mRNAs susceptible to degradation by RNases [33,34], and miRNAs secreted from THP-1 cells similarly lose protection following treatment with detergents [36]. As postulated by many researchers since the 1970s, it appears that at least one mechanism for the extracellular stability of RNAs is the natural encapsulation of these molecules in vesicles [37].

Stability and function of extracellular RNA

Vesicles are secreted by many (if not all) cell types and have been detected in body fluids through density sedimentation, electron microscopy and analysis of specific markers on their surfaces. Owing to a lack of precise nomenclature, many terms are used to describe extracellular vesicles, including microparticles, microvesicles, exosomes and membrane particles; in the present paper, we refer to exosomes, apoptotic bodies and shedding microvesicles as defined in a recent review [38]. The term exosome defines vesicles ~40–100 nm in diameter, of endocytic origin, derived from MVBs (multivesicular bodies) that fuse with the plasma membrane [39]. Shedding microvesicles are ~100–1000 nm

Figure 1 | Diverse origins of stabilized extracellular miRNA

Extracellular miRNAs are protected from degradation by RNases through encapsulation within exosomes, shedding microvesicles and apoptotic cells. They have also been identified in lower-molecular-mass complexes bound to Ago2, NPM1 or HDL.

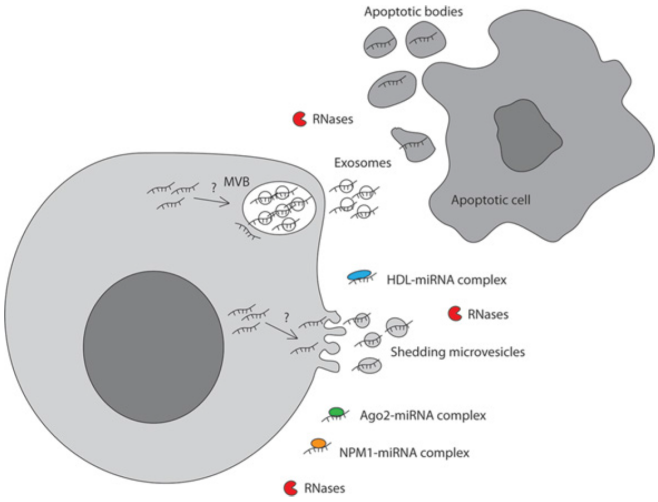

in diameter and derive directly from cell membranes by budding. Apoptotic bodies are ~50–5000 nm in diameter and are membranous vesicles shed from the plasma membranes of dying/apoptotic cells via blebbing. A description of the biogenesis and distinguishing features of these vesicles is summarized in [38]. Of interest is the fact that RNA has been identified in vesicles (cartoon in Figure 1) and specific small RNAs are enriched in vesicles in relation to the pool of intracellular small RNA [6,40]. Furthermore, various reports suggest that vesicular miRNAs are a medium for cell–cell communication. For example, *miR-150* is selectively packaged into exosomes secreted by THP-1 cells (a human acute monocytic leukaemia cell line), which are taken up by HMEC-1 cells (a human microvascular endothelial cell line). Increased concentrations of *miR-150* in HMEC-1 cells leads to down-regulation of *miR-150* targets, including the transcription factor c-Myb, resulting in enhanced cell migration [36]. Functional transfer of RNA between cells also occurs through apoptotic bodies: *miR-126* is the most abundant miRNA in endothelium-derived apoptotic bodies generated during atherosclerosis and can be transferred and taken up by vascular cells [41]. Using a variety of controls, including apoptotic bodies from cells derived from *miR-126*$^{-/-}$ mice, Zernecke et al. [41] demonstrated that the uptake of *miR-126* is responsible for the down-regulation of its target, RGS16, an inhibitor of G-protein-coupled receptors. Regulation of RGS16 by *miR-126* leads to an increase in CXCL12 (CXC chemokine ligand 12), which causes mobilization of progenitor cells and incorporation into plaques, conferring protective effects in diet-induced atherosclerosis [41].

Before it was known that RNA was contained within secreted vesicles, numerous studies have demonstrated important functions of exosomes in cell–cell communication, in particular in neuronal and immune signalling (reviewed in [42]). On the basis of the work cited in the present paper, it seems likely that RNAs within these vesicles could be involved directly in altering the functional properties of recipient cells. However, the actual mechanisms governing specificity, in terms of which RNAs are selectively packaged into vesicles, remain unknown. Given the short length of a mature miRNA, there are limited *cis*-acting elements within the sequence to dictate specificity. However, it is possible that miRNA-interaction partners could somehow be involved in localization of miRNAs for export. Gibbings et al. [43] demonstrated that exosomes secreted from monocytes contain components of the RISC machinery, including Ago2 (Argonaute 2) and GW182, which co-migrate with endosomal–MVB fractions in density gradients [43]. miRNA–RISC silencing activity is also enhanced when MVB turnover is impaired and MVBs positively regulate RISC loading [44]. However, to date, there is no experimental support for a mechanism whereby specific miRNAs are loaded into MVBs for secretion; neither is it known how specificity is achieved in apoptotic bodies and shedding microvesicles.

Non-vesicular extracellular miRNA

The studies cited above support the existence of miRNA-containing vesicles, but this may not be the most prevalent form of extracellular miRNA. Several reports suggest that

a substantial fraction of extracellular miRNAs are not encapsulated within vesicles, but are protected against RNase digestion by association with proteins. Wang et al. [45] showed that miRNAs secreted by A549 and HepG2 cells associate with RNA-binding protein nucleophosmin (NPM1), a multifunctional histone-binding protein. On the basis of size-exclusion chromatography, Arroyo et al. [46] reported that the majority of plasma miRNAs (~90%) are present as Ago2–miRNA complexes not contained within vesicles. They showed further that these miRNAs become susceptible to RNase digestion following proteinase K treatment of plasma [46]. Similarly, Turchinovich et al. [47] showed that the majority of miRNAs found in human plasma, as well as those secreted from the MCF7 breast cancer cell line, are associated with Ago2, but exist in a form that is <300 kDa. The authors suggested that the high proportion of Ago–miRNA may represent by-products of dead cells, since Ago–miRNA complexes are known to be extremely stable within cells [47]. However, Ago2 is also present within exosomes [36,43], and it may be that some of the Ago2–RNA complexes identified derive from vesicles, potentially damaged during purification. Another study has shown that specific miRNAs are complexed to HDL (high-density lipoprotein) in serum, and this also protects miRNAs from degradation and mediates transport into recipient cells [48]. The mechanisms controlling which export/import pathways are active in a cell are unknown. However, exosome release is blocked by inhibiting nSMase2 (neutral sphingomyelinase 2), an enzyme involved in ceramide biosynthesis [49]. Interestingly, inhibition of nSMase2 actually increases the export of miRNAs by HDL [48], suggesting distinct mechanisms and/or competition in the export pathways. Further research is required to understand the mechanisms dictating specificity in the secretion and uptake pathways. Nonetheless, the capacity to mimic and exploit these natural RNA-transport vehicles, whether they be vesicles or protein co-factors, has exciting implications for therapeutic RNA delivery [50].

The extracellular communicator hypothesis revisited

In a hypothesis paper in 1988, entitled "Extracellular 'communicator RNA'", Steven Benner proposed that RNA could be involved in cell–cell communication as a short distance messenger [51]. He based this on the fact that extracellular fluid is full of proteins with RNase activity, as well as RNase inhibitors, and the balance between these molecules is associated with disease conditions including cancer and angiogenesis. We are now aware of even more secretory RNase-like proteins with functions in innate and acquired immunity [52]. One might expect, as Benner proposed [51], that it is the substrates of extracellular RNases, i.e. extracellular RNA, that are important. However, all of the examples cited in the present paper suggest that extracellular RNA is protected from RNases through association with proteins and/or encapsulation within vesicles. It is therefore possible that we have just scratched the surface in understanding the functions of short- or long-lived extracellular RNAs, and the meaning of the numerous RNase-like proteins that have evolved in different species [53].

Funding

A.H. is supported by a studentship from the National Environmental Research Council. A.B. is supported by a Wellcome Trust Research Career Development Fellowship [grant number 097394/Z/11/Z].

References

1 Mandel, P. and Métais, P. (1948) Les acides nucleiques du plasma sanguin chez l'homme. C. R. Seances Soc. Biol. Ses Fil. **142**, 241–243
2 Kolodny, G.M. (1971) Evidence for transfer of macromolecular RNA between mammalian cells in culture. Exp. Cell Res. **65**, 313–324
3 Kolodny, G.M. (1972) Cell to cell transfer of RNA into transformed cells. J. Cell. Physiol. **79**, 147–150
4 Stroun, M., Anker, P., Beljanski, M., Henri, J., Lederrey, C., Ojha, M. and Maurice, P.A. (1978) Presence of RNA in the nucleoprotein complex spontaneously released by human lymphocytes and frog auricles in culture. Cancer Res. **38**, 3546–3554
5 Niu, M.C., Cordova, C.C., Niu, L.C. and Radbill, C.L. (1962) RNA-induced biosynthesis of specific enzymes. Proc. Natl. Acad. Sci. U.S.A. **48**, 1964–1969
6 Valadi, H., Ekstrom, K., Bossios, A., Sjostrand, M., Lee, J.J. and Lotvall, J.O. (2007) Exosome-mediated transfer of mRNAs and microRNAs is a novel mechanism of genetic exchange between cells. Nat. Cell Biol. **9**, 654–659
7 Ghildiyal, M. and Zamore, P.D. (2009) Small silencing RNAs: an expanding universe. Nat. Rev. Genet. **10**, 94–108
8 Winter, J., Jung, S., Keller, S., Gregory, R.I. and Diederichs, S. (2009) Many roads to maturity: microRNA biogenesis pathways and their regulation. Nat. Cell Biol. **11**, 228–234
9 Bartel, D.P. (2009) MicroRNAs: target recognition and regulatory functions. Cell **136**, 215–233
10 Kozomara, A. and Griffiths-Jones, S. (2011) miRBase: integrating microRNA annotation and deep-sequencing data. Nucleic Acids Res. **39**, D152–D157
11 Friedman, R.C., Farh, K.K., Burge, C.B. and Bartel, D.P. (2009) Most mammalian mRNAs are conserved targets of microRNAs. Genome Res. **19**, 92–105
12 Chang, T.C. and Mendell, J.T. (2007) microRNAs in vertebrate physiology and human disease. Annu. Rev. Genomics Hum. Genet. **8**, 215–239
13 Lawrie, C.H., Gal, S., Dunlop, H.M., Pushkaran, B., Liggins, A.P., Pulford, K., Banham, A.H., Pezzella, F., Boultwood, J., Wainscoat, J.S. et al. (2008) Detection of elevated levels of tumour-associated microRNAs in serum of patients with diffuse large B-cell lymphoma. Br. J. Haematol. **141**, 672–675
14 Mitchell, P.S., Parkin, R.K., Kroh, E.M., Fritz, B.R., Wyman, S.K., Pogosova-Agadjanyan, E.L., Peterson, A., Noteboom, J., O'Briant, K.C., Allen, A. et al. (2008) Circulating microRNAs as stable blood-based markers for cancer detection. Proc. Natl. Acad. Sci. U.S.A. **105**, 10513–10518
15 Chen, X., Ba, Y., Ma, L., Cai, X., Yin, Y., Wang, K., Guo, J., Zhang, Y., Chen, J., Guo, X. et al. (2008) Characterization of microRNAs in serum: a novel class of biomarkers for diagnosis of cancer and other diseases. Cell Res. **18**, 997–1006
16 Chim, S.S., Shing, T.K., Hung, E.C., Leung, T.Y., Lau, T.K., Chiu, R.W. and Lo, Y.M. (2008) Detection and characterization of placental microRNAs in maternal plasma. Clin. Chem. **54**, 482–490
17 Brase, J.C., Wuttig, D., Kuner, R. and Sultmann, H. (2010) Serum microRNAs as non-invasive biomarkers for cancer. Mol. Cancer **9**, 306
18 Wang, K., Zhang, S., Marzolf, B., Troisch, P., Brightman, A., Hu, Z., Hood, L.E. and Galas, D.J. (2009) Circulating microRNAs, potential biomarkers for drug-induced liver injury. Proc. Natl. Acad. Sci. U.S.A. **106**, 4402–4407

19 Starkey Lewis, P.J., Dear, J., Platt, V., Simpson, K.J., Craig, D.G., Antoine, D.J., French, N.S., Dhaun, N., Webb, D.J., Costello, E.M. et al. (2011) Circulating microRNAs as potential markers of human drug-induced liver injury. Hepatology **54**, 1767–1776

20 Zhang, Y., Jia, Y., Zheng, R., Guo, Y., Wang, Y., Guo, H., Fei, M. and Sun, S. (2010) Plasma microRNA-122 as a biomarker for viral-, alcohol-, and chemical-related hepatic diseases. Clin. Chem. **56**, 1830–1838

21 Cheng, Y., Tan, N., Yang, J., Liu, X., Cao, X., He, P., Dong, X., Qin, S. and Zhang, C. (2010) A translational study of circulating cell-free microRNA-1 in acute myocardial infarction. Clin. Sci. **119**, 87–95

22 Liang, Y., Ridzon, D., Wong, L. and Chen, C. (2007) Characterization of microRNA expression profiles in normal human tissues. BMC Genomics **8**, 166

23 Hunter, M.P., Ismail, N., Zhang, X., Aguda, B.D., Lee, E.J., Yu, L., Xiao, T., Schafer, J., Lee, M.L., Schmittgen, T.D. et al. (2008) Detection of microRNA expression in human peripheral blood microvesicles. PLoS ONE **3**, e3694

24 Cortez, M.A., Bueso-Ramos, C., Ferdin, J., Lopez-Berestein, G., Sood, A.K. and Calin, G.A. (2011) MicroRNAs in body fluids: the mix of hormones and biomarkers. Nat. Rev. Clin. Oncol. **8**, 467–477

25 Calin, G.A. and Croce, C.M. (2006) MicroRNA signatures in human cancers. Nat. Rev. Cancer **6**, 857–866

26 Semenov, D.V., Kuligina, E.V., Shevyrina, O.N., Richter, V.A. and Vlassov, V.V. (2004) Extracellular ribonucleic acids of human milk. Ann. N.Y. Acad. Sci. **1022**, 190–194

27 Appaiah, H.N., Goswami, C.P., Mina, L.A., Badve, S., Sledge, Jr, G.W., Liu, Y. and Nakshatri, H. (2011) Persistent upregulation of U6:SNORD44 small RNA ratio in the serum of breast cancer patients. Breast Cancer Res. **13**, R86

28 Yang, Q., Lu, J., Wang, S., Li, H., Ge, Q. and Lu, Z. (2011) Application of next-generation sequencing technology to profile the circulating microRNAs in the serum of preeclampsia versus normal pregnant women. Clin. Chim. Acta **412**, 2167–2173

29 Li, H., Guo, L., Wu, Q., Lu, J., Ge, Q. and Lu, Z. (2012) A comprehensive survey of maternal plasma miRNAs expression profiles using high-throughput sequencing. Clin. Chim. Acta **413**, 568–576

30 Weber, J.A., Baxter, D.H., Zhang, S., Huang, D.Y., Huang, K.H., Lee, M.J., Galas, D.J. and Wang, K. (2010) The microRNA spectrum in 12 body fluids. Clin. Chem. **56**, 1733–1741

31 Kamm, R.C. and Smith, A.G. (1972) Ribonuclease activity in human plasma. Clin. Biochem. **5**, 198–200

32 Blank, A. and Dekker, C.A. (1981) Ribonucleases of human serum, urine, cerebrospinal fluid, and leukocytes: activity staining following electrophoresis in sodium dodecyl sulfate-polyacrylamide gels. Biochemistry **20**, 2261–2267

33 Tsui, N.B., Ng, E.K. and Lo, Y.M. (2002) Stability of endogenous and added RNA in blood specimens, serum, and plasma. Clin. Chem. **48**, 1647–1653

34 El-Hefnawy, T., Raja, S., Kelly, L., Bigbee, W.L., Kirkwood, J.M., Luketich, J.D. and Godfrey, T.E. (2004) Characterization of amplifiable, circulating RNA in plasma and its potential as a tool for cancer diagnostics. Clin. Chem. **50**, 564–573

35 Li, Y., Jiang, Z., Xu, L., Yao, H., Guo, J. and Ding, X. (2011) Stability analysis of liver cancer-related microRNAs. Acta Biochim. Biophys. Sin. **43**, 69–78

36 Zhang, Y., Liu, D., Chen, X., Li, J., Li, L., Bian, Z., Sun, F., Lu, J., Yin, Y., Cai, X. et al. (2010) Secreted monocytic *miR-150* enhances targeted endothelial cell migration. Mol. Cell **39**, 133–144

37 Ng, E.K., Tsui, N.B., Lam, N.Y., Chiu, R.W., Yu, S.C., Wong, S.C., Lo, E.S., Rainer, T.H., Johnson, P.J. and Lo, Y.M. (2002) Presence of filterable and nonfilterable mRNA in the plasma of cancer patients and healthy individuals. Clin. Chem. **48**, 1212–1217

38 Gyorgy, B., Szabo, T.G., Pasztoi, M., Pal, Z., Misjak, P., Aradi, B., Laszlo, V., Pallinger, E., Pap, E., Kittel, A. et al. (2011) Membrane vesicles, current state-of-the-art: emerging role of extracellular vesicles. Cell. Mol. Life Sci. **68**, 2667–2688

39 Stoorvogel, W., Kleijmeer, M.J., Geuze, H.J. and Raposo, G. (2002) The biogenesis and functions of exosomes. Traffic **3**, 321–330

40 Pigati, L., Yaddanapudi, S.C., Iyengar, R., Kim, D.J., Hearn, S.A., Danforth, D., Hastings, M.L. and Duelli, D.M. (2010) Selective release of microRNA species from normal and malignant mammary epithelial cells. PLoS ONE **5**, e13515

41 Zernecke, A., Bidzhekov, K., Noels, H., Shagdarsuren, E., Gan, L., Denecke, B., Hristov, M., Koppel, T., Jahantigh, M.N., Lutgens, E. et al. (2009) Delivery of microRNA-126 by apoptotic bodies induces CXCL12-dependent vascular protection. Sci. Signaling **2**, ra81

42 Thery, C. (2011) Exosomes: secreted vesicles and intercellular communications. F1000 Biol. Rep. **3**, 15

43 Gibbings, D.J., Ciaudo, C., Erhardt, M. and Voinnet, O. (2009) Multivesicular bodies associate with components of miRNA effector complexes and modulate miRNA activity. Nat. Cell Biol. **11**, 1143–1149

44 Lee, Y.S., Pressman, S., Andress, A.P., Kim, K., White, J.L., Cassidy, J.J., Li, X., Lubell, K., Lim, D.H., Cho, I.S. et al. (2009) Silencing by small RNAs is linked to endosomal trafficking. Nat. Cell Biol. **11**, 1150–1156

45 Wang, K., Zhang, S., Weber, J., Baxter, D. and Galas, D.J. (2011) Export of microRNAs and microRNA-protective protein by mammalian cells. Nucleic Acids Res. **38**, 7248–7259

46 Arroyo, J.D., Chevillet, J.R., Kroh, E.M., Ruf, I.K, Pritchard, C.C., Gibson, D.F., Mitchell, P.S., Bennett, C.F., Pogosova-Agadjanyan, E.L., Stirewalt, D.L. et al. (2011) Argonaute2 complexes carry a population of circulating microRNAs independent of vesicles in human plasma. Proc. Natl. Acad. Sci. U.S.A. **108**, 5003–5008

47 Turchinovich, A., Weiz, L., Langheinz, A. and Burwinkel, B. (2011) Characterization of extracellular circulating microRNA. Nucleic Acids Res. **39**, 7223–7233

48 Vickers, K.C., Palmisano, B.T., Shoucri, B.M., Shamburek, R.D. and Remaley, A.T. (2011) MicroRNAs are transported in plasma and delivered to recipient cells by high-density lipoproteins. Nat. Cell Biol. **13**, 423–433

49 Kosaka, N., Iguchi, H., Yoshioka, Y., Takeshita, F., Matsuki, Y. and Ochiya, T. (2010) Secretory mechanisms and intercellular transfer of microRNAs in living cells. J. Biol. Chem. **285**, 17442–17452

50 Alvarez-Erviti, L., Seow, Y., Yin, H., Betts, C., Lakhal, S. and Wood, M.J. (2011) Delivery of siRNA to the mouse brain by systemic injection of targeted exosomes. Nat. Biotechnol. **29**, 341–345

51 Benner, S.A. (1988) Extracellular 'communicator RNA'. FEBS Lett. **233**, 225–228

52 Rosenberg, H.F. (2011) Vertebrate secretory (RNase A) ribonucleases and host defense. Nucleic Acids Mol. Biol. **26**, 35–53

53 Sorrentino, S. (1998) Human extracellular ribonucleases: multiplicity, molecular diversity and catalytic properties of the major RNase types. Cell. Mol. Life Sci. **54**, 785–794

Received 21 March 2012
doi:10.1042/BST20120019

REFERENCES

Aad, G., Abajyan, T., Abbott, B., Abdallah, J., Abdel Khalek, S., Abdinov, O., Aben, R., Abi, B., Abolins, M., Abouzeid, O.S.*, et al.* (2014). Search for quantum black hole production in high-invariant-mass lepton+jet final states using pp collisions at radicals=8 TeV and the ATLAS detector. Physical review letters *112*, 091804.

Alvarez-Erviti, L., Seow, Y., Yin, H., Betts, C., Lakhal, S., and Wood, M.J. (2011). Delivery of siRNA to the mouse brain by systemic injection of targeted exosomes. Nat Biotechnol *29*, 341-345.

Ameres, S.L., and Zamore, P.D. (2013). Diversifying microRNA sequence and function. Nature reviews. Molecular cell biology *14*, 475-488.

Andersen, C.L., Jensen, J.L., and Orntoft, T.F. (2004). Normalization of real-time quantitative reverse transcription-PCR data: a model-based variance estimation approach to identify genes suited for normalization, applied to bladder and colon cancer data sets. Cancer Res *64*, 5245-5250.

Andersen, K.L., and Collins, K. (2012). Several RNase T2 enzymes function in induced tRNA and rRNA turnover in the ciliate Tetrahymena. Molecular biology of the cell *23*, 36-44.

Anthony, B., Allen, J.T., Li, Y.S., and McManus, D.P. (2010). Hepatic stellate cells and parasite-induced liver fibrosis. Parasites & vectors *3*, 60.

Anthony, B.J., James, K.R., Gobert, G.N., Ramm, G.A., and McManus, D.P. (2013). Schistosoma Eggs Induce a Proinflammatory, Anti-Fibrogenic Phenotype in Hepatic Stellate Cells. PloS one *8*, e68479.

Appaiah, H.N., Goswami, C.P., Mina, L.A., Badve, S., Sledge, G.W., Jr., Liu, Y., and Nakshatri, H. (2011). Persistent upregulation of U6:SNORD44 small RNA ratio in the serum of breast cancer patients. Breast Cancer Res *13*, R86.

Araujo, A.P., Frezza, T.F., Allegretti, S.M., and Giorgio, S. (2010). Hypoxia, hypoxia-inducible factor-1alpha and vascular endothelial growth factor in a murine model of Schistosoma mansoni infection. Experimental and molecular pathology *89*, 327-333.

Arroyo, J.D., Chevillet, J.R., Kroh, E.M., Ruf, I.K., Pritchard, C.C., Gibson, D.F., Mitchell, P.S., Bennett, C.F., Pogosova-Agadjanyan, E.L., Stirewalt, D.L.*, et al.* (2011). Argonaute2 complexes carry a population of circulating

microRNAs independent of vesicles in human plasma. Proc Natl Acad Sci U S A *108*, 5003-5008.

Arthur, M.J. (2000). Fibrogenesis II. Metalloproteinases and their inhibitors in liver fibrosis. American journal of physiology. Gastrointestinal and liver physiology *279*, G245-249.

Bagga, S., Bracht, J., Hunter, S., Massirer, K., Holtz, J., Eachus, R., and Pasquinelli, A.E. (2005). Regulation by let-7 and lin-4 miRNAs results in target mRNA degradation. Cell *122*, 553-563.

Bandyopadhyay, S., Friedman, R.C., Marquez, R.T., Keck, K., Kong, B., Icardi, M.S., Brown, K.E., Burge, C.B., Schmidt, W.N., Wang, Y., and McCaffrey, A.P. (2011). Hepatitis C virus infection and hepatic stellate cell activation downregulate miR-29: miR-29 overexpression reduces hepatitis C viral abundance in culture. The Journal of infectious diseases *203*, 1753-1762.

Barbosa Junior Ade, A., Pfeifer, U., and Andrade, Z.A. (1993). Role of fat-storing cells in schistosomal hepatic fibrosis of mice. Virchows Archiv. B, Cell pathology including molecular pathology *64*, 91-96.

Bartel, D.P. (2009). MicroRNAs: target recognition and regulatory functions. Cell *136*, 215-233.

Bartley, P.B., Ramm, G.A., Jones, M.K., Ruddell, R.G., Li, Y., and McManus, D.P. (2006). A contributory role for activated hepatic stellate cells in the dynamics of Schistosoma japonicum egg-induced fibrosis. International journal for parasitology *36*, 993-1001.

Bataller, R., and Brenner, D.A. (2005). Liver fibrosis. The Journal of clinical investigation *115*, 209-218.

Behm-Ansmant, I., Rehwinkel, J., Doerks, T., Stark, A., Bork, P., and Izaurralde, E. (2006). mRNA degradation by miRNAs and GW182 requires both CCR4:NOT deadenylase and DCP1:DCP2 decapping complexes. Genes & development *20*, 1885-1898.

Bennett, C.F., and Swayze, E.E. (2010). RNA targeting therapeutics: molecular mechanisms of antisense oligonucleotides as a therapeutic platform. Annual review of pharmacology and toxicology *50*, 259-293.

Berezikov, E., Chung, W.J., Willis, J., Cuppen, E., and Lai, E.C. (2007). Mammalian mirtron genes. Mol Cell *28*, 328-336.

Bethune, J., Artus-Revel, C.G., and Filipowicz, W. (2012). Kinetic analysis reveals successive steps leading to miRNA-mediated silencing in mammalian cells. EMBO reports *13*, 716-723.

Blank, A., and Dekker, C.A. (1981). Ribonucleases of human serum, urine, cerebrospinal fluid, and leukocytes. Activity staining following electrophoresis in sodium dodecyl sulfate-polyacrylamide gels. Biochemistry *20*, 2261-2267.

Bohnsack, M.T., Czaplinski, K., and Gorlich, D. (2004). Exportin 5 is a RanGTP-dependent dsRNA-binding protein that mediates nuclear export of pre-miRNAs. Rna *10*, 185-191.

Boloukhere, M., Baldo-Correa, E., and Borojevic, R. (1993). Experimental schistosomiasis mansoni: characterization of connective tissue cells in hepatic periovular granulomas. Journal of submicroscopic cytology and pathology *25*, 505-517.

Booth, M., Mwatha, J.K., Joseph, S., Jones, F.M., Kadzo, H., Ireri, E., Kazibwe, F., Kemijumbi, J., Kariuki, C., Kimani, G.*, et al.* (2004). Periportal fibrosis in human Schistosoma mansoni infection is associated with low IL-10, low IFN-gamma, high TNF-alpha, or low RANTES, depending on age and gender. Journal of immunology *172*, 1295-1303.

Borchert, G.M., Lanier, W., and Davidson, B.L. (2006). RNA polymerase III transcribes human microRNAs. Nat Struct Mol Biol *13*, 1097-1101.

Borel, F., Konstantinova, P., and Jansen, P.L. (2012). Diagnostic and therapeutic potential of miRNA signatures in patients with hepatocellular carcinoma. J Hepatol *56*, 1371-1383.

Bottieau, E., Clerinx, J., de Vega, M.R., Van den Enden, E., Colebunders, R., Van Esbroeck, M., Vervoort, T., Van Gompel, A., and Van den Ende, J. (2006). Imported Katayama fever: clinical and biological features at presentation and during treatment. The Journal of infection *52*, 339-345.

Braun, J.E., Huntzinger, E., Fauser, M., and Izaurralde, E. (2011). GW182 proteins directly recruit cytoplasmic deadenylase complexes to miRNA targets. Mol Cell *44*, 120-133.

Brennecke, J., Hipfner, D.R., Stark, A., Russell, R.B., and Cohen, S.M. (2003). bantam encodes a developmentally regulated microRNA that controls cell proliferation and regulates the proapoptotic gene hid in Drosophila. Cell *113*, 25-36.

Brennecke, J., Stark, A., Russell, R.B., and Cohen, S.M. (2005). Principles of microRNA-target recognition. PLoS Biol *3*, e85.

Britton, C., Winter A.D., Gillan, V., Devaney, E., (2014). microRNAs of parasitic helminths – Identification, characterization and potential as drug targets. International Journal for Parasitology: Drugs and Drug Resistance *4*, 85-94.

Broderick, J.A., and Zamore, P.D. (2011). MicroRNA therapeutics. Gene therapy *18*, 1104-1110.

Brunet, L.R., Finkelman, F.D., Cheever, A.W., Kopf, M.A., and Pearce, E.J. (1997). IL-4 protects against TNF-alpha-mediated cachexia and death during acute schistosomiasis. Journal of immunology *159*, 777-785.

Buhler, M., Spies, N., Bartel, D.P., and Moazed, D. (2008). TRAMP-mediated RNA surveillance prevents spurious entry of RNAs into the Schizosaccharomyces pombe siRNA pathway. Nat Struct Mol Biol *15*, 1015-1023.

Bumcrot, D., Manoharan, M., Koteliansky, V., and Sah, D.W. (2006). RNAi therapeutics: a potential new class of pharmaceutical drugs. Nature chemical biology *2*, 711-719.

Burroughs, A.M., Ando, Y., de Hoon, M.J., Tomaru, Y., Suzuki, H., Hayashizaki, Y., and Daub, C.O. (2011). Deep-sequencing of human Argonaute-associated small RNAs provides insight into miRNA sorting and reveals Argonaute association with RNA fragments of diverse origin. Rna Biol *8*, 158-177.

Cai, P., Piao, X., Liu, S., Hou, N., Wang, H., and Chen, Q. (2013). MicroRNA-gene expression network in murine liver during Schistosoma japonicum infection. PloS one *8*, e67037.

Cai, X., Hagedorn, C.H., and Cullen, B.R. (2004). Human microRNAs are processed from capped, polyadenylated transcripts that can also function as mRNAs. Rna *10*, 1957-1966.

Calin, G.A., and Croce, C.M. (2006). MicroRNA signatures in human cancers. Nat Rev Cancer *6*, 857-866.

Camps, C., Buffa, F.M., Colella, S., Moore, J., Sotiriou, C., Sheldon, H., Harris, A.L., Gleadle, J.M., and Ragoussis, J. (2008). hsa-miR-210 Is induced by hypoxia and is an independent prognostic factor in breast cancer. Clinical cancer research : an official journal of the American Association for Cancer Research *14*, 1340-1348.

Carthew, R.W., and Sontheimer, E.J. (2009). Origins and Mechanisms of miRNAs and siRNAs. Cell *136*, 642-655.

Chan, Y.C., Banerjee, J., Choi, S.Y., and Sen, C.K. (2012). miR-210: the master hypoxamir. Microcirculation *19*, 215-223.

Chang, D., Ramalho, L.N., Ramalho, F.S., Martinelli, A.L., and Zucoloto, S. (2006). Hepatic stellate cells in human schistosomiasis mansoni: a comparative immunohistochemical study with liver cirrhosis. Acta Trop *97*, 318-323.

Chang, T.C., and Mendell, J.T. (2007). microRNAs in vertebrate physiology and human disease. Annu Rev Genomics Hum Genet *8*, 215-239.

Chau, B.N., Xin, C., Hartner, J., Ren, S., Castano, A.P., Linn, G., Li, J., Tran, P.T., Kaimal, V., Huang, X*., et al.* (2012). MicroRNA-21 promotes fibrosis of the kidney by silencing metabolic pathways. Science translational medicine *4*, 121ra118.

Cheloufi, S., Dos Santos, C.O., Chong, M.M., and Hannon, G.J. (2010). A dicer-independent miRNA biogenesis pathway that requires Ago catalysis. Nature *465*, 584-589.

Chen, C., Wu, C.Q., Zhang, Z.Q., Yao, D.K., and Zhu, L. (2011a). Loss of expression of miR-335 is implicated in hepatic stellate cell migration and activation. Experimental cell research *317*, 1714-1725.

Chen, C.J., liu, Q., Zhang, Y.C., Qu, L.H., Chen, Y.Q., and Gautheret, D. (2011b). Genome-wide discovery and analysis of microRNAs and other small RNAs from rice embryogenic callus. Rna Biol *8*, 538-547.

Chen, S.Y., Wang, Y., Telen, M.J., and Chi, J.T. (2008a). The genomic analysis of erythrocyte microRNA expression in sickle cell diseases. PloS one *3*, e2360.

Chen, X., Ba, Y., Ma, L., Cai, X., Yin, Y., Wang, K., Guo, J., Zhang, Y., Chen, J., Guo, X*., et al.* (2008b). Characterization of microRNAs in serum: a novel class of biomarkers for diagnosis of cancer and other diseases. Cell Res *18*, 997-1006.

Chen, X.M. (2009). MicroRNA signatures in liver diseases. World J Gastroenterol *15*, 1665-1672.

Chendrimada, T.P., Gregory, R.I., Kumaraswamy, E., Norman, J., Cooch, N., Nishikura, K., and Shiekhattar, R. (2005). TRBP recruits the Dicer complex to Ago2 for microRNA processing and gene silencing. Nature *436*, 740-744.

Cheng, G., Luo, R., Hu, C., Cao, J., and Jin, Y. (2013). Deep sequencing-based identification of pathogen-specific microRNAs in the plasma of rabbits infected with Schistosoma japonicum. Parasitology *140*, 1751-1761.

Cheng, Y., Tan, N., Yang, J., Liu, X., Cao, X., He, P., Dong, X., Qin, S., and Zhang, C. (2010). A translational study of circulating cell-free microRNA-1 in acute myocardial infarction. Clin Sci (Lond) *119*, 87-95.

Cheung, O., Puri, P., Eicken, C., Contos, M.J., Mirshahi, F., Maher, J.W., Kellum, J.M., Min, H., Luketic, V.A., and Sanyal, A.J. (2008). Nonalcoholic steatohepatitis is associated with altered hepatic MicroRNA expression. Hepatology *48*, 1810-1820.

Chiaramonte, M.G., Donaldson, D.D., Cheever, A.W., and Wynn, T.A. (1999). An IL-13 inhibitor blocks the development of hepatic fibrosis during a T-helper type 2-dominated inflammatory response. The Journal of clinical investigation *104*, 777-785.

Chim, S.S., Shing, T.K., Hung, E.C., Leung, T.Y., Lau, T.K., Chiu, R.W., and Lo, Y.M. (2008). Detection and characterization of placental microRNAs in maternal plasma. Clin Chem *54*, 482-490.

Cifuentes, D., Xue, H., Taylor, D.W., Patnode, H., Mishima, Y., Cheloufi, S., Ma, E., Mane, S., Hannon, G.J., Lawson, N.D*., et al.* (2010). A novel miRNA processing pathway independent of Dicer requires Argonaute2 catalytic activity. Science *328*, 1694-1698.

Cole, C., Sobala, A., Lu, C., Thatcher, S.R., Bowman, A., Brown, J.W., Green, P.J., Barton, G.J., and Hutvagner, G. (2009). Filtering of deep sequencing data reveals the existence of abundant Dicer-dependent small RNAs derived from tRNAs. Rna *15*, 2147-2160.

Cortez, M.A., Bueso-Ramos, C., Ferdin, J., Lopez-Berestein, G., Sood, A.K., and Calin, G.A. (2011). MicroRNAs in body fluids--the mix of hormones and biomarkers. Nat Rev Clin Oncol *8*, 467-477.

Coulibaly, J.T., N'Gbesso, Y.K., Knopp, S., N'Guessan, N.A., Silue, K.D., van Dam, G.J., N'Goran, E.K., and Utzinger, J. (2013). Accuracy of urine circulating cathodic antigen test for the diagnosis of Schistosoma mansoni in preschool-aged children before and after treatment. PLoS Negl Trop Dis *7*, e2109.

Coulouarn, C., Factor, V.M., Andersen, J.B., Durkin, M.E., and Thorgeirsson, S.S. (2009). Loss of miR-122 expression in liver cancer correlates with suppression of the hepatic phenotype and gain of metastatic properties. Oncogene *28*, 3526-3536.

Couvillion, M.T., Sachidanandam, R., and Collins, K. (2010). A growth-essential Tetrahymena Piwi protein carries tRNA fragment cargo. Genes & development *24*, 2742-2747.

de Jesus, A.R., Magalhaes, A., Miranda, D.G., Miranda, R.G., Araujo, M.I., de Jesus, A.A., Silva, A., Santana, L.B., Pearce, E., and Carvalho, E.M. (2004). Association of type 2 cytokines with hepatic fibrosis in human Schistosoma mansoni infection. Infection and immunity *72*, 3391-3397.

de Oliveira, R.B., Senger, M.R., Vasques, L.M., Gasparotto, J., dos Santos, J.P., Pasquali, M.A., Moreira, J.C., Silva, F.P., Jr., and Gelain, D.P. (2013). Schistosoma mansoni infection causes oxidative stress and alters receptor for advanced glycation endproduct (RAGE) and tau levels in multiple organs in mice. International journal for parasitology *43*, 371-379.

de Souza Gomes, M., Muniyappa, M.K., Carvalho, S.G., Guerra-Sa, R., and Spillane, C. (2011). Genome-wide identification of novel microRNAs and their target genes in the human parasite Schistosoma mansoni. Genomics *98*, 96-111.

Denli, A.M., Tops, B.B., Plasterk, R.H., Ketting, R.F., and Hannon, G.J. (2004). Processing of primary microRNAs by the Microprocessor complex. Nature *432*, 231-235.

Derry, M.C., Yanagiya, A., Martineau, Y., and Sonenberg, N. (2006). Regulation of poly(A)-binding protein through PABP-interacting proteins. Cold Spring Harbor symposia on quantitative biology *71*, 537-543.

Dhahbi, J.M., Spindler, S.R., Atamna, H., Yamakawa, A., Boffelli, D., Mote, P., and Martin, D.I. (2013). 5' tRNA halves are present as abundant complexes in serum, concentrated in blood cells, and modulated by aging and calorie restriction. BMC Genomics *14*, 298.

Diederichs, S., and Haber, D.A. (2007). Dual role for argonautes in microRNA processing and posttranscriptional regulation of microRNA expression. Cell *131*, 1097-1108.

Djuranovic, S., Nahvi, A., and Green, R. (2012). miRNA-mediated gene silencing by translational repression followed by mRNA deadenylation and decay. Science *336*, 237-240.

Doench, J.G., and Sharp, P.A. (2004). Specificity of microRNA target selection in translational repression. Genes & development *18*, 504-511.

Doenhoff, M.J., Chiodini, P.L., and Hamilton, J.V. (2004). Specific and sensitive diagnosis of schistosome infection: can it be done with antibodies? Trends Parasitol *20*, 35-39.

Dunne, D.W., Jones, F.M., and Doenhoff, M.J. (1991). The purification, characterization, serological activity and hepatotoxic properties of two cationic

glycoproteins (alpha 1 and omega 1) from Schistosoma mansoni eggs. Parasitology *103 Pt 2*, 225-236.

Dunne, D.W., Lucas, S., Bickle, Q., Pearson, S., Madgwick, L., Bain, J., and Doenhoff, M.J. (1981). Identification and partial purification of an antigen (omega 1) from Schistosoma mansoni eggs which is putatively hepatotoxic in T-cell deprived mice. Trans R Soc Trop Med Hyg *75*, 54-71.

Dunne, D.W., Vennervald, B.J., Booth, M., Joseph, S., Fitzsimmons, C.M., Cahen, P., Sturrock, R.F., Ouma, J.H., Mwatha, J.K., Kimani, G.*, et al.* (2006). Applied and basic research on the epidemiology, morbidity, and immunology of schistosomiasis in fishing communities on Lake Albert, Uganda. Trans R Soc Trop Med Hyg *100*, 216-223.

Durdevic, Z., Mobin, M.B., Hanna, K., Lyko, F., and Schaefer, M. (2013). The RNA methyltransferase Dnmt2 is required for efficient Dicer-2-dependent siRNA pathway activity in Drosophila. Cell reports *4*, 931-937.

Duttagupta, R., Jiang, R., Gollub, J., Getts, R.C., and Jones, K.W. (2011). Impact of cellular miRNAs on circulating miRNA biomarker signatures. PloS one *6*, e20769.

Ebert, M.S., Neilson, J.R., and Sharp, P.A. (2007). MicroRNA sponges: competitive inhibitors of small RNAs in mammalian cells. Nature methods *4*, 721-726.

Ebert, M.S., and Sharp, P.A. (2010). Emerging roles for natural microRNA sponges. Current biology : CB *20*, R858-861.

El-Hefnawy, T., Raja, S., Kelly, L., Bigbee, W.L., Kirkwood, J.M., Luketich, J.D., and Godfrey, T.E. (2004). Characterization of amplifiable, circulating RNA in plasma and its potential as a tool for cancer diagnostics. Clin Chem *50*, 564-573.

Elkayam, E., Kuhn, C.D., Tocilj, A., Haase, A.D., Greene, E.M., Hannon, G.J., and Joshua-Tor, L. (2012). The structure of human argonaute-2 in complex with miR-20a. Cell *150*, 100-110.

Emara, M.M., Ivanov, P., Hickman, T., Dawra, N., Tisdale, S., Kedersha, N., Hu, G.F., and Anderson, P. (2010). Angiogenin-induced tRNA-derived stress-induced RNAs promote stress-induced stress granule assembly. The Journal of biological chemistry *285*, 10959-10968.

Ender, C., and Meister, G. (2010). Argonaute proteins at a glance. Journal of cell science *123*, 1819-1823.

Enk, M.J., Oliveira e Silva, G., and Rodrigues, N.B. (2012). Diagnostic accuracy and applicability of a PCR system for the detection of Schistosoma mansoni DNA in human urine samples from an endemic area. PloS one *7*, e38947.

Etheridge, A., Lee, I., Hood, L., Galas, D., and Wang, K. (2011). Extracellular microRNA: A new source of biomarkers. Mutat Res-Fund Mol M *717*, 85-90.

Eulalio, A., Huntzinger, E., and Izaurralde, E. (2008). Getting to the root of miRNA-mediated gene silencing. Cell *132*, 9-14.

Eulalio, A., Rehwinkel, J., Stricker, M., Huntzinger, E., Yang, S.F., Doerks, T., Dorner, S., Bork, P., Boutros, M., and Izaurralde, E. (2007). Target-specific requirements for enhancers of decapping in miRNA-mediated gene silencing. Genes & development *21*, 2558-2570.

Everts, B., Perona-Wright, G., Smits, H.H., Hokke, C.H., van der Ham, A.J., Fitzsimmons, C.M., Doenhoff, M.J., van der Bosch, J., Mohrs, K., Haas, H.*, et al.* (2009). Omega-1, a glycoprotein secreted by Schistosoma mansoni eggs, drives Th2 responses. The Journal of experimental medicine *206*, 1673-1680.

Fabian, M.R., Cieplak, M.K., Frank, F., Morita, M., Green, J., Srikumar, T., Nagar, B., Yamamoto, T., Raught, B., Duchaine, T.F., and Sonenberg, N. (2011). miRNA-mediated deadenylation is orchestrated by GW182 through two conserved motifs that interact with CCR4-NOT. Nat Struct Mol Biol *18*, 1211-1217.

Fabian, M.R., Mathonnet, G., Sundermeier, T., Mathys, H., Zipprich, J.T., Svitkin, Y.V., Rivas, F., Jinek, M., Wohlschlegel, J., Doudna, J.A.*, et al.* (2009). Mammalian miRNA RISC recruits CAF1 and PABP to affect PABP-dependent deadenylation. Mol Cell *35*, 868-880.

Fabian, M.R., and Sonenberg, N. (2012). The mechanics of miRNA-mediated gene silencing: a look under the hood of miRISC. Nat Struct Mol Biol *19*, 586-593.

Fallon, P.G., Richardson, E.J., McKenzie, G.J., and McKenzie, A.N. (2000). Schistosome infection of transgenic mice defines distinct and contrasting pathogenic roles for IL-4 and IL-13: IL-13 is a profibrotic agent. Journal of immunology *164*, 2585-2591.

Fallon, P.G., Smith, P., and Dunne, D.W. (1998). Type 1 and type 2 cytokine-producing mouse CD4+ and CD8+ T cells in acute Schistosoma mansoni infection. European journal of immunology *28*, 1408-1416.

Fett, J.W., Strydom, D.J., Lobb, R.R., Alderman, E.M., Bethune, J.L., Riordan, J.F., and Vallee, B.L. (1985). Isolation and characterization of angiogenin, an angiogenic protein from human carcinoma cells. Biochemistry *24*, 5480-5486.

Filipowicz, W., Bhattacharyya, S.N., and Sonenberg, N. (2008). Mechanisms of post-transcriptional regulation by microRNAs: are the answers in sight? Nature reviews. Genetics *9*, 102-114.

Franzen, O., Arner, E., Ferella, M., Nilsson, D., Respuela, P., Carninci, P., Hayashizaki, Y., Aslund, L., Andersson, B., and Daub, C.O. (2011). The short non-coding transcriptome of the protozoan parasite Trypanosoma cruzi. PLoS Negl Trop Dis *5*, e1283.

Friedlander, M.R., Mackowiak, S.D., Li, N., Chen, W., and Rajewsky, N. (2012). miRDeep2 accurately identifies known and hundreds of novel microRNA genes in seven animal clades. Nucleic acids research *40*, 37-52.

Friedman, R.C., Farh, K.K., Burge, C.B., and Bartel, D.P. (2009). Most mammalian mRNAs are conserved targets of microRNAs. Genome Res *19*, 92-105.

Friedman, S.L. (2008). Hepatic stellate cells: protean, multifunctional, and enigmatic cells of the liver. Physiological reviews *88*, 125-172.

Fu, H., Feng, J., Liu, Q., Sun, F., Tie, Y., Zhu, J., Xing, R., Sun, Z., and Zheng, X. (2009). Stress induces tRNA cleavage by angiogenin in mammalian cells. FEBS letters *583*, 437-442.

Garcia-Silva, M.R., Frugier, M., Tosar, J.P., Correa-Dominguez, A., Ronalte-Alves, L., Parodi-Talice, A., Rovira, C., Robello, C., Goldenberg, S., and Cayota, A. (2010). A population of tRNA-derived small RNAs is actively produced in Trypanosoma cruzi and recruited to specific cytoplasmic granules. Mol Biochem Parasitol *171*, 64-73.

Gebetsberger, J., Zywicki, M., Kunzi, A., and Polacek, N. (2012). tRNA-derived fragments target the ribosome and function as regulatory non-coding RNA in Haloferax volcanii. Archaea *2012*, 260909.

Gibbings, D.J., Ciaudo, C., Erhardt, M., and Voinnet, O. (2009). Multivesicular bodies associate with components of miRNA effector complexes and modulate miRNA activity. Nat Cell Biol *11*, 1143-1149.

Giege, R., Juhling, F., Putz, J., Stadler, P., Sauter, C., and Florentz, C. (2012). Structure of transfer RNAs: similarity and variability. Wiley interdisciplinary reviews. RNA *3*, 37-61.

Girard, M., Jacquemin, E., Munnich, A., Lyonnet, S., and Henrion-Caude, A. (2008). miR-122, a paradigm for the role of microRNAs in the liver. J Hepatol *48*, 648-656.

Glinz, D., Silue, K.D., Knopp, S., Lohourignon, L.K., Yao, K.P., Steinmann, P., Rinaldi, L., Cringoli, G., N'Goran, E.K., and Utzinger, J. (2010). Comparing diagnostic accuracy of Kato-Katz, Koga agar plate, ether-concentration, and FLOTAC for Schistosoma mansoni and soil-transmitted helminths. PLoS Negl Trop Dis *4*, e754.

Gomes, L.I., Enk, M.J., and Rabello, A. (2014). Diagnosing schistosomiasis: where are we? Revista da Sociedade Brasileira de Medicina Tropical *47*, 3-11.

Goren, Y., Kushnir, M., Zafrir, B., Tabak, S., Lewis, B.S., and Amir, O. (2012). Serum levels of microRNAs in patients with heart failure. Eur J Heart Fail *14*, 147-154.

Gori, M., Arciello, M., and Balsano, C. (2014). MicroRNAs in Nonalcoholic Fatty Liver Disease: Novel Biomarkers and Prognostic Tools during the Transition from Steatosis to Hepatocarcinoma. BioMed research international *2014*, 741465.

Gray, D.J., Ross, A.G., Li, Y.S., and McManus, D.P. (2011). Diagnosis and management of schistosomiasis. Bmj *342*, d2651.

Gregory, R.I., Yan, K.P., Amuthan, G., Chendrimada, T., Doratotaj, B., Cooch, N., and Shiekhattar, R. (2004). The Microprocessor complex mediates the genesis of microRNAs. Nature *432*, 235-240.

Grimson, A., Farh, K.K., Johnston, W.K., Garrett-Engele, P., Lim, L.P., and Bartel, D.P. (2007). MicroRNA targeting specificity in mammals: determinants beyond seed pairing. Mol Cell *27*, 91-105.

Grishok, A., Pasquinelli, A.E., Conte, D., Li, N., Parrish, S., Ha, I., Baillie, D.L., Fire, A., Ruvkun, G., and Mello, C.C. (2001). Genes and mechanisms related to RNA interference regulate expression of the small temporal RNAs that control C. elegans developmental timing. Cell *106*, 23-34.

Gryseels, B., Polman, K., Clerinx, J., and Kestens, L. (2006). Human schistosomiasis. Lancet *368*, 1106-1118.

Gu, S., and Kay, M.A. (2010). How do miRNAs mediate translational repression? Silence *1*, 11.

Guo, C.J., Pan, Q., Jiang, B., Chen, G.Y., and Li, D.G. (2009a). Effects of upregulated expression of microRNA-16 on biological properties of culture-

activated hepatic stellate cells. Apoptosis : an international journal on programmed cell death *14*, 1331-1340.

Guo, C.J., Pan, Q., Li, D.G., Sun, H., and Liu, B.W. (2009b). miR-15b and miR-16 are implicated in activation of the rat hepatic stellate cell: An essential role for apoptosis. J Hepatol *50*, 766-778.

Guo, C.J., Pan, Q., Xiong, H., Qiao, Y.Q., Bian, Z.L., Zhong, W., Sheng, L., Li, H., Shen, L., Hua, J., and Ma, X. (2014). Therapeutic Potential of MicroRNA: A New Target to Treat Intrahepatic Portal Hypertension? BioMed research international *2014*, 797898.

Guo, C.J., Pan, Q., Xiong, H., Qiao, Y.Q., Bian, Z.L., Zhong, W., Sheng, L., Li, H., Shen, L., Hua, J.*, et al.* (2013). Dynamic expression of miR-126* and its effects on proliferation and contraction of hepatic stellate cells. FEBS letters *587*, 3792-3801.

Guo, H., Ingolia, N.T., Weissman, J.S., and Bartel, D.P. (2010). Mammalian microRNAs predominantly act to decrease target mRNA levels. Nature *466*, 835-840.

Gyorgy, B., Szabo, T.G., Pasztoi, M., Pal, Z., Misjak, P., Aradi, B., Laszlo, V., Pallinger, E., Pap, E., Kittel, A.*, et al.* (2011). Membrane vesicles, current state-of-the-art: emerging role of extracellular vesicles. Cell Mol Life Sci *68*, 2667-2688.

Haas, G., Braun, J.E., Igreja, C., Tritschler, F., Nishihara, T., and Izaurralde, E. (2010). HPat provides a link between deadenylation and decapping in metazoa. The Journal of cell biology *189*, 289-302.

Haase, A.D., Jaskiewicz, L., Zhang, H., Laine, S., Sack, R., Gatignol, A., and Filipowicz, W. (2005). TRBP, a regulator of cellular PKR and HIV-1 virus expression, interacts with Dicer and functions in RNA silencing. EMBO reports *6*, 961-967.

Haiser, H.J., Karginov, F.V., Hannon, G.J., and Elliot, M.A. (2008). Developmentally regulated cleavage of tRNAs in the bacterium Streptomyces coelicolor. Nucleic acids research *36*, 732-741.

Hams, E., Aviello, G., and Fallon, P.G. (2013). The schistosoma granuloma: friend or foe? Frontiers in immunology *4*, 89.

Han, H., Peng, J., Hong, Y., Zhang, M., Han, Y., Liu, D., Fu, Z., Shi, Y., Xu, J., Tao, J., and Lin, J. (2013). MicroRNA expression profile in different tissues of BALB/c mice in the early phase of Schistosoma japonicum infection. Mol Biochem Parasitol *188*, 1-9.

Han, J., Lee, Y., Yeom, K.H., Kim, Y.K., Jin, H., and Kim, V.N. (2004). The Drosha-DGCR8 complex in primary microRNA processing. Genes & development *18*, 3016-3027.

Han, J., Lee, Y., Yeom, K.H., Nam, J.W., Heo, I., Rhee, J.K., Sohn, S.Y., Cho, Y., Zhang, B.T., and Kim, V.N. (2006). Molecular basis for the recognition of primary microRNAs by the Drosha-DGCR8 complex. Cell *125*, 887-901.

Hanada, T., Weitzer, S., Mair, B., Bernreuther, C., Wainger, B.J., Ichida, J., Hanada, R., Orthofer, M., Cronin, S.J., Komnenovic, V.*, et al.* (2013). CLP1 links tRNA metabolism to progressive motor-neuron loss. Nature *495*, 474-480.

Hansen, T.B., Jensen, T.I., Clausen, B.H., Bramsen, J.B., Finsen, B., Damgaard, C.K., and Kjems, J. (2013). Natural RNA circles function as efficient microRNA sponges. Nature *495*, 384-388.

Haussecker, D., Huang, Y., Lau, A., Parameswaran, P., Fire, A.Z., and Kay, M.A. (2010). Human tRNA-derived small RNAs in the global regulation of RNA silencing. Rna *16*, 673-695.

He, X., Sai, X., Chen, C., Zhang, Y., Xu, X., Zhang, D., and Pan, W. (2013). Host serum miR-223 is a potential new biomarker for Schistosoma japonicum infection and the response to chemotherapy. Parasites & vectors *6*, 272.

He, Y., Huang, C., Sun, X., Long, X.R., Lv, X.W., and Li, J. (2012a). MicroRNA-146a modulates TGF-beta1-induced hepatic stellate cell proliferation by targeting SMAD4. Cellular signalling *24*, 1923-1930.

He, Y., Huang, C., Zhang, S.P., Sun, X., Long, X.R., and Li, J. (2012b). The potential of microRNAs in liver fibrosis. Cellular signalling *24*, 2268-2272.

Henke, J.I., Goergen, D., Zheng, J., Song, Y., Schuttler, C.G., Fehr, C., Junemann, C., and Niepmann, M. (2008). microRNA-122 stimulates translation of hepatitis C virus RNA. The EMBO journal *27*, 3300-3310.

Hernandez-Gea, V., and Friedman, S.L. (2011). Pathogenesis of liver fibrosis. Annual review of pathology *6*, 425-456.

Heyer, R., Dorr, M., Jellen-Ritter, A., Spath, B., Babski, J., Jaschinski, K., Soppa, J., and Marchfelder, A. (2012). High throughput sequencing reveals a plethora of small RNAs including tRNA derived fragments in Haloferax volcanii. Rna Biol *9*, 1011-1018.

Hoffmann, K.F., Cheever, A.W., and Wynn, T.A. (2000). IL-10 and the dangers of immune polarization: excessive type 1 and type 2 cytokine

responses induce distinct forms of lethal immunopathology in murine schistosomiasis. Journal of immunology *164*, 6406-6416.

Horak, P., and Kolarova, L. (2005). Molluscan and vertebrate immune responses to bird schistosomes. Parasite immunology *27*, 247-255.

Hou, J., Lin, L., Zhou, W., Wang, Z., Ding, G., Dong, Q., Qin, L., Wu, X., Zheng, Y., Yang, Y.*, et al.* (2011). Identification of miRNomes in human liver and hepatocellular carcinoma reveals miR-199a/b-3p as therapeutic target for hepatocellular carcinoma. Cancer cell *19*, 232-243.

Hoy, A.M., and Buck, A.H. (2012). Extracellular small RNAs: what, where, why? Biochem Soc Trans *40*, 886-890.

Hsieh, L.C., Lin, S.I., Kuo, H.F., and Chiou, T.J. (2010). Abundance of tRNA-derived small RNAs in phosphate-starved Arabidopsis roots. Plant signaling & behavior *5*, 537-539.

Hsieh, L.C., Lin, S.I., Shih, A.C., Chen, J.W., Lin, W.Y., Tseng, C.Y., Li, W.H., and Chiou, T.J. (2009). Uncovering small RNA-mediated responses to phosphate deficiency in Arabidopsis by deep sequencing. Plant physiology *151*, 2120-2132.

Hu, J., Xu, Y., Hao, J., Wang, S., Li, C., and Meng, S. (2012). MiR-122 in hepatic function and liver diseases. Protein Cell *3*, 364-371.

Huang, X., Le, Q.T., and Giaccia, A.J. (2010). MiR-210--micromanager of the hypoxia pathway. Trends in molecular medicine *16*, 230-237.

Huang, X., and Zuo, J. (2014). Emerging roles of miR-210 and other non-coding RNAs in the hypoxic response. Acta Biochim Biophys Sin (Shanghai) *46*, 220-232.

Hunter, M.P., Ismail, N., Zhang, X., Aguda, B.D., Lee, E.J., Yu, L., Xiao, T., Schafer, J., Lee, M.L., Schmittgen, T.D.*, et al.* (2008). Detection of microRNA expression in human peripheral blood microvesicles. PLoS One *3*, e3694.

Huntzinger, E., and Izaurralde, E. (2011). Gene silencing by microRNAs: contributions of translational repression and mRNA decay. Nature reviews. Genetics *12*, 99-110.

Hutvagner, G., McLachlan, J., Pasquinelli, A.E., Balint, E., Tuschl, T., and Zamore, P.D. (2001). A cellular function for the RNA-interference enzyme Dicer in the maturation of the let-7 small temporal RNA. Science *293*, 834-838.

Hutvagner, G., Simard, M.J., Mello, C.C., and Zamore, P.D. (2004). Sequence-specific inhibition of small RNA function. PLoS Biol *2*, E98.

Ibironke, O.A., Phillips, A.E., Garba, A., Lamine, S.M., and Shiff, C. (2011). Diagnosis of Schistosoma haematobium by detection of specific DNA fragments from filtered urine samples. Am J Trop Med Hyg *84*, 998-1001.

Iizuka, M., Ogawa, T., Enomoto, M., Motoyama, H., Yoshizato, K., Ikeda, K., and Kawada, N. (2012). Induction of microRNA-214-5p in human and rodent liver fibrosis. Fibrogenesis Tissue Repair *5*, 12.

Iredale, J.P. (2003). Cirrhosis: new research provides a basis for rational and targeted treatments. Bmj *327*, 143-147.

Iredale, J.P., Benyon, R.C., Pickering, J., McCullen, M., Northrop, M., Pawley, S., Hovell, C., and Arthur, M.J. (1998). Mechanisms of spontaneous resolution of rat liver fibrosis. Hepatic stellate cell apoptosis and reduced hepatic expression of metalloproteinase inhibitors. The Journal of clinical investigation *102*, 538-549.

Ivanov, P., Emara, M.M., Villen, J., Gygi, S.P., and Anderson, P. (2011). Angiogenin-induced tRNA fragments inhibit translation initiation. Mol Cell *43*, 613-623.

Jankovic, D., Kullberg, M.C., Noben-Trauth, N., Caspar, P., Ward, J.M., Cheever, A.W., Paul, W.E., and Sher, A. (1999). Schistosome-infected IL-4 receptor knockout (KO) mice, in contrast to IL-4 KO mice, fail to develop granulomatous pathology while maintaining the same lymphokine expression profile. Journal of immunology *163*, 337-342.

Janssen, H.L., Reesink, H.W., Lawitz, E.J., Zeuzem, S., Rodriguez-Torres, M., Patel, K., van der Meer, A.J., Patick, A.K., Chen, A., Zhou, Y.*, et al.* (2013). Treatment of HCV infection by targeting microRNA. The New England journal of medicine *368*, 1685-1694.

Ji, J., Zhang, J., Huang, G., Qian, J., Wang, X., and Mei, S. (2009). Over-expressed microRNA-27a and 27b influence fat accumulation and cell proliferation during rat hepatic stellate cell activation. FEBS letters *583*, 759-766.

Jiang, X., Tsitsiou, E., Herrick, S.E., and Lindsay, M.A. (2010). MicroRNAs and the regulation of fibrosis. Febs J *277*, 2015-2021.

Jinek, M., and Doudna, J.A. (2009). A three-dimensional view of the molecular machinery of RNA interference. Nature *457*, 405-412.

Jochl, C., Rederstorff, M., Hertel, J., Stadler, P.F., Hofacker, I.L., Schrettl, M., Haas, H., and Huttenhofer, A. (2008). Small ncRNA transcriptome analysis from Aspergillus fumigatus suggests a novel mechanism for regulation of protein synthesis. Nucleic acids research *36*, 2677-2689.

Jopling, C. (2012). Liver-specific microRNA-122: Biogenesis and function. Rna Biol *9*, 137-142.

Jopling, C.L., Yi, M., Lancaster, A.M., Lemon, S.M., and Sarnow, P. (2005). Modulation of hepatitis C virus RNA abundance by a liver-specific MicroRNA. Science *309*, 1577-1581.

Kabatereine, N.B., Kemijumbi, J., Ouma, J.H., Kariuki, H.C., Richter, J., Kadzo, H., Madsen, H., Butterworth, A.E., Ornbjerg, N., and Vennervald, B.J. (2004). Epidemiology and morbidity of Schistosoma mansoni infection in a fishing community along Lake Albert in Uganda. Trans R Soc Trop Med Hyg *98*, 711-718.

Kabatereine, N.B., Vennervald, B.J., Ouma, J.H., Kemijumbi, J., Butterworth, A.E., Dunne, D.W., and Fulford, A.J. (1999). Adult resistance to schistosomiasis mansoni: age-dependence of reinfection remains constant in communities with diverse exposure patterns. Parasitology *118 (Pt 1)*, 101-105.

Kamm, R.C., and Smith, A.G. (1972). Ribonuclease activity in human plasma. Clin Biochem *5*, 198-200.

Kanda, T., Ishibashi, O., Kawahigashi, Y., Mishima, T., Kosuge, T., Mizuguchi, Y., Shimizu, T., Arima, Y., Yokomuro, S., Yoshida, H.*, et al.* (2010). Identification of obstructive jaundice-related microRNAs in mouse liver. Hepato-gastroenterology *57*, 1013-1023.

Kapp, L.D., and Lorsch, J.R. (2004). The molecular mechanics of eukaryotic translation. Annual review of biochemistry *73*, 657-704.

Karanja, D.M., Boyer, A.E., Strand, M., Colley, D.G., Nahlen, B.L., Ouma, J.H., and Secor, W.E. (1998). Studies on schistosomiasis in western Kenya: II. Efficacy of praziquantel for treatment of schistosomiasis in persons coinfected with human immunodeficiency virus-1. Am J Trop Med Hyg *59*, 307-311.

Katz, N., Chaves, A., and Pellegrino, J. (1972). A simple device for quantitative stool thick-smear technique in Schistosomiasis mansoni. Rev Inst Med Trop Sao Paulo *14*, 397-400.

Kaviratne, M., Hesse, M., Leusink, M., Cheever, A.W., Davies, S.J., McKerrow, J.H., Wakefield, L.M., Letterio, J.J., and Wynn, T.A. (2004). IL-13

activates a mechanism of tissue fibrosis that is completely TGF-beta independent. Journal of immunology *173*, 4020-4029.

Kawaji, H., Nakamura, M., Takahashi, Y., Sandelin, A., Katayama, S., Fukuda, S., Daub, C.O., Kai, C., Kawai, J., Yasuda, J.*, et al.* (2008). Hidden layers of human small RNAs. BMC Genomics *9*, 157.

Ketting, R.F., Fischer, S.E., Bernstein, E., Sijen, T., Hannon, G.J., and Plasterk, R.H. (2001). Dicer functions in RNA interference and in synthesis of small RNA involved in developmental timing in C. elegans. Genes & development *15*, 2654-2659.

Khvorova, A., Reynolds, A., and Jayasena, S.D. (2003). Functional siRNAs and miRNAs exhibit strand bias. Cell *115*, 209-216.

Kisseleva, T., Cong, M., Paik, Y., Scholten, D., Jiang, C., Benner, C., Iwaisako, K., Moore-Morris, T., Scott, B., Tsukamoto, H.*, et al.* (2012). Myofibroblasts revert to an inactive phenotype during regression of liver fibrosis. Proc Natl Acad Sci U S A *109*, 9448-9453.

Kolodny, G.M. (1971). Evidence for transfer of macromolecular RNA between mammalian cells in culture. Exp Cell Res *65*, 313-324.

Kolodny, G.M. (1972). Cell to cell transfer of RNA into transformed cells. J Cell Physiol *79*, 147-150.

Kosaka, N., Iguchi, H., and Ochiya, T. (2010a). Circulating microRNA in body fluid: a new potential biomarker for cancer diagnosis and prognosis. Cancer Sci *101*, 2087-2092.

Kosaka, N., Iguchi, H., Yoshioka, Y., Takeshita, F., Matsuki, Y., and Ochiya, T. (2010b). Secretory mechanisms and intercellular transfer of microRNAs in living cells. J Biol Chem *285*, 17442-17452.

Kosaka, N., Iguchi, H., Yoshioka, Y., Takeshita, F., Matsuki, Y., and Ochiya, T. (2010c). Secretory mechanisms and intercellular transfer of microRNAs in living cells. The Journal of biological chemistry *285*, 17442-17452.

Kozomara, A., and Griffiths-Jones, S. (2011). miRBase: integrating microRNA annotation and deep-sequencing data. Nucleic acids research *39*, D152-157.

Krek, A., Grun, D., Poy, M.N., Wolf, R., Rosenberg, L., Epstein, E.J., MacMenamin, P., da Piedade, I., Gunsalus, K.C., Stoffel, M., and Rajewsky, N. (2005). Combinatorial microRNA target predictions. Nature genetics *37*, 495-500.

Kresina, T.F., He, Q., Degli Esposti, S., and Zern, M.A. (1994). Gene expression of transforming growth factor beta 1 and extracellular matrix proteins in murine Schistosoma mansoni infection. Gastroenterology *107*, 773-780.

Krizhanovsky, V., Yon, M., Dickins, R.A., Hearn, S., Simon, J., Miething, C., Yee, H., Zender, L., and Lowe, S.W. (2008). Senescence of activated stellate cells limits liver fibrosis. Cell *134*, 657-667.

Krutzfeldt, J., Rajewsky, N., Braich, R., Rajeev, K.G., Tuschl, T., Manoharan, M., and Stoffel, M. (2005). Silencing of microRNAs in vivo with 'antagomirs'. Nature *438*, 685-689.

Kumar, P.C.M.L. (2000). Kumar and Clark's Clinical Medicine (Elsevier Health).

Kuzuoglu-Ozturk, D., Huntzinger, E., Schmidt, S., and Izaurralde, E. (2012). The Caenorhabditis elegans GW182 protein AIN-1 interacts with PAB-1 and subunits of the PAN2-PAN3 and CCR4-NOT deadenylase complexes. Nucleic acids research *40*, 5651-5665.

Kwiecinski, M., Elfimova, N., Noetel, A., Tox, U., Steffen, H.M., Hacker, U., Nischt, R., Dienes, H.P., and Odenthal, M. (2012). Expression of platelet-derived growth factor-C and insulin-like growth factor I in hepatic stellate cells is inhibited by miR-29. Laboratory investigation; a journal of technical methods and pathology *92*, 978-987.

Kwiecinski, M., Noetel, A., Elfimova, N., Trebicka, J., Schievenbusch, S., Strack, I., Molnar, L., von Brandenstein, M., Tox, U., Nischt, R.*, et al.* (2011). Hepatocyte growth factor (HGF) inhibits collagen I and IV synthesis in hepatic stellate cells by miRNA-29 induction. PLoS One *6*, e24568.

Lakner, A.M., Steuerwald, N.M., Walling, T.L., Ghosh, S., Li, T., McKillop, I.H., Russo, M.W., Bonkovsky, H.L., and Schrum, L.W. (2012). Inhibitory effects of microRNA 19b in hepatic stellate cell-mediated fibrogenesis. Hepatology *56*, 300-310.

Landthaler, M., Yalcin, A., and Tuschl, T. (2004). The human DiGeorge syndrome critical region gene 8 and Its D. melanogaster homolog are required for miRNA biogenesis. Current biology : CB *14*, 2162-2167.

Lanford, R.E., Hildebrandt-Eriksen, E.S., Petri, A., Persson, R., Lindow, M., Munk, M.E., Kauppinen, S., and Orum, H. (2010). Therapeutic silencing of microRNA-122 in primates with chronic hepatitis C virus infection. Science *327*, 198-201.

Lawrie, C.H., Gal, S., Dunlop, H.M., Pushkaran, B., Liggins, A.P., Pulford, K., Banham, A.H., Pezzella, F., Boultwood, J., Wainscoat, J.S*., et al.* (2008). Detection of elevated levels of tumour-associated microRNAs in serum of patients with diffuse large B-cell lymphoma. Br J Haematol *141*, 672-675.

Lee, R.C., Feinbaum, R.L., and Ambros, V. (1993). The C. elegans heterochronic gene lin-4 encodes small RNAs with antisense complementarity to lin-14. Cell *75*, 843-854.

Lee, S.R., and Collins, K. (2005). Starvation-induced cleavage of the tRNA anticodon loop in Tetrahymena thermophila. The Journal of biological chemistry *280*, 42744-42749.

Lee, Y., Ahn, C., Han, J., Choi, H., Kim, J., Yim, J., Lee, J., Provost, P., Radmark, O., Kim, S., and Kim, V.N. (2003). The nuclear RNase III Drosha initiates microRNA processing. Nature *425*, 415-419.

Lee, Y., Hur, I., Park, S.Y., Kim, Y.K., Suh, M.R., and Kim, V.N. (2006). The role of PACT in the RNA silencing pathway. The EMBO journal *25*, 522-532.

Lee, Y., Jeon, K., Lee, J.T., Kim, S., and Kim, V.N. (2002). MicroRNA maturation: stepwise processing and subcellular localization. The EMBO journal *21*, 4663-4670.

Lee, Y., Kim, M., Han, J., Yeom, K.H., Lee, S., Baek, S.H., and Kim, V.N. (2004). MicroRNA genes are transcribed by RNA polymerase II. The EMBO journal *23*, 4051-4060.

Lee, Y.S., Pressman, S., Andress, A.P., Kim, K., White, J.L., Cassidy, J.J., Li, X., Lubell, K., Lim do, H., Cho, I.S*., et al.* (2009a). Silencing by small RNAs is linked to endosomal trafficking. Nat Cell Biol *11*, 1150-1156.

Lee, Y.S., Shibata, Y., Malhotra, A., and Dutta, A. (2009b). A novel class of small RNAs: tRNA-derived RNA fragments (tRFs). Genes & development *23*, 2639-2649.

Lewis, B.P., Burge, C.B., and Bartel, D.P. (2005). Conserved seed pairing, often flanked by adenosines, indicates that thousands of human genes are microRNA targets. Cell *120*, 15-20.

Lewis, B.P., Shih, I.H., Jones-Rhoades, M.W., Bartel, D.P., and Burge, C.B. (2003). Prediction of mammalian microRNA targets. Cell *115*, 787-798.

Li, F., Ma, N., Zhao, R., Wu, G., Zhang, Y., Qiao, Y., Han, D., Xu, Y., Xiang, Y., Yan, B*., et al.* (2014a). Overexpression of miR-483-5p/3p cooperate to inhibit mouse liver fibrosis by suppressing the TGF-beta stimulated HSCs in transgenic mice. Journal of cellular and molecular medicine.

Li, J., Ghazwani, M., Zhang, Y., Lu, J., Li, J., Fan, J., Gandhi, C.R., and Li, S. (2013). miR-122 regulates collagen production via targeting hepatic stellate cells and suppressing P4HA1 expression. J Hepatol *58*, 522-528.

Li, L.M., Hu, Z.B., Zhou, Z.X., Chen, X., Liu, F.Y., Zhang, J.F., Shen, H.B., Zhang, C.Y., and Zen, K. (2010). Serum microRNA profiles serve as novel biomarkers for HBV infection and diagnosis of HBV-positive hepatocarcinoma. Cancer Res *70*, 9798-9807.

Li, W.Q., Chen, C., Xu, M.D., Guo, J., Li, Y.M., Xia, Q.M., Liu, H.M., He, J., Yu, H.Y., and Zhu, L. (2011a). The rno-miR-34 family is upregulated and targets ACSL1 in dimethylnitrosamine-induced hepatic fibrosis in rats. Febs J *278*, 1522-1532.

Li, Y., Jiang, Z., Xu, L., Yao, H., Guo, J., and Ding, X. (2011b). Stability analysis of liver cancer-related microRNAs. Acta Biochim Biophys Sin (Shanghai) *43*, 69-78.

Li, Y., Luo, J., Zhou, H., Liao, J.Y., Ma, L.M., Chen, Y.Q., and Qu, L.H. (2008). Stress-induced tRNA-derived RNAs: a novel class of small RNAs in the primitive eukaryote Giardia lamblia. Nucleic acids research *36*, 6048-6055.

Li, Y., and Zhou, H. (2009). tRNAs as regulators in gene expression. Science in China. Series C, Life sciences / Chinese Academy of Sciences *52*, 245-252.

Li, Z.J., Ou-Yang, P.H., and Han, X.P. (2014b). Profibrotic effect of miR-33a with Akt activation in hepatic stellate cells. Cellular signalling *26*, 141-148.

Liang, Y., Ridzon, D., Wong, L., and Chen, C. (2007). Characterization of microRNA expression profiles in normal human tissues. BMC Genomics *8*, 166.

Liao, J.Y., Ma, L.M., Guo, Y.H., Zhang, Y.C., Zhou, H., Shao, P., Chen, Y.Q., and Qu, L.H. (2010). Deep sequencing of human nuclear and cytoplasmic small RNAs reveals an unexpectedly complex subcellular distribution of miRNAs and tRNA 3' trailers. PloS one *5*, e10563.

Lingel, A., Simon, B., Izaurralde, E., and Sattler, M. (2004). Nucleic acid 3'-end recognition by the Argonaute2 PAZ domain. Nat Struct Mol Biol *11*, 576-577.

Lino Cardenas, C.L., Henaoui, I.S., Courcot, E., Roderburg, C., Cauffiez, C., Aubert, S., Copin, M.C., Wallaert, B., Glowacki, F., Dewaeles, E.*, et al.* (2013). miR-199a-5p Is upregulated during fibrogenic response to tissue injury and mediates TGFbeta-induced lung fibroblast activation by targeting caveolin-1. PLoS genetics *9*, e1003291.

Liu, G., Friggeri, A., Yang, Y., Milosevic, J., Ding, Q., Thannickal, V.J., Kaminski, N., and Abraham, E. (2010). miR-21 mediates fibrogenic activation of pulmonary fibroblasts and lung fibrosis. The Journal of experimental medicine *207*, 1589-1597.

Liu, J., Carmell, M.A., Rivas, F.V., Marsden, C.G., Thomson, J.M., Song, J.J., Hammond, S.M., Joshua-Tor, L., and Hannon, G.J. (2004). Argonaute2 is the catalytic engine of mammalian RNAi. Science *305*, 1437-1441.

Liu, W.H., Yeh, S.H., and Chen, P.J. (2011). Role of microRNAs in hepatitis B virus replication and pathogenesis. Biochimica et biophysica acta *1809*, 678-685.

Livak, K.J., and Schmittgen, T.D. (2001). Analysis of relative gene expression data using real-time quantitative PCR and the 2(T)(-Delta Delta C) method. Methods *25*, 402-408.

Llave, C., Xie, Z., Kasschau, K.D., and Carrington, J.C. (2002). Cleavage of Scarecrow-like mRNA targets directed by a class of Arabidopsis miRNA. Science *297*, 2053-2056.

Lodh, N., Mwansa, J.C., Mutengo, M.M., and Shiff, C.J. (2013). Diagnosis of Schistosoma mansoni without the Stool: Detecting DNA from Filtered Urine Comparison of Three Diagnostic Tests to Detect Schistosoma mansoni Infection from Filtered Urine in Zambia. Am J Trop Med Hyg.

Loebel, D.A., Tsoi, B., Wong, N., and Tam, P.P. (2005). A conserved noncoding intronic transcript at the mouse Dnm3 locus. Genomics *85*, 782-789.

Lowe, T.M., and Eddy, S.R. (1997). tRNAscan-SE: a program for improved detection of transfer RNA genes in genomic sequence. Nucleic acids research *25*, 955-964.

Lund, E., and Dahlberg, J.E. (1998). Proofreading and aminoacylation of tRNAs before export from the nucleus. Science *282*, 2082-2085.

Lund, E., Guttinger, S., Calado, A., Dahlberg, J.E., and Kutay, U. (2004). Nuclear export of microRNA precursors. Science *303*, 95-98.

Madala, S.K., Pesce, J.T., Ramalingam, T.R., Wilson, M.S., Minnicozzi, S., Cheever, A.W., Thompson, R.W., Mentink-Kane, M.M., and Wynn, T.A. (2010). Matrix metalloproteinase 12-deficiency augments extracellular matrix degrading metalloproteinases and attenuates IL-13-dependent fibrosis. Journal of immunology *184*, 3955-3963.

Mah, S.M., Buske, C., Humphries, R.K., and Kuchenbauer, F. (2010). miRNA*: a passenger stranded in RNA-induced silencing complex? Critical reviews in eukaryotic gene expression *20*, 141-148.

Marco, A., Kozomara, A., Hui, J.H., Emery, A.M., Rollinson, D., Griffiths-Jones, S., and Ronshaugen, M. (2013). Sex-biased expression of microRNAs in Schistosoma mansoni. PLoS Negl Trop Dis *7*, e2402.

Marquez, R.T., Bandyopadhyay, S., Wendlandt, E.B., Keck, K., Hoffer, B.A., Icardi, M.S., Christensen, R.N., Schmidt, W.N., and McCaffrey, A.P. (2010). Correlation between microRNA expression levels and clinical parameters associated with chronic hepatitis C viral infection in humans. Laboratory investigation; a journal of technical methods and pathology *90*, 1727-1736.

Mathonnet, G., Fabian, M.R., Svitkin, Y.V., Parsyan, A., Huck, L., Murata, T., Biffo, S., Merrick, W.C., Darzynkiewicz, E., Pillai, R.S.*, et al.* (2007). MicroRNA inhibition of translation initiation in vitro by targeting the cap-binding complex eIF4F. Science *317*, 1764-1767.

Mattie, M.D., Benz, C.C., Bowers, J., Sensinger, K., Wong, L., Scott, G.K., Fedele, V., Ginzinger, D., Getts, R., and Haqq, C. (2006). Optimized high-throughput microRNA expression profiling provides novel biomarker assessment of clinical prostate and breast cancer biopsies. Molecular cancer *5*, 24.

McDaniel, K., Herrera, L., Zhou, T., Francis, H., Han, Y., Levine, P., Lin, E., Glaser, S., Alpini, G., and Meng, F. (2014). The functional role of microRNAs in alcoholic liver injury. Journal of cellular and molecular medicine *18*, 197-207.

McDonald, J.S., Milosevic, D., Reddi, H.V., Grebe, S.K., and Algeciras-Schimnich, A. (2011). Analysis of circulating microRNA: preanalytical and analytical challenges. Clinical chemistry *57*, 833-840.

Mduluza, T., Mutapi, F., Ruwona, T., Kaluka, D., Midzi, N., and Ndhlovu, P.D. (2009). Similar cellular responses after treatment with either praziquantel or oxamniquine in Schistosoma mansoni infection. Malawi medical journal : the journal of Medical Association of Malawi *21*, 176-182.

Meister, G., Landthaler, M., Patkaniowska, A., Dorsett, Y., Teng, G., and Tuschl, T. (2004). Human Argonaute2 mediates RNA cleavage targeted by miRNAs and siRNAs. Mol Cell *15*, 185-197.

Mendell, J.T., and Olson, E.N. (2012). MicroRNAs in stress signaling and human disease. Cell *148*, 1172-1187.

Meng, F., Glaser, S.S., Francis, H., Yang, F., Han, Y., Stokes, A., Staloch, D., McCarra, J., Liu, J., Venter, J.*, et al.* (2012). Epigenetic regulation of miR-34a expression in alcoholic liver injury. The American journal of pathology *181*, 804-817.

Mentink-Kane, M.M., Cheever, A.W., Thompson, R.W., Hari, D.M., Kabatereine, N.B., Vennervald, B.J., Ouma, J.H., Mwatha, J.K., Jones, F.M., Donaldson, D.D.*, et al.* (2004). IL-13 receptor alpha 2 down-modulates granulomatous inflammation and prolongs host survival in schistosomiasis. Proc Natl Acad Sci U S A *101*, 586-590.

Merrick, W.C. (2004). Cap-dependent and cap-independent translation in eukaryotic systems. Gene *332*, 1-11.

Mestdagh, P., Van Vlierberghe, P., De Weer, A., Muth, D., Westermann, F., Speleman, F., and Vandesompele, J. (2009). A novel and universal method for microRNA RT-qPCR data normalization. Genome biology *10*, R64.

Mitchell, P.S., Parkin, R.K., Kroh, E.M., Fritz, B.R., Wyman, S.K., Pogosova-Agadjanyan, E.L., Peterson, A., Noteboom, J., O'Briant, K.C., Allen, A.*, et al.* (2008). Circulating microRNAs as stable blood-based markers for cancer detection. Proc Natl Acad Sci U S A *105*, 10513-10518.

Moore, D.V., and Sandground, J.H. (1956). The relative egg producing capacity of Schistosoma mansoni and Schistosoma japonicum. Am J Trop Med Hyg *5*, 831-840.

Motorin, Y., and Helm, M. (2010). tRNA stabilization by modified nucleotides. Biochemistry *49*, 4934-4944.

Mott, K.E. (1983). A reusable polyamide filter for diagnosis of S. haematobium infection by urine filtration. Bull Soc Pathol Exot Filiales *76*, 101-104.

Murakami, Y., Toyoda, H., Tanaka, M., Kuroda, M., Harada, Y., Matsuda, F., Tajima, A., Kosaka, N., Ochiya, T., and Shimotohno, K. (2011). The progression of liver fibrosis is related with overexpression of the miR-199 and 200 families. PLoS One *6*, e16081.

Mutapi, F., Mduluza, T., and Ndhlovu, P.D. (2002). The effect of treatment on the age-antibody relationship in children infected with Schistosoma mansoni and Schistosoma haematobium. Memorias do Instituto Oswaldo Cruz *97 Suppl 1*, 173-180.

Nagase, H., Visse, R., and Murphy, G. (2006). Structure and function of matrix metalloproteinases and TIMPs. Cardiovascular research *69*, 562-573.

Naus, C.W., Booth, M., Jones, F.M., Kemijumbi, J., Vennervald, B.J., Kariuki, C.H., Ouma, J.H., Kabatereine, N.B., and Dunne, D.W. (2003). The relationship between age, sex, egg-count and specific antibody responses against Schistosoma mansoni antigens in a Ugandan fishing community. Tropical medicine & international health : TM & IH *8*, 561-568.

Ng, E.K., Tsui, N.B., Lam, N.Y., Chiu, R.W., Yu, S.C., Wong, S.C., Lo, E.S., Rainer, T.H., Johnson, P.J., and Lo, Y.M. (2002). Presence of filterable and nonfilterable mRNA in the plasma of cancer patients and healthy individuals. Clin Chem *48*, 1212-1217.

Nishihara, T., Zekri, L., Braun, J.E., and Izaurralde, E. (2013). miRISC recruits decapping factors to miRNA targets to enhance their degradation. Nucleic acids research *41*, 8692-8705.

Niu, M.C., Cordova, C.C., Niu, L.C., and Radbill, C.L. (1962). Rna-Induced Biosynthesis of Specific Enzymes. Proc Natl Acad Sci U S A *48*, 1964-1969.

Nowacka, M., Strozycki, P.M., Jackowiak, P., Hojka-Osinska, A., Szymanski, M., and Figlerowicz, M. (2013). Identification of stable, high copy number, medium-sized RNA degradation intermediates that accumulate in plants under non-stress conditions. Plant molecular biology *83*, 191-204.

Obernosterer, G., Tafer, H., and Martinez, J. (2008). Target site effects in the RNA interference and microRNA pathways. Biochem Soc Trans *36*, 1216-1219.

Ogawa, T., Enomoto, M., Fujii, H., Sekiya, Y., Yoshizato, K., Ikeda, K., and Kawada, N. (2012). MicroRNA-221/222 upregulation indicates the activation of stellate cells and the progression of liver fibrosis. Gut *61*, 1600-1609.

Ogawa, T., Iizuka, M., Sekiya, Y., Yoshizato, K., Ikeda, K., and Kawada, N. (2010). Suppression of type I collagen production by microRNA-29b in cultured human stellate cells. Biochemical and biophysical research communications *391*, 316-321.

Okamura, K., Hagen, J.W., Duan, H., Tyler, D.M., and Lai, E.C. (2007). The mirtron pathway generates microRNA-class regulatory RNAs in Drosophila. Cell *130*, 89-100.

Orom, U.A., Nielsen, F.C., and Lund, A.H. (2008). MicroRNA-10a binds the 5'UTR of ribosomal protein mRNAs and enhances their translation. Mol Cell *30*, 460-471.

Pall, G.S., and Hamilton, A.J. (2008). Improved northern blot method for enhanced detection of small RNA. Nature protocols *3*, 1077-1084.

Pasquinelli, A.E., Reinhart, B.J., Slack, F., Martindale, M.Q., Kuroda, M.I., Maller, B., Hayward, D.C., Ball, E.E., Degnan, B., Muller, P.*, et al.* (2000). Conservation of the sequence and temporal expression of let-7 heterochronic regulatory RNA. Nature *408*, 86-89.

Pearce, E.J., and MacDonald, A.S. (2002). The immunobiology of schistosomiasis. Nat Rev Immunol *2*, 499-511.

Pellicoro, A., Ramachandran, P., Iredale, J.P., and Fallowfield, J.A. (2014). Liver fibrosis and repair: immune regulation of wound healing in a solid organ. Nat Rev Immunol *14*, 181-194.

Perron, M.P., and Provost, P. (2008). Protein interactions and complexes in human microRNA biogenesis and function. Frontiers in bioscience : a journal and virtual library *13*, 2537-2547.

Petersen, C.P., Bordeleau, M.E., Pelletier, J., and Sharp, P.A. (2006). Short RNAs repress translation after initiation in mammalian cells. Mol Cell *21*, 533-542.

Pfaffl, M.W. (2001). A new mathematical model for relative quantification in real-time RT-PCR. Nucleic acids research *29*, e45.

Pfeffer, S., and Baumert, T.F. (2010). Impact of microRNAs for pathogenesis and treatment of hepatitis C virus infection. Gastroenterologie clinique et biologique *34*, 431-435.

Phizicky, E.M., and Hopper, A.K. (2010). tRNA biology charges to the front. Genes & development *24*, 1832-1860.

Pigati, L., Yaddanapudi, S.C., Iyengar, R., Kim, D.J., Hearn, S.A., Danforth, D., Hastings, M.L., and Duelli, D.M. (2010). Selective release of microRNA species from normal and malignant mammary epithelial cells. PloS one *5*, e13515.

Pogribny, I.P., Starlard-Davenport, A., Tryndyak, V.P., Han, T., Ross, S.A., Rusyn, I., and Beland, F.A. (2010). Difference in expression of hepatic microRNAs miR-29c, miR-34a, miR-155, and miR-200b is associated with strain-specific susceptibility to dietary nonalcoholic steatohepatitis in mice. Laboratory investigation; a journal of technical methods and pathology *90*, 1437-1446.

Pontes, L.A., Oliveira, M.C., Katz, N., Dias-Neto, E., and Rabello, A. (2003a). Comparison of a polymerase chain reaction and the Kato-Katz technique for diagnosing infection with Schistosoma mansoni. Am J Trop Med Hyg *68*, 652-656.

Pontes, L.A., Oliveira, M.C., Katz, N., Dias-Neto, E., and Rabello, A. (2003b). Comparison of a polymerase chain reaction and the Kato-Katz technique for diagnosing infection with Schistosoma mansoni. Am J Trop Med Hyg *68*, 652-656.

Popiel, I., Cioli, D., and Erasmus, D.A. (1984). The morphology and reproductive status of female Schistosoma mansoni following separation from male worms. International journal for parasitology *14*, 183-190.

Pottier, N., Cauffiez, C., Perrais, M., Barbry, P., and Mari, B. (2014). FibromiRs: translating molecular discoveries into new anti-fibrotic drugs. Trends in pharmacological sciences *35*, 119-126.

Qi, Y., Cui, L., Ge, Y., Shi, Z., Zhao, K., Guo, X., Yang, D., Yu, H., Shan, Y., Zhou, M.*, et al.* (2012). Altered serum microRNAs as biomarkers for the early diagnosis of pulmonary tuberculosis infection. BMC Infect Dis *12*, 384.

Ramachandran, S., Ilias Basha, H., Sarma, N.J., Lin, Y., Crippin, J.S., Chapman, W.C., and Mohanakumar, T. (2013). Hepatitis C virus induced miR200c down modulates FAP-1, a negative regulator of Src signaling and promotes hepatic fibrosis. PloS one *8*, e70744.

Rehwinkel, J., Behm-Ansmant, I., Gatfield, D., and Izaurralde, E. (2005). A crucial role for GW182 and the DCP1:DCP2 decapping complex in miRNA-mediated gene silencing. Rna *11*, 1640-1647.

Reinhart, B.J., Slack, F.J., Basson, M., Pasquinelli, A.E., Bettinger, J.C., Rougvie, A.E., Horvitz, H.R., and Ruvkun, G. (2000). The 21-nucleotide let-7 RNA regulates developmental timing in Caenorhabditis elegans. Nature *403*, 901-906.

Robertson, H.D., Altman, S., and Smith, J.D. (1972). Purification and properties of a specific Escherichia coli ribonuclease which cleaves a tyrosine transfer ribonucleic acid presursor. The Journal of biological chemistry *247*, 5243-5251.

Roderburg, C., Urban, G.W., Bettermann, K., Vucur, M., Zimmermann, H., Schmidt, S., Janssen, J., Koppe, C., Knolle, P., Castoldi, M.*, et al.* (2011). Micro-RNA profiling reveals a role for miR-29 in human and murine liver fibrosis. Hepatology *53*, 209-218.

Rollinson, D., Knopp, S., Levitz, S., Stothard, J.R., Tchuem Tchuente, L.A., Garba, A., Mohammed, K.A., Schur, N., Person, B., Colley, D.G., and Utzinger, J. (2013). Time to set the agenda for schistosomiasis elimination. Acta Trop *128*, 423-440.

Rollinson, D.S., V. R. (1987). The genus Schistosoma: A Taxonomic Appraisal.

Ross, A.G., Bartley, P.B., Sleigh, A.C., Olds, G.R., Li, Y., Williams, G.M., and McManus, D.P. (2002). Schistosomiasis. The New England journal of medicine *346*, 1212-1220.

Ruby, J.G., Jan, C.H., and Bartel, D.P. (2007). Intronic microRNA precursors that bypass Drosha processing. Nature *448*, 83-86.

Ruckerl, D., Jenkins, S.J., Laqtom, N.N., Gallagher, I.J., Sutherland, T.E., Duncan, S., Buck, A.H., and Allen, J.E. (2012). Induction of IL-4Ralpha-dependent microRNAs identifies PI3K/Akt signaling as essential for IL-4-driven murine macrophage proliferation in vivo. Blood *120*, 2307-2316.

Rybak, S.M., and Vallee, B.L. (1988). Base cleavage specificity of angiogenin with Saccharomyces cerevisiae and Escherichia coli 5S RNAs. Biochemistry *27*, 2288-2294.

Saikia, M., Krokowski, D., Guan, B.J., Ivanov, P., Parisien, M., Hu, G.F., Anderson, P., Pan, T., and Hatzoglou, M. (2012). Genome-wide identification and quantitative analysis of cleaved tRNA fragments induced by cellular stress. The Journal of biological chemistry *287*, 42708-42725.

Sato, M., Suzuki, S., and Senoo, H. (2003). Hepatic stellate cells: unique characteristics in cell biology and phenotype. Cell structure and function *28*, 105-112.

Saxena, S.K., Rybak, S.M., Davey, R.T., Jr., Youle, R.J., and Ackerman, E.J. (1992). Angiogenin is a cytotoxic, tRNA-specific ribonuclease in the RNase A superfamily. The Journal of biological chemistry *267*, 21982-21986.

Schaedel, O.N., Gerisch, B., Antebi, A., and Sternberg, P.W. (2012). Hormonal signal amplification mediates environmental conditions during development and controls an irreversible commitment to adulthood. PLoS Biol *10*, e1001306.

Schaefer, M., Pollex, T., Hanna, K., Tuorto, F., Meusburger, M., Helm, M., and Lyko, F. (2010). RNA methylation by Dnmt2 protects transfer RNAs against stress-induced cleavage. Genes & development *24*, 1590-1595.

Schiffer, S., Rosch, S., and Marchfelder, A. (2002). Assigning a function to a conserved group of proteins: the tRNA 3'-processing enzymes. The EMBO journal *21*, 2769-2777.

Schirle, N.T., and MacRae, I.J. (2012). The crystal structure of human Argonaute2. Science *336*, 1037-1040.

Scholer, N., Langer, C., Dohner, H., Buske, C., and Kuchenbauer, F. (2010). Serum microRNAs as a novel class of biomarkers: a comprehensive review of the literature. Exp Hematol *38*, 1126-1130.

Schramm, G., Gronow, A., Knobloch, J., Wippersteg, V., Grevelding, C.G., Galle, J., Fuller, H., Stanley, R.G., Chiodini, P.L., Haas, H., and Doenhoff, M.J. (2006). IPSE/alpha-1: a major immunogenic component secreted from Schistosoma mansoni eggs. Mol Biochem Parasitol *147*, 9-19.

Schur, N., Gosoniu, L., Raso, G., Utzinger, J., and Vounatsou, P. (2011a). Modelling the geographical distribution of co-infection risk from single-disease surveys. Statistics in medicine *30*, 1761-1776.

Schur, N., Hurlimann, E., Garba, A., Traore, M.S., Ndir, O., Ratard, R.C., Tchuem Tchuente, L.A., Kristensen, T.K., Utzinger, J., and Vounatsou, P. (2011b). Geostatistical model-based estimates of Schistosomiasis prevalence among individuals aged </= 20 years in West Africa. PLoS Negl Trop Dis *5*, e1194.

Schwarz, D.S., Hutvagner, G., Du, T., Xu, Z., Aronin, N., and Zamore, P.D. (2003). Asymmetry in the assembly of the RNAi enzyme complex. Cell *115*, 199-208.

Sekiya, Y., Ogawa, T., Iizuka, M., Yoshizato, K., Ikeda, K., and Kawada, N. (2011a). Down-regulation of cyclin E1 expression by microRNA-195 accounts for interferon-beta-induced inhibition of hepatic stellate cell proliferation. Journal of cellular physiology *226*, 2535-2542.

Sekiya, Y., Ogawa, T., Yoshizato, K., Ikeda, K., and Kawada, N. (2011b). Suppression of hepatic stellate cell activation by microRNA-29b. Biochemical and biophysical research communications *412*, 74-79.

Semenov, D.V., Baryakin, D.N., Brenner, E.V., Kurilshikov, A.M., Vasiliev, G.V., Bryzgalov, L.A., Chikova, E.D., Filippova, J.A., Kuligina, E.V., and Richter, V.A. (2012). Unbiased approach to profile the variety of small non-coding RNA of human blood plasma with massively parallel sequencing technology. Expert opinion on biological therapy *12 Suppl 1*, S43-51.

Semenov, D.V., Kuligina, E.V., Shevyrina, O.N., Richter, V.A., and Vlassov, V.V. (2004). Extracellular ribonucleic acids of human milk. Ann N Y Acad Sci *1022*, 190-194.

Shane, H.L., Verani, J.R., Abudho, B., Montgomery, S.P., Blackstock, A.J., Mwinzi, P.N., Butler, S.E., Karanja, D.M., and Secor, W.E. (2011). Evaluation of urine CCA assays for detection of Schistosoma mansoni infection in Western Kenya. PLoS Negl Trop Dis *5*, e951.

Shapiro, R., Strydom, D.J., Olson, K.A., and Vallee, B.L. (1987). Isolation of angiogenin from normal human plasma. Biochemistry *26*, 5141-5146.

Shell, S., Park, S.M., Radjabi, A.R., Schickel, R., Kistner, E.O., Jewell, D.A., Feig, C., Lengyel, E., and Peter, M.E. (2007). Let-7 expression defines two differentiation stages of cancer. Proc Natl Acad Sci U S A *104*, 11400-11405.

Shimoyama, S., Gansauge, F., Gansauge, S., Negri, G., Oohara, T., and Beger, H.G. (1996). Increased angiogenin expression in pancreatic cancer is related to cancer aggressiveness. Cancer Res *56*, 2703-2706.

Shrivastava, S., Petrone, J., Steele, R., Lauer, G.M., Bisceglie, A.M., and Ray, R.B. (2013). Upregulation of circulating miR-20a is correlated with hepatitis C virus mediated liver disease progression. Hepatology.

Singh, K.P., Gerard, H.C., Hudson, A.P., and Boros, D.L. (2004a). Dynamics of collagen, MMP and TIMP gene expression during the granulomatous, fibrotic process induced by Schistosoma mansoni eggs. Annals of tropical medicine and parasitology *98*, 581-593.

Singh, K.P., Gerard, H.C., Hudson, A.P., and Boros, D.L. (2004b). Expression of matrix metalloproteinases and their inhibitors during the resorption of schistosome egg-induced fibrosis in praziquantel-treated mice. Immunology *111*, 343-352.

Skelly, P. (2008). Fighting killer worms. Scientific American *298*, 94-99.

Sobala, A., and Hutvagner, G. (2013). Small RNAs derived from the 5' end of tRNA can inhibit protein translation in human cells. Rna Biol *10*, 553-563.

Song, G., and Wang, L. (2008). MiR-433 and miR-127 arise from independent overlapping primary transcripts encoded by the miR-433-127 locus. PloS one *3*, e3574.

Song, J.J., Smith, S.K., Hannon, G.J., and Joshua-Tor, L. (2004). Crystal structure of Argonaute and its implications for RISC slicer activity. Science *305*, 1434-1437.

Sousa-Figueiredo, J.C., Betson, M., Kabatereine, N.B., and Stothard, J.R. (2013). The urine circulating cathodic antigen (CCA) dipstick: a valid substitute for microscopy for mapping and point-of-care diagnosis of intestinal schistosomiasis. PLoS Negl Trop Dis *7*, e2008.

Starkey Lewis, P.J., Dear, J., Platt, V., Simpson, K.J., Craig, D.G., Antoine, D.J., French, N.S., Dhaun, N., Webb, D.J., Costello, E.M.*, et al.* (2011). Circulating microRNAs as potential markers of human drug-induced liver injury. Hepatology *54*, 1767-1776.

Starkey Lewis, P.J., Merz, M., Couttet, P., Grenet, O., Dear, J., Antoine, D.J., Goldring, C., Park, B.K., and Moggs, J.G. (2012). Serum microRNA biomarkers for drug-induced liver injury. Clin Pharmacol Ther *92*, 291-293.

Steinmann, P., Keiser, J., Bos, R., Tanner, M., and Utzinger, J. (2006). Schistosomiasis and water resources development: systematic review, meta-analysis, and estimates of people at risk. The Lancet infectious diseases *6*, 411-425.

Stenvang, J., and Kauppinen, S. (2008). MicroRNAs as targets for antisense-based therapeutics. Expert opinion on biological therapy *8*, 59-81.

Stoorvogel, W., Kleijmeer, M.J., Geuze, H.J., and Raposo, G. (2002). The biogenesis and functions of exosomes. Traffic *3*, 321-330.

Stothard, J.R., Sousa-Figueiredo, J.C., Betson, M., Adriko, M., Arinaitwe, M., Rowell, C., Besiyge, F., and Kabatereine, N.B. (2011). Schistosoma mansoni Infections in young children: when are schistosome antigens in urine, eggs in stool and antibodies to eggs first detectable? PLoS Negl Trop Dis *5*, e938.

Stroun, M., Anker, P., Beljanski, M., Henri, J., Lederrey, C., Ojha, M., and Maurice, P.A. (1978). Presence of RNA in the nucleoprotein complex spontaneously released by human lymphocytes and frog auricles in culture. Cancer Res *38*, 3546-3554.

Sullivan, C.S., and Ganem, D. (2005). MicroRNAs and viral infection. Mol Cell *20*, 3-7.

Szabo, G., and Bala, S. (2013). MicroRNAs in liver disease. Nature reviews. Gastroenterology & hepatology *10*, 542-552.

Tafer, H., Ameres, S.L., Obernosterer, G., Gebeshuber, C.A., Schroeder, R., Martinez, J., and Hofacker, I.L. (2008). The impact of target site accessibility on the design of effective siRNAs. Nature biotechnology *26*, 578-583.

Takahashi, S., Dunn, M.A., and Seifter, S. (1980). Liver collagenase in murine schistosomiasis. Gastroenterology *78*, 1425-1431.

Thery, C. (2011). Exosomes: secreted vesicles and intercellular communications. F1000 Biol Rep *3*, 15.

Thompson, D.M., Lu, C., Green, P.J., and Parker, R. (2008). tRNA cleavage is a conserved response to oxidative stress in eukaryotes. Rna *14*, 2095-2103.

Thompson, D.M., and Parker, R. (2009). The RNase Rny1p cleaves tRNAs and promotes cell death during oxidative stress in Saccharomyces cerevisiae. The Journal of cell biology *185*, 43-50.

Trebicka, J., Anadol, E., Elfimova, N., Strack, I., Roggendorf, M., Viazov, S., Wedemeyer, I., Drebber, U., Rockstroh, J., Sauerbruch, T.*, et al.* (2013). Hepatic and serum levels of miR-122 after chronic HCV-induced fibrosis. J Hepatol *58*, 234-239.

Troeger, J.S., Mederacke, I., Gwak, G.Y., Dapito, D.H., Mu, X., Hsu, C.C., Pradere, J.P., Friedman, R.A., and Schwabe, R.F. (2012). Deactivation of hepatic stellate cells during liver fibrosis resolution in mice. Gastroenterology *143*, 1073-1083 e1022.

Tsui, N.B., Ng, E.K., and Lo, Y.M. (2002). Stability of endogenous and added RNA in blood specimens, serum, and plasma. Clinical chemistry *48*, 1647-1653.

Tu, X., Zhang, H., Zhang, J., Zhao, S., Zheng, X., Zhang, Z., Zhu, J., Chen, J., Dong, L., Zang, Y., and Zhang, J. (2014). MicroRNA-101 suppresses liver fibrosis by targeting TGFbeta signaling pathway. The Journal of pathology.

Tuck, A.C., and Tollervey, D. (2011). RNA in pieces. Trends Genet *27*, 422-432.

Turchinovich, A., Weiz, L., Langheinz, A., and Burwinkel, B. (2011). Characterization of extracellular circulating microRNA. Nucleic acids research *39*, 7223-7233.

Vaillant, B., Chiaramonte, M.G., Cheever, A.W., Soloway, P.D., and Wynn, T.A. (2001). Regulation of hepatic fibrosis and extracellular matrix genes by the th response: new insight into the role of tissue inhibitors of matrix metalloproteinases. Journal of immunology *167*, 7017-7026.

Valadi, H., Ekstrom, K., Bossios, A., Sjostrand, M., Lee, J.J., and Lotvall, J.O. (2007). Exosome-mediated transfer of mRNAs and microRNAs is a novel mechanism of genetic exchange between cells. Nat Cell Biol *9*, 654-659.

van Dam, G.J., Bogitsh, B.J., van Zeyl, R.J., Rotmans, J.P., and Deelder, A.M. (1996). Schistosoma mansoni: in vitro and in vivo excretion of CAA and CCA by developing schistosomula and adult worms. J Parasitol *82*, 557-564.

van Dam, G.J., de Dood, C.J., Lewis, M., Deelder, A.M., van Lieshout, L., Tanke, H.J., van Rooyen, L.H., and Corstjens, P.L. (2013). A robust dry reagent lateral flow assay for diagnosis of active schistosomiasis by detection of Schistosoma circulating anodic antigen. Exp Parasitol *135*, 274-282.

van der Werf, M.J., de Vlas, S.J., Brooker, S., Looman, C.W., Nagelkerke, N.J., Habbema, J.D., and Engels, D. (2003). Quantification of clinical morbidity associated with schistosome infection in sub-Saharan Africa. Acta Trop *86*, 125-139.

van Lieshout, L., De Jonge, N., Mansour, M.M., Bassily, S., Krijger, F.W., and Deelder, A.M. (1993). Circulating cathodic antigen levels in serum and urine of schistosomiasis patients before and after chemotherapy with praziquantel. Trans R Soc Trop Med Hyg *87*, 311-312.

van Rooij, E., Purcell, A.L., and Levin, A.A. (2012). Developing microRNA therapeutics. Circulation research *110*, 496-507.

Vasudevan, S., Tong, Y., and Steitz, J.A. (2007). Switching from repression to activation: microRNAs can up-regulate translation. Science *318*, 1931-1934.

Venter, J.C., Adams, M.D., Myers, E.W., Li, P.W., Mural, R.J., Sutton, G.G., Smith, H.O., Yandell, M., Evans, C.A., Holt, R.A.*, et al.* (2001). The sequence of the human genome. Science *291*, 1304-1351.

Venugopal, S.K., Jiang, J., Kim, T.H., Li, Y., Wang, S.S., Torok, N.J., Wu, J., and Zern, M.A. (2010). Liver fibrosis causes downregulation of miRNA-150 and miRNA-194 in hepatic stellate cells, and their overexpression causes decreased stellate cell activation. American journal of physiology. Gastrointestinal and liver physiology *298*, G101-106.

Vettori, S., Gay, S., and Distler, O. (2012). Role of MicroRNAs in Fibrosis. The open rheumatology journal *6*, 130-139.

Vickers, K.C., Palmisano, B.T., Shoucri, B.M., Shamburek, R.D., and Remaley, A.T. (2011). MicroRNAs are transported in plasma and delivered to recipient cells by high-density lipoproteins. Nat Cell Biol *13*, 423-433.

Villarroya-Beltri, C., Gutierrez-Vazquez, C., Sanchez-Cabo, F., Perez-Hernandez, D., Vazquez, J., Martin-Cofreces, N., Martinez-Herrera, D.J., Pascual-Montano, A., Mittelbrunn, M., and Sanchez-Madrid, F. (2013). Sumoylated hnRNPA2B1 controls the sorting of miRNAs into exosomes through binding to specific motifs. Nature communications *4*, 2980.

Wahid, F., Shehzad, A., Khan, T., and Kim, Y.Y. (2010). MicroRNAs: synthesis, mechanism, function, and recent clinical trials. Biochimica et biophysica acta *1803*, 1231-1243.

Walker, S.C., and Engelke, D.R. (2006). Ribonuclease P: the evolution of an ancient RNA enzyme. Critical reviews in biochemistry and molecular biology *41*, 77-102.

Wang, B., Li, W., Guo, K., Xiao, Y., Wang, Y., and Fan, J. (2012a). miR-181b promotes hepatic stellate cells proliferation by targeting p27 and is elevated in the serum of cirrhosis patients. Biochemical and biophysical research communications *421*, 4-8.

Wang, K., Li, H., Yuan, Y., Etheridge, A., Zhou, Y., Huang, D., Wilmes, P., and Galas, D. (2012b). The complex exogenous RNA spectra in human plasma: an interface with human gut biota? PloS one *7*, e51009.

Wang, K., Zhang, S., Marzolf, B., Troisch, P., Brightman, A., Hu, Z., Hood, L.E., and Galas, D.J. (2009). Circulating microRNAs, potential biomarkers for drug-induced liver injury. Proc Natl Acad Sci U S A *106*, 4402-4407.

Wang, K., Zhang, S., Weber, J., Baxter, D., and Galas, D.J. (2011). Export of microRNAs and microRNA-protective protein by mammalian cells. Nucleic acids research *38*, 7248-7259.

Wang, M., Abais, J.M., Meng, N., Zhang, Y., Ritter, J.K., Li, P.L., and Tang, W.X. (2014). Upregulation of cannabinoid receptor-1 and fibrotic activation of mouse hepatic stellate cells during Schistosoma J. infection: Role of NADPH oxidase. Free radical biology & medicine *71C*, 109-120.

Wang, Q., Lee, I., Ren, J., Ajay, S.S., Lee, Y.S., and Bao, X. (2013). Identification and functional characterization of tRNA-derived RNA fragments (tRFs) in respiratory syncytial virus infection. Molecular therapy : the journal of the American Society of Gene Therapy *21*, 368-379.

Wang, V., and Wu, W. (2009). MicroRNA-based therapeutics for cancer. BioDrugs : clinical immunotherapeutics, biopharmaceuticals and gene therapy *23*, 15-23.

Wang, Z., Xue, X., Sun, J., Luo, R., Xu, X., Jiang, Y., Zhang, Q., and Pan, W. (2010). An "in-depth" description of the small non-coding RNA population of Schistosoma japonicum schistosomulum. PLoS Negl Trop Dis *4*, e596.

Weber, J.A., Baxter, D.H., Zhang, S., Huang, D.Y., Huang, K.H., Lee, M.J., Galas, D.J., and Wang, K. (2010). The microRNA spectrum in 12 body fluids. Clin Chem *56*, 1733-1741.

Wee, L.M., Flores-Jasso, C.F., Salomon, W.E., and Zamore, P.D. (2012). Argonaute divides its RNA guide into domains with distinct functions and RNA-binding properties. Cell *151*, 1055-1067.

Wei, J., Feng, L., Li, Z., Xu, G., and Fan, X. (2013). MicroRNA-21 activates hepatic stellate cells via PTEN/Akt signaling. Biomedicine & pharmacotherapy = Biomedecine & pharmacotherapie *67*, 387-392.

Weiland, M., Gao, X.H., Zhou, L., and Mi, Q.S. (2012a). Small RNAs have a large impact Circulating microRNAs as biomarkers for human diseases. Rna Biol *9*, 850-859.

Weiland, M., Gao, X.H., Zhou, L., and Mi, Q.S. (2012b). Small RNAs have a large impact: circulating microRNAs as biomarkers for human diseases. RNA Biol *9*, 850-859.

Wells, S.E., Hillner, P.E., Vale, R.D., and Sachs, A.B. (1998). Circularization of mRNA by eukaryotic translation initiation factors. Mol Cell *2*, 135-140.

White, R.J. (2011). Transcription by RNA polymerase III: more complex than we thought. Nature reviews. Genetics *12*, 459-463.

WHO (2002). Prevention and Control of Schistosomiasia and Soil Transmitted helminthiasia- Report of a WHO Expert Committee. (Geneva).

WHO (2008). Elimination of schistosomiasis from low‐transmission areas

Report of a WHO Informal Consultation.

WHO (2013a). Schistosomiasis-Fact scheet 115. (WHO).

WHO (2013b). Schistosomiasis: progress report 2001–2011 and strategic plan 2012–2020.

Wichmann, D., Panning, M., Quack, T., Kramme, S., Burchard, G.D., Grevelding, C., and Drosten, C. (2009). Diagnosing schistosomiasis by detection of cell-free parasite DNA in human plasma. PLoS Negl Trop Dis *3*, e422.

Wiggins, J.F., Ruffino, L., Kelnar, K., Omotola, M., Patrawala, L., Brown, D., and Bader, A.G. (2010). Development of a lung cancer therapeutic based on the tumor suppressor microRNA-34. Cancer Res *70*, 5923-5930.

Wightman, B., Ha, I., and Ruvkun, G. (1993). Posttranscriptional regulation of the heterochronic gene lin-14 by lin-4 mediates temporal pattern formation in C. elegans. Cell *75*, 855-862.

Wu, L., Fan, J., and Belasco, J.G. (2006). MicroRNAs direct rapid deadenylation of mRNA. Proc Natl Acad Sci U S A *103*, 4034-4039.

Wynn, T.A., Thompson, R.W., Cheever, A.W., and Mentink-Kane, M.M. (2004). Immunopathogenesis of schistosomiasis. Immunol Rev *201*, 156-167.

Xiao, C., and Rajewsky, K. (2009). MicroRNA control in the immune system: basic principles. Cell *136*, 26-36.

Xiong, Y., and Steitz, T.A. (2006). A story with a good ending: tRNA 3'-end maturation by CCA-adding enzymes. Current opinion in structural biology *16*, 12-17.

Xue, X., Sun, J., Zhang, Q., Wang, Z., Huang, Y., and Pan, W. (2008). Identification and characterization of novel microRNAs from Schistosoma japonicum. PloS one *3*, e4034.

Yamasaki, S., Ivanov, P., Hu, G.F., and Anderson, P. (2009). Angiogenin cleaves tRNA and promotes stress-induced translational repression. The Journal of cell biology *185*, 35-42.

Yang, J.S., Maurin, T., Robine, N., Rasmussen, K.D., Jeffrey, K.L., Chandwani, R., Papapetrou, E.P., Sadelain, M., O'Carroll, D., and Lai, E.C. (2010). Conserved vertebrate mir-451 provides a platform for Dicer-independent, Ago2-mediated microRNA biogenesis. Proc Natl Acad Sci U S A *107*, 15163-15168.

Yekta, S., Shih, I.H., and Bartel, D.P. (2004). MicroRNA-directed cleavage of HOXB8 mRNA. Science *304*, 594-596.

Yeung, M.L., Bennasser, Y., Watashi, K., Le, S.Y., Houzet, L., and Jeang, K.T. (2009). Pyrosequencing of small non-coding RNAs in HIV-1 infected cells: evidence for the processing of a viral-cellular double-stranded RNA hybrid. Nucleic acids research *37*, 6575-6586.

Yi, R., Qin, Y., Macara, I.G., and Cullen, B.R. (2003). Exportin-5 mediates the nuclear export of pre-microRNAs and short hairpin RNAs. Genes & development *17*, 3011-3016.

Youssef, Y.M., White, N.M., Grigull, J., Krizova, A., Samy, C., Mejia-Guerrero, S., Evans, A., and Yousef, G.M. (2011). Accurate molecular classification of kidney cancer subtypes using microRNA signature. European urology *59*, 721-730.

Yu, F., Lin, Z., Zheng, J., Gao, S., Lu, Z., and Dong, P. (2014). Suppression of collagen synthesis by Dicer gene silencing in hepatic stellate cells. Molecular medicine reports *9*, 707-714.

Zekri, L., Huntzinger, E., Heimstadt, S., and Izaurralde, E. (2009). The silencing domain of GW182 interacts with PABPC1 to promote translational repression and degradation of microRNA targets and is required for target release. Molecular and cellular biology *29*, 6220-6231.

Zernecke, A., Bidzhekov, K., Noels, H., Shagdarsuren, E., Gan, L., Denecke, B., Hristov, M., Koppel, T., Jahantigh, M.N., Lutgens, E.*, et al.* (2009). Delivery of microRNA-126 by apoptotic bodies induces CXCL12-dependent vascular protection. Sci Signal *2*, ra81.

Zhang, H., Kolb, F.A., Jaskiewicz, L., Westhof, E., and Filipowicz, W. (2004). Single processing center models for human Dicer and bacterial RNase III. Cell *118*, 57-68.

Zhang, L., Hou, D., Chen, X., Li, D., Zhu, L., Zhang, Y., Li, J., Bian, Z., Liang, X., Cai, X.*, et al.* (2012). Exogenous plant MIR168a specifically targets mammalian LDLRAP1: evidence of cross-kingdom regulation by microRNA. Cell Res *22*, 107-126.

Zhang, Y., Jia, Y., Zheng, R., Guo, Y., Wang, Y., Guo, H., Fei, M., and Sun, S. (2010a). Plasma microRNA-122 as a biomarker for viral-, alcohol-, and chemical-related hepatic diseases. Clinical chemistry *56*, 1830-1838.

Zhang, Y., Liu, D., Chen, X., Li, J., Li, L., Bian, Z., Sun, F., Lu, J., Yin, Y., Cai, X.*, et al.* (2010b). Secreted monocytic miR-150 enhances targeted endothelial cell migration. Mol Cell *39*, 133-144.

Zhang, Z., Sun, H., Dai, H., Walsh, R.M., Imakura, M., Schelter, J., Burchard, J., Dai, X., Chang, A.N., Diaz, R.L.*, et al.* (2009). MicroRNA miR-210 modulates cellular response to hypoxia through the MYC antagonist MNT. Cell cycle *8*, 2756-2768.

Zhang, Z., Zha, Y., Hu, W., Huang, Z., Gao, Z., Zang, Y., Chen, J., Dong, L., and Zhang, J. (2013). The autoregulatory feedback loop of microRNA-21/programmed cell death protein 4/activation protein-1 (MiR-21/PDCD4/AP-1) as a driving force for hepatic fibrosis development. The Journal of biological chemistry *288*, 37082-37093.

Zheng, J., Lin, Z., Dong, P., Lu, Z., Gao, S., Chen, X., Wu, C., and Yu, F. (2013). Activation of hepatic stellate cells is suppressed by microRNA-150. International journal of molecular medicine *32*, 17-24.

Zhou, X., Duan, X., Qian, J., and Li, F. (2009). Abundant conserved microRNA target sites in the 5'-untranslated region and coding sequence. Genetica *137*, 159-164.